



Flinders
UNIVERSITY

Peri-infarct Glial Cell Responses and Functional Recovery After Stroke

Wai Ping Yew

BMedSci, BSc(Hons)

School of Medicine

Faculty of Medicine, Nursing and Health Sciences

Flinders University

1 July, 2016

TABLE OF CONTENTS

Thesis Summary	iii
Declaration	v
Acknowledgments	vi
Contributions of investigators to this project	viii
Published abstracts arising from this project	x
List of abbreviations	xi
List of figures and tables	xiv
Organisation of the thesis	xix
Chapter 1 <i>General Introduction</i>	1
1.1 What is Stroke?.....	2
1.2 Acute Interventions - Thrombolytics & Neuroprotective Treatments	4
1.3 Spontaneous Recovery After Stroke	6
1.4 Post-Stroke Peri-infarct Glial Cell Responses	8
1.4.1 Astroglial Responses	10
1.4.2 Microglial Responses	15
1.5 Modulating Glial Cell Responses to Promote Functional Recovery	27
1.5.1 Anti-inflammatory agents	27
1.5.2 Anti-proliferative agents	29
1.5.3 Stem Cell Transplantation	31
1.6 Modeling Stroke	33
1.6.1 Animal Models	33
1.6.2 Tissue Culture Models	35
1.7 Objectives of the Study	36
Chapter 2 <i>General Materials and Methods</i>	38
2.1 Animals	39
2.2 General Materials.....	39
2.3 General Methods	41
2.3.1 Habituation of Animals to Handling and Functional Testing.....	41
2.3.2 Forelimb Placing Assessment	41
2.3.3 Photothrombotic Stroke Surgery	42
2.3.4 Perfusion-Fixation of the Brain	45
2.3.5 Cryoprotection of Brain Samples.....	46
2.3.6 Cryosectioning of Brain Samples	46
2.3.7 Cresyl Violet Staining and Calculation of Infarct Volume	47
2.3.8 Immunohistochemistry	48
2.3.9 Image Acquisition.....	49
2.3.10 Image Analysis.....	52
2.3.11 Western Blot	55
2.3.12 Statistical Analysis	56
Chapter 3 <i>Microglial and Astroglial Responses in a Photothrombotic Model of Stroke</i>	57
3.1 Introduction	58
3.2 Materials and Methods.....	62
3.2.1 Experimental Design.....	62
3.2.2 NeuroTrace Staining Vs. NeuN Immunolabelling	63
3.2.3 Additional Analysis of Changes in Microglial Response to Photothrombotic Stroke.....	64

3.3	Results.....	65
3.3.1	Infarct Volume.....	65
3.3.2	Forelimb Placing Reflex.....	66
3.3.3	Microglial Response – Circularity.....	68
3.3.4	Microglial Response – Area Fraction.....	72
3.3.5	Microglial Response – Particle Count & Average Size.....	74
3.3.6	Microglial Response – Additional Analysis.....	77
3.3.7	Astroglial Response.....	79
3.4	Discussion.....	83
3.5	Conclusion.....	93
Chapter 4 <i>Effects of Treatment Using Minocycline on Post-Stroke Glial Cell Responses and Functional Recovery</i>		94
4.1	Introduction.....	95
4.2	Materials and Methods.....	98
4.2.1	Initial Investigations of Treatment Using Minocycline.....	98
4.2.2	High Dose Minocycline Treatment.....	100
4.2.3	Image Acquisition and Analysis for ED1-Immunolabelled Sections.....	103
4.3	Results.....	105
4.3.1	Initial Investigations of Treatment Using Minocycline.....	105
4.3.2	High Dose Minocycline Treatment.....	112
4.4	Discussion.....	119
4.5	Conclusion.....	126
Chapter 5 <i>A Cell Culture Model of the Peri-infarct Tissue</i>.....		127
5.1	Introduction.....	128
5.1.1	Studying Glial Cell Activation in Cell Cultures.....	129
5.1.2	Inducing Focal Injury in Cell Cultures.....	131
5.1.3	A Cell Culture Model of the Peri-infarct Tissue after Stroke.....	131
5.2	Materials and Methods.....	133
5.2.1	Primary Mixed Glial Cell Culture.....	133
5.2.3	Coating of Coverslips with Poly-L-lysine.....	134
5.2.3	Depletion of Microglial Cells from Mixed Glial Cultures.....	134
5.2.4	Minocycline Treatment.....	135
5.2.5	Induction of Cryo-lesion.....	135
5.2.6	Thermal imaging of cell culture surfaces during Cryo-lesion induction.....	137
5.2.7	Assessment of Cell Death and Viability Following Cryo-lesioning.....	137
5.2.8	Immunocytochemistry.....	138
5.2.9	Image Acquisition.....	139
5.2.10	Image Analysis.....	141
5.2.11	Measuring Nitrite Content Using the Griess Reaction.....	143
5.3	Results.....	144
5.3.1	Characterisation of the Cell Culture Model.....	144
5.3.2	Modifying Glial Responses to Cold-Induced Focal Cell Death.....	159
5.4	Discussion.....	168
5.5	Conclusion.....	178
Chapter 6 <i>General Conclusions and Future Directions</i>.....		179
Bibliography.....		185

THESIS SUMMARY

Recovery of function following stroke depends, at least in part, on the re-organisation of neurons within the viable tissue immediately surrounding the infarct. The processes underlying neuronal plasticity are critically influenced by the responses of microglia and astroglia within this tissue region, also known as the "peri-infarct" tissue. However, the development of these responses and the nature of their influence are not well understood. The investigations described in this thesis aimed to (i) further characterise the changes induced in peri-infarct glial cells, (ii) develop novel approaches for evaluating key changes in these cells in the brain and in a cell culture model and (iii) assess the consequences of early treatment with the anti-inflammatory drug, minocycline, on the peri-infarct glial cell responses and functional recovery.

In the first part of this thesis, quantitative measures were developed based on the changes in morphology, proliferation and migration of glial cells that occur after stroke. These measures were applied to the characterisation of the photothrombotic model of stroke and enabled the detection of activation in peri-infarct microglia by 3 hours following infarction and the novel observation of a loss of these cells at 24 hours. Using the characterised model, the influence of the early post-stroke glial cell responses on functional recovery was investigated by time-targeted treatment with minocycline, a drug widely reported to inhibit microglial activation. Surprisingly, minocycline treatment had limited effects on the quantitative measures of microglial activation following stroke. Despite this, the treatment resulted in improved functional recovery that was associated with increased astroglial reactivity as assessed by GFAP and vimentin expression. Crucially, the early treatment did not result in changes to the infarct volume indicative of neuroprotection. These results provided evidence that minocycline treatment can improve functional recovery after stroke via non-neuroprotective mechanisms, including the enhancement of aspects of the astroglial response that are beneficial to recovery. However, the limited effects on microglial activation suggested the possibility that either microglia were not the primary targets of minocycline, or there were subtle changes that were not detected by the measures used.

In the second part of the thesis, a cell culture model of focal injury was developed based on a method of inducing cell death by rapid, localised cooling. Characterisation of the model in primary mixed glial cultures revealed that it recapitulated key features of the peri-infarct glial cell responses following stroke. Using the model, the role of microglial activation in the development of astrogliosis was investigated by (i) depleting microglial cells from the cultures and, (ii) pre-treatment with minocycline. Depletion of microglial cells led to an increase in the baseline astroglial reactivity as measured by nestin expression, but did not prevent the development of the astroglial response to focal injury. Minocycline treatment did not result in changes to the microglial and astroglial response. The results suggested that the development of the astroglial response is not dependent on microglial activity but may be modulated by it. The lack of effects of minocycline treatment further suggested that microglia may not be its primary target.

DECLARATION

I certify that this thesis does not incorporate without acknowledgment any material previously submitted for a degree or diploma in any university; and that to the best of my knowledge and belief it does not contain any material previously published or written by another person except where due reference is made in the text.

Signed.....

Date.....

ACKNOWLEDGMENTS

I would like to acknowledge and express my gratitude to the following people for their contributions to this project. The thesis could not have been completed or at the very least greatly impoverished without their involvement.

First and foremost, I would like to thank my principal supervisor, Professor Neil R. Sims, and co-supervisor, Dr. Håkan Muyderman. I am especially indebted to Neil for his invaluable advice, guidance and mentorship over the years. His patience, insightful comments and feedback (and good humour, mostly!) over the course of the protracted writing of the thesis is greatly appreciated. Håkan provided some very helpful feedback during the drafting of this thesis. He also assisted during the early stages of the cell culture studies by providing advice on the design of the model.

Much credit and thanks to our research assistants, Mr. Jaya S.P. Jayaseelan and Ms. Natalia D. Djukic, who performed a significant portion of the work for some of the experiments that formed the basis of this thesis.

Special thanks are due to Dr. F. Rohan Walker at the University of Newcastle in New South Wales. Rohan provided the additional analysis of microglia morphology in the animal studies using the NeuroLucida image analysis software.

Further thanks go out to the following people who provided assistance in various aspects of the project. Dr. Tim K. Chataway provided assistance and advice on the technique and analysis of Western blots and access to the Flinders Proteomics Facility. Professor Simon J. Brookes and Ms. Bao Nan Chen provided access to the Olympus IX-71 fluorescence microscope in the Neurogastroenterology laboratory. Professor Rainer V. Haberberger is an associate supervisor and provided valuable feedback on the thesis write-up. Emeritus Professor Ian L. Gibbins provided much appreciated and helpful advice on image analysis techniques and statistical analysis. Ms. Yvette de Graf provided support and training for the confocal and epifluorescence microscopes, and the cryo-microtomes, at the Flinders Microscopy facility.

I would also like to give special mention to one of our previous research assistants, Ms. Alison L. Wadey. Alison was a research assistant in the Stroke Laboratory years

ago during my summer internship and honours project in the laboratory. She was the one most responsible for imparting to me the basics of laboratory work, including cell culturing and animal handling and surgery.

Finally and most importantly, to my parents, Yew Ching Chwan and Chua Pheck Lan. They have given me unquestioning and unstinting support since all those years ago, when I decided to leave the safe and stable career of an engineer to pursue my childhood aspiration of becoming a scientist. This is dedicated to them.

CONTRIBUTIONS OF INVESTIGATORS TO THIS PROJECT

The entirety of this thesis was written by me, with guidance and feedback from Professor Neil R. Sims. Additional comments and feedback on the manuscript were received from Dr. Håkan Muyderman and Professor Rainer V. Haberberger.

The thesis was organised around the three main studies described in chapters 3, 4 and 5. I was responsible for the development of the techniques and procedures used throughout all the studies. These included the surgery for photothrombotic stroke induction, functional testing of the animals, tissue processing, immunohistochemistry, microscopy, image analysis and data collection. I was also responsible for the teaching of these techniques to our research assistants, Mr. Jaya S.P. Jayaseelan and Ms. Natalia D. Djukic, as well as providing guidance and supervision where necessary.

In chapter 3, "Microglial and Astroglial Responses in a Photothrombotic Model of Stroke", Neil and I were responsible for the experimental design of the study and for the analysis of most of the data and interpretation of the findings. I have performed all the surgeries during the establishment of the model and around half of the surgeries used in the characterisation of the model. I also performed the functional testing for the animals that I have operated on, as well as essentially all of the microscopy and image analysis. Jaya performed the remaining half of the surgeries and functional testing for the characterisation of the model. Natalia was primarily responsible for all the work on Western blots under the supervision of Neil. The tissue processing and immunohistochemistry work was shared between Jaya, Natalia and myself. Additional image analysis using Neurolucida for microglial morphology was performed by Dr. F. Rohan Walker at the University of Newcastle.

In chapter 4, "Effects of Treatment Using Minocycline on Post-stroke Glial Cell Responses and Functional recovery", Neil and I were responsible for the experimental design of the study and for the analysis of most of the data and the interpretation of the findings. The techniques and procedures used in this study were largely identical to those that were established in chapter 3. Jaya was responsible for all the surgeries and functional testing for the low dose and around two-thirds of the

surgeries for the high dose minocycline treatment experiments. I was responsible for the remaining surgeries and functional testing for the high dose experiments. The tissue processing, immunohistochemistry and microscope work was shared between Jaya, Natalia and myself. Image analysis was performed by Jaya and myself. Western blotting was performed by Natalia.

In chapter 5, "A Cell Culture Model of the Peri-infarct Tissue", I was primarily responsible for the experimental design of the study with guidance from Neil. The cell culture model was designed and developed by myself with advice and feedback from Neil and Håkan. Essentially the entirety of the work for this study was conducted by myself.

All statistical analyses in the studies were performed by myself with advice from Neil.

PUBLISHED ABSTRACTS ARISING FROM THIS PROJECT

Yew, WP, Jayaseelan, J, Djukic, N, Muyderman, H & Sims, N 2015, 'Early post-stroke treatment with minocycline promotes functional recovery without modulating key aspects of microglial activation', *Journal of Neurochemistry*, vol. 134, no. S1, pp. 298.

Djukic, N, **Yew, WP**, Jayaseelan, J, Muyderman, H & Sims, N 2015, 'Minocycline treatment increases peri-infarct astrocytic responses and functional recovery following photothrombotic stroke', *Journal of Neurochemistry*, vol. 134, no. S1, pp. 291-2.

Yew WP, Djukic ND, Jayaseelan JSP, Muyderman H and Sims NR 2014, 'Minocycline has limited effects on early microglial activation following photothrombotic stroke in rats', POS-THU-077, *ANS 2014 Conference in Adelaide*, SA, Australia. 30 January, 2014.

Djukic ND, **Yew WP**, Jayaseelan JSP, Muyderman H and Sims NR 2014, 'Glial cell activation in peri-infarct tissue in a photothrombotic model of stroke in rats', POS-WED-050, *ANS 2014 Conference in Adelaide*, SA, Australia. 29 January, 2014.

W. YEW, J. S. P. JAYASEELAN, N. D. DJUKIC, H. MUYDERMAN, N. R. SIMS. Early responses of microglia to tissue infarction in a photothrombotic model of stroke in rats. Program No. 251.15. Neuroscience 2013 Abstracts. San Diego, CA: Society for Neuroscience, 2013. Online.

N. R. SIMS, **W. YEW**, N. D. DJUKIC, J. S. P. JAYASEELAN, H. MUYDERMAN. Peri-infarct responses of microglia and astrocytes in a photothrombotic model of stroke in rats. Program No. 251.14. Neuroscience 2013 Abstracts. San Diego, CA: Society for Neuroscience, 2013. Online.

Yew WP, Djukic ND, Jayaseelan JSP, Muyderman H and Sims NR 2013, 'Peri-infarct glial cell responses in a photothrombotic model of stroke in rats', ORAL-16-8, *ANS 2013 Conference in Melbourne*, VIC, Australia. 6 February, 2013.

Yew WP, Muyderman H, Sims NR 2012, 'A cell culture model for investigating microglial responses to focal cell death', POS-WED-082, *ANS 2012 Conference in Gold Coast*, QLD, Australia. 1 February, 2012.

LIST OF ABBREVIATIONS

$^{\circ}\text{C}$	degree Celsius
<i>5-LOX</i>	5-lipoxygenase
<i>bFGF</i>	basic Fibroblast Growth Factor
<i>d, h, min</i>	day, hour, minute
<i>g, kg, mg, μg</i>	gram, kilogram, milligram, microgram
<i>iNOS</i>	inducible Nitric Oxide Synthase
<i>m, mm, μm</i>	metre, millimetre, micrometre
<i>mRNA</i>	messenger RNA
<i>tβ₄</i>	Thymosin beta 4
<i>tPA</i>	Tissue Plasminogen Activator
<i>Ara-C</i>	Cytosine β -d-Arabinofuranoside
<i>Arg-1</i>	Arginase-1
<i>ANOVA</i>	Analysis of Variance
<i>ATP</i>	Adenosine Triphosphate
<i>BDNF</i>	Brain-Derived Neurotrophic Factor
<i>BMSC</i>	Bone Marrow Stromal/Stem Cells
<i>BSA</i>	Bovine Serum Albumin
<i>Cox-2</i>	Cyclooxygenase 2
<i>CB2R</i>	Cannabinoid Type 2 Receptor
<i>CD</i>	Cluster of Differentiation
<i>CINC-1</i>	Cytokine-Induced Chemoattractant protein 1

<i>CNS</i>	Central Nervous System
<i>CNTF</i>	Ciliary Neurotrophic Factor
<i>CSPG</i>	Chondroitin Sulfate Proteoglycan
<i>Da, kDa</i>	Dalton, kilodalton
<i>DAMP</i>	Danger-Associated Molecular Pattern
<i>DIV</i>	Days <i>in vitro</i>
<i>DMEM</i>	Dulbecco's Modified Eagle's Medium
<i>EDTA</i>	Ethylenediaminetetraacetic Acid
<i>ERK, pERK</i>	Extracellular Receptor Kinase, phosphorylated ERK
<i>FCM</i>	Fresh Culture Medium
<i>GCM</i>	Glia-Conditioned Medium
<i>GDNF</i>	Glial cell-Derived Neurotrophic Factor
<i>GFAP</i>	Glial Fibrillary Acidic Protein
<i>GFP</i>	Green Fluorescent Protein
<i>HBSS</i>	Hepes-Buffered Salt Solution
<i>HMGB1</i>	High Mobility Group Box-1
<i>Iba1</i>	Ionised-calcium Binding Adapter protein 1
<i>IFN-γ</i>	Interferon gamma
<i>IL</i>	Interleukin
<i>L, mL, μL</i>	litre, millilitre, microlitre
<i>LME</i>	L-leucine Methyl Ester
<i>LPS</i>	Lipopolysaccharides
<i>M, mM, μM</i>	molar, millimolar, micromolar

<i>MCA, MCAo</i>	Middle Cerebral Artery, Middle Cerebral Artery occlusion
<i>MCP-1</i>	Monocyte Chemoattractant Protein 1
<i>MIP-1α</i>	Macrophage Inflammatory Protein 1 alpha
<i>MMP</i>	Matrix Metalloproteinases
<i>MRI</i>	Magnetic Resonance Imaging
<i>NeuN</i>	Neuronal Nuclei
<i>NO</i>	Nitric Oxide
<i>OGD</i>	Oxygen-Glucose Deprivation
<i>PBS</i>	Phosphate-Buffered Saline
<i>PI</i>	Propidium Iodide
<i>PVDF</i>	Polyvinylidene fluoride
<i>RCF</i>	Relative Centrifugal Force
<i>ROI</i>	Region Of Interest
<i>ROS</i>	Reactive Oxygen Species
<i>RNA</i>	Ribonucleic Acid
<i>SD</i>	Standard Deviation
<i>TBS</i>	Tris-Buffered Saline
<i>TGF-β</i>	Transforming Growth Factor beta
<i>TNF-α</i>	Tumor Necrosis Factor alpha
<i>U</i>	unit
<i>VEGF</i>	Vascular Endothelial Growth Factor

LIST OF FIGURES AND TABLES

FIGURE 1.1.1 ISCHEMIC STROKE ARISING FROM OCCLUSION OF THE MIDDLE CEREBRAL ARTERY.....	3
FIGURE 1.4.1 EXPRESSION OF CYTOSKELETAL PROTEINS ARE UPREGULATED IN PERI-INFARCT ASTROGLIA FOLLOWING STROKE.....	9
FIGURE 1.4.2 STRUCTURE OF THE GLIA LIMITANS AT THE MENINGEAL AND LESION BOUNDARIES.	10
FIGURE 1.4.3 MORPHOLOGICAL TRANSFORMATION OF MICROGLIA DURING ACTIVATION.....	16
TABLE 2.2.1 LIST OF COMMON LABORATORY CHEMICALS AND REAGENTS	39
FIGURE 2.3.1 FORELIMB PLACING TEST PLATFORM.....	41
FIGURE 2.3.2 THE THREE VARIANTS OF THE FORELIMB PLACING TEST.....	42
FIGURE 2.3.3 PLACEMENT OF BRASS SHIM AND FIBRE OPTIC CABLE FROM LIGHT SOURCE.....	44
FIGURE 2.3.4 SAMPLE IMAGE OF BRAIN SECTION STAINED WITH CRESYL VIOLET.	48
TABLE 2.3.1 LIST OF ANTIBODIES AND DILUTIONS USED IN IMMUNOHISTOCHEMISTRY.....	49
FIGURE 2.3.5 LOCATION OF IMAGES ACQUIRED FOR THE CHARACTERISATION OF MICROGLIAL CHANGES FOLLOWING STROKE.	50
FIGURE 2.3.6 LOCATION OF IMAGES ACQUIRED FOR THE CHARACTERISATION OF ASTROGLIAL CHANGES FOLLOWING STROKE.....	51
FIGURE 2.3.7 SPECIFYING THE AREA FOR PARTICLE ANALYSIS OF IBA1 IMMUNOLABELLING WITHIN THE PERI-INFARCT REGION.....	53
FIGURE 2.3.8 OVERLAY OUTLINES OF MICROGLIAL CELLS IMMUNOLABELLED WITH IBA1 AS IDENTIFIED BY "ANALYZE PARTICLE" FUNCTION IN IMAGEJ.....	54
FIGURE 2.3.9 SPECIFYING THE AREA FOR AREA FRACTION ANALYSIS OF VIMENTIN IMMUNOLABELLING WITHIN THE PERI-INFARCT REGION.....	54
FIGURE 2.3.10 DISSECTION OF BRAIN TISSUE FOR WESTERN BLOT.....	56
TABLE 2.3.2 LIST OF ANTIBODIES AND DILUTIONS USED IN WESTERN BLOTS	56
FIGURE 3.2.1 EXPERIMENTAL TIMELINE FOR THE CHARACTERISATION OF THE PHOTOTHROMBOTIC STROKE MODEL.	62
TABLE 3.2.1 LIST OF ANTIBODIES, STAINS AND DILUTIONS USED FOR NEUROTRACE AND NEUN CO-LABELLING.....	64
FIGURE 3.3.1 VOLUME OF INFARCT FOLLOWING PHOTOTHROMBOTIC STROKE INDUCTION.	65
FIGURE 3.3.2 COMPARISON BETWEEN NEUROTRACE™ NISSL STAINING AND NEUN IMMUNOLABELLING.....	66
FIGURE 3.3.3 FORELIMB PLACING SCORES FOLLOWING STROKE INDUCTION.....	67
FIGURE 3.3.4 LOCATIONS WITHIN EACH BRAIN SECTION ANALYZED FOR MICROGLIAL CHANGES AFTER STROKE.	68

FIGURE 3.3.5 MICROGLIA CIRCULARITY AT 3 HOURS AFTER STROKE INDUCTION.	69
FIGURE 3.3.6 MICROGLIA CIRCULARITY AT 24 HOURS AFTER STROKE INDUCTION.....	70
FIGURE 3.3.7 TIME-COURSE OF CHANGES IN MICROGLIAL CIRCULARITY AFTER STROKE INDUCTION.	71
FIGURE 3.3.8 MICROGLIA AREA FRACTION AT 3 HOURS AFTER STROKE INDUCTION.	72
FIGURE 3.3.9 MICROGLIA AREA FRACTION AT 24 HOURS AFTER STROKE INDUCTION.	73
FIGURE 3.3.10 TIME-COURSE OF CHANGES IN MICROGLIAL AREA FRACTION AFTER STROKE INDUCTION.	74
FIGURE 3.3.11 PARTICLE COUNTS OF IBA1-IMUNOLABELLED PARTICLES WITHIN THE PERI-INFARCT AND CORRESPONDING CONTRALATERAL REGIONS AFTER PHOTOTHROMBOTIC STROKE.	75
FIGURE 3.3.12 AVERAGE SIZE OF IBA1-IMMUNOLABELLED PARTICLES WITHIN THE PERI-INFARCT AND CORRESPONDING CONTRALATERAL REGIONS AFTER PHOTOTHROMBOTIC STROKE.	76
FIGURE 3.3.13 CO-LOCALISATION OF KI67 AND IBA1 WITHIN THE PERI-INFARCT TISSUE AT 3 DAYS AFTER STROKE.	76
FIGURE 3.3.14 MICROGLIAL CELL AREA AT 24 HOURS AND 7 DAYS AFTER STROKE.....	77
FIGURE 3.3.15 MICROGLIAL SOMA AREA AT 24 HOURS AND 7 DAYS AFTER STROKE.....	78
FIGURE 3.3.16 MICROGLIAL CELL PERIMETER AT 24 HOURS AND 7 DAYS AFTER STROKE.....	78
FIGURE 3.3.17 GFAP AND VIMENTIN EXPRESSION AT 3 DAYS AFTER STROKE.....	79
FIGURE 3.3.17 REPRESENTATIVE FLUORESCENCE IMAGES OF VIMENTIN-IMMUNOLABELLED SECTIONS AT DIFFERENT TIME-POINTS AFTER STROKE INDUCTION.	80
FIGURE 3.3.18 INCREASE IN VIMENTIN AREA FRACTION IN THE PERI-INFARCT AFTER STROKE INDUCTION.	81
FIGURE 3.3.19 WESTERN BLOTS FOR VIMENTIN AND GFAP FOLLOWING PHOTOTHROMBOTIC STROKE.	82
FIGURE 4.2.1 EXPERIMENTAL TIMELINE FOR THE INVESTIGATION OF THE EFFECTS OF LOW DOSE MINOCYCLINE TREATMENT FOLLOWING PHOTOTHROMBOTIC STROKE..	99
FIGURE 4.2.2 EXPERIMENTAL TIMELINE FOR THE INVESTIGATION OF THE EFFECTS OF HIGH DOSE MINOCYCLINE TREATMENT FOLLOWING PHOTOTHROMBOTIC STROKE..	101
FIGURE 4.2.3 LOCATION OF IMAGES ACQUIRED FOR ANALYSIS OF ED1 EXPRESSION.....	104
FIGURE 4.2.3 AREA SELECTION FOR ANALYSIS OF ED1 ⁺ PARTICLES.	104

FIGURE 4.3.1 INFARCT VOLUME IN ANIMALS TREATED WITH LOW DOSE MINOCYCLINE OR VEHICLE FOLLOWING STROKE.....	105
FIGURE 4.3.2 FORELIMB PLACING SCORE OF THE AFFECTED FORELIMB OF ANIMALS TREATED WITH LOW DOSE MINOCYCLINE OR VEHICLE AT BASELINE AND UP TO 7 DAYS AFTER STROKE.....	106
FIGURE 4.3.3 CIRCULARITY OF MICROGLIAL CELLS IN THE CONTRALATERAL CORTEX AND PERI-INFARCT TISSUE OF ANIMALS TREATED WITH LOW DOSE MINOCYCLINE OR VEHICLE.	107
FIGURE 4.3.4 AREA FRACTION OF MICROGLIAL CELLS IN THE CONTRALATERAL CORTEX AND PERI-INFARCT TISSUE OF ANIMALS TREATED WITH LOW DOSE MINOCYCLINE OR VEHICLE.	108
FIGURE 4.3.5 AREA FRACTION OF VIMENTIN IMMUNOLABELLING IN THE PERI- INFARCT TISSUE AND CONTRALATERAL CORTEX OF ANIMALS TREATED WITH LOW DOSE MINOCYCLINE AT 7 DAYS AFTER STROKE.	109
FIGURE 4.3.6 DENSITOMETRIC ANALYSIS OF WESTERN BLOTS OF VIMENTIN EXPRESSION IN THE PERI-INFARCT TISSUE OF ANIMALS TREATED WITH LOW DOSE MINOCYCLINE AT 7 DAYS AFTER STROKE.....	110
FIGURE 4.3.7 DENSITOMETRIC ANALYSIS OF WESTERN BLOTS OF NEUROCAN EXPRESSION IN THE PERI-INFARCT TISSUE OF ANIMALS TREATED WITH LOW DOSE MINOCYCLINE AT 7 DAYS AFTER STROKE.....	111
FIGURE 4.3.8 FORELIMB PLACING SCORE OF THE AFFECTED FORELIMB OF ANIMALS TREATED WITH HIGH DOSE MINOCYCLINE OR VEHICLE AT BASELINE AND UP TO 7 DAYS AFTER STROKE.....	113
FIGURE 4.3.9 CIRCULARITY OF MICROGLIAL CELLS IN THE CONTRALATERAL CORTEX AND PERI-INFARCT TISSUE OF ANIMALS TREATED WITH HIGH DOSE MINOCYCLINE OR VEHICLE.	114
FIGURE 4.3.10 AREA FRACTION OF MICROGLIAL CELLS IN THE CONTRALATERAL CORTEX AND PERI-INFARCT TISSUE OF ANIMALS TREATED WITH HIGH DOSE MINOCYCLINE OR VEHICLE.	115
FIGURE 4.3.11 ED1-IMMUNOLABELLING WITHIN THE PERI-INFARCT TISSUE AT 3 DAYS AFTER STROKE.....	116
FIGURE 4.3.12 ED1 ⁺ PARTICLE DENSITY IN THE CONTRALATERAL CORTEX AND PERI-INFARCT TISSUE OF ANIMALS TREATED WITH HIGH DOSE MINOCYCLINE OR VEHICLE.	117
FIGURE 4.3.13 DENSITOMETRIC ANALYSIS OF WESTERN BLOTS OF VIMENTIN AND GFAP EXPRESSION IN THE PERI-INFARCT TISSUE OF ANIMALS TREATED WITH HIGH DOSE MINOCYCLINE AT 7 DAYS AFTER STROKE.....	118
FIGURE 4.3.14 DENSITOMETRIC ANALYSIS OF WESTERN BLOT NEUROCAN EXPRESSION IN THE PERI-INFARCT TISSUE OF ANIMALS TREATED WITH HIGH DOSE MINOCYCLINE AT 7 DAYS AFTER STROKE.....	118
FIGURE 5.2.1 EXPERIMENTAL SET-UP FOR INDUCTION OF CRYO-LESION IN CELL CULTURES.....	136

TABLE 5.2.1 LIST OF ANTIBODIES AND DILUTIONS USED IN IMMUNOCYTOCHEMISTRY	138
FIGURE 5.2.2 DIAGRAM ILLUSTRATING REGIONS OF INTEREST FOR IMAGE ACQUISITION ON EACH COVERSIP	140
FIGURE 5.3.1 UNFIXED PRIMARY MIXED GLIAL CULTURE 24 HOURS AFTER 7 SECONDS CONTACT WITH LIQUID NITROGEN COOLED COPPER ROD	144
FIGURE 5.3.2 THERMAL IMAGES OF CELL CULTURE SURFACE BEFORE AND IMMEDIATELY AFTER INDUCTION OF CRYO-LESION	145
FIGURE 5.3.3 FLUORESCENCE IMAGES OF LIVE CULTURES STAINED WITH CALCEIN AND PROPIDIUM IODIDE AT 2 HOURS AFTER CRYO-LESION	146
FIGURE 5.3.4 MICROGLIAL CELLS IN CONTROL CULTURES AT 14 DIV	147
FIGURE 5.3.5 MICROGLIAL CELLS ALONG THE LESION BORDER AT 2 HOURS AFTER CRYO-LESION	148
FIGURE 5.3.6 INFILTRATION OF MICROGLIA INTO THE LESION CORE OVER TIME	149
FIGURE 5.3.7 CHANGES IN TOTAL AND MICROGLIAL CELL DENSITIES ALONG THE LESION BORDER FOLLOWING CRYO-LESIONING	151
FIGURE 5.3.8 CHANGES IN TOTAL AND MICROGLIAL CELL DENSITIES AT 5 MM FROM THE LESION BORDER FOLLOWING CRYO-LESIONING	152
FIGURE 5.3.9 CHANGES IN THE PROPORTIONS OF RAMIFIED AND AMOEBOID MICROGLIA ALONG THE LESION BORDER FOLLOWING CRYO-LESIONING	153
FIGURE 5.3.10 CHANGES IN THE PROPORTIONS OF RAMIFIED AND AMOEBOID MICROGLIA AT 5 MM FROM THE LESION BORDER FOLLOWING CRYO-LESIONING	154
FIGURE 5.3.11 GFAP EXPRESSION IN CONTROL CULTURES AT 14 DIV	156
FIGURE 5.3.12 CHANGES IN ASTROGLIAL GFAP EXPRESSION ALONG LESION BORDER FOLLOWING CRYO-LESIONING	157
FIGURE 5.3.13 CHANGES IN NESTIN EXPRESSION IN ASTROGLIA ALONG LESION BORDER FOLLOWING CRYO-LESIONING	158
FIGURE 5.3.14 QUANTIFICATION OF MICROGLIAL AREA FRACTION AND CIRCULARITY IN CONTROL AND CRYO-LESIONED CULTURES	160
FIGURE 5.3.15 EFFECTS OF MINOCYCLINE TREATMENT ON AREA FRACTION AND CIRCULARITY OF MICROGLIAL CELLS ALONG THE LESION BORDER FOLLOWING CRYO-LESIONING	161
FIGURE 5.3.16 EFFECTS OF MINOCYCLINE TREATMENT ON AREA FRACTION AND CIRCULARITY OF MICROGLIAL CELLS AT 5 MM FROM THE LESION BORDER FOLLOWING CRYO-LESIONING	162
FIGURE 5.3.17 PARTICLE COUNT OF INOS-IMMUNOLABELLED PARTICLES AT THE LESION BORDER AND 5 MM AWAY 24 HOURS AFTER CRYO-LESIONING	163
FIGURE 5.3.18 INCREASE IN NITRITE CONTENT AT 24 AND 48 HOURS AFTER CRYO-LESIONING	164
FIGURE 5.3.19 PRIMARY MIXED GLIAL CULTURE 6 DAYS AFTER MICROGLIA DEPLETION TREATMENT	165

FIGURE 5.3.20 NORMALISED GFAP FLUORESCENCE INTENSITY AT 48 HOURS AFTER CRYO-LESIONING.....	166
FIGURE 5.3.21. NORMALISED NESTIN FLUORESCENCE INTENSITY AT 48 HOURS AFTER CRYO-LESIONING.....	167

ORGANISATION OF THE THESIS

This thesis is a report on a series of investigations into the characteristics of the responses of glial cells, specifically the microglia and astroglia, to infarction as a result of ischemic stroke and the subsequent functional recovery. The first chapter provides an introduction to the current understanding of these glial cell responses and how they influence the mechanisms that underlie the recovery of function following stroke. This is followed by a chapter describing the common materials and methods employed in the experiments conducted in the investigations. The next three chapters, chapters 3, 4 and 5, present the experimental investigations that formed the core of this thesis. The investigations in chapter 3 were designed to characterise the glial cell responses following photothrombotic stroke in rats using a quantitative approach that can be applied to subsequent investigations aimed at modifying these responses. Chapter 4 describes investigations into the effects of modifying the glial cell responses in the photothrombotic stroke model and the influence of these changes on functional recovery. In chapter 5, a new cell culture model was developed for the investigation of glial cell responses to focal injuries such as stroke. The cell culture model was then applied to the investigation of the influence of microglial activation on the development of astroglial responses. These three chapters have been written in a self-contained manner and each include a chapter-specific introduction, methods, results, discussion and conclusions. Finally, chapter 6 concludes the thesis with a brief discussion of the general findings of the investigations and potential directions for future studies.

CHAPTER 1
GENERAL INTRODUCTION

1.1 What is Stroke?

Stroke is a neurological disorder caused by a disruption of blood supply that results in an injury to the brain. It is the second leading cause of death and third leading cause of disability worldwide (Feigin et al. 2014; Lozano et al. 2012; Murray et al. 2012). Globally, there were 25.7 million stroke survivors, 10.3 million new strokes and 6.5 million deaths resulting from stroke in 2013 (Feigin et al. 2015). In Australia, it has been estimated that more than 50,000 persons each year are affected by stroke with an associated lifetime cost per patient of more than AUD 80,000 (Cadilhac et al. 2009; Gloede et al. 2014).

Hemorrhagic and ischemic stroke are the two main types of stroke, with ischemic stroke accounting for approximately 70 % of all stroke cases globally (Feigin et al. 2015). Ischemic stroke is the result of cerebral arterial occlusion due to the formation of a thrombus or a travelling embolus that leads to ischemia of the brain region supplied by the blood vessel (Caplan 2006; Flynn, MacWalter & Doney 2008) (figure 1.1.1). Within the brain, there is very little overlap between the arterial territories supplying the different brain regions. As a result, the initial functional impairments reflect the neuronal dysfunction due to restriction in blood supply to the territory of the occluded artery. However, if the blood supply is not restored rapidly, infarction which is the death of essentially all cells within the affected tissue occurs. This results in permanent damage and long-term loss of function associated with the infarcted brain region.

The development of the infarct in focal ischemic stroke has been investigated in many studies using animal models (Chen, F et al. 2007; Chen, H et al. 1993; Chiamulera et al. 1993; Clark et al. 1993; Garcia et al. 1993; Liu, F, Schafer & McCullough 2009; Zhang, X et al. 2015) as well as in human patients (Back & Schuler 2004; Baird et al. 1997; Karonen et al. 2000). The results of the animal studies revealed that maturation of the infarct is essentially complete by 1 – 3 days after stroke, where the infarct core can be clearly distinguished from the "peri-infarct", the region of surviving tissue immediately surrounding the infarct, in magnetic resonance imaging (MRI) and histological examinations (Chen, F et al. 2007; Garcia et al. 1993). MRI data in human patients are in general agreement with the animal studies where the majority of patients exhibit rapid expansion of the

lesion within the first 2 days but minimal changes in lesion volume afterwards (Baird et al. 1997; Karonen et al. 2000).

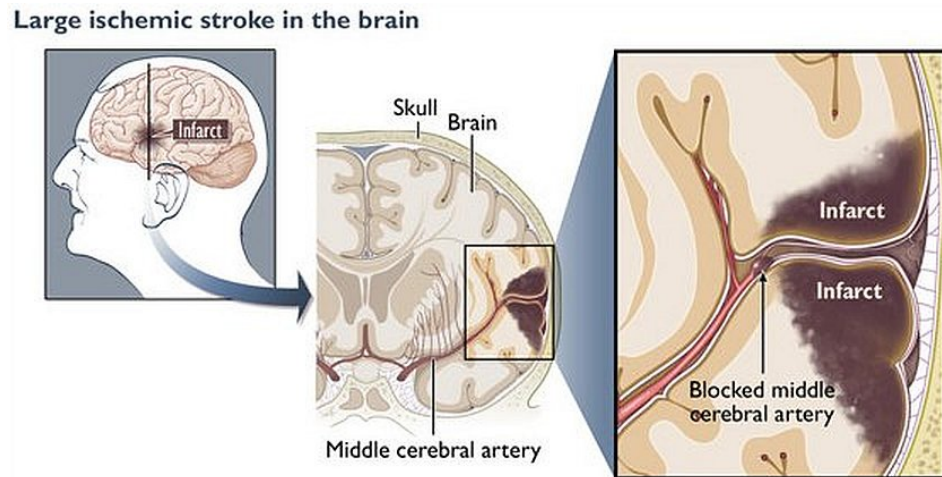


Figure 1.1.1 Ischemic stroke arising from occlusion of the middle cerebral artery.

Blockage of a cerebral artery due a travelling embolus or formation of a thrombus results in the interruption of blood supply to brain regions downstream of the occlusion. Infarction of the affected brain tissue eventually results if blood supply is not rapidly restored. The diagram illustrates an ischemic stroke arising from blockage of a distal branch of the middle cerebral artery (© University of Washington 2016, reprinted with permission).

The mechanisms of infarct development in stroke have been the subject of intense research over the past decades and various factors have been proposed to contribute towards infarct expansion. These factors include glutamate excitotoxicity, calcium influx, mitochondrial dysfunction, activation of intracellular enzymes, reactive oxygen species (ROS) and nitric oxide (NO) production and inflammatory responses (Brouns & De Deyn 2009; Doyle, Simon & Stenzel-Poore 2008; Lipton 1999; Sutherland et al. 2012). The results of these studies have served as the basis of extensive efforts to develop treatments to protect neurons following stroke.

1.2 Acute Interventions - Thrombolytics & Neuroprotective Treatments

Despite the considerable efforts expended in the development of neuroprotective treatments for ischemic stroke, until recently there has been only one treatment that has been demonstrated to be effective in humans. Tissue plasminogen activator (tPA) is a thrombolytic agent that was originally developed for the treatment of acute myocardial infarction. The observation of the similarities in the cause of myocardial infarction and cerebral ischemia prompted investigations into the use of tPA for the treatment of acute ischemic stroke (Levine & Brott 1992). Indeed, acute treatment with intravenous tPA has been shown to improve outcome at 3 to 6 months after stroke onset and is currently the only approved treatment in most countries for acute ischemic stroke up to 3 – 4.5 hours following onset ('Tissue plasminogen activator for acute ischemic stroke. The National Institute of Neurological Disorders and Stroke rt-PA Stroke Study Group' 1995; Wardlaw, JM et al. 2014). However, the usefulness of tPA treatment is limited by its narrow therapeutic window and increased risk of hemorrhagic transformations (Moretti, Ferrari & Villa 2015; Tsivgoulis, Katsanos & Alexandrov 2014). In fact, the effectiveness of treatment using tPA beyond 3 hours after stroke onset remains controversial (Alper et al. 2015a, 2015b; Shy 2014; Wardlaw, J & Berge 2015).

In recent years, newer treatments based on mechanical thrombectomy have been demonstrated to be highly effective with an extended treatment window of 6 to 8 hours in clinical trials (Balami et al. 2015; Chen, CJ et al. 2015; Goyal et al. 2016; Palaniswami & Yan 2015). However, despite the wider therapeutic window compared to tPA thrombolysis, the thrombectomy approach is currently only viable in strokes involving the large arteries of the anterior cerebral circulation, such as the proximal middle cerebral artery (Goyal et al. 2016; Przybylowski et al. 2014).

Numerous other pharmacological agents have also been investigated or are currently undergoing evaluation as potential neuroprotective agents in animal models as well as clinical trials (Ginsberg 2008, 2009; Minnerup et al. 2012; Moretti, Ferrari & Villa 2015). These agents include calcium channel blockers, antioxidants and glutamate antagonists amongst many others that are designed to protect potentially salvageable neurons by modifying various aspects of the biochemical cascade that follows from ischemic stroke (Ginsberg 2009; Minnerup et al. 2012; Turner et al. 2013). Despite

the large number of studies, none of the agents found to be neuroprotective in animal studies have so far been demonstrated to be effective in clinical trials (Ginsberg 2009; Minnerup et al. 2014; Moretti, Ferrari & Villa 2015; Sutherland et al. 2012; Xu, SY & Pan 2013). It is instructive to note that very few of the prospective neuroprotective agents have been found to be effective when administered beyond 6 hours following stroke onset in the animal studies whereas the overwhelming majority of clinical trials have utilised treatment windows in excess of 6 hours (Ginsberg 2008, 2009; Moretti, Ferrari & Villa 2015).

There are various factors that may explain the lack of success of the neuroprotective approach in the treatment of ischemic stroke (Ginsberg 2009; Hossmann 2012; Minnerup et al. 2014; Moretti, Ferrari & Villa 2015; Turner et al. 2013). These factors include potentially critical differences in the preclinical animal studies and human clinical trials and include the inability to achieve adequate dosing in humans, use of different primary outcomes in the animal studies and clinical trials and the frequent presentation of multiple co-morbidities in human patients. Perhaps most important amongst the factors are the use of animal stroke models that are not clinically relevant in many preclinical studies and the use of an excessively wide treatment window in most clinical trials (Ginsberg 2009; Hossmann 2009, 2012).

However, regardless of translational success, the fact that a significant number of stroke patients may not be able to access treatment within a limited time window is likely to remain a crucial limitation on the effectiveness of neuroprotective therapies.

1.3 Spontaneous Recovery After Stroke

Some spontaneous recovery of function usually occurs in the days and weeks following stroke even in the absence of treatment (Cramer 2008b; Murphy, TH & Corbett 2009). This spontaneous functional recovery is highly variable between patients and may be dependent on the location and severity of the infarct (Cramer 2008b; Starkey & Schwab 2014). Although the largest extent of recovery has generally been observed to occur within the first 3 months following stroke, continued improvements may occur even out to a year and longer (Cramer 2008b; Kotila et al. 1984; Murphy, TH & Corbett 2009; Skilbeck et al. 1983).

Most of the recovery over the first few days following stroke is likely to be due to the resolution of oedema and restoration of perfusion and function to hypo-perfused tissue. Other mechanisms during this early recovery phase may also include the strengthening of alternative parallel neuronal pathways and the unmasking of pre-existing but inactive or latent connections (Chen, R, Cohen & Hallett 2002; Cramer 2008b; Dancause & Nudo 2011; Hallett 2001). However, recovery over longer periods is likely to involve the establishment of new connections by the surviving neurons through neurite outgrowth and synaptogenesis.

It is now widely accepted that spontaneous recovery following stroke is due, in part, to neuroplasticity in surviving neurons that reorganise their connections to compensate for the neurons that do not survive (Carmichael 2003; Chen, R, Cohen & Hallett 2002; Murphy, TH & Corbett 2009; Nudo 2007; Starkey & Schwab 2014; Winship & Murphy 2009). Evidence supporting post-stroke neuroplasticity has come from longitudinal studies using functional mapping techniques in rats (Jablonka et al. 2010; van der Zijden et al. 2008), mice (Clarkson et al. 2013; Harrison et al. 2013) and monkeys (Dancause et al. 2005; Xerri et al. 1998) as well as in humans (Jaillard et al. 2005). Further evidence was provided in a series of studies by Murphy and co-workers who demonstrated that synaptic plasticity within the tissue regions immediately adjacent to the infarct was enhanced in the subsequent weeks after stroke using *in vivo* imaging techniques in live animals (Brown et al. 2009; Brown, Boyd & Murphy 2010; Harrison et al. 2013; Sigler & Murphy 2010). These studies have revealed that spontaneous functional recovery after stroke is associated with a remapping of activity from the injured brain regions to adjacent intact regions. Consistent with these findings are studies that have found increases in the expression

of proteins associated with neuronal growth and synaptogenesis within the same tissue regions (Li, S et al. 2010; Li, Y, Jiang, et al. 1998; Stroemer, Kent & Hulsebosch 1995; Ueno et al. 2012).

Although it is likely that the most important changes are occurring within the peri-infarct tissue, the region of intact tissue nearest to the infarct (Carmichael 2006; Cramer 2008b; Johnston et al. 2013; Starkey & Schwab 2014), other studies have suggested that changes in neuronal connectivity occurring in distant regions, including the contralateral hemisphere (Butefisch et al. 2005; Gerloff et al. 2006; Riecker et al. 2010; Takatsuru, Nabekura & Koibuchi 2014) and the lower motor pathways (Liu, Z et al. 2013; Sist, Fouad & Winship 2014; Starkey et al. 2012) may also contribute to functional recovery.

The occurrence of spontaneous recovery after stroke points to an alternative to the neuroprotective approach in the treatment of stroke with a greatly extended therapeutic window. There is now an increasing interest in the development of neurorestorative therapies that can improve the outcome of stroke even when initiated long after maturation of the infarct by augmenting the intrinsic mechanisms underlying spontaneous recovery. Of particular interest in the present study, are the mechanisms of glial cell responses to stroke that can influence functional recovery and are therefore potential therapeutic targets.

1.4 Post-Stroke Peri-infarct Glial Cell Responses

Normal neuronal function is supported by glial cells that greatly outnumber neurons within the brain (Jha, Kim & Suk 2014). Two of the major types of glial cells, that are also the most studied in stroke, are astroglia and microglia. Astroglial cells make up the largest population of glia within the central nervous system (CNS) and over the past decades have been discovered to serve wide-ranging functions including providing metabolic support to neurons, regulation of fluid, pH and ion homeostasis, modulation of synaptic transmission and regulation of neurogenesis and synaptogenesis (Barker & Ullian 2010; Newman 2003; Pekny & Pekna 2014; Sofroniew & Vinters 2010). Microglial cells are the resident immune cells of the CNS that share a common lineage with other tissue-resident macrophages and are closely related to blood monocytes (Chan, Kohsaka & Rezaie 2007; Cuadros & Navascues 1998; Dey, Allen & Hankey-Giblin 2015; Ginhoux et al. 2013; Katsumoto et al. 2014). In addition to mediating immune responses, microglia have also been found to play important roles in the surveillance and regulation of the brain microenvironment, shaping and maturation of neuronal circuits during development, as well as plasticity in the mature brain (Ginhoux et al. 2013; Graeber & Streit 2010; Hanisch & Kettenmann 2007; Tremblay et al. 2011).

Following a stroke event, coincident with the neuronal changes involved in plasticity, striking changes can also be observed in glial cells within the same critical region of the post-stroke peri-infarct tissue. Astroglial cells respond to the infarction in a process termed reactive astrogliosis that is characterised by cellular hypertrophy, proliferation and increased expression of cytoskeletal proteins including GFAP, vimentin and nestin (Duggal, Schmidt-Kastner & Hakim 1997; Hol & Pekny 2015; Katsman et al. 2003; Li, Y & Chopp 1999; Sofroniew 2009) (figure 1.4.1). Prolonged reactive astrogliosis eventually leads to the formation of a glial scar along the border of the lesion that isolates the infarct core from the surrounding healthy tissue.

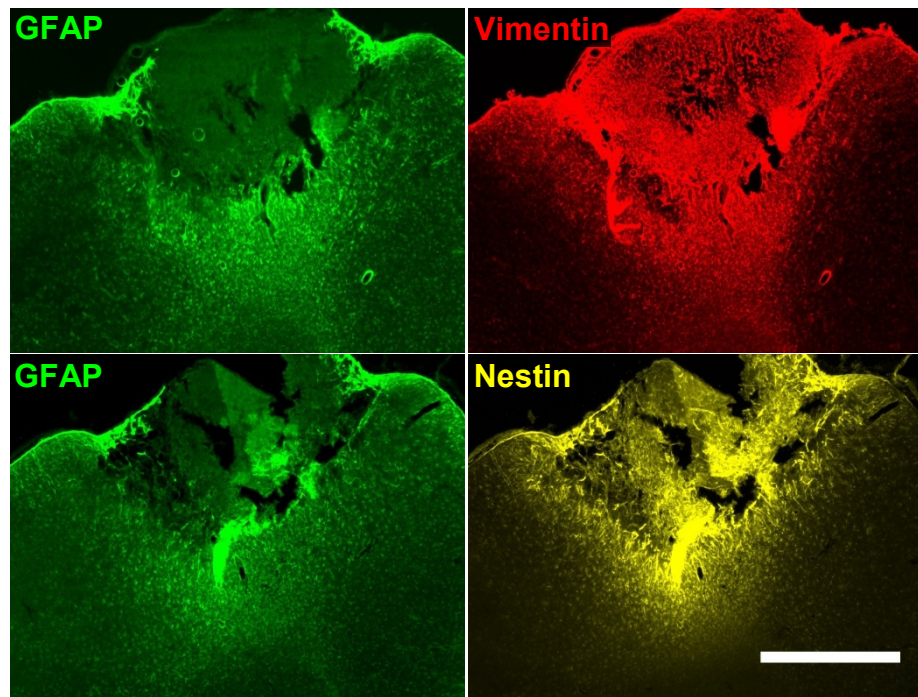


Figure 1.4.1 Expression of cytoskeletal proteins are upregulated in peri-infarct astroglia following stroke.

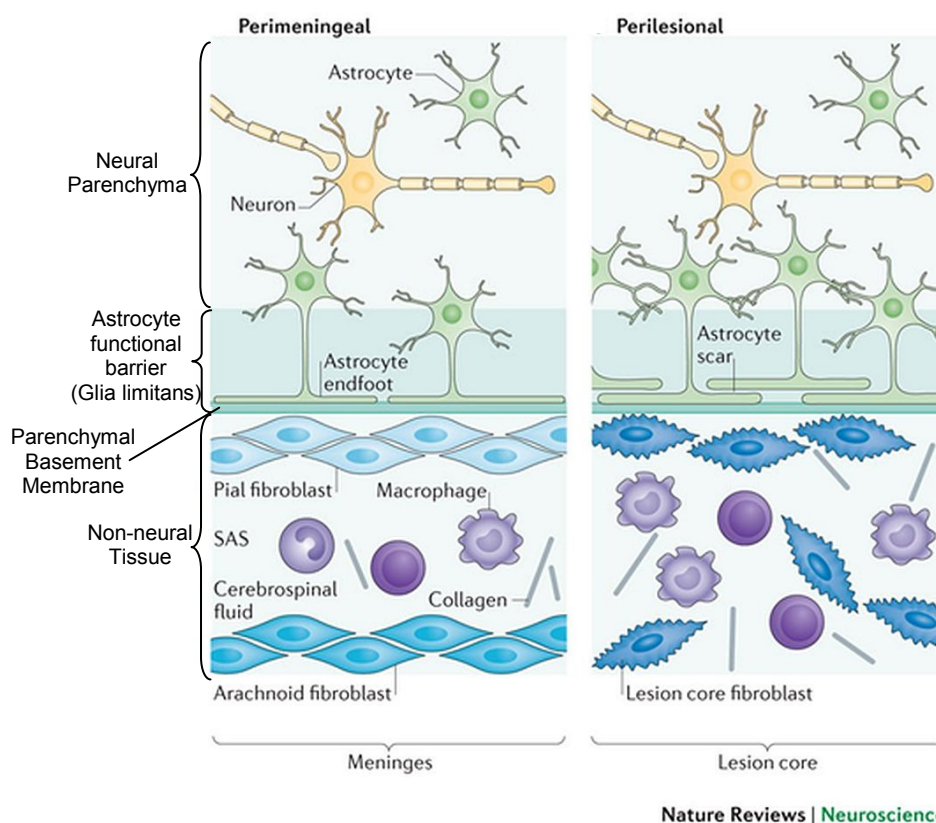
GFAP, vimentin and nestin expression is upregulated in reactive astroglial cells surrounding an infarct. The images were taken from immunolabelled brain sections of a rat at 7 days after photothrombotic stroke (scale bar = 1 mm).

In contrast to astrogliosis that may take one to two days to develop observable morphological changes, the activation of microglia in response to stroke can be detected within hours following infarction. Microglial activation is characterised by a rapid and dramatic change in morphology where the normally highly ramified cells retract their processes and assume an amoeboid form (Kettenmann et al. 2011; Streit 2000). Activated microglia proliferate and migrate towards the infarct where they are involved in the clearance of dead cells and cellular debris (Napoli & Neumann 2009; Schilling, M et al. 2005; Schroeter et al. 1997).

In addition to these stereotypical glial responses to injury, reactive astroglia and activated microglia also exhibit extensive changes in gene expression that can affect the stroke outcome by influencing neuroplasticity within the surviving tissue.

1.4.1 Astroglial Responses

As mentioned above, the long term effect of reactivity in astroglial cells after stroke is the formation of a glial scar that surrounds the infarcted tissue. It has long been recognised from studies of spinal cord injury that the glial scar is inhibitory to axonal regeneration and is likely to be an important factor in limiting functional recovery after stroke (Fitch & Silver 2008; Silver & Miller 2004; Sofroniew & Vinters 2010; Yiu & He 2006). However, glial scar formation is also thought to serve the beneficial function of isolating the infarct and limiting the spread of injury and invasion of blood-borne inflammatory cells into the healthy tissue (Pekny & Pekna 2014; Sofroniew 2015). It reflects the reparative response of the brain to establish a new *glia limitans* that defines the altered boundary of the CNS after injury (Kawano et al. 2012; Li, Y et al. 2012; Shearer & Fawcett 2001; Sofroniew 2015) (figure 1.4.2).



Nature Reviews | Neuroscience

Figure 1.4.2 Structure of the glia limitans at the meningeal and lesion boundaries.

Astroglia form structural borders (*glia limitans*) along all interfaces between CNS and non-neural tissue, including the meninges and blood vessels. Following an injury, such as stroke, an astroglial scar forms around the lesion boundary that is similar in appearance, organisation and function to the *glia limitans* in the intact CNS and similarly restricts entry of peripheral immune cells into the adjacent CNS parenchyma (Adapted by permission from Macmillan Publishers Ltd: Nature Reviews Neuroscience, Sofroniew 2015, ©2015).

The major inhibitory component of the glial scar are the chondroitin sulfate proteoglycans (CSPGs) that are upregulated in reactive astroglial cells (McKeon, Juryneec & Buck 1999; Sharma, Selzer & Li 2012; Siebert, Conta Steencken & Osterhout 2014; Wiese, Karus & Faissner 2012) and can be detected even during the early stages of scar formation (Asher et al. 2000; Morgenstern, Asher & Fawcett 2002). In particular, upregulation of neurocan can be detected within the peri-infarct tissue within days following stroke in rat models (Deguchi et al. 2005; Shen et al. 2008).

Although inhibitory signalling by CSPGs may be an impediment to axonal regeneration following stroke they play a critical role in axonal guidance during CNS development (Bandtlow & Zimmermann 2000) and are involved in the regulation of synaptic plasticity and maintenance of stable neuronal connections in the adult CNS (Brakebusch et al. 2002; Bukalo, Schachner & Dityatev 2001; Levy, Omar & Koleske 2014). Furthermore, quite apart from merely being an impediment to recovery after stroke, the upregulation of CSPGs within the infarct core and glial scar may serve to prevent the futile re-extension of axons into the infarct where there are few if any surviving neurons (Liu, Z & Chopp 2015; Liu, Z et al. 2014; Liu, Z, Xin & Chopp 2014).

In addition to the production and secretion of CSPGs, other aspects of the astroglial responses to tissue infarction can also influence the stroke outcome long before the maturation of the glial scar. As discussed below, a few studies based on different approaches to manipulate the post-stroke response of astroglial cells have revealed that, in general, suppression of astroglial reactivity appeared to inhibit plasticity and functional recovery.

Of particular note is a series of studies based on genetically modified mice lacking both GFAP and vimentin intermediate filaments (GFAP^{-/-}/Vim^{-/-}). Astroglial reactivity and glial scar formation is suppressed in these mice following focal ischemia and traumatic CNS injuries (Li, L et al. 2008; Pekny et al. 1999; Wilhelmsson et al. 2004). However, using a photothrombotic stroke model in which cortical infarction is induced by light irradiation following injection of a photosensitive dye (Watson et al. 1985), Liu, Z et al. (2014) observed that post-stroke functional recovery was significantly impaired in GFAP^{-/-}/Vim^{-/-} mice compared to their wild-type counterparts. Similar results were observed in a study

using fluorocitrate to inhibit the metabolic activity of astroglial cells in another stroke model in which infarction was induced by temporary occlusion of the middle cerebral artery (MCA) with a nylon filament. Fluorocitrate treatment following stroke was found to impair functional recovery along with decreased expression of markers associated with neuroplasticity (Hayakawa et al. 2010).

Interestingly, some studies using interventions aimed at improving functional outcome, including environmental enrichment (Komitova et al. 2005; Komitova et al. 2006), skilled reaching training (Keiner et al. 2008) and a combination of anti-inflammatory drug treatment with skilled reaching training (Liebigt et al. 2012), have observed improved functional recovery together with increased survival of newly proliferated astroglial cells.

These observations may be explained by other studies that have identified the reactive astroglia as a source of molecules that may facilitate neuroplasticity and promote functional recovery after stroke (Liberto et al. 2004; Liu, Z & Chopp 2015; Zhao, Y & Rempe 2010). These molecules include thrombospondins, clusterin, matrix metalloproteinase (MMP) and various trophic factors such as CNTF, GDNF, BDNF, VEGF and bFGF.

Thrombospondins-1 and 2 are extracellular glycoproteins expressed by astroglial cells that have been found to promote synaptogenesis (Christopherson et al. 2005). By using transgenic mice with homozygous deletion of both thrombospondin-1 and 2 genes, Liauw et al. (2008) demonstrated that a deficiency of these glycoproteins resulted in impaired functional recovery after stroke along with decreased synaptic density and axonal sprouting within the peri-infarct tissue. Similarly, clusterin is another glycoprotein upregulated in reactive astroglia following stroke that has been proposed to play a role in facilitating neuronal remodelling (Charnay et al. 2012; Imhof et al. 2006).

The upregulation of matrix metalloproteinases (MMPs) has long been implicated as a detrimental factor that exacerbated the injury in acute stroke, but there is now evidence to suggest that MMPs may have an opposing beneficial function in facilitating neuroplasticity in the post-acute phase of stroke (Morancho et al. 2010; Phillips et al. 2014; Rosell & Lo 2008; Sood et al. 2008). In support of this, Zhao, BQ et al. (2006) observed that delayed treatment at seven days post-stroke with MMP inhibitors suppressed neurovascular remodelling and resulted in impaired

functional recovery. The authors attributed the results, in part, to the expression of MMP-9 in peri-infarct astroglial cells that may be involved in the processing of pro- and matrix-bound VEGF into active molecules.

Astroglial cells are also a rich source of trophic factors, many of which have been found to be upregulated following stroke and are likely to be important regulators of neuroplasticity. BDNF is a neurotrophic factor that is usually expressed by neurons and is involved in learning and memory formation in the normal adult brain (Binder & Scharfman 2004). It has also been found to be strongly upregulated in astroglial cells within the peri-infarct tissue during the post-acute phase following ischemic stroke (Bejot et al. 2011). Although various studies have found that manipulation of BDNF levels after stroke can influence neuroplastic changes and functional recovery, it has only more recently been demonstrated that endogenous production of BDNF by neural cells, including astroglia, is involved in the facilitation of spontaneous post-stroke neuroplasticity (Madinier et al. 2013).

Similar to BDNF, GDNF is also a neurotrophic factor that has been found to be upregulated in the peri-infarct tissue following stroke. Studies using animal models of stroke have observed that GDNF is expressed in neurons early following ischemia but becomes strongly localised to astroglial cells during the post-acute stages (Kuric, Wieloch & Ruscher 2013; Wei, Wu & Cao 2000). More significantly, the timing of the upregulation of astroglial GDNF appeared to coincide with the period of maximum spontaneous functional recovery following photothrombotic stroke in rats (Horinouchi et al. 2007). This coincidence of timing suggests that astroglial production of GDNF may play an important role in the recovery of function after stroke.

Unlike BDNF and GDNF, CNTF expression appears to be highly specific to reactive astroglial cells in the CNS. Studies have found that CNTF appear to be expressed at low or undetectable levels in control animals but becomes rapidly induced in astroglial cells following focal ischemia (Kang et al. 2012; Lin et al. 1998). In the studies, CNTF immunolabelling and mRNA expression was observed to be the most intense within the peri-infarct tissue and both protein and mRNA expression continued to increase over the first two weeks following stroke. A possible involvement of CNTF in the facilitation of neuronal plasticity has been suggested from studies using traumatic injury models where astroglial expression of CNTF has

been found to be correlated with axonal sprouting following injury (Askvig, Leiphon & Watt 2012; Guthrie et al. 1997).

VEGF and bFGF are trophic factors involved in angiogenesis and are thought to promote neovascularisation in ischemic tissue (Greenberg & Jin 2013; Hermann & Zechariah 2009). Both VEGF and bFGF have been found to be upregulated in peri-infarct astroglial cells after stroke in animal models (Chen, HH, Chien & Liu 1994; Cobbs et al. 1998) as well as in humans (Issa et al. 2005; Margaritescu, Pirici & Margaritescu 2011). However, although treatment using both trophic factors appeared to improve functional recovery following stroke, the neuroplastic changes accompanying recovery were observed to occur predominantly in the intact contralesional hemisphere (Kawamata et al. 1997; Reitmeir et al. 2012). These results suggest that peri-infarct astroglia-derived VEGF and bFGF may play only a limited role, if any, in functional recovery after stroke.

Although the studies cited earlier involving the direct inhibition of astroglial reactivity either by genetic (Liu, Z, Xin & Chopp 2014) or pharmacological manipulation (Hayakawa et al. 2010) provided evidence for an overall beneficial role of astrogliosis, there have also been other studies that appear to suggest the opposite. These studies reported a reduced or suppressed astroglial response following treatments that resulted in improved stroke outcomes (Brunkhorst et al. 2013; Lopez-Valdes et al. 2014; Schabitz et al. 2004). These contrasting studies serve to highlight the fact that the astroglial response to injury may either inhibit or promote neuroplasticity and that the balance of this response is likely to shift over time following stroke and vary depending on brain region and proximity to the infarct.

Heterogeneity of the astroglial response can also further contribute to the complexity of their influence on neuroplasticity. In two separate studies, investigators found that CSPG expression in the brain of adult mice was associated with only a subpopulation of astroglial cells (Hayashi et al. 2007; Liu, Z et al. 2014). Furthermore, Liu, Z et al. (2014) found using GFAP^{-/-}/Vim^{-/-} mice that the attenuated astroglial response to focal ischemic injury due to the lack of the two intermediate filaments differentially modulated CSPG expression depending on the brain region and distance from the infarct. In fact, evidence for the presence of different reactive astroglial phenotypes can be found in earlier studies that observed that reactive astroglia are not always inhibitory to axonal growth and that there are regional differences in the astroglial

response to injury (Bovolenta, Wandosell & Nieto-Sampedro 1991; Ridet et al. 1997). Zamanian et al. (2012) further demonstrated that even astroglial cells located in close proximity to each other can exhibit differential expression of reactive genes in mouse models of stroke and neuroinflammation.

There is much that is unknown at present about the diversity of the reactive astroglial phenotypes and how they may evolve over time following injury. An improved understanding will greatly benefit future efforts to develop treatments to enhance functional recovery after stroke.

1.4.2 Microglial Responses

In the normal adult brain, the microglia exhibit a highly ramified form and have in the past been frequently described as “resting” or “quiescent”. These terms are misleading as studies have more recently shown that the ramified microglia exhibit highly motile processes that are constantly surveying the microenvironment (Davalos et al. 2005; Nimmerjahn, Kirchhoff & Helmchen 2005; Wake et al. 2009). These studies have also shown that even while in their ramified form the microglia may respond to local injury almost instantly by extending their processes toward the injured site to shield it from the healthy tissue.

Following more extensive injuries such as those caused by stroke, signals released by dying and injured cells within the ischemic core trigger a marked morphological transformation in the microglial cells. Microglia activated by the signals, also known as danger-associated molecular patterns (DAMPs) (Famakin 2014; Kigerl et al. 2014; Savage et al. 2012), retract their processes and transform into amoeboid forms resembling peripheral macrophages (figure 1.4.3). Within the peri-infarct tissue, microglial activation can be detected within a few hours following infarction (Ito et al. 2001; Rupalla et al. 1998).

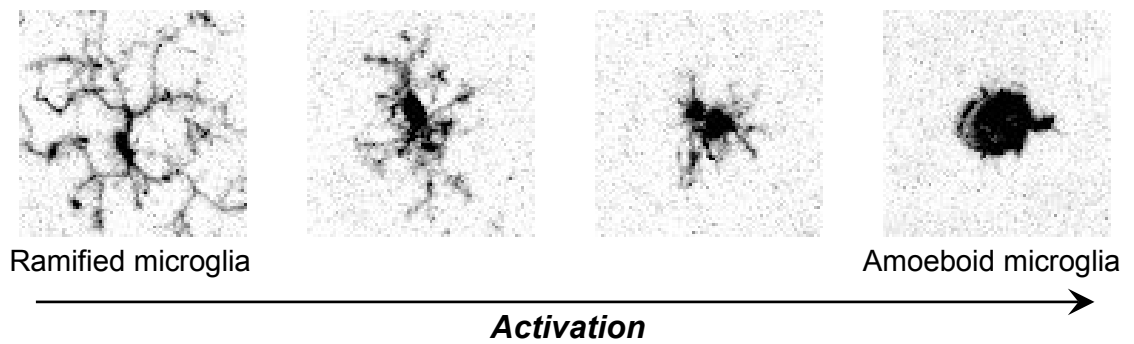


Figure 1.4.3 Morphological transformation of microglia during activation.

The unactivated microglia exhibits a ramified morphology with several long, thin and highly branched processes extending from its cell soma. Following activation, the microglia retracts its processes and assumes an amoeboid form. Hypertrophy of the cell soma can also be observed over the course of activation. Representative images ($60 \times 60 \mu\text{m}$) of microglia at various stages of activation in rat brain sections immunolabelled for Iba1 following photothrombotic stroke are shown.

Along with the striking morphological transformation, microglial activation also results in the upregulation of expression of a host of molecules including chemokines, cytokines, proteases, ROS, prostanoids, NO and various trophic factors (Iadecola & Anrather 2011; Kriz 2006; Stoll, Jander & Schroeter 1998, 2002; Taylor & Sansing 2013; Tuttolomondo et al. 2008). Many of these molecules are potentially neurotoxic or may mediate an inflammatory cascade that exacerbates the injury in stroke and other neurological disorders (Amor et al. 2010; Kim, JY, Kim & Yenari 2015). Indeed, various studies based on the pharmacological inhibition of microglial activation have observed beneficial effects in acute stroke (Hailer 2008; Yrjanheikki et al. 1999).

These observations would appear to suggest a detrimental role for microglial activation in acute stroke. However, a few studies based on direct manipulation of the microglial population have obtained results that suggested the contrary. These studies have observed that the depletion of brain resident microglia led to exacerbated injuries whereas the transplantation of exogenous microglial cells provided neuroprotection following stroke in animal models (Kitamura et al. 2004; Kitamura et al. 2005; Lalancette-Hebert et al. 2007; Szalay et al. 2016) and oxygen-glucose deprivation (OGD) in organotypic hippocampal slice cultures (Montero, Gonzalez & Zimmer 2009; Neumann et al. 2006). In particular, the study by Szalay

and co-workers (2016) provided a striking demonstration of the neuroprotective potential of microglial cells in stroke. In the study, microglia was depleted in mice by treatment with a colony-stimulating factor 1 receptor (CSF1R) kinase inhibitor. Microglia-depleted mice exhibited a 60 % increase in infarct size compared to control animals with normal microglial population 24 hours after MCA occlusion. When stroke was induced after microglia was allowed to repopulate the brains of microglia-depleted mice, following withdrawal of the CSF1R kinase inhibitor treatment, the infarct sizes were similar to control animals.

A mechanism that may underlie the neuroprotective potential of microglia was proposed in a study by Neumann et al. (2008). In their study, Neumann and co-workers observed that externally applied polymorphonuclear neutrophils (PMNs) resulted in marked increases in neuronal death in organotypic hippocampal slice cultures that were subjected to oxygen-glucose depletion. However, this increased neurotoxicity was counteracted by additional application of primary microglia that were grown in culture. Furthermore, using time-lapse microscopy, the investigators also observed that microglia were capable of phagocytosis of active PMNs. Based on these results and observations from an earlier study (Neumann et al. 2006), the authors suggested that activated microglia may provide neuroprotection through the direct engulfment of invading peripheral immune cells that can exacerbate injury by releasing neurotoxic molecules. Overall, although the inhibition of microglial activation appears to be a promising approach for the treatment of acute stroke, the contrasting outcomes in some studies suggest that there are aspects of the early microglial response that are beneficial.

1.4.2.1 Microglial Influence on Post-Stroke Functional Recovery

Although there is a large body of literature regarding microglial activation and its effects in stroke, most of the research has focussed on the acute microglial responses and the influence of these cells on the development of injury. However, a small but increasing number of studies are finding evidence for the involvement of microglial cells in promoting functional recovery following stroke and other injuries of the CNS (Aldskogius 2001; Kriz & Lalancette-Hebert 2009; Lloyd-Burton et al. 2013; Peruzzotti-Jametti et al. 2014).

An early study that suggested a potential role for microglia in post-stroke functional recovery observed that thymosin β_4 ($t\beta_4$), a trophic factor that is thought to promote neurite outgrowth, is highly expressed in macrophages and microglia within the infarct and peri-infarct tissue at 7 days after stroke (Vartiainen et al. 1996). The beneficial effects of $t\beta_4$ were demonstrated in a more recent study where treatment using $t\beta_4$ starting at 24 hours after stroke improved functional recovery without affecting the infarct size in an embolic stroke model in which infarction was induced by the injection of a blood clot at the origin of the MCA (Morris et al. 2010). Evidence from the study also suggested that $t\beta_4$ facilitated functional recovery by promoting angiogenesis and the re-myelination of axons.

Although most studies have only investigated the involvement of neuron or astroglia-derived neurotrophic factors in facilitating functional recovery, there is some evidence that activated microglia may also produce neurotrophic factors such as BDNF and GDNF following CNS injury. Batchelor et al. (2002) observed that sprouting neurites in the peri-lesional tissue were closely associated with activated microglial cells following traumatic injury to the striatum in a mouse model. Using *in situ* hybridisation for BDNF and GDNF, the authors determined that the regenerating axons were sprouting along a BDNF/GDNF trophic gradient that was generated by the expression of the neurotrophic factors in activated microglia and macrophages. Another group of researchers found that the inhibition of acute microglial activation led to a chronic decrease in the expression of proteins associated with neuronal plasticity in a photothrombotic stroke model (Madinier et al. 2009). The decreased neuroplasticity was associated with a significant decrease in tissue BDNF levels that was attributed to the suppression of microglial BDNF production.

Interestingly, some studies have also found evidence suggesting that IL-6 and TNF- α , cytokines produced by activated microglia that are associated with deleterious effects in acute stroke (Hallenbeck 2002; Planas, Gorina & Chamorro 2006; Tuttolomondo et al. 2008; Tuttolomondo, Pecoraro & Pinto 2014), may actually facilitate recovery in the later stages of stroke (Lippoldt, Moenning & Reichel 2005).

IL-6 expression is upregulated in peri-infarct microglia and neurons following stroke (Suzuki et al. 1999) and is thought to mediate inflammatory responses that exacerbates the extent of injury. However, there is increasing evidence suggesting

that IL-6 may also play an important role in facilitating neurotrophic and tissue remodelling processes (Suzuki, Tanaka & Suzuki 2009). In particular, Gertz et al. (2012) showed that IL-6 knockout mice exhibited significantly worse functional outcome than wild type controls at 4 weeks after stroke. Similar results were observed in another study using IL-6 knockout mice in a traumatic brain injury model (Swartz et al. 2001). In both studies, the impairment in functional recovery was associated with an impaired angiogenic response in the IL-6 knockout animals. In addition, Swartz et al. (2001) also observed that mice genetically altered to over-express IL-6 exhibited enhanced re-vascularisation and repair of the injured tissue.

Much like IL-6, TNF- α expression has also been found to be upregulated in peri-infarct microglial cells following stroke (Gregersen, Lambertsen & Finsen 2000; Lambertsen et al. 2005) and associated with neurotoxic effects following stroke in many studies (Lambertsen, Biber & Finsen 2012). However, results from other studies have suggested a potential role for TNF- α in facilitating recovery following CNS injury. Oshima et al. (2009) observed that TNF- α knockout mice exhibited impaired functional recovery compared to wild type mice following traumatic brain injury. An earlier work by Arnett et al. (2001) suggested that TNF- α may be involved in neurorestorative processes following CNS injuries through promoting the proliferation of oligodendroglial cells and re-myelination of axons. Interestingly, there is also evidence that suggests TNF- α may promote survival and proliferation of neural progenitor cells following stroke (Bernardino et al. 2008; Heldmann et al. 2005).

Microglia within the infarct and peri-infarct tissue have also been observed to rapidly upregulate TGF- β following stroke (Doyle et al. 2010; Lehrmann et al. 1998; Pal et al. 2012; Yamashita, K et al. 1999). Although the expression of this cytokine in peri-infarct microglia has been found to persist for up to a month or longer after stroke, most of the existing studies have only focussed on its neuroprotective effects during the acute phase. The timing and duration as well as the region of expression of this protein following stroke suggests a potentially significant influence on functional recovery. Indeed, studies based on other disease models have found that TGF- β has anti-inflammatory effects and can promote angiogenesis and synaptogenesis (Dobolyi et al. 2012) suggesting a beneficial influence of peri-infarct microglial TGF- β on post-stroke recovery (Amantea, Diana et al. 2015; Yamashita, K et al. 1999).

Much of our current understanding of the influence of microglial responses on post-stroke functional recovery is confounded by the rapid and early activation of microglia following stroke and a heterogeneity of activated phenotypes that continue to evolve over a prolonged duration. In particular, as discussed previously, expression of molecules such as the cytokines IL-6, TNF- α and TGF- β are all induced in microglia in the early post-stroke phase where they may influence neuronal survival, but all three cytokines can also be detected in microglia during the later stages where they may also influence the regenerative processes.

1.4.2.2 Classical and Alternative Activation of Microglia in Stroke

In recent years there has been an increasing use of the terminology of M1 and M2, otherwise known as “classical” and “alternative” activation to describe different microglial phenotypes that may be induced in stroke and other neurological disorders (Cherry, Olschowka & O'Banion 2014). This is a concept that has been borrowed from studies of peripheral macrophages where M1 refers to a pro-inflammatory neurotoxic phenotype and M2 refers to an anti-inflammatory pro-regenerative phenotype (Boche, Perry & Nicoll 2013; Dey, Allen & Hankey-Giblin 2015; Mantovani et al. 2013). Despite the trend, there is at present very little that is known regarding the microglial expression of M1/M2 markers following stroke and their actual influence on the regenerative processes underlying functional recovery.

However, some studies have started to address this deficiency by examining the expression of various putative M1/M2 markers after stroke. Perego, Fumagalli and De Simoni (2011) investigated the spatiotemporal expression of a few specific M1/M2 markers, including CD68, Ym1 and CD206 by immunohistochemical labelling, in a permanent MCA occlusion model of stroke in mice. However, the study focussed primarily on the changes occurring within the infarcted tissue and furthermore did not include time points between 48 hours and 7 days. The gap in the time points investigated is particularly salient as another study has observed that the expression of many of the M1/M2 markers may peak during this time period (Hu et al. 2012).

In that study, Hu et al. (2012) quantified the changes in the expression of multiple M1/M2 markers over several time points up to 14 days after stroke induced by

temporary MCA occlusion in mice. However, the authors performed the bulk of their investigations using real-time polymerase chain reaction (RT-PCR) with whole brain samples that does not distinguish between changes occurring within and outside of the infarct core. Although the data from RT-PCR was complemented with immunohistochemical labelling for CD16/32 and CD206, the authors only looked at changes in expression of these markers within the infarct core using this approach. Nonetheless, the results from the study revealed that, within the infarct core, the expression of all of the M2 markers that were investigated peaked at 3 to 5 days whereas expression of most of the M1 markers continued to increase beyond 7 days after stroke.

Very few studies have investigated the changes in M1/M2 expression in microglia within the peri-infarct tissue where they are more likely to influence the processes involved in functional recovery. Where studies have looked at changes in this tissue region, they have generally only focussed on specific markers at limited time points. For example, Verma et al. (2014) investigated microglial/macrophage responses within the peri-infarct tissue in a mouse stroke model, but only looked at the changes in a single M2 marker, Arginase-1 (Arg-1), and only at 6 weeks post-stroke. Similarly, Brifault et al. (2015) also investigated the changes in microglial expression of Arg-1 at a single time point (7 days).

Of particular note however, is a study by Zarruk et al. (2012) that investigated the effect of treatment using a cannabinoid type 2 receptor (CB2R) agonist on the expression of a large number of M1/M2 markers within the peri-infarct tissue following permanent MCA occlusion in mice. The authors reported increases in the mRNA and protein expression of all of the measured M1 and M2 markers within the peri-infarct tissue at 15 and 24 hours post-stroke. Treatment with the CB2R agonist resulted in a reduction of the infarct volume and improved functional outcome at 48 hours. Interestingly, the improved outcome was associated with a general decrease in the expression of both the M1 and M2 markers within the peri-infarct tissue at 15 and 24 hours post-stroke. However, because the improved outcome was accompanied by a reduction in the infarct volume and furthermore the study only looked at the changes occurring within the first 24 hours, the data from the study provided little information on the relationship between the expression of the M1/M2 markers and the neuro-regenerative processes underlying long-term functional recovery. Similarly, Xu, Y et al. (2012) also reported stroke-induced increases in the

expression of M1 and M2 markers within the peri-infarct tissue but only investigated these changes at 24 hours post-stroke.

Of greater relevance is a study by Jin et al. (2014) where the authors investigated the effects of delayed metformin treatment following temporary MCA occlusion in mice. Although only a limited number of markers were examined, specifically CD16/32 (M1) and CD206 (M2), within the peri-infarct tissue, the changes in expression of these markers were quantified at time points (3 and 14 days post-stroke) that are more relevant to neuroregenerative processes. Their results revealed that the experimental stroke induced upregulation in the expression of both CD16/32 and CD206 within the peri-infarct tissue in immunohistochemically labelled brain sections. Metformin treatment at 24 hours improved functional recovery at up to 28 days after stroke and was associated with decreased expression of CD16/32 and increased expression of CD206 at 3 and 14 days. Crucially, the delayed treatment with metformin did not lead to changes in the infarct volume that can complicate interpretation of the results.

Most of the M1/M2 markers that have been used in stroke studies have come from the study of peripheral macrophages and very few have been well characterised for microglia in the context of CNS disorders. At present, the evidence is limited or in some cases ambiguous for an association with either an inhibitory or pro-regenerative phenotype for most of the M1/M2 markers that have been used in stroke studies. For example, IL-6 and TNF- α are markers that are commonly regarded to be indicative of the M1 or pro-inflammatory phenotype but, as discussed previously, there is evidence to suggest that they may also be involved in facilitating functional recovery after stroke. It is likely that other markers may also reflect similarly complex and evolving functions of microglia during the different stages following stroke.

It has been recognised for some time now that the concept of M1/M2 polarisation is an oversimplification and that there is a continuum of phenotypes reflecting the diverse roles and functions of microglia and macrophages (Gertig & Hanisch 2014; Hanisch 2013; Hu et al. 2015; Mosser & Edwards 2008). It is also apparent that the markers by themselves are insufficient to define the role of microglia without an understanding of the context in which they are expressed, whether it is during the acute or post-acute stages of disease, and its location within the brain and in relation

to the infarcted tissue (Gertig & Hanisch 2014; Hu et al. 2015; Kriz 2006; Stoll, Jander & Schroeter 2002). Further studies designed with these distinctions in mind are clearly necessary to identify and properly characterise potentially useful markers for the investigation of microglial responses in stroke.

1.4.2.3 Infiltrating Immune Cells vs. Brain Resident Microglia

Although it is now known that the brain resident microglia are derived during development from cell populations that are distinct from those giving rise to the blood monocytes and other peripheral immune cells, it remains a matter of debate if the peripheral cell population may contribute to the microglial pool in the normal adult brain (Chan, Kohsaka & Rezaie 2007; Dey, Allen & Hankey-Giblin 2015). However, it is clear that the two populations express many common cellular markers that make it difficult to distinguish between them in immunohistochemical investigations. For example, essentially all of the commonly used microglial markers such as Ionised-calcium binding adapter molecule 1 (Iba1), CD11b, CD68 and Isolectin B4 also label peripheral immune cells such as macrophages and neutrophils (Guillemin & Brew 2004; Matsumoto et al. 2007; Patel et al. 2013).

Under normal conditions, this does not present a problem as microglia are separated from the peripheral immune cell population by the blood brain barrier within the intact brain. However, in neuropathological conditions resulting in the breakdown of the blood brain barrier such as stroke and traumatic brain injury, immune cells are rapidly recruited from the blood circulation to the site of injury and may invade into the peri-lesional tissue. Furthermore, microglia activated by the insult adopt amoeboid forms that are morphologically identical to the infiltrating peripheral macrophages. Consequently, it is difficult, if not impossible, to distinguish between the infiltrating cells and the resident microglia and their respective involvement in the development of such conditions.

Various attempts have been made to address this problem using different approaches, highlighted by studies using bone marrow chimeras and parabiotic animals. However, there were two studies that were notable early attempts that utilised only immunohistochemical approaches to clarify the nature of the peripheral immune cell infiltration in permanent MCA occlusion (Schroeter et al. 1994) and photothrombotic

stroke (Jander et al. 1995). In the two studies, the invading immune cells were identified immunohistochemically by using a host of antibodies directed against markers specific for different subsets of the peripheral immune cells. Although there were some differences in the timing and pattern of infiltration by macrophages in the two different models, it was observed in both models that the macrophages were mostly localised to the infarct core and boundary region of the peri-infarct tissue even at peak response. Although the investigators did not look specifically at the local microglial response, their observation that few peripheral macrophages invaded into the peri-infarct tissue suggested that the microglia would be the predominant immune cell type within that region.

Later studies conducted using green fluorescent protein transgenic bone marrow chimeric mice provided greater clarity on the relative contributions of the peripheral immune cells and microglial cells to the immune response around the infarct after stroke (Schilling, M et al. 2003; Schilling, M et al. 2005; Tanaka, R et al. 2003). In these studies bone marrow from green fluorescent protein (GFP) transgenic mice was transplanted into wild-type mice that had been exposed to sub-lethal irradiation. These mice exhibit bone marrow chimerism in which their bone marrow derived cells, including the peripheral macrophages, express GFP whereas the brain resident microglial cells do not.

Using the bone marrow chimeric mice in a temporary MCA occlusion model of stroke, Schilling, M et al. (2003) observed that, within the infarct, microglial cells greatly outnumbered the infiltrating macrophages across all the time points investigated. In the study, the peripheral macrophages and microglia were identified in brain sections by immunolabelling with an anti-F4/80 antibody that targeted a receptor protein expressed by both cell populations. Infarcted tissue was visualised by the loss of NeuN immunolabelling. The investigators reported that infiltrating macrophages, identified by both F4/80 and GFP expression, were first detected in significant numbers within the infarct only at 4 days after stroke. Their numbers peaked at 7 days and declined thereafter. However, microglial cells that were F4/80-positive and GFP-negative were always present in far greater numbers than the infiltrating macrophages. Although the relative cell numbers within the peri-infarct tissue were not quantified in the study, very few GFP-positive cells can be seen outside of the infarcted regions in the 7 day images provided in the paper.

Similarly using bone marrow chimeric mice, Tanaka, R et al. (2003) investigated the infiltration of peripheral macrophages into the stroke infarct following permanent MCA occlusion. In this study, the peripheral macrophages and microglia were identified by immunolabelling for Iba1 and the infarct was visualised by loss of immunolabelling for microtubule associated protein-2, a neuron specific marker. In contrast to the study by Schilling, M et al. (2003), the authors reported that infiltrating macrophages can be detected within the infarct by 24 hours and continued to increase in numbers up to 14 days after stroke, by which time they vastly outnumbered the microglia cells. Furthermore, it was also observed that the macrophages can similarly be detected within the peri-infarct tissue by 24 hours and reached numbers comparable to the resident microglial cells by 7 day after stroke.

The disparity in the results between the two studies using bone marrow chimeras described above was discussed in a later study by Schilling, M et al. (2005). In their study, Schilling and co-workers utilised an Iba1 antibody identical to that used by Tanaka, R et al. (2003) and confirmed the results of their earlier study using an F4/80 antibody (Schilling, M et al. 2003) that identified microglia as the predominant immune cell type within the infarct and peri-infarct regions after stroke. The authors suggested that the duration of occlusion used in stroke induction in MCA occlusion models may have a major influence on the kinetics of the responses of the different immune cell populations. Therefore, the use of different MCA occlusion models (*i.e.* temporary *vs.* permanent occlusion) may have resulted in the differences observed between the two earlier studies.

A later study by Li, T et al. (2013) provided evidence that following photothrombotic stroke, similar to the observations from studies using temporary MCA occlusion, microglial cells are the predominant immune cell type recruited to the infarct. In the study, the blood circulation of GFP transgenic mice were joined surgically via anastomoses to wild-type mice to generate parabiotic pairs exhibiting GFP chimerism in their circulating blood cells. The investigators reported that by 13 to 14 days following parabiotic surgery, at which time the animals were used in the stroke experiments, nearly half of all monocytes within the blood circulation of the wild-type mice were GFP-positive. It was observed that the immune cell population recruited to the infarct, as identified by Iba1 immunolabelling, increased over the first 7 days following photothrombotic stroke. Over the same time period, in the wild-type mice, infiltrating cells that can be distinguished by GFP expression

increased in numbers up to day 5 and declined on days 6 and 7. Most importantly, the investigators reported that at the infarct boundary, microglial cells outnumbered the infiltrating immune cells by 30 fold even at peak infiltration. Similar results were observed regardless of whether only the wild-type or both animals in each parabiotic pair were subjected to stroke.

In recent years, investigations using mouse transcriptome datasets have identified a microglia-specific transmembrane protein, TMEM119, that may potentially be used to differentiate microglial cells from peripheral immune cells (Butovsky et al. 2014; Satoh et al. 2016). Based on these studies, Bennett, ML et al. (2016) have developed antibodies against TMEM119 that were demonstrated to be highly specific to microglia in human and mouse brain tissue. Although further validation of these reports will be required, microglial markers based on TMEM119 will provide a powerful approach in future investigations to clarify the roles of microglia and infiltrating immune cells in the development of and recovery after stroke.

To date, the lack of a unique identifying marker for microglia has been an obstacle in investigations of the relative contributions of the peripheral immune cells and microglia to the immune responses following stroke. Nonetheless, the sum of evidence from the different studies suggest that, in most cases, locally recruited microglia are the major source of immune cell activity within the brain following stroke. This is especially true in the case of the peri-infarct regions where microglial cell numbers predominate over the infiltrating immune cells across all the time points investigated in the studies utilising either the temporary MCA occlusion or photothrombotic stroke models. As a result of these observations, all the cells that were identified by the Iba1 marker in the investigations described in the subsequent chapters of this thesis will be collectively referred to as microglia or microglial cells.

1.5 Modulating Glial Cell Responses to Promote Functional Recovery

Although spontaneous recovery of function occurs in almost all cases following stroke, the extent of recovery is usually limited (Cramer 2008a; Di Giovanni 2009). As discussed in the preceding sections, glial cells play important roles in supporting the processes underlying spontaneous recovery following stroke and present potential therapeutic targets for enhancing the functional outcome in stroke. This potential has been investigated in various studies that have utilised interventions aimed at manipulating the post-stroke astroglial and microglial responses. In addition, there is increasing evidence that the beneficial effects observed in other interventions such as stem cell transplantation may also be mediated, at least in part, through the modulation of glial cell responses.

1.5.1 Anti-inflammatory agents

Activation of the brain resident immune cells, the microglia, is generally viewed to have detrimental consequences on the stroke outcome (Biber, Owens & Boddeke 2014; Hailer 2008; Hellwig, Heinrich & Biber 2013). As a result, there have been many studies investigating the use of anti-inflammatory and immunosuppressive agents such as minocycline, rapamycin, cyclosporine A and FK506 to suppress microglial activation for the treatment of stroke (Hailer 2008; Liguz-Lecznar & Kossut 2013). However, the major focus of these studies has been on the neuroprotective potential of these drugs in acute stroke. Although it has been suggested that prolonged microglial activation may inhibit functional recovery (Kriz & Lalancette-Hebert 2009; Liguz-Lecznar & Kossut 2013), there has been far fewer studies that have looked specifically at the effects of anti-inflammatory treatment in the post-acute stages of stroke.

Of the studies that have investigated the use of anti-inflammatory drugs in the treatment of stroke during the post-acute stages, many have used minocycline as it has been widely reported to be an effective inhibitor of microglial activation in various *in vitro* and *in vivo* models (Garrido-Mesa, Zarzuelo & Galvez 2013a, 2013b; Suk 2004; Tikka et al. 2001; Yrjanheikki et al. 1998; Yrjanheikki et al. 1999).

Liu, Z et al. (2007) reported that minocycline treatment started at 4 days and continued daily for 4 weeks following experimental stroke in rats led to enhanced functional recovery without affecting the infarct volume. Along with the improved function, it was also reported that at 4 weeks after stroke there was increased survival of newborn neurons as well as decreased tissue labelling of ED1, a lysosome-associated membrane protein expressed in activated microglia and macrophages indicative of phagocytic activity. The authors concluded that the effect of minocycline treatment on functional recovery was at least in part due to the suppression of microglial activation based on the reduction in ED1-positive cell counts in minocycline treated animals.

Using a similar model, Chu et al. (2010) also reported that treatment with minocycline resulted in functional improvements with associated changes in astroglia and macrophages/microglia. In the study, minocycline treatment reduced glial scar thickness and GFAP expression in peri-infarct astroglial cells at 36 days post-stroke. The authors also detected a decrease in the expression of 5-lipoxygenase, an enzyme involved in the mediation of inflammatory responses, in peri-infarct astroglia and microglia/macrophages within the infarct core. However, minocycline treatment in the study was initiated 2 hours after stroke and early minocycline treatment has been previously shown to be neuroprotective (Hewlett & Corbett 2006; Yrjanheikki et al. 1999). Although the authors reported that the treatment did not result in changes to the infarct volume at 36 days, it would be difficult to detect the effects of neuroprotection by minocycline during early infarct development at such a late stage due to contraction of the lesion.

In a recent paper, Yang, Y et al. (2015) reported that a single intravenous infusion of minocycline administered at reperfusion following temporary MCA occlusion in rats led to enhanced neurovascular remodelling and a shift towards the M2 phenotype in peri-infarct microglia/macrophages at four weeks after stroke. It is unclear if the treatment resulted in improved functional recovery due to the lack of functional assessments in the study design. Furthermore, similar to other studies, the infarct volume was reduced by the early minocycline treatment. Regardless, the authors claimed that their results provided evidence that minocycline treatment facilitated neurological recovery by promoting alternative (M2) activation of microglia/macrophages.

Interestingly, in contrast to the above studies, Kim, BJ et al. (2009) reported that minocycline treatment initiated immediately after stroke suppressed microglial/macrophage activation without resulting in any significant effects on functional outcome at 7 days, suggesting both an absence of neuroprotective effects as well as a lack of effects on the neurorestorative processes. However, as the authors have alluded to in their discussions, 7 days may be too short a duration to fully assess the functional effects of the treatment.

Although overall there is strong evidence that minocycline treatment can improve the functional outcome in stroke, the majority of studies so far have focussed on its neuroprotective effect in early intervention. Studies that have asserted that the functional improvements were the results of enhanced neurorestorative processes have generally failed to distinguish these effects from those arising from neuroprotection leading to reduced infarct volumes. Although the results of the study by Liu, Z et al. (2007) do provide evidence that minocycline treatment may enhance recovery following stroke through the modification of glial responses, the data is limited to a single marker, ED1, that by itself is not indicative of a pro-restorative or inhibitory state in microglia. Despite the limited evidence, the observation of an effect of minocycline in modulating the post-stroke microglial response appear to be in agreement with the results in a mouse model of motor neuron disease where minocycline treatment inhibited the expression of M1 markers in activated microglia (Kobayashi et al. 2013). Further studies are clearly necessary to clarify the role of glial cells in mediating the non-neuroprotective effects of minocycline in the treatment of stroke.

1.5.2 Anti-proliferative agents

Ischemic stroke triggers the upregulation of cell cycle related proteins that are associated with apoptosis in post-mitotic cells and have been suggested to contribute to secondary neuronal loss and infarct expansion (O'Hare, Wang & Park 2002; Osuga et al. 2000; Yang, Y & Herrup 2007). Within the peri-infarct tissue, upregulation of these proteins also triggers the proliferation of astroglial and microglial cells that are thought to contribute to the formation of the glial scar and the release of inflammatory mediators from glial cells that can inhibit post-stroke recovery (Byrnes & Faden 2007; Wanner et al. 2013).

Studies using models of traumatic brain and spinal cord injuries have suggested that treatment using cell cycle inhibitors can inhibit microglial activation and glial scar formation, and thereby promote recovery (Cernak et al. 2005; Di Giovanni et al. 2005; Tian et al. 2006). However, there has been few studies examining the effects of such treatments using stroke models.

Of the limited number of studies that have investigated the use of anti-proliferative drugs in the treatment of stroke, most have only looked at the effects of treatment in acute stroke and very few have assessed the effects on functional outcomes. For example, both Zhu et al. (2007) and Wang, W et al. (2008) investigated the effects of treatment using olomoucine, a cyclin-dependent kinase inhibitor, in stroke models in rats. In both studies, the olomoucine treatment was administered at 1 hour and 24 hours after reperfusion following temporary MCA occlusion. Both studies reported a reduction in cellular proliferation and astrogliosis within the peri-infarct tissue, as measured by proliferating cell nuclear antigen and GFAP expression, at 7 and 30 days after stroke. However, Zhu and co-workers did not report the effect of the treatment on infarct volume and, while Wang and co-workers reported a no changes in infarct volume, they also detected a significant decrease in apoptosis within the peri-infarct tissue. Crucially however, neither study have reported functional measures as part of their assessments. Thus, it is unclear whether the decreased proliferation and astroglial response led to improved functional recovery.

Similarly, Zhang, Q et al. (2009) investigated the effects of treatment using roscovitine, a different cyclin-dependent kinase inhibitor, in an identical stroke model. The investigators reported that the treatment resulted in decreased microglial proliferation within the peri-infarct tissue as well as reduced expression of pro-inflammatory markers IL-1 β , MIP-1 α and iNOS, along with improved neurobehavioural function at 1, 3 and 7 days after stroke. However, the roscovitine treatment was initiated at 24 hours before stroke induction and the infarct volume was reduced by more than half in the treated animals. The neuroprotective effect of pre-treatment using roscovitine, as evidenced by the marked reduction in infarct volume, renders it extremely difficult if not impossible to determine if the drug had any effect on the neurorestorative processes involved in functional recovery.

Overall, investigations into the effects of treatment using anti-proliferative agents have so far not yielded any clear evidence for a beneficial effect in promoting functional recovery following stroke due to a lack of properly designed studies.

1.5.3 Stem Cell Transplantation

The early studies of stem cell transplantation therapies were conducted to investigate their potential in improving stroke outcome by replacing some of the neurons that were lost to infarction. However, it was quickly apparent that very few of the transplanted cells survive for long durations and there was little evidence to show that the surviving cells differentiated into neurons that functionally integrated into the existing neuronal network (Bjorklund & Lindvall 2000; Ramos-Cabrer et al. 2010; Roitberg 2004).

Regardless, an increasing number of studies investigating stem cell transplantation have reported long-term functional improvements that persist for up to one year in rodent stroke models and even when transplantation is performed up to one month after stroke (Li, Y et al. 2005; Shen, Li, Chen, Cui, et al. 2007; Shen, Li, Chen, Zacharek, et al. 2007; Zhang, L et al. 2011). The evidence from these studies suggest that the transplanted cells may improve functional recovery not via direct neuronal replacement, but rather through promoting endogenous neurogenesis and neuroplasticity (Liu, Z et al. 2010; Ramos-Cabrer et al. 2010).

Investigations over the past decade, most notably the studies using bone marrow stromal cells (BMSC) by Chopp and co-workers, have contributed greatly to our current understanding of how transplanted stem cells may facilitate the neurorestorative processes underlying post-stroke functional recovery (Chen, J et al. 2014; Chopp, Li & Zhang 2009). The results of these investigations have revealed that neurorestorative effects of stem cell transplantation are mediated, at least in part, through the modulation of the post-stroke glial cell responses (Chopp, Li & Zhang 2009; Goldmacher et al. 2013). Some of the changes in protein expression in glial cells that have been identified include the upregulation of trophic factors such as angiopoetin-1, bone morphogenetic proteins 2 and 4, VEGF and GDNF (Shen, Li & Chopp 2010; Zacharek et al. 2007; Zhang, C et al. 2006), and gap junction protein connexin-43 (Zhang, C et al. 2006) and downregulation of neurocan (Shen et al.

2008) and plasminogen activator inhibitor-1 (Xin et al. 2011). Although most of the investigations so far have focussed on the astroglial changes, studies using other disease models have also demonstrated that the beneficial effects of BMSC transplantation may also be mediated via the promotion of M2 polarisation in activated microglia (Ohtaki et al. 2008; Zanier et al. 2014)

The studies mentioned above have mostly been conducted using BMSCs. Investigations into other sources of stem cells such as olfactory ensheathing cells, dental pulp stem cells and induced pluripotent stem cells have also begun to demonstrate potential in enhancing functional recovery after stroke (Chou et al. 2014; Leong et al. 2012; Yuan et al. 2013).

1.6 Modeling Stroke

Various models of stroke in animals (Bacigaluppi, Comi & Hermann 2010a, 2010b; Canazza et al. 2014; Carmichael 2005) and tissue culture systems (Giffard & Swanson 2005; Murphy, EJ & Horrocks 1993; Wu & Schwartz 1998) have been devised for use in the investigations of mechanisms underlying infarction and recovery, as well as in the development of treatments and interventions. These animal and tissue culture stroke models approximate the various aspects of stroke in humans to differing extents and enable the study of the disease under conditions that are more controlled and reproducible while minimising the ethical issues associated with studies involving human patients.

1.6.1 Animal Models

Animal models of stroke have typically utilised rodents such as mice, rats and gerbils as the model animal. However, larger animals such as rabbits, cats, dogs, sheep, pigs and monkeys, exhibiting greater complexity in brain structure that more closely resemble human brains, have also been used (Canazza et al. 2014; Traystman 2003). Although rodents exhibit lesser brain complexity, there are many comparative advantages for their use in stroke models compared to larger animals. These advantages include a lower cost of maintenance, ease of breeding and handling, and fast maturation, all of which facilitate studies with high throughput and greater statistical power. Furthermore, a large variety of transgenic strains are available, particularly in mice, that enable investigations of specific genes and molecular pathways that are not feasible in other model animals. These advantages are reflected in the fact that the large majority of reported studies have employed rodent models of stroke.

Middle cerebral artery occlusion (MCAo) is the most common form of clinical stroke in humans (Bogousslavsky, Van Melle & Regli 1988; Olsen, Skriver & Herning 1985). Consequently, occlusion of the middle cerebral artery is the prevalent approach to infarct induction in animal stroke models and many different techniques that has been devised to achieve this, including endothelin-1 injection, intraluminal thread, embolic clot, microvascular clip, suture ligation and electrocoagulation (Carmichael 2005; Fluri, Schuhmann & Kleinschnitz 2015; Hossmann 2008; Macrae

2011). Furthermore, depending on the technique used, the arterial occlusion may be reversed to model the consequences of reperfusion due to spontaneous or pharmacologically induced recanalisation. However, depending on the technique and surgical conditions used, the size and location of infarct can be highly variable (Carmichael 2006; Fluri, Schuhmann & Kleinschnitz 2015; Hossmann 2008; Traystman 2003).

An alternative approach is the photothrombotic stroke model that is used in the investigations presented in this thesis. In this model, infarction is induced by the translumination of the brain through the skull from a cold light source following injection of rose bengal, a photosensitive dye, into the blood circulation of the animal (Watson et al. 1985). Rose bengal is activated by light exposure triggering the generation of oxygen radicals that lead to platelet activation and clotting within the microvasculature of the pia and parenchyme resulting in rapid cell death and infarct development. However, the model has been criticised for a lack of clinical relevance as it results in little or no ischemic penumbra and endothelial damage caused by the oxygen radicals also lead to early vasogenic oedema that is uncharacteristic of stroke in humans (Carmichael 2005; Fluri, Schuhmann & Kleinschnitz 2015; Hossmann 2008). Despite this, the photothrombotic stroke model exhibits several key advantages over the MCAo models particularly in the study of neurorestorative mechanisms and functional recovery following stroke.

The infarcts generated by photothrombotic stroke are highly reproducible with well-defined boundaries and can be targeted to specific brain regions to generate functional deficits that are easily assessed. Furthermore, the relative size of infarcts generated by photothrombotic stroke are more comparable to the average size of infarcts compatible with survival in humans than the much larger infarctions typically obtained in MCAo stroke models (Carmichael 2005). The results from a study by Alaverdashvili et al. (2008) is of particular pertinence here as they suggested that the long term outcome of injuries such as stroke is more dependent on the severity and size of the infarct rather than the nature or cause of the injury. As a final point, the rapid development and lack of an ischemic penumbra may be an advantage as the infarct is more resistant to modification by neuroprotective mechanisms that can confound investigations into the effects of neurorestorative interventions. Indeed, this model has been used in many studies investigating neuroplastic changes within the peri-infarct tissue that underlie post-stroke functional

recovery (Brown, Boyd & Murphy 2010; Brown, Wong & Murphy 2008; Clarkson et al. 2013; Harrison et al. 2013; Hinman, Rasband & Carmichael 2013; Jablonka et al. 2010; Jablonka et al. 2012; Sigler & Murphy 2010).

1.6.2 Tissue Culture Models

Although the use of animal models is indispensable to the development of treatments and studies of post-stroke functional recovery that cannot be replicated *in vitro*, the use of tissue culture systems have also contributed greatly to the understanding of specific mechanisms and pathways that are involved in the responses of different neural cell types to ischemia (Almeida et al. 2002; Dugan & Kim-Han 2004; Goldberg, WJ, Kadingo & Barrett 1986; Yenari & Giffard 2001).

There are in general two different types of tissue culture systems used in the study of stroke-related mechanisms, organotypic slice cultures and cell cultures (Dugan & Kim-Han 2004; Gahwiler et al. 1997; Norberg et al. 2005; Wu & Schwartz 1998). Organotypic cultures using brain slices have the advantages of retaining the structure, intercellular organisation and neuronal connections of the intact brain while allowing for direct manipulation of the cells and ease of assessment of the responses to manipulation. However, these cultures are difficult to maintain for long durations (Wilhelmi et al. 2002) and are therefore unsuitable for the study of mechanisms involved in recovery following stroke as these processes typically take place over prolonged periods of time.

In contrast, cultures of cells from dissociated brain tissue can be easily maintained for up to several weeks and the cellular composition of the cultures can be easily manipulated to allow the investigation of specific interactions between different neural cell types (Costantini et al. 2010; Langan & Slater 1991; Szabo & Gulya 2013). However, there is at present no cell culture model that allows the study of peri-infarct cellular responses. The challenges of modeling the peri-infarct tissue in cell culture will be discussed in detail in the study described in chapter 5.

1.7 Objectives of the Study

Although it is clear that the responses of glial cells within the peri-infarct tissue are important determinants of the long term outcome of stroke, there is much that remains unknown about their influence on the processes involved in the recovery of function, and even less about how these responses may be manipulated to enhance recovery.

The experiments described in this thesis were designed to investigate the processes involved in the development of the post-stroke peri-infarct glial cell responses. Of particular interest were the early microglial responses that may influence functional recovery during the post-acute phase of stroke. Specifically, it is commonly held that microglial activation is detrimental to the stroke outcome and that this may in part be attributed to the effects of the early microglial responses and its influence on the subsequent development of astrogliosis following stroke.

The investigations were organised into three parts, of which the first two were based on the photothrombotic model of stroke in rats. The photothrombotic model of stroke, despite having been used in numerous studies over the past three decades, is still incompletely characterised, particularly in terms of a quantitative approach to characterise the peri-infarct glial cell responses over time. This deficiency was addressed in the first part of the investigations where quantitative measures were developed and applied to the characterisation of microglial and astroglial responses within the tissue regions surrounding the infarct over the first 7 days following stroke.

In the second part of the investigations, the characterised model was used as a basis to study the effects of treatment with the anti-inflammatory drug minocycline on the early microglial responses and the subsequent development of astrogliosis and functional recovery. Minocycline was selected for these studies as it has been widely reported to be an effective inhibitor of microglial activation.

The third and final part of the investigations addressed the current lack of *in vitro* models that can be used to study peri-infarct cellular responses. Here, a previously reported technique of inducing focal cell death in cultured cells was used as the basis to develop a cell culture model that enabled the investigation of glial cell responses under conditions that simulate the environment of the peri-infarct tissue. The cell

culture model was characterised using a similar quantitative approach as in the photothrombotic model and was applied to the investigation of microglial activation and its influence on the development of astrogliosis within the simulated peri-infarct environment. Minocycline was again used to inhibit the microglial responses to the focal injury.

The objectives of the study are summarised as follows:

1. To characterise the photothrombotic model of stroke using a quantitative approach
 - a. To develop quantitative measures for microglial activation and astrogliosis
 - b. To characterise the spatiotemporal changes in the microglial and astroglial responses in the intact tissue surrounding the infarct core following photothrombotic stroke
2. To investigate the effectiveness of early treatment with minocycline on the modulation of microglial and astroglial responses and its influence on the subsequent functional recovery after stroke
3. To develop an *in vitro* model of the post-stroke peri-infarct tissue
 - a. To characterise the spatiotemporal changes in the microglial and astroglial responses within the peri-focal regions of the model
 - b. To investigate the role of microglial activation on the development of astrogliosis following focal lesioning by treatment with minocycline and by depletion of microglial cells from the cultures

CHAPTER 2
GENERAL MATERIALS AND METHODS

Materials and methods that are common to the experiments in this thesis are described in the following sections. Variations and modifications or methods that are specific to the chapters are described in the methods sections within those chapters. In particular, the methods pertaining to cell culture and immunocytochemistry are described only within the methods section of chapter 5 (section 5.2).

2.1 Animals

Male Sprague-Dawley rats (Laboratory Animal Services, University of Adelaide, SA, Australia) between 270 and 340 g body weight were used in the experiments. The animals were kept in a temperature and humidity controlled room with a 12 h / 12 h light/dark cycle and *ad libitum* access to water and standard rat chow. The use of animals in this study was approved by the Animal Welfare Committee of Flinders University (Project Number 754/10).

2.2 General Materials

The common laboratory chemicals and reagents used in the experiments described in this thesis are listed in Table 2.2.1.

Table 2.2.1 List of common laboratory chemicals and reagents

Description	Product / Catalogue No.	Supplier / Manufacturer
Acetic acid, glacial	1-2.5L GL	Ajax Finechem
Bovine Serum Albumin	A6003	Sigma-Aldrich
Calcein, AM	C3099	ThermoFisher / Molecular Probes™
Calcium chloride dihydrate	127-500G	Ajax Finechem
Chondroitinase ABC from <i>Proteus vulgaris</i>	C3667	Sigma-Aldrich
Cresyl Violet acetate	C5042	Sigma-Aldrich
Cytosine β-D-arabinofuranoside	C1768	Sigma-Aldrich
Denatured Absolute Alcohol F3	4546	Ajax Finechem
Dulbecco's modified Eagle's medium – low glucose	D6046	Sigma-Aldrich
Donkey serum	D9663	Sigma-Aldrich
DPX Mountant for histology	06522	Sigma-Aldrich
Ethanol Udenatured 100% AR	EA043	Chem-Supply
Fetal Bovine Serum, qualified, Australia origin	10099141	ThermoFisher / Gibco™
D-(+)-Glucose	G8270	Sigma-Aldrich

Griess Reagent (modified)	G4410	Sigma-Aldrich
HEPES	H3375	Sigma-Aldrich
Heptane, anhydrous, 99%	246654	Sigma-Aldrich
Hoechst 33258	H3569	ThermoFisher / Molecular Probes™
Hydrochloric acid, 36%	AJA1367-2.5LGL	Ajax Finechem
L-Leucine Methyl Ester	L1002	Sigma-Aldrich
Magnesium chloride hexahydrate	M2393	Sigma-Aldrich
Magnesium sulphate	105886	Merck Millipore
Minocycline Hydrochloride	M9511	Sigma-Aldrich
NeuroTrace™ 500/525 Green Fluorescent Nissl Stain	N-21480	ThermoFisher / Molecular Probes™
Paraformaldehyde, prilled, 95%	441244	Sigma-Aldrich
Penicillin-Streptomycin (10,000 U/mL)	15140122	ThermoFisher / Gibco™
Poly-L-lysine hydrobromide	P1274	Sigma-Aldrich
Potassium chloride	P9541	Sigma-Aldrich
Potassium dihydrogen orthophosphate	391-500G	Ajax Finechem
ProLong® Gold Antifade Mountant	P36934	ThermoFisher / Molecular Probes™
Propidium iodide solution	P4864	Sigma-Aldrich
Protease Inhibitor Cocktail	P8340	Sigma-Aldrich
Rose bengal	330000	Sigma-Aldrich
Sodium acetate	S2889	Sigma-Aldrich
Sodium azide	S2002	Sigma-Aldrich
Sodium bicarbonate	S5761	Sigma-Aldrich
Sodium chloride	S9625	Sigma-Aldrich
Sodium hydroxide	S5881	Sigma-Aldrich
Sodium nitrite	S2252	Sigma-Aldrich
Sodium phosphate dibasic	S3264	Sigma-Aldrich
Sodium phosphate monobasic	S3139	Sigma-Aldrich
Sucrose	S0389	Sigma-Aldrich
Trizma® base	T1503	Sigma-Aldrich
Triton™ X-100	T8787	Sigma-Aldrich
Tween® 20	P9416	Sigma-Aldrich

2.3 General Methods

2.3.1 Habituation of Animals to Handling and Functional Testing

Each animal was handled by an investigator for at least 10 minutes a day on 3 separate days leading up to the surgical induction of photothrombotic stroke. These sessions included the familiarisation of the animals to the testing platform (figure 2.2.1) and trial attempts at the forelimb placing assessment (described below) to habituate the animals to the handling required to successfully perform the assessment.



Figure 2.3.1 Forelimb placing test platform.

Animals were habituated to handling on the forelimb placing test platform on three separate days for 10 minutes each time before photothrombotic stroke surgery.

2.3.2 Forelimb Placing Assessment

The forelimb placing assessment tests for the reflexive motor response of the rat to reach for the nearest detected surface when held suspended with all of its limbs hanging in space. This functional test was originally developed by Schallert et al. (2000) and has been described in detail elsewhere (Schallert & Woodlee 2005). The rat being tested was held firmly by its torso in both hands such that all four limbs hang freely. Placing response in the forelimb was elicited by brushing the vibrissae of the rat against the testing platform.

Three variants of the test, the head-on, same-side and cross-midline, were used in the assessment (figure 2.3.2). The rats were given ten trials for each variant of the test on both forelimbs during each assessment. The placing score for each forelimb was

calculated by summing the successful trials in all three variants, giving a maximum score of 30 for the test.

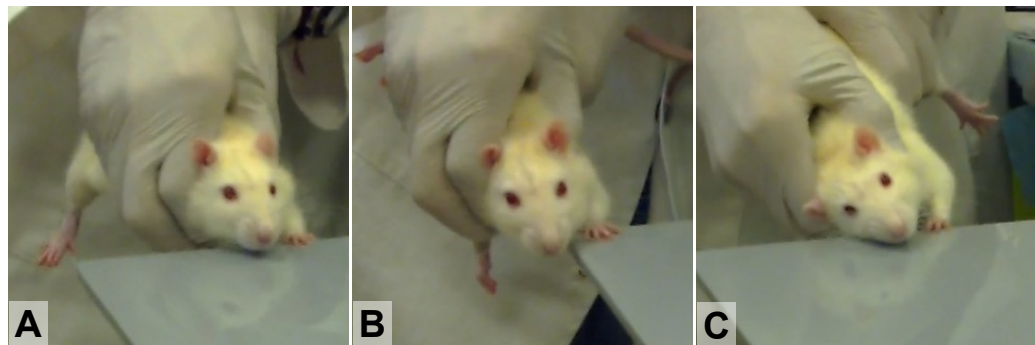


Figure 2.3.2 The three variants of the forelimb placing test.

A) Head on - In the head on test, the rat is held with its body level to the platform. The vibrissae from both sides of its face brush the edge when the rat is moved towards the platform. B) Same side - The rat is held in the same manner as in the head on test. The rat is moved towards the platform from the corner so that only the vibrissae on the same side as the forelimb being tested contacts the platform. C) Cross midline - The rat is held tilted towards the side opposite to the forelimb being tested so that only the vibrissae on the opposite side contacts the platform.

2.3.3 Photothrombotic Stroke Surgery

The photothrombotic stroke surgery was based on the method described in the original study by Watson et al. (1985) and the study by Alaverdashvili et al. (2008) with some modifications in the surgical technique and equipment used.

The rats were anaesthetised for surgery using ketamine (100 mg/kg; Ketamine Hydrochloride; Ceva Animal Health Pty Ltd, NSW, Australia) and xylazine (10 mg/kg; Ilium Xylazil-20; Troy Laboratories Pty Ltd, NSW, Australia) via intraperitoneal injections. Adequate depth of anaesthesia was determined by the lack of response to a pinch on the hindlimb footpad. Rose-bengal dye was prepared by dissolving in saline at 10 mg/mL then sterile filtered through a 0.20 μm (16534K ; Sartorius Stedim Australia Pty Ltd, VIC, Australia) syringe filter before use in the surgery. Anaesthesia was maintained for the duration of the surgery using 250 μL boluses of ketamine, diluted 1:10 in saline, that were administered as necessary. Rose-bengal and additional ketamine were administered via a femoral vein cannula introduced in the first part of the surgery. Core temperatures of the rats were

monitored by a rectal temperature probe (YSI Precision 4000 A Thermometer; YSI Inc., OH, USA) that was inserted after anaesthesia. The temperature was maintained at between 36.5 and 37.5 °C using heating pads during the surgery and heat lamps that were switched on as necessary during recovery from anaesthesia following the surgery. The scalp and inner surface of the right thigh were shaved using electric clippers and sterilised by swabbing with 70% alcohol before surgical incisions were made at each site.

The surgery was carried out in two parts, the first of which was the cannulation of the femoral vein. An incision approximately 2 cm in length was made on the inner surface of the right thigh directly along the femoral sheath that contains the femoral nerve, artery and vein. An approximately 1cm segment of the femoral vein was isolated from the femoral sheath and ligated at the distal end using 4-0 braided silk suture (SA4040; Dynek Pty Ltd, London, UK). Another ligature was tied loosely at the proximal end of the isolated vein. A small incision was made into the femoral vein just proximal to the distal ligature and a cannula (Polyethylene tubing, ID 0.28 mm OD 0.61 mm, Product Code: I-10338; SteriHealth Pty Ltd, SA, Australia) was introduced into the vein via the incision. The cannula was advanced approximately 2 cm past the proximal (loose) ligature. The proximal ligature was then tightened to secure the cannula. Approximately 50 µL bupivacaine (Bupivacaine Injection BP 0.5%; Pfizer Inc., NY, USA) was administered directly onto the surgical site and the wound was temporarily closed with a single simple interrupted suture (S207; Dynek Pty Ltd, London, UK). The cannula was further secured by using masking tape to hold the cannula around the right ankle.

Following femoral vein cannulation, the head of the rat was immobilised in a stereotaxic frame (Model 900 Small Animal Stereotaxic Instrument; David Kopf Instruments, CA, USA). An approximately 2 cm long midline incision was made along the scalp with a disposable sterile blade (Surgical scalpel blade No. 21, REF 0206; Swann-Morton Limited, Sheffield, UK) and the scalp was retracted to expose the skull. The periosteum was cleared from the skull surface by gentle scraping with the blade and blood was cleaned by swabbing with cotton buds. Bleeding was stopped by cauterisation using low temperature electrocautery (Accu-Temp® Low Temperature Cautery, Product No. 8441000; Beaver Visitec International, MA, USA). The location of the infarct was fixed by placement of a brass shim stencil with a rectangular window (3 × 5 mm) positioned over the forelimb motor cortex of

the right hemisphere, at 1.5 mm anterior to bregma and 2.5 mm lateral to midline (figure 2.3.3).

Translumination of the skull for stroke induction was performed using a 150 W light source (Intralux 5000; Volpi AG, Schlieren, Switzerland) equipped with a green filter (532.5 - 587.5 nm pass band) and attached fibre-optic cable (6 mm diameter). Intensity of the emitted light from the fibre-optic cable was measured using a digital light meter (LX-1330B; GX Pro, Gain Express Holdings Ltd, Kowloon, Hong Kong) to ensure an intensity of at least 140,000 lux at the point of emission from the cable when the shutter dial was at maximum. The lamp of the light source was replaced as soon as the light intensity fell below 140,000 lux. The shutter dial was turned to minimum and the fibre-optic cable was positioned directly over the window of the brass shim stencil and as close as possible without contacting the skull (figure 2.3.3).

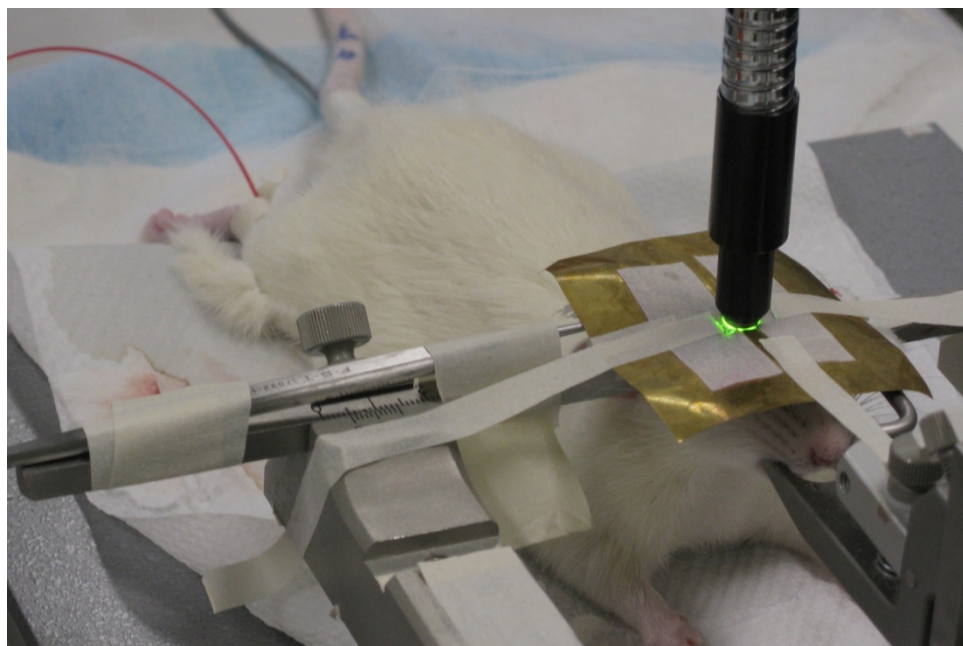


Figure 2.3.3 Placement of brass shim and fibre optic cable from light source.

A brass shim with a 3×5 mm window is positioned over the forelimb motor cortex, centred at bregma +1.5 mm, midline +2.5 mm. The brass shim is held in position with masking tape. The fibre-optic cable of the light source is positioned with the aperture directly over the cut-out and as close as possible without contacting the skull.

Rose-bengal dye, at a dose of 13 mg/kg bodyweight (1.3 mL/kg), was injected via the femoral vein cannula using a syringe pump (sp200i syringe pump; World Precision Instruments Inc, FL, USA) at a rate of 200 μ L/min. At the same time, the shutter dial of the light source was turned to maximum to begin stroke induction. The translumination was maintained for 15 min before the light source was removed. The duration of light exposure was determined from initial experiments to reliably generate infarcts that reached the full cortical depth without extending into the subcortical layers.

Following completion of stroke induction, the incision on the scalp was closed with a simple running suture and 100 μ L bupivacaine was administered by subcutaneous injections around the surgical site. Next, the femoral vein cannula was withdrawn and the proximal ligature that was used to secure the cannula was then further tightened to close the vein. The incision at this site was closed using several simple interrupted sutures and 100 μ L bupivacaine was administered around the site via subcutaneous injections. The rat was then returned to its cage and its temperature was monitored and maintained between 36.5 and 37.5 $^{\circ}$ C using a heat lamp that was turned on as necessary until it had recovered from anaesthesia.

2.3.4 Perfusion-Fixation of the Brain

The rats were sacrificed by transcardial perfusion-fixation for brain samples that were used in immunohistochemistry and cresyl violet staining.

The rats were anaesthetised using ketamine (100 mg/kg) and xylazine (10 mg/kg) administered via intraperitoneal injections. The anaesthetised rat was placed in a supine position and the limbs were secured using masking tape. The pleural cavity was exposed by dissecting into the ribcage and diaphragm to allow access to the heart. The thymus was dissected to allow visualisation of the ascending aorta. The heart was gripped loosely across the middle using a haemostat and the lower wall of the left ventricle was punctured with a blunted 18 gauge needle (BD PrecisionGlide™ 18G 1 1/2TW; Becton, Dickinson and Company, NJ, USA) attached via tubing to a peristaltic pump (7401 Blood Pump; Drake Willock). The needle was gently advanced upwards past the left ventricle until the tip was visible in the ascending aorta. The haemostat was then clamped to secure the needle for perfusion-fixation. An incision was made in the right atrium of the heart just before

starting the peristaltic pump to allow the blood and perfusion solutions to leave the circulation. The peristaltic pump was set to a flow rate of 60 mL/min for both perfusion and fixation. Perfusion was performed using 1 % NaNO₂ in 0.01 M sodium phosphate buffer (pH 7.4) followed by fixation using 4 % paraformaldehyde in 0.1 M sodium phosphate buffer (pH 7.4). Perfusion was continued for at least 3 min until the solution flowing out of the incision ran clear. Fixation was performed using approximately 200 mL of the fixative. Following fixation, the rat was decapitated and the brain was extracted from the skull. The brain was then placed into a vial filled with fixative and post-fixed overnight at 4 °C.

2.3.5 Cryoprotection of Brain Samples

Following post-fixation, the brain samples were transferred into 20 % cyoprotectant (20 % sucrose solution with 0.02 % sodium azide in PBS, pH 7.4) and incubated at 4 °C until the brains sank to the base of the containers. The samples were then transferred into 30 % cryoprotectant (30 % sucrose solution with 0.02 % sodium azide in PBS, pH 7.4) and again incubated at 4 °C until the brains sank to the base of the containers. Finally, the samples were transferred into fresh 30 % cryoprotectant and stored at 4 °C until they were processed for cryosectioning.

2.3.6 Cryosectioning of Brain Samples

The brain samples were first placed into a brain matrix and trimmed by cutting away the tissue approximately 1 mm anterior and posterior to the infarct. The block of brain tissue containing the infarct was blotted gently with tissue paper to remove excess cryoprotectant, then placed into a cryomold (18646A; Polysciences Inc., PA, USA). The cryomold was then filled with OCT compound (Tissue-Tek[®] O.C.T. Compound; Sakura Finetek USA Inc., CA, USA) until the brain block was completely covered.

The cryomold was then immersed in heptane that was cooled to near freezing in liquid nitrogen. Once the OCT compound had completely frozen, the cryomold was kept in a freezer at -20 °C overnight to allow the temperature to equilibrate before sectioning.

The brain blocks embedded in OCT were cut in a cryo-microtome (Leica Cryocut 1800 equipped with Leica Microtome 2020; Leica Microsystems Pty Ltd, NSW, Australia) into 20 μm thick coronal sections. For every 25 sections cut (*i.e.* at 0.5 mm intervals), sections were mounted onto poly-L-lysine-coated glass slides for cresyl violet staining. The glass slides (76 \times 26 mm, HD 41808 1P0; HD Scientific Supplies Pty Ltd, NSW, Australia) were prepared beforehand by incubating in poly-L-lysine (0.01 %) dissolved in double-distilled water for 15 minutes and then dried in an oven at 60 $^{\circ}\text{C}$.

The slide-mounted sections were kept in a desiccated slide container at 4 $^{\circ}\text{C}$ until they were processed for cresyl violet staining. Other sections were kept free floating in PBS with 0.02 % sodium azide also at 4 $^{\circ}\text{C}$.

2.3.7 Cresyl Violet Staining and Calculation of Infarct Volume

Slide-mounted brain sections were stained with cresyl violet to allow visualisation of the infarct. Cresyl violet staining solution was prepared by dissolving cresyl violet acetate (0.1 %) in double-distilled water, filtered through a 0.20 μm syringe filter, then acidified with acetic acid (0.0006 %).

The sections were rehydrated by incubation in decreasing concentrations of ethanol: 2 min at 100 % ethanol, 2 min in 95 % ethanol, 3 min in 75 % ethanol, and finally, 5 min in 50 % ethanol. The sections were then stained by incubation in cresyl violet staining solution for 10 min. The sections were then carefully rinsed with double-distilled water and de-stained by 2 incubations in 95 % ethanol for 5 min each time. Finally, the sections were dehydrated by 2 incubations in 100 % ethanol for 5 min each time. The sections were air dried for 15 min in a fume cabinet, then mounted and coverslipped in DPX mountant.

Images of the stained sections were taken using a digital camera (Canon PowerShot A650 IS; Canon Australia, NSW, Australia), together with a microscope calibration slide for scale (figure 2.3.4). The images were processed using the image processing and analysis software, "ImageJ" (Schneider, Rasband & Eliceiri 2012), for the calculation of infarct volume. The area of infarction in each section as identified by pale staining was measured in ImageJ. Then the infarct volumes within the intervals between sections were approximated by the trapezoidal method (*i.e.* Interval

$\text{volume}_{a,b} = 1/2 \times (\text{Area}_a + \text{Area}_b) \times \text{interval distance}$). The interval volumes were then summed to obtain the total infarct volume.

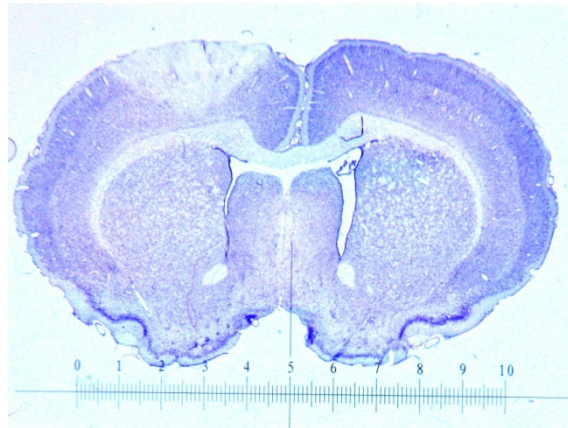


Figure 2.3.4 Sample image of brain section stained with cresyl violet.

The brain section was taken from an animal at 24 h after photothrombotic stroke. The infarcted tissue was weakly stained by cresyl violet as can be clearly seen in the image. A microscope calibration slide (1 mm per numbered division) was placed at the base of the section to allow for the calculation of infarct volume.

2.3.8 Immunohistochemistry

A list of primary and secondary antibodies, dilutions used, and the suppliers are provided in Table 2.3.1. In addition, cell nuclei were counterstained with Hoechst 33258 (1:1000 dilution).

Free floating brain sections were blocked and permeabilised in blocking buffer (0.3% Triton-X100, 5% Donkey serum in PBS, pH 7.4) for 2 h at room temperature before incubating in primary antibodies. Primary antibodies were diluted in blocking buffer and the sections were incubated overnight at 4 °C. The sections were then washed four times in PBS before incubating in secondary antibodies. Secondary antibodies and Hoechst 33258 were diluted in PBS and the sections were incubated for 2 h at room temperature on an orbital shaker (Bioline orbital shaker, BL8136; Bioline Global Pty Ltd, NSW, Australia). The sections were then washed four times in PBS before being mounted on glass slides in Prolong[®] Gold antifade mountant and coverslipped.

Table 2.3.1 List of antibodies and dilutions used in immunohistochemistry

Primary Antibodies			
Description	Dilution	Catalogue #	Supplier
Goat polyclonal anti-Iba1	1:1000	ab5076	Abcam
Mouse monoclonal anti-NeuN [Clone A60]	1:500	MAB377	Millipore / Chemicon®
Rabbit monoclonal anti-Ki67 [Clone SP6]	1:500	ab16667	Abcam
Rabbit monoclonal anti-Vimentin [Clone EPR3776]	1:500	ab92547	Abcam
Rabbit polyclonal anti-CD68	1:1000	ab125212	Abcam
Rabbit polyclonal anti-GFAP	1:500	G4546	Sigma-Aldrich
Secondary Antibodies			
Description	Dilution	Catalogue #	Supplier
Donkey anti-Mouse IgG (H+L) Alexa Fluor® 488 conjugate	1:2000	A-21202	ThermoFisher / Invitrogen™
Donkey anti-Mouse IgG (H+L) Alexa Fluor® 647 conjugate	1:2000	A-31571	ThermoFisher / Invitrogen™
Donkey anti-Rabbit IgG (H+L) Alexa Fluor® 488 conjugate	1:2000	A-21206	ThermoFisher / Invitrogen™
Donkey anti-Rabbit IgG (H+L) Alexa Fluor® 647 conjugate	1:2000	A-31573	ThermoFisher / Invitrogen™
Donkey anti-Goat IgG (H+L) Alexa Fluor® 647 conjugate	1:2000	A-31571	ThermoFisher / Invitrogen™

2.3.9 Image Acquisition

Images were acquired using a Leica TCS SP5 confocal microscope (Leica Microsystems Pty Ltd, NSW, Australia) from Iba1-immunolabelled sections for the determination of microglial circularity and area fraction. The 20× objective lens was used for image acquisition on the confocal microscope. Images for vimentin-immunolabelled sections were acquired using an Olympus IX71 inverted microscope (Olympus Australia Pty Ltd, NSW, Australia) with the 4× objective lens. Images were acquired from two brain sections separated by at least 25 sections (*i.e.* 0.5 mm) from each brain sample and the results reported were averages of the two sections.

For the characterisation of changes in the microglial response, images were scanned from Iba1 and NeuN double-immunolabelled sections at the 8 regions of interests (ROIs) as shown in figure 2.3.5 A. "Ipsi01A" and "Ipsi01B" are ROIs within the peri-infarct tissue along the boundary on the lateral and midline edges of the infarct. "Ipsi01A + 1mm" is located 1 mm away from the infarct boundary on the same side of the infarct as "Ipsi01A". "Ipsi02" and "Ipsi03" are ROIs within the ipsilateral cortex in regions that are distant to the infarct. "Contra01", "Contra02" and "Contra03" are corresponding regions within the contralateral cortex. The contralateral region, "Contra01" was used as the corresponding control for "Ipsi01A"

and "Ipsi01B" as no changes were expected within the contralateral cortex. Loss of immunolabelling for NeuN was used as the method of locating the infarct boundary for the acquisition of images in the peri-infarct regions (figure 2.3.5 B & C). Image stacks were scanned at 1 μm steps through the full thickness of the sections using confocal microscopy with the 20 \times objective lens.

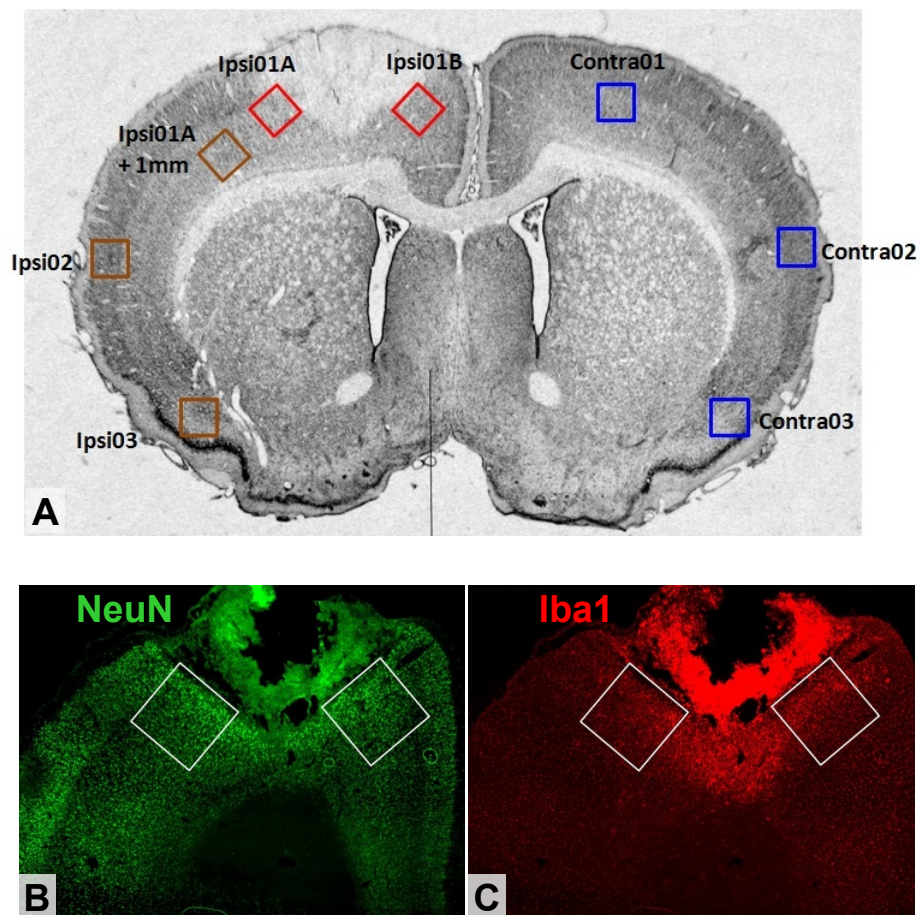


Figure 2.3.5 Location of images acquired for the characterisation of microglial changes following stroke.

(A) The boxes show the positions of the ROIs that were scanned by confocal microscopy. (B) The loss of NeuN immunolabelling was used to identify the infarct and locate the boundary between the infarct and peri-infarct tissue. The white boxes ($775 \times 775 \mu\text{m}$) correspond to Ipsi01A and Ipsi01B in (A) and are located within the peri-infarct tissue regions on either side of the infarct. The ROIs were aligned along the boundary of the infarct so that a small area of the infarct was just visible in the scanned images. (C) The corresponding ROIs in the Iba1 fluorescence channel is shown.

For the characterisation of changes in the astroglial response, images were scanned from vimentin and NeuN double-immunolabelled sections. For this characterisation only the peri-infarct tissue regions on either side of the infarct and the corresponding contralateral region were scanned (figure 2.3.6 A). Loss of immunolabelling for NeuN was again used as the method for positioning the ROI during image acquisition (figure 2.3.6 B & C). The images here were acquired on the Olympus IX71 microscope using the 4× objective lens. Identical camera exposure settings were used to capture all images for vimentin immunofluorescence.

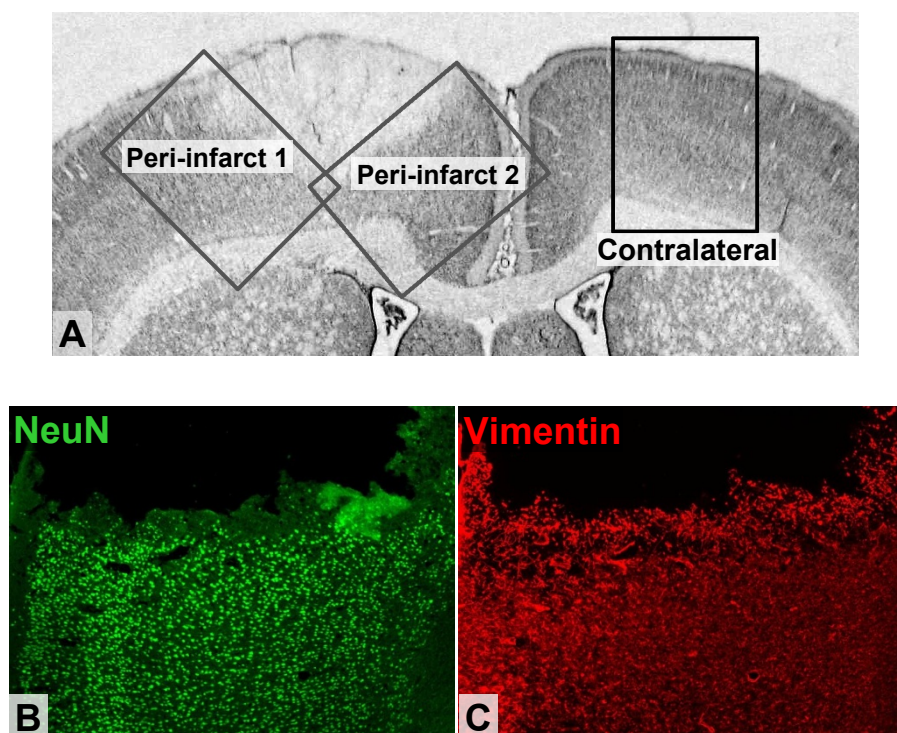


Figure 2.3.6 Location of images acquired for the characterisation of astroglial changes following stroke.

(A) The boxes ($2250 \times 1681 \mu\text{m}$) show the positions of the images taken using the 4× objective lens within the peri-infarct tissue and corresponding contralateral region. The images taken within the peri-infarct tissue on either side of the infarct were aligned along the boundary using NeuN immunolabelling as a guide. (B) An example of an image ($2250 \times 1681 \mu\text{m}$) taken at the "Peri-infarct 1" position in the NeuN fluorescence channel. The loss of NeuN immunolabelling was again used to identify the infarct and locate the boundary between the infarct and peri-infarct tissue. The images taken within the peri-infarct tissue were positioned so that they were aligned with the edge of the infarct with the infarct clearly visible in the top portion of the image. (C) The corresponding image in the vimentin fluorescence channel is shown.

2.3.10 Image Analysis

Images from the Iba1-immunolabelled sections acquired using confocal microscopy were analyzed to determine microglial circularity and area fraction. The image stacks were opened in ImageJ and maximum intensity projections were obtained. All subsequent image processing and analyses were performed using these projected images. The images for the Iba1 fluorescence channel were processed to reduce background noise using the "subtract background noise" function with "rolling ball radius" set at 100 pixels and the sliding paraboloid box checked. The mean background fluorescence intensity was then determined by sampling and averaging the fluorescence intensity at 5 random positions that were devoid of cells. The image was then thresholded at a level that was twice the mean background fluorescence intensity rounded down to the nearest integer.

An area $500 \times 500 \mu\text{m}$ in size was selected for analysis using the "specify" function. For images in the peri-infarct regions (*i.e.* Ipsi01A and Ipsi01B), the position was chosen so that the selected area was immediately adjacent to the infarct, within the tissue region where NeuN immunolabelling was preserved (figure 2.3.7). For all other ROIs, the selection box was simply placed in the centre of the image.

Finally, the selected areas within thresholded Iba1 images were analysed using the "Analyze Particles" function, with the particle size set to a lower limit of 200 pixel units. This particle size limit corresponds to circular particles of approximately $12 \mu\text{m}$ in diameter and was chosen in order to exclude cell debris or cells that are only partially within the section. An overlay outline of the analyzed image is shown in figure 2.3.8. The results of the analyses for "particle count", "average size", "%Area" and "circularity" were transferred into spreadsheets for collation and statistical analysis.

Images from the vimentin-immunolabelled sections were analyzed using ImageJ to determine the area fraction of immunolabelling as a measure of the astroglial response. The mean background fluorescence intensity was calculated for each of the images in the vimentin fluorescence channel. This was done by sampling and averaging the fluorescence intensity at 5 random positions that were not occupied by astroglial cells. The images were then thresholded at levels that are twice their respective mean background fluorescence intensity, rounded down to the nearest integer. The corresponding images in the NeuN fluorescence channel were again

used to visualise the infarct for the placement of the selection box for analyses. The selection box was positioned immediately along the boundary of the infarct within the region where NeuN immunolabelling was preserved (figure 2.3.9). The size of the selection box was defined so that it extended 500 μm from the edge of the infarct and covered the full depth of the cortical layer. The area fraction of vimentin immunolabelling within the selection box was then determined by using the "Measure" function in ImageJ. The results were transferred into spreadsheets for collation and statistical analyses.

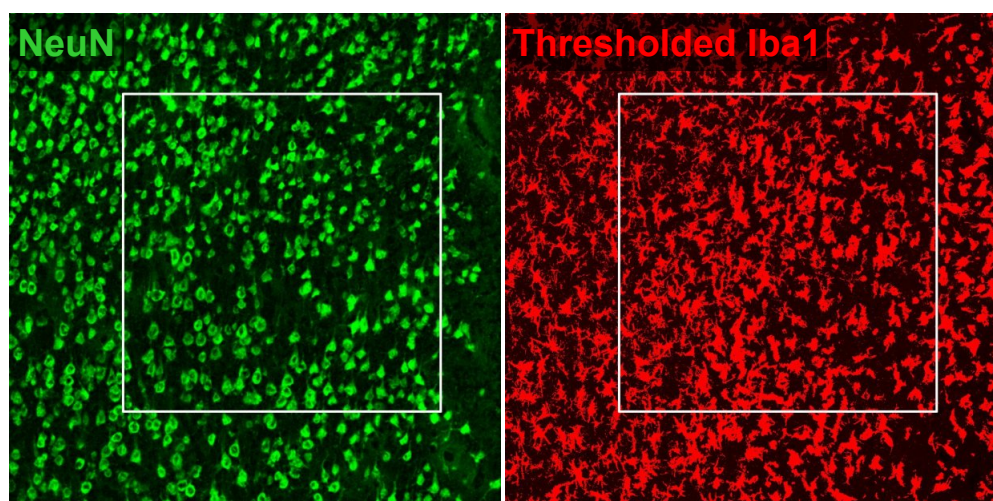


Figure 2.3.7 Specifying the area for particle analysis of Iba1 immunolabelling within the peri-infarct region.

The images shown are examples of area selection for analysis of Iba1 immunolabelling within the peri-infarct regions, "Ipsi01A" and "Ipsi01B". The images ($775 \times 775 \mu\text{m}$) are maximum intensity projections from image stacks of the NeuN and Iba1 fluorescence channels. The Iba1 image has additionally been thresholded at a level that is twice the mean background fluorescence intensity. The infarct can be seen along the right edge of the image in the NeuN channel based on the loss of immunolabelling for NeuN. The selection box ($500 \times 500 \mu\text{m}$) is positioned so that it is immediately alongside the infarct, within the tissue region where NeuN immunolabelling is preserved. The same selection box was then used on the Iba1 channel for analysis of microglial circularity and area fraction.

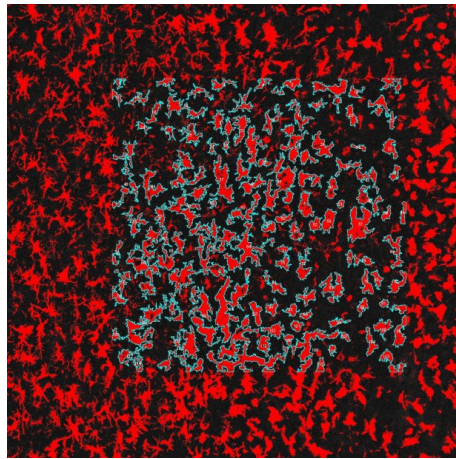


Figure 2.3.8 Overlay outlines of microglial cells immunolabelled with Iba1 as identified by "Analyze Particle" function in ImageJ.

The image shows the thresholded Iba1 image in figure 2.3.7 after particle analysis in ImageJ. All microglial cells identified by the analysis are outlined in cyan. Numerous particles that were smaller than the particle size limit can be seen in between the outlined cells.

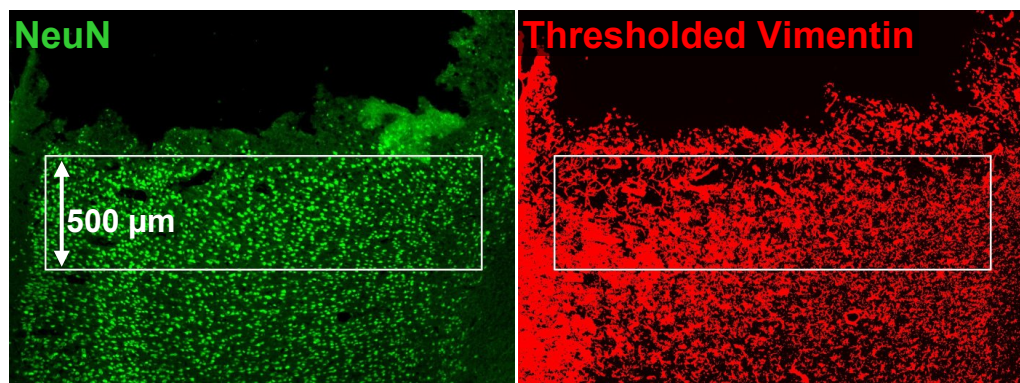


Figure 2.3.9 Specifying the area for area fraction analysis of vimentin immunolabelling within the peri-infarct region.

The images shown are examples of area selection for area fraction analysis of vimentin immunolabelling within the peri-infarct regions. The vimentin image has been thresholded at a level that is twice the mean background fluorescence intensity. The selection box was positioned along the boundary of the infarct within the tissue region where NeuN immunolabelling was preserved. The width of the selection box was specified so that it extended 500 μm from the edge of the infarct. The length of the box was specified so that it covered the entire cortical layer.

2.3.11 Western Blot

The rats that were used for western blots were sacrificed by decapitation following anaesthesia using ketamine (100 mg/kg) and xylazine (10 mg/kg) administered via intraperitoneal injections. The brains were extracted and the subcortical structures were dissected away. The infarct can be identified by the paleness of the tissue from the lack of blood flow and cell death (figure 2.3.10). The region of tissue containing the infarct and approximately 2 mm of the surrounding viable tissue was dissected out and designated as the peri-infarct tissue for analysis by western blot. A similar region of tissue was dissected from the contralateral cortex as control.

The tissue samples were homogenised in TES buffer (0.1 M Tris, 0.01 mM EDTA, 0.32 M sucrose, pH 7.4) with protease inhibitor cocktail (1:100 dilution) using the Retsch TissueLyser (Qiagen Pty Ltd, VIC, Australia) at a frequency of 30 Hz for 2 min. The homogenised samples were then assayed for protein concentration using the Bio-Rad DC protein assay kit (5000112; Bio-Rad Laboratories Pty Ltd, NSW Australia) following the manufacturer's protocol with BSA protein standards. Samples used for Neurocan blots were pre-digested, before gel electrophoresis, by incubation in an equal volume of chondroitinase ABC (1 unit/mL) in Tris-acetate buffer (0.2 M Tris, 0.6M sodium acetate, pH 8.0) for 3 h at 37 °C.

20 µg of each sample and molecular weight standards (Precision Plus Protein™ Dual Color Standards, #1610394; Bio-Rad Laboratories Pty Ltd) were loaded for gel electrophoresis (4–20% Criterion™ TGX Stain-Free™ Protein Gel, #5678094; Bio-Rad Laboratories Pty Ltd) and Western blotting (Trans-Blot® Turbo™ Transfer System with RTA Midi LF PVDF Transfer Kit, #1704155 & #1704275; Bio-Rad Laboratories Pty Ltd). The PVDF membranes were blocked in 5% skim milk and 0.1% Tween 20 in PBS (pH 7.4) for 1 hour at room temperature. All primary and secondary antibodies were diluted in 2.5% skim milk and 0.05% Tween 20 in PBS (pH 7.4). A list of the antibodies and dilutions used is shown in table 2.3.2. The membranes were incubated in primary antibodies for 30 min at room temperature with regular manual agitation. This was followed by overnight incubation at 4 °C on an orbital shaker. This membranes were then incubated in secondary antibody for 2 h at room temperature. The bands were developed by incubation in 5 mL ECL substrate (Clarity™ Western ECL Blotting Substrate, #1705061; Bio-Rad Laboratories Pty Ltd) for 5 min at room temperature. Chemiluminescence from the

blots were captured digitally on a Gel Doc™ EZ Imager (#1708270; Bio-Rad Laboratories Pty Ltd) and the band intensities were analyzed using the Carestream Molecular Imaging Software (Version 5.0; Carestream Health Inc, NY, USA).

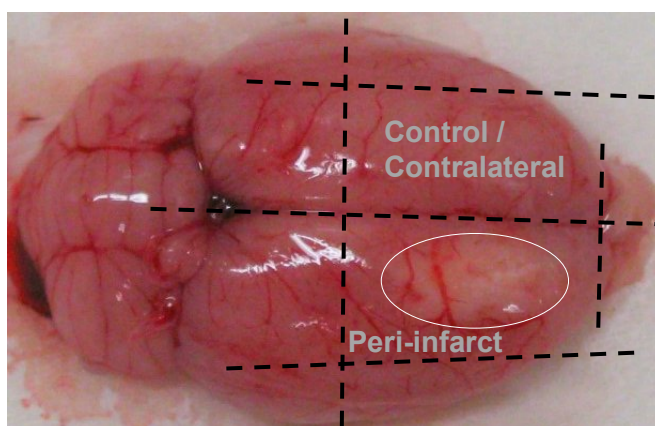


Figure 2.3.10 Dissection of brain tissue for western blot.

The picture shows a freshly extracted brain sample. The infarct can be clearly identified in the right hemisphere from the pale appearance of the tissue (thin white line). The region of cortical tissue around the infarct, including approximately 2 mm of the surrounding viable tissue was dissected out for analysis by western blot as indicated by the broken black lines. The corresponding region of tissue in the left hemisphere was dissected out and used as control.

Table 2.3.2 List of antibodies and dilutions used in western blots

Primary Antibodies			
Description	Dilution	Catalogue #	Supplier
Mouse monoclonal anti-Neurocan [Clone 650.24]	1:1000	MAB5212	Millipore / Chemicon®
Rabbit monoclonal anti-Vimentin	1:1000	ab92547	Abcam
Rabbit polyclonal anti-Actin	1:1000	A2066	Sigma-Aldrich
Rabbit polyclonal anti-GFAP	1:1000	G3893	Sigma-Aldrich
Secondary Antibodies			
Description	Dilution	Catalogue #	Supplier
Peroxidase AffiniPure Donkey Anti-Rabbit IgG (H+L)	1:2000	711-035-152	Jackson ImmunoResearch Laboratories

2.3.12 Statistical Analysis

Statistical Analyses of the experimental data were performed using the SPSS software package (IBM SPSS Statistics for Windows. Version 23.0; IBM Corp., Armonk, NY, USA). Details of individual analysis are given in the results section of subsequent chapters.

CHAPTER 3
***MICROGLIAL AND ASTROGLIAL
RESPONSES IN A PHOTOTHROMBOTIC
MODEL OF STROKE***

3.1 Introduction

Glial cells greatly outnumber neurons within the CNS and serve important roles in the regulation of the brain microenvironment that modulate and support normal neuronal functions. In acute neurological disorders such as stroke, glial cells become activated in response to the injury and act in concert to isolate and limit the extent of damage and also to promote resolution and recovery.

The astroglial response, termed astrogliosis, is characterised by cellular hypertrophy and upregulated expression of intermediate filaments including GFAP, vimentin and nestin. Over time, hypertrophic and newly proliferated astroglial cells form a glial scar along the boundary of the infarct that serves to wall off the damaged tissue (Burda & Sofroniew 2014; Sofroniew 2015).

Microglial activation occurs rapidly and typically precedes astrogliosis after stroke and is likely to be an important factor in the initiation and modulation of post-stroke astroglial responses. Activation of microglial cells is characterised by a striking morphological transformation where the normally highly ramified cells retract their processes and assume an amoeboid form. Activated microglia proliferate and migrate towards the infarct where they are involved in the clearance of debris and dead cells (Napoli & Neumann 2009).

Spontaneous partial recovery of function is usually observed over several weeks to months following stroke. This recovery in function is generally attributed to neuroplastic changes within the peri-infarct tissue, which is the region immediately surrounding the infarct. It is thought that surviving neuronal cells within the peri-infarct tissue may establish new connections that partially compensate for the neurons that are lost within the infarct (Brown & Murphy 2008).

Astroglial responses may alternatively inhibit or facilitate these neuroplastic processes (Sofroniew 2005). It has long been observed that the glial scar that is formed following prolonged astrogliosis is a barrier to axonal regeneration, but it was only more recently identified that expression of CSPGs in reactive astroglia are largely responsible for the observed inhibitory effects on axons (Fitch & Silver 1997; McKeon, Jurynek & Buck 1999). Indeed, evidence from various studies suggests that CSPGs released from reactive astroglia within the peri-infarct tissue after stroke may inhibit plasticity and limit recovery long before the formation of a mature glial scar

(Carmichael et al. 2005; Shen et al. 2008). However, reactive astroglia may also play important roles in facilitating functional recovery through the expression of molecules such as thrombospondins, clusterin and various trophic factors that promote neuroplasticity (Allred, Kim & Jones 2014; Imhof et al. 2006; Liu, Z, Xin & Chopp 2014; Zhao, Y & Rempe 2010).

In addition to the physical changes, microglial activation is also accompanied by a host of changes in protein expression including upregulation of various cytokines (Jordan et al. 2008; Kim, JY, Kawabori & Yenari 2014), many of which have been observed to induce or modulate astroglial reactivity (Chen, SH et al. 2015; Gao, Z et al. 2013; Zhang, D et al. 2010), as well as neurotrophic factors such as BDNF and GDNF that promote neuroplasticity (Batchelor et al. 2002; Lai & Todd 2008; Madinier et al. 2009; Yang, H et al. 2012).

The timing of the respective responses of microglia and astroglia and their interactions are likely to be critical in determining the balance of factors favouring or inhibiting neuroplasticity. A detailed characterisation of the spatio-temporal progression of microglial and astroglial responses following stroke will be useful in furthering the understanding of the cross-interactions of these responses and in aiding the development of interventions to enhance functional recovery. However there have so far been very few attempts at a quantitative approach to characterise these glial cell changes.

The present study was designed with the aim of providing a detailed characterisation of the changes in microglia in relation to astroglial responses within the peri-infarct tissue over the first 7 days following photochemically induced stroke in rats. A major focus of the study was to develop reliable measures that can be used to quantify the glial cell responses and evaluate the effectiveness of treatments aimed at modifying them.

The photothrombotic model of stroke was chosen for this study as it generates more reproducible and well-defined infarcts than most other models. It also allows the infarct to be targeted to specific regions such as the motor cortex to generate functional deficits that can be readily assessed. As a result, this model has been frequently used in studies investigating mechanisms of neuroplasticity underlying functional recovery following stroke.

There are perhaps two main difficulties to developing a quantitative approach to the characterisation of glial cell changes in the peri-infarct tissue. The first is the lack of quantifiable markers of microglial activation that can reliably measure microglial changes over an extended period of time. Previous studies have looked at changes in the expression of proteins associated with microglial activation such as interleukins, IL-1 β , IL-6, and IL-18, TNF- α and iNOS, or their mRNAs. However these changes are generally transient and their expression are often not specific to microglia. For example, although early upregulation of IL-1 β has been detected in microglia following focal ischemia, its expression peaked very rapidly and generally did not persist beyond 48 hours (Clausen et al. 2005; Lambertsen, Biber & Finsen 2012). In addition, upregulation of IL-1 β expression has also been detected in astroglia and neurons following ischemic stroke (Amantea, D. et al. 2010).

The second is the lack of a method to objectively and consistently identify the boundary between the infarct and peri-infarct tissue. Most studies have relied on histological stains such as cresyl-violet in alternate sections to identify the infarct boundary. However, this is an imprecise and unreliable approach as the differences in staining intensities between the infarct and peri-infarct tissue can be subtle at the early time points. At later time points, infiltration into the infarct by microglia and macrophages can also make the boundary difficult to identify.

In the present study, the above issues were addressed in part by adopting a direct approach of quantifying the morphological changes in microglial activation through the measurement of the circularity of cellular profiles in brain sections labelled for the microglial marker, Iba1. Further analysis of the physical parameters of microglial cells, including cell and soma sizes, provided additional information on the changes in microglial morphology during activation. Whereas changes in most of the protein markers associated with microglial activation tend to be transient or slow developing, the corresponding change in morphology occurs rapidly and persists even at 7 days after ischemia.

In addition, the area fractions for microglia and astroglia, in respectively Iba1 and vimentin-labelled brain sections, were used as composite measures of their responses to infarction in terms of cellular hypertrophy and changes in cell numbers as a result of cell death, proliferation and migration.

The infarct was identified by the loss of immunoreactivity to the neuronal marker NeuN and allowed for an unambiguous definition of the peri-infarct regions. NeuN immunolabelling revealed a well-defined boundary between the infarct and peri-infarct tissue across all the time-points investigated in this study.

The results from the study reveal that morphological changes in microglia can be detected as early as 3 hours following focal ischemia via assessment of the circularity of microglial profiles. In addition, these changes spread transiently to regions distant from the infarct at 24 hours within the ipsilateral cortex and persist up to 7 days within the immediate peri-infarct regions. Area fraction of Iba1 immunolabelling within the peri-infarct region exhibited an initial decrease at 24 hours followed by marked increases at 3 and 7 days. The microglial response was accompanied by a marked and progressive increase in the area fraction of vimentin immunolabelling from 24 hours to 7 days after stroke.

3.2 Materials and Methods

3.2.1 Experimental Design

The common materials and methods used in the experiments in this chapter have been described previously in chapter 2. Additional details and methods specific to this part of the study are provided in the following sections.

The photothrombotic model of stroke was characterised for the first 7 days after stroke induction by functional assessment, infarct volume measurement, immunohistochemical labelling and Western blot. A timeline of the experimental procedures is shown in figure 3.2.1.

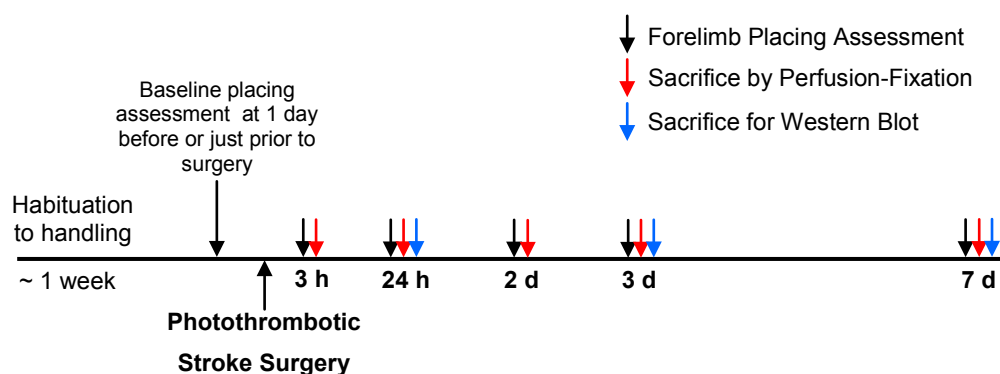


Figure 3.2.1 Experimental timeline for the characterisation of the photothrombotic stroke model.

All animals used in the experiments were habituated to handling during the week before photothrombotic stroke surgery. Baseline forelimb placing scores were assessed either on the day before surgery or just prior to surgery. Following surgery, the animals were assessed for inclusion at 3 h by forelimb placing scores (≤ 15). Forelimb placing scores were also assessed at 24 h, 2 d, 3 d and 7 d until the rats were sacrificed. Groups of animals were sacrificed by perfusion-fixation at each of the listed time points. Additional animals were also sacrificed at 24 h, 3 d and 7 d by decapitation for assessment by Western blots.

All animals were habituated (section 2.3.1) to handling during the week before photothrombotic stroke surgery in 10 min sessions on 3 separate days. Baseline forelimb placing scores of the rats were assessed (section 2.3.2) either on the day before surgery or just before the surgery. Following stroke surgery (section 2.3.3),

the rats were assessed again at 3 h by the forelimb placing assessment to ensure that the stroke surgery was successful. Only animals that scored 15 or less were included in this study. For the rats that met the inclusion criterion, recovery of function was further characterised by forelimb placing assessments that were conducted at 24 h, 2 d, 3 d and 7 d until the animals were sacrificed.

At each of the time points indicated, following forelimb placing assessments, animals were sacrificed by perfusion-fixation (section 2.3.4). The brains were then extracted and processed for cryosectioning (sections 2.3.5 & 2.3.6). The brain sections were then used for cresyl violet staining and immunohistochemical labelling.

The infarct volumes were determined from the cresyl violet stained sections (section 2.3.7) and changes in the microglial and astroglial responses were assessed from the immunolabelled sections. In addition, brain sections were taken from 3 h, 3 d and 7 d samples for the analysis of infarct visualisation by Nissl staining using NeuroTrace™ compared against immunolabelling for the neuron-specific marker NeuN (described below).

Brain sections were immunolabelled for Iba1 and vimentin to characterise the changes in microglial and astroglial responses following photothrombotic stroke as described in sections 2.3.8, 2.3.9 and 2.3.10.

Animals were also sacrificed by decapitation at 24 h, 3 d and 7 d for Western blots to assess the changes in the expression of astroglial markers GFAP and vimentin (section 2.3.11).

3.2.2 NeuroTrace Staining Vs. NeuN Immunolabelling

Visualisation of the infarct by Nissl staining is compared against immunolabelling for NeuN by co-labelling using NeuroTrace™, a fluorescent Nissl stain, with an anti-NeuN antibody. The co-labelling was performed using slide-mounted sections from 3 h, 3 d and 7 d samples. The antibodies and NeuroTrace stain used are listed in table 3.2.1.

The slide-mounted sections were rehydrated by washing twice in PBS for 10 min each time. The sections were blocked and permeabilised in blocking buffer for 1 h at room temperature. Anti-NeuN antibody was diluted in blocking buffer and the

sections were incubated overnight at room temperature. Following incubation in primary antibody, the sections were washed 4 times in PBS for 10 min each time. Secondary antibody and NeuroTrace stain were diluted in PBS and the sections were incubated for 3 h at room temperature. The sections were washed 4 times in PBS for 10 min each time, then mounted in Prolong[®] Gold antifade mountant and coverslipped. Fluorescence images of the immunolabelled sections were taken on the Olympus IX71 microscope.

Table 3.2.1 List of antibodies, stains and dilutions used for NeuroTrace and NeuN co-labelling

Description	Dilution	Catalogue #	Supplier
Donkey anti-Mouse IgG (H+L) Alexa Fluor [®] 647 conjugate	1:500	A-31571	ThermoFisher / Invitrogen [™]
Mouse monoclonal anti-NeuN [Clone A60]	1:200	MAB377	Millipore / Chemicon [®]
NeuroTrace [™] 500/525 Green Fluorescent Nissl Stain	1:100	N-21480	ThermoFisher / Molecular Probes [™]

3.2.3 Additional Analysis of Changes in Microglial Response to Photothrombotic Stroke

In addition to the analysis for microglial circularity and area fraction using ImageJ as described in section 2.3.10, further analysis was performed using the image analysis software, "NeuroLucida" (version 8; MBF Bioscience, VT, USA).

Images were acquired from Iba1-immunolabelled sections of 24 h and 7 d brain samples at the positions "Ipsi01A", "Ipsi01B" and "Contra01" (see figure 2.3.5 in section 2.3.9). These images were then analysed for the morphological measures of cell area, soma area and cell perimeter. These are alternative indicators of the changes in microglial morphology during activation that provide additional morphological data and complement the results from circularity analysis using ImageJ. The time points 24 h and 7 d were selected for the additional analyses as the change in microglial circularity was already maximal at 24 h and has started to return to baseline at 7 d.

3.3 Results

3.3.1 Infarct Volume

Using cresyl violet staining, the infarct was detectable as early as 3 h after stroke induction. The infarct reached maximum volume by 24 h and contracted significantly by 7 days (figure 3.3.1).

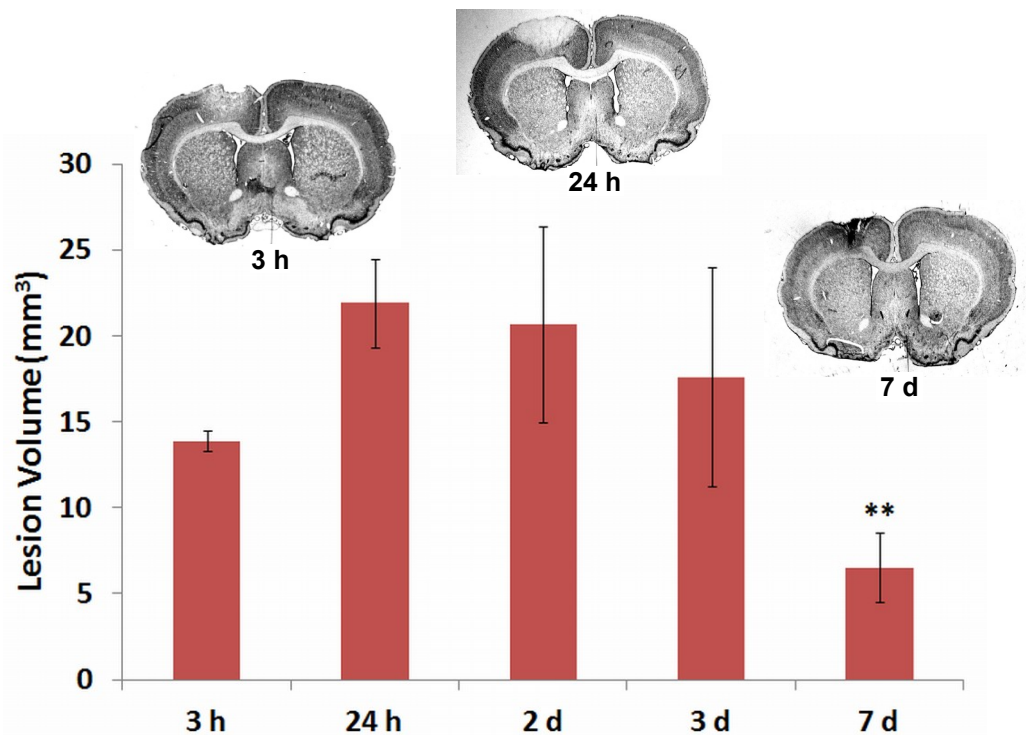


Figure 3.3.1 Volume of infarct following photothrombotic stroke induction.

The infarct as defined by the lack of or weaker staining of cresyl violet was detected at 3 h after stroke induction, reached maximum volume by 24 h and contracted significantly by 7 d (** $p < 0.01$, vs. all other time points, One-way ANOVA with Tukey's HSD). Values are shown as mean \pm SD ($n = 4 - 6$ per time point). Representative images of cresyl violet-stained sections at 3 h, 24 h and 7 d after stroke are shown in the insets.

NeuN immunolabelling was used to identify the boundary between the infarct core and peri-infarct tissue in all parts of the study involving immunohistochemistry as it was a highly sensitive marker of neuronal loss. As a comparison, brain sections from 3 h, 3 d and 7 d after stroke were immunolabelled for NeuN and counterstained with NeuroTrace™, a fluorescent Nissl stain (figure 3.3.2).

In all the cases examined, NeuN immunolabelling provided a clear distinction between the infarct core and the peri-infarct regions. Although it was possible to detect the infarct through NeuroTrace staining at all 3 time points, it was difficult to define the boundary of the infarct. NeuroTrace also appeared to underestimate the region of neuronal loss, especially at the base of the infarct.

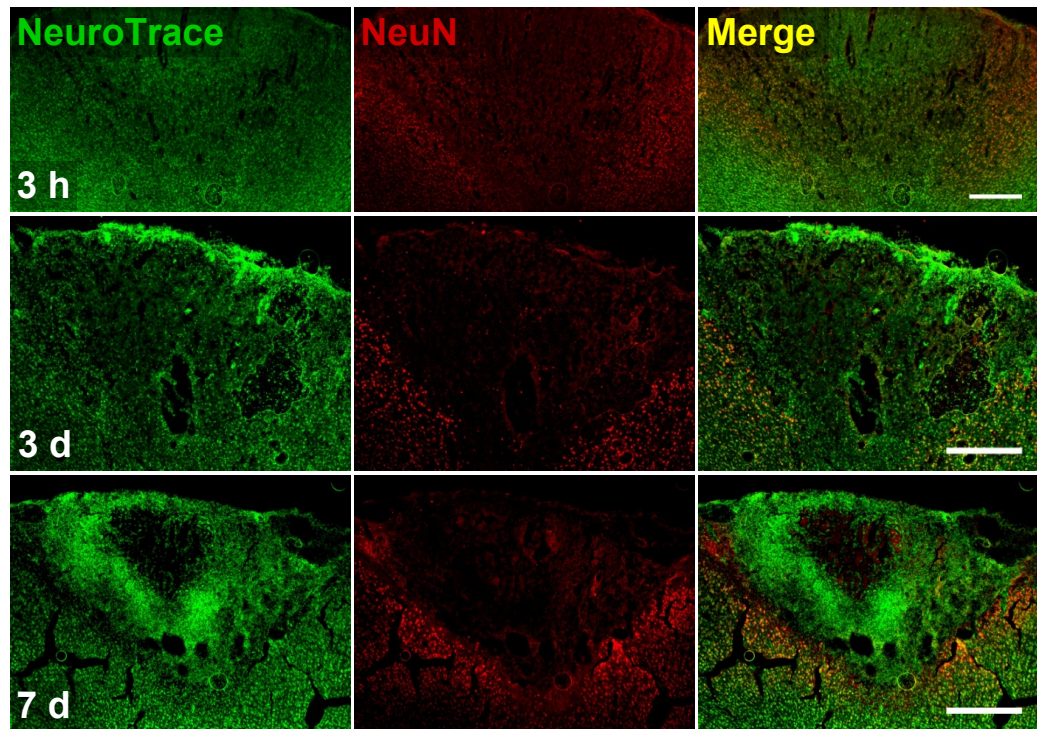


Figure 3.3.2 Comparison between NeuroTrace™ Nissl staining and NeuN immunolabelling.

Although it was possible to detect the infarct using either NeuroTrace staining or NeuN immunolabelling, the loss of NeuN immunoreactivity more clearly defined the infarct border (scale bar = 500 μ m).

3.3.2 Forelimb Placing Reflex

The development of the infarct was accompanied by a measurable impairment of the placing reflex of the affected (contralateral) forelimb (figure 3.3.3). The impairment could be detected by 3 h after stroke and the placing score of the affected (contralateral) forelimb at this time was used as the inclusion criterion for the study. Although, the inclusion criterion was set at a placing score of 15 or less for this part of the study, most of the animals that have met the criterion have in fact scored 5 or less (21 of 29 animals).

The deficit in the placing reflex was most severe at between 3 h and 2 d post-stroke and partial recovery was observed at 3 and 7 d after stroke.

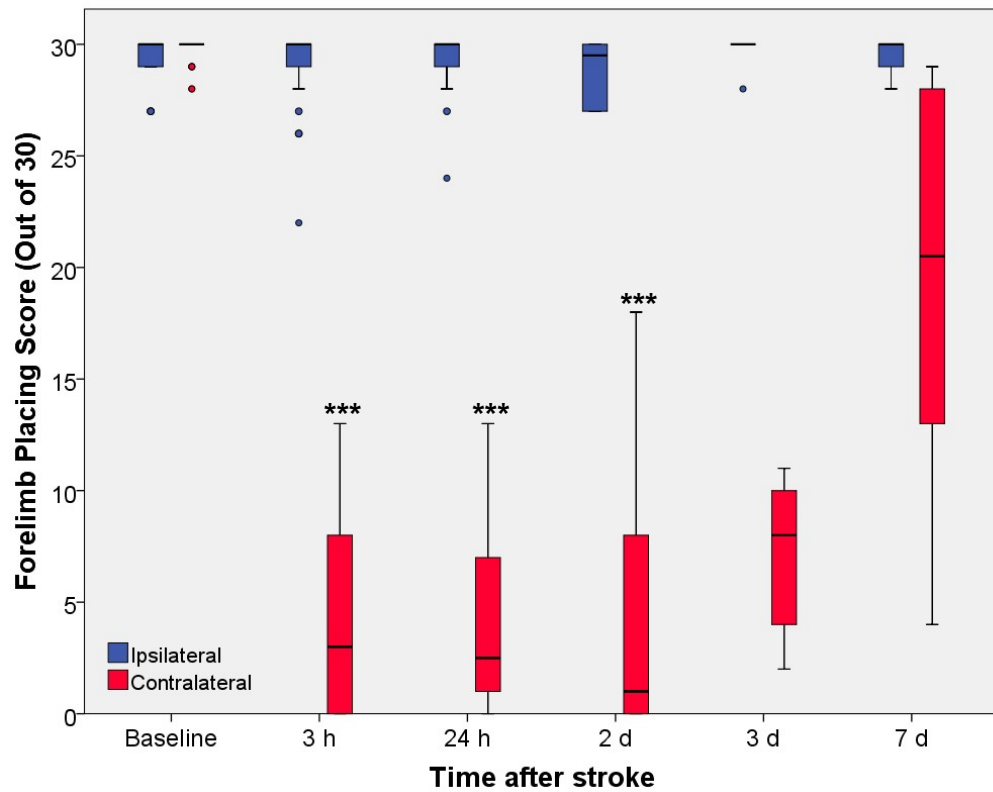


Figure 3.3.3 Forelimb placing scores following stroke induction.

Impairment of placing reflex of the affected forelimb was easily detected by 3 h after stroke induction and remained markedly impaired up to 2 d after stroke (** $p < 0.001$ vs. *Baseline*, *Kruskal-Wallis test*, *pair-wise comparison with Bonferroni correction*). The data is presented in a box plot with outliers shown in circles ($n \geq 5$ per time point).

3.3.3 Microglial Response – Circularity

Increased circularity as a result of process retraction was used as a measure of morphological changes associated with microglial activation in the brain sections. Iba1-immunolabelled brain sections were scanned using confocal microscopy at several locations in both the ipsilateral and contralateral cortices (figure 3.3.4). Maximum projections of z-stacks were thresholded and the average circularity of microglial cells within each image field was determined using the “Analyze Particles” function in ImageJ.

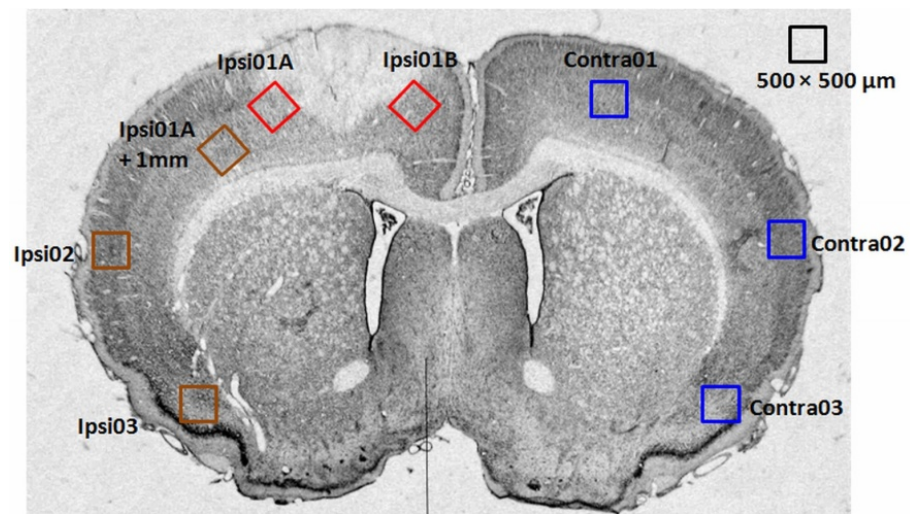


Figure 3.3.4 Locations within each brain section analyzed for microglial changes after stroke.

Z-stacks were scanned using confocal microscopy at the 8 locations in each brain section as shown. Microglial changes were analyzed within a 500 μ m by 500 μ m ROI at each location.

i. 3 Hours Post-Stroke

At just 3 h after stroke induction, the circularity of microglial cells in the peri-infarct regions on either side of the infarct at "Ipsi01A" and "Ipsi01B" had become significantly higher than in the corresponding contralateral region at "Contra01" (figure 3.3.5). The circularity of microglia in other regions was unaffected at this time.

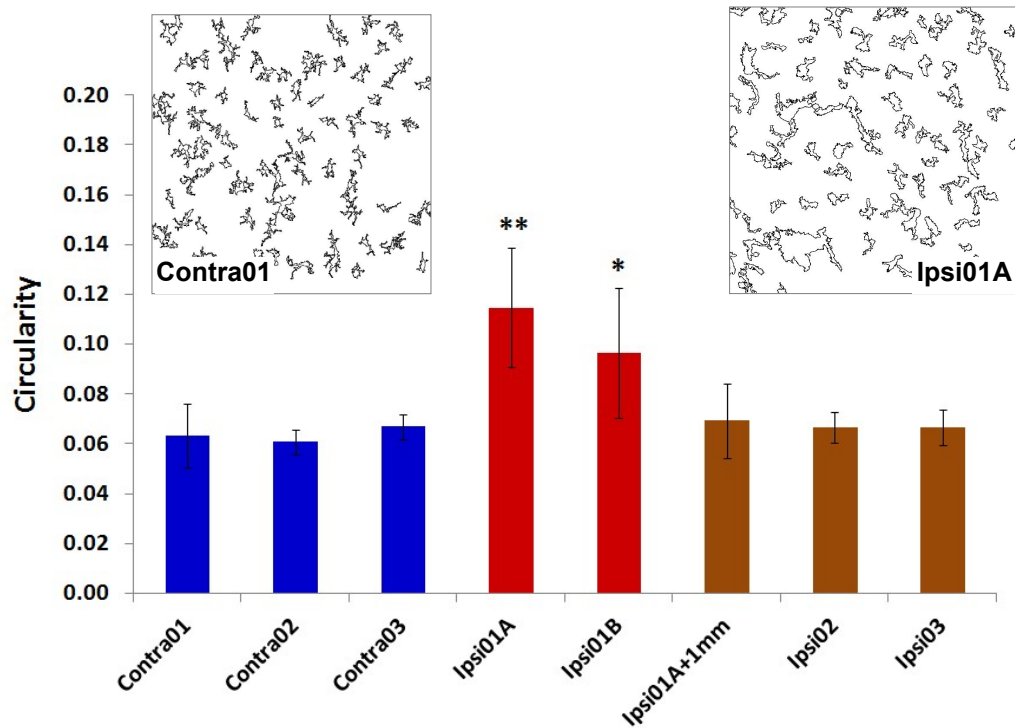


Figure 3.3.5 Microglia circularity at 3 hours after stroke induction.

Changes in microglial morphology as determined by the circularity parameter could be detected in the peri-infarct regions at just 3 h after stroke ($*p < 0.05$, $**p < 0.01$ vs. "Contra01", *One-way ANOVA with Tukey's HSD*). Values are shown as mean \pm SD (n = 4). Representative images of microglia outlines in the "Contra01" and "Ipsi01A" regions are shown in the insets.

ii. 24 Hours Post-Stroke

At 24 hours the circularity of peri-infarct ("Ipsi01A" and "Ipsi01B") microglia had further increased. The changes in microglia morphology in the ipsilateral cortex had also spread further out and even distant regions approximately 4 to 5 mm away ("Ipsi02") exhibited significantly higher circularities than contralateral regions (figure 3.3.6).

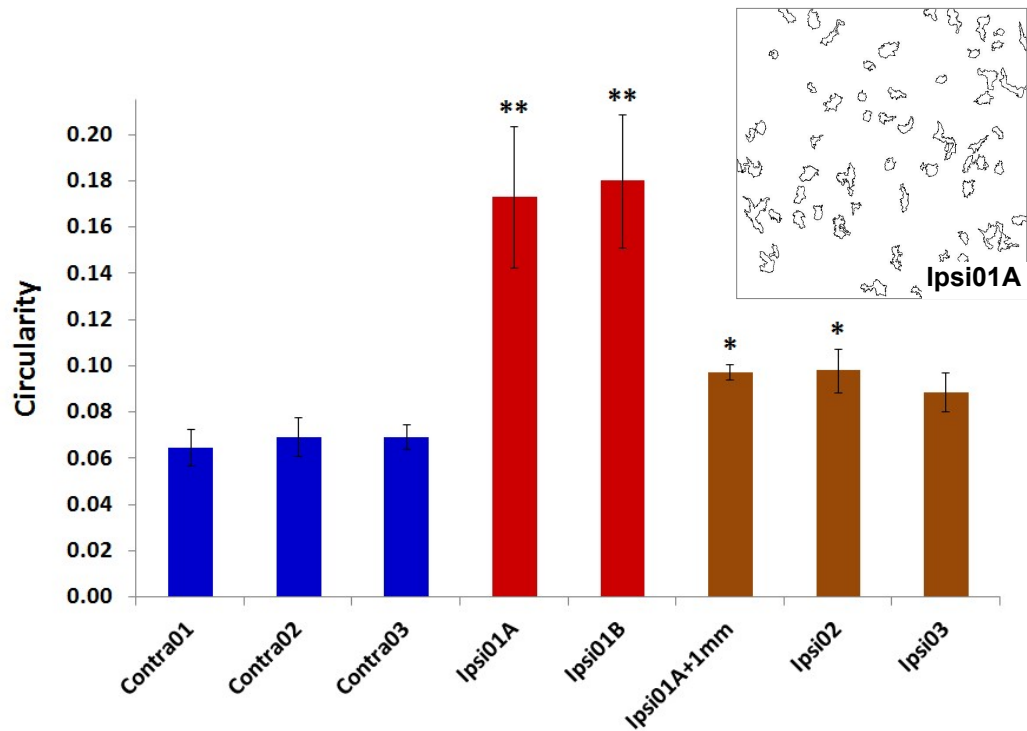


Figure 3.3.6 Microglia circularity at 24 hours after stroke induction.

At 24 h, circularity of the peri-infarct microglia had further increased and these changes had also spread to distant regions of the ipsilateral cortex ($*p < 0.05$, $**p < 0.01$ vs. corresponding contralateral regions, One-way ANOVA with Tukey's HSD). Values are shown as mean \pm SD (n = 4). A representative image of microglia outlines in the "Ipsi01A" region is shown in the inset.

iii. Time-course

At 3 d the increase in the circularity of the peri-infarct microglia persisted, but the changes at distant regions observed at 24 h had reversed and returned to levels comparable to the contralateral cortex. Circularity was still elevated within the peri-infarct region at 3 d and even though there was a decrease by 7 d, it remained significantly higher than the contralateral cortex (figure 3.3.7).

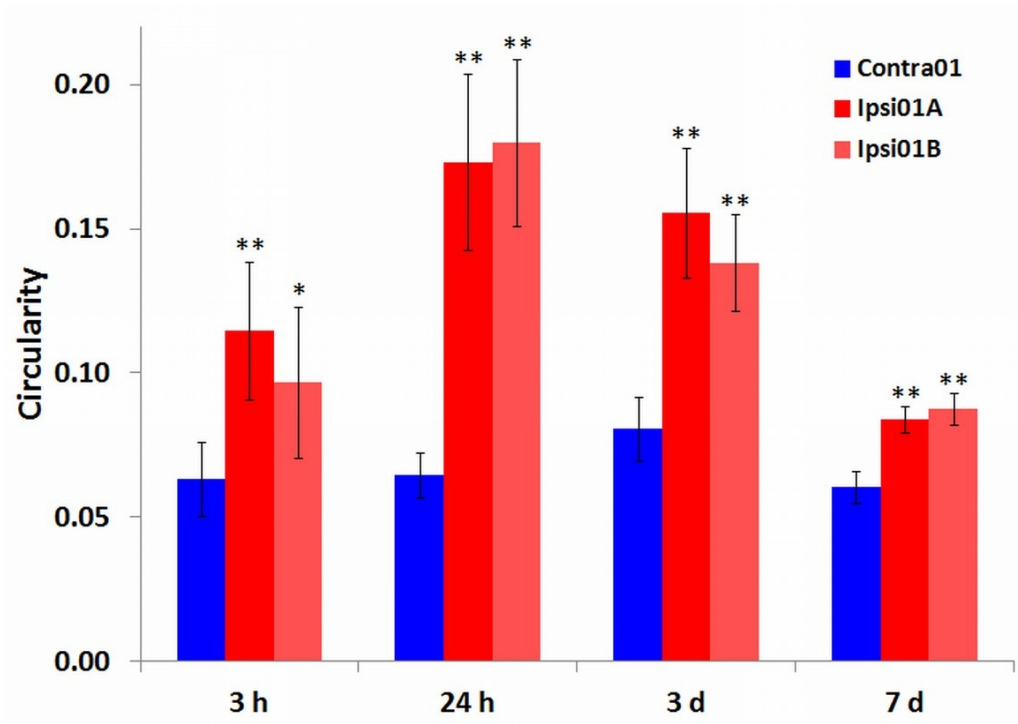


Figure 3.3.7 Time-course of changes in microglial circularity after stroke induction. Circularity of microglia in the peri-infarct regions remained significantly higher than the contralateral regions up to 7 d after stroke (* $p < 0.05$, ** $p < 0.01$ vs. "Contra01", One-way ANOVA with Tukey's HSD). Values are shown as mean \pm SD (n = 4).

3.3.4 Microglial Response – Area Fraction

Microglial area fraction was used as a measure of changes including cellular hypertrophy and increase in cell numbers as a result of migration and proliferation that are the typical responses of microglia to stroke. The area fraction was determined at the same locations as described previously (see figure 3.3.4 above) using the same procedure for analysis as for circularity.

i. 3 Hours Post-Stroke

At 3 h after stroke induction the distribution of microglia as assessed by area fraction around the peri-infarct and other ipsilateral cortical regions were unaffected and very similar to that in the contralateral regions (figure 3.3.8). Microglial cells within the peri-infarct appear to have enlarged cell soma but overall area fractions within those regions were not significantly different from the contralateral regions (see figure 3.3.8 insets).

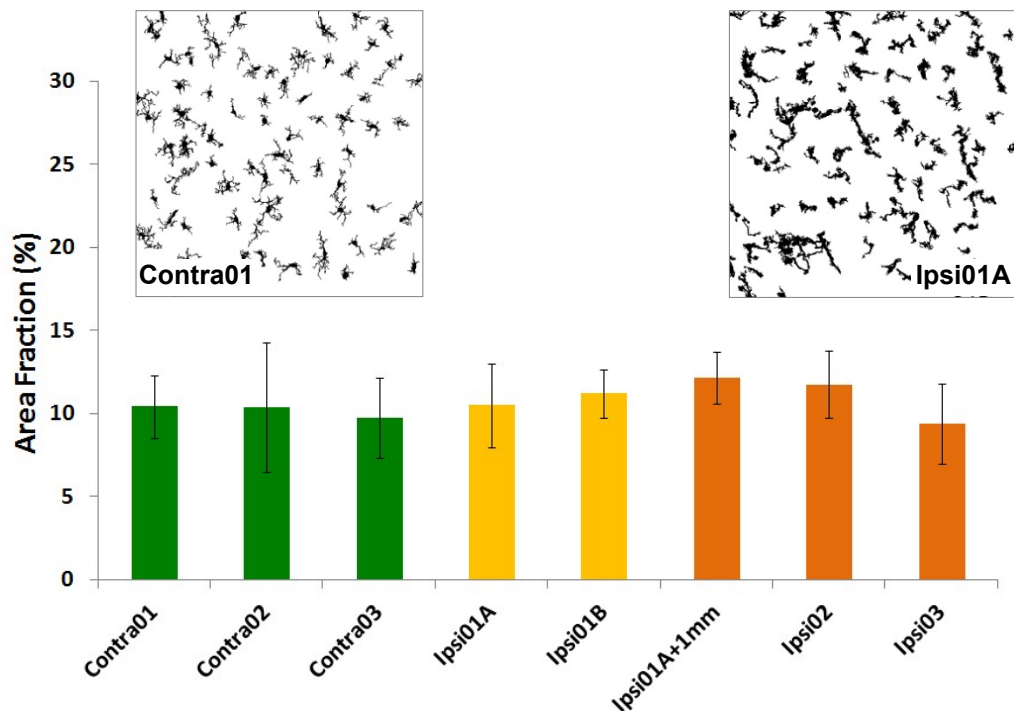


Figure 3.3.8 Microglia area fraction at 3 hours after stroke induction.

Distribution of microglia as assessed by area fraction was relatively uniform and unchanged across the contralateral and ipsilateral regions, although microglial cells appeared hypertrophic within the peri-infarct regions. Values are shown as mean \pm SD ($n = 4$). Representative images of microglia masks in the "Contra01" and "Ipsi01A" regions are shown in the insets.

ii. 24 Hours Post-Stroke

At 24 h, there was a decrease in the peri-infarct microglia area fraction relative to the neighbouring ipsilateral regions (figure 3.3.9). This decrease in microglia area fractions in the peri-infarct regions at 24 h was also observed in the minocycline studies (see section 4.3.1.4) where similar decreases in the peri-infarct microglia area fraction were detected in both the vehicle and minocycline-treated groups. The cell soma appears to be enlarged at this time, similar to observations at 3 h. This was confirmed by additional morphological analysis in section 3.3.6 (figure 3.3.14) that revealed an increase in the soma area of peri-infarct microglial cells at 24 h post-stroke.

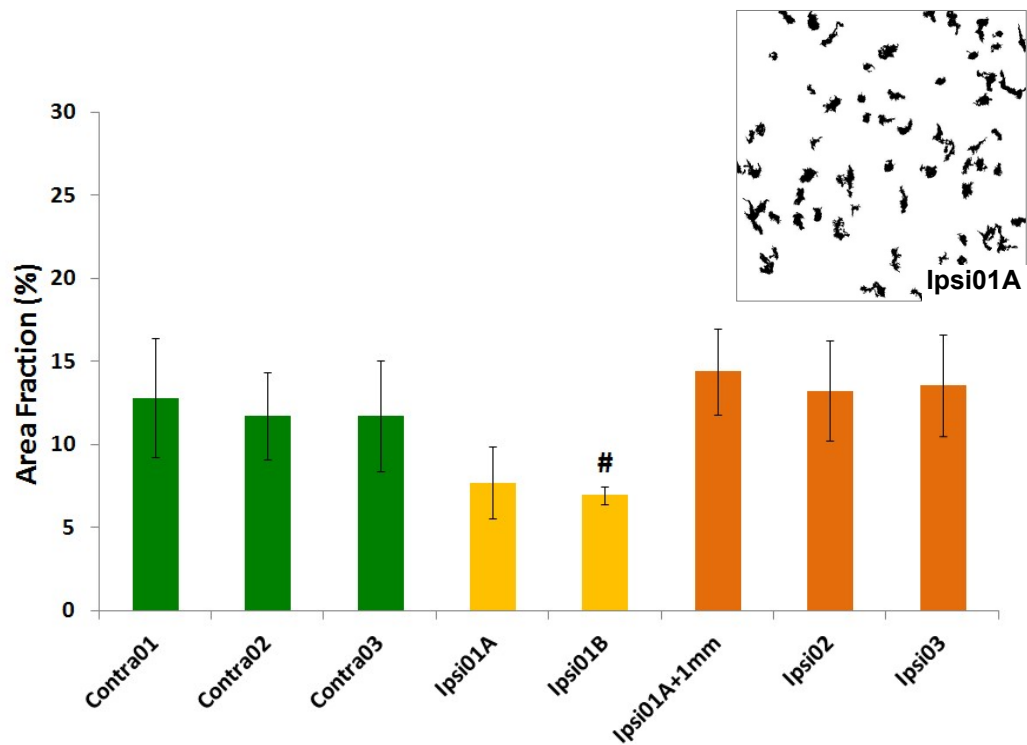


Figure 3.3.9 Microglia area fraction at 24 hours after stroke induction.

At 24 h, area fraction of microglia in the peri-infarct region was decreased relative to neighbouring ipsilateral regions ($^{\#}p < 0.05$ vs. "Ipsi01A+1mm", One-way ANOVA with Tukey's HSD). Values are shown as mean \pm SD (n = 4). A representative image of the microglia masks in the "Ipsi01A" region is shown in the inset.

iii. Time-course

At 3 d, the area fraction of peri-infarct microglia had recovered and became higher than the contralateral regions. Further increases were observed at 7 d after stroke (figure 3.3.10).

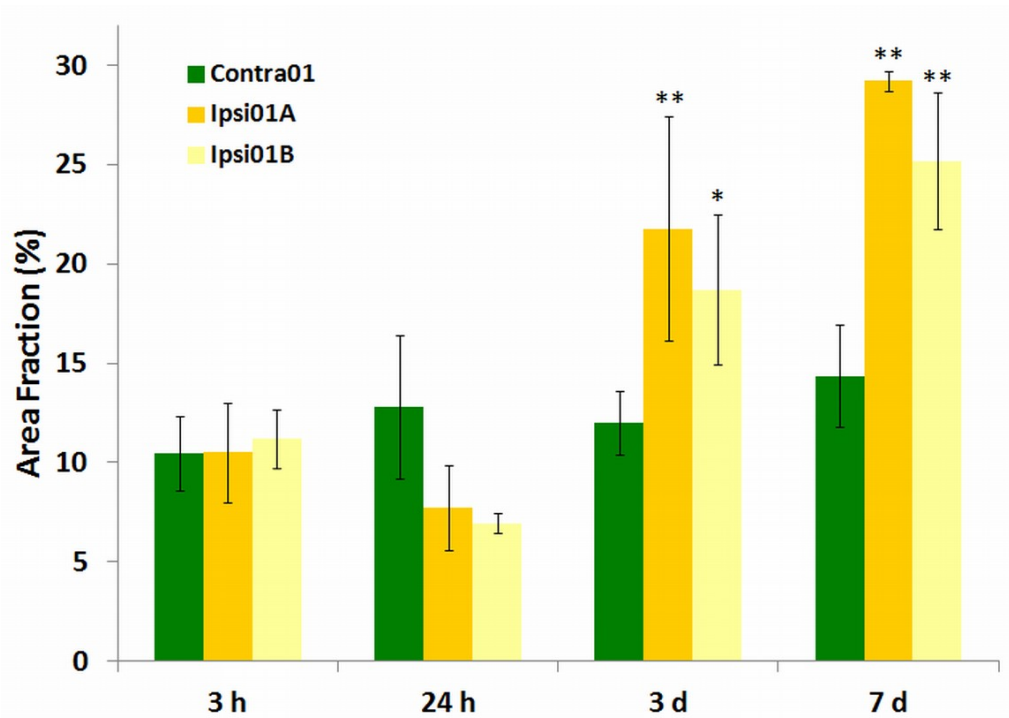


Figure 3.3.10 Time-course of changes in microglial area fraction after stroke induction.

Area fraction of microglia in the peri-infarct region had increased at 3 d and 7 d after stroke ($*p < 0.05$, $**p < 0.01$ vs. "Contra01", One-way ANOVA with Tukey's HSD). Values are shown as mean \pm SD (n = 4).

3.3.5 Microglial Response – Particle Count & Average Size

Counts of Iba1-immunolabelled particles (figure 3.3.11) and their average sizes (figure 3.3.12) in each of the ROIs (500 by 500 μm) were also determined from the ImageJ analysis. These data provided an indication of the changes in microglial cell numbers and their sizes following stroke. Only the data from "Contra01", "Ipsi01A" and "Ipsi01B" are shown as the other regions did not exhibit significant changes.

The data from the particle counts and particle area revealed that the decrease in microglial area fraction within the peri-infarct regions, "Ipsi01A" and "Ipsi01B", at 24 h after stroke was due primarily to a decrease in microglial cell numbers. Similarly, the increase in area fraction within the same regions at 3 d was due to increases in microglial cell numbers. Double-immunolabelling of Iba1 with Ki67, a cell proliferation marker, shows that the increase in microglial cell numbers was due, at least in part, to proliferation *in situ* (figure 3.3.13).

Particle counts became unreliable at 7 d after stroke due to the high microglial cell densities within the peri-infarct regions. This high density meant that a large proportion of the cellular profiles overlapped or were in contact and as a result were mis-identified by the ImageJ software as single large particles. This can be seen from the large increase in the average particle size within the peri-infarct regions at 7 d.

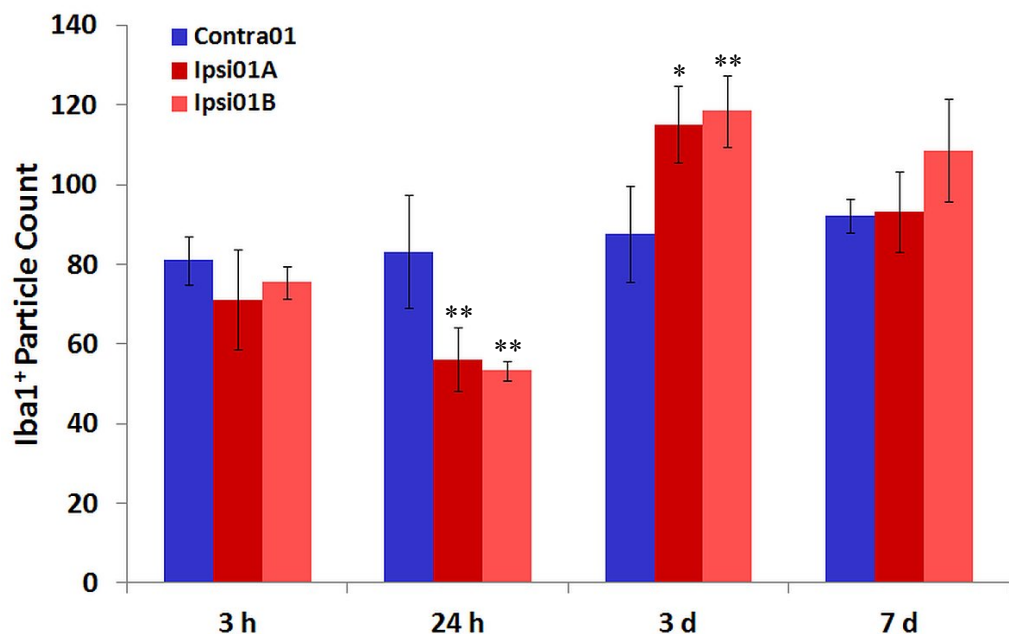


Figure 3.3.11 Particle counts of Iba1-immunolabelled particles within the peri-infarct and corresponding contralateral regions after photothrombotic stroke.

Following photothrombotic stroke, the Iba1⁺ particle counts within the peri-infarct regions, "Ipsi01A" and "Ipsi01B", decreased initially at 24 h but became elevated at 3 d compared to the corresponding contralateral regions (* $p < 0.05$, ** $p < 0.01$ vs. "Contra01", One-way ANOVA with Tukey's HSD). Values are shown as mean \pm SD (n = 4).

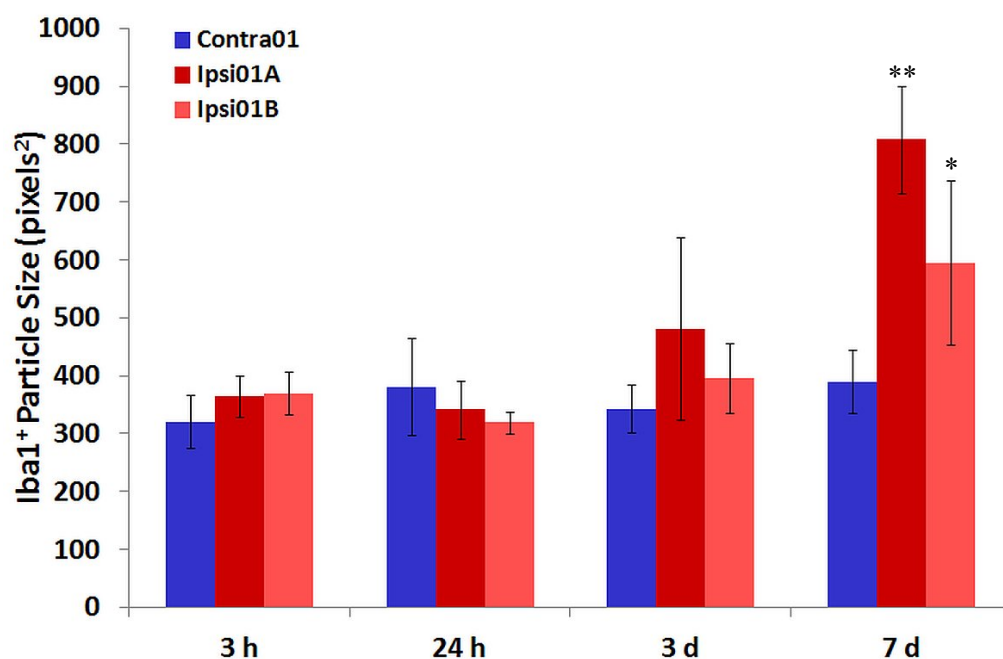


Figure 3.3.12 Average size of Iba1-immunolabelled particles within the peri-infarct and corresponding contralateral regions after photothrombotic stroke.

The size of the Iba⁺ particles within the peri-infarct regions, "Ipsi01A" and "Ipsi01B", were not significantly different compared to those within the corresponding regions at up to 3 d after stroke. However, at 7 d there was a marked increase in the peri-infarct particle size relative to the contralateral region ($*p < 0.05$, $***p < 0.01$ vs. "Contra01", *One-way ANOVA with Tukey's HSD*). Values are shown as mean \pm SD (n = 4).

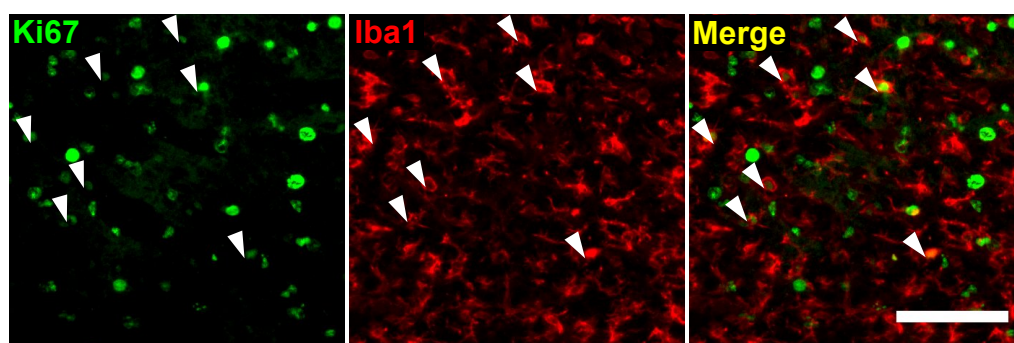


Figure 3.3.13 Co-localisation of Ki67 and Iba1 within the peri-infarct tissue at 3 days after stroke.

The fluorescence images show co-localisation (arrowheads) of the proliferation marker, Ki67, with microglial marker, Iba1. Representative images from the peri-infarct region, "Ipsi01A", of a 3 d brain sample are shown (scale bar = 100 μ m).

3.3.6 Microglial Response – Additional Analysis

Additional analysis was performed using the image analysis software, "Neurolucida" (section 3.2.2), to measure the changes in the morphological parameters of cell area, soma area and cell perimeter. These are alternative measures to circularity (section 3.3.3) that provided additional information on the changes in microglial morphology during activation.

Microglial cell area within the peri-infarct regions, "Ipsi01A and "Ipsi01B", was decreased compared to the corresponding contralateral region, "Contra01", at 24 h and these changes persisted at 7 d after stroke (figure 3.3.14). In contrast, the soma area of peri-infarct microglial cells increased at 24 h but returned to values that were similar to that within the contralateral regions by 7 d (figure 3.3.15). Microglial cell perimeter exhibited changes that were similar to the cell area. The perimeter of microglial cells within the peri-infarct regions were decreased at both 24 h and 7 d after stroke (figure 3.3.16).

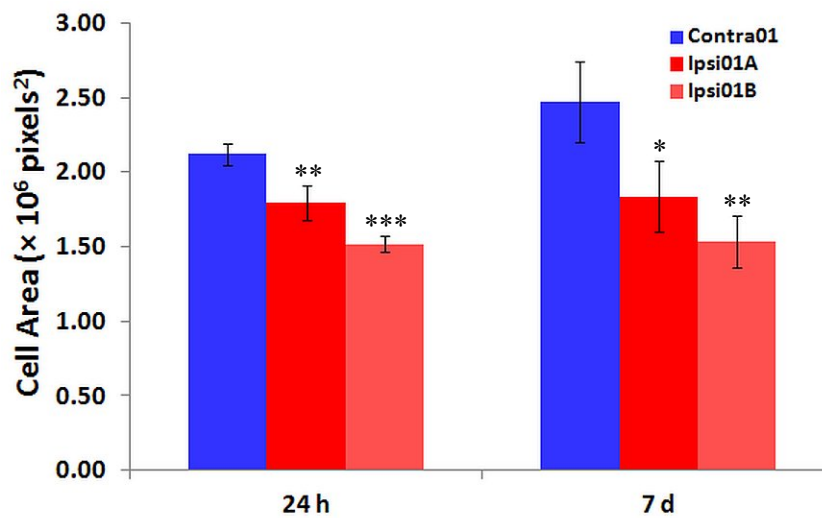


Figure 3.3.14 Microglial cell area at 24 hours and 7 days after stroke.

One-way analysis of variance at each of the time points revealed significant differences between the cell area of microglia within the peri-infarct regions, "Ipsi01A" and "Ipsi01B", and the corresponding contralateral region "Contra01" ($*p < 0.05$, $**p < 0.01$, $***p < 0.001$, vs. *Contra01*, One-way ANOVA with Tukey's HSD). Values are shown as mean \pm SD (n = 3 - 4 per group).

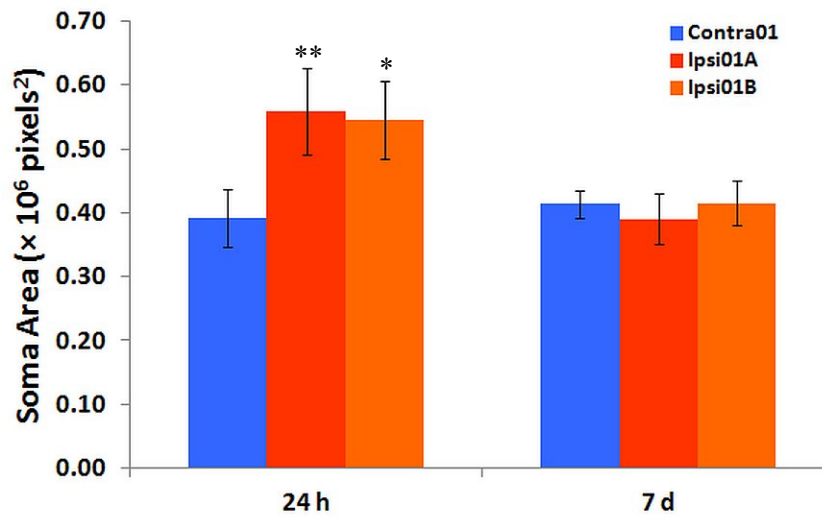


Figure 3.3.15 Microglial soma area at 24 hours and 7 days after stroke.

One-way analysis of variance revealed significant differences between the soma area of microglial cells within the peri-infarct regions and the corresponding contralateral region at 24 h, but not at 7 d after stroke ($*p < 0.05$, $*p < 0.01$, vs. *Contra01*, *One-way ANOVA with Tukey's HSD*). Values are shown as mean \pm SD (n = 3 - 4 per group).

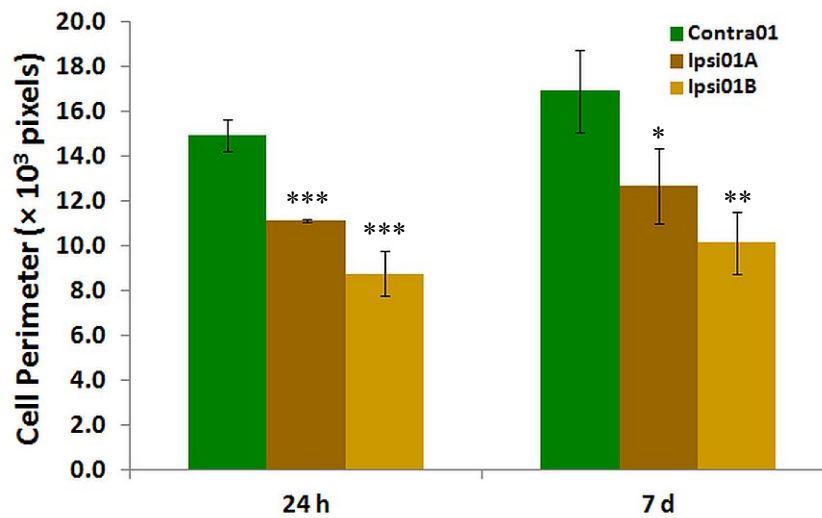


Figure 3.3.16 Microglial cell perimeter at 24 hours and 7 days after stroke.

One-way analysis of variance at each of the time points revealed significant differences between the cell perimeter of microglia within the peri-infarct regions and the corresponding contralateral region ($*p < 0.05$, $**p < 0.01$, $***p < 0.001$, vs. *Contra01*, *One-way ANOVA with Tukey's HSD*). Values are shown as mean \pm SD (n = 3 - 4 per group).

3.3.7 Astroglial Response

The astroglial response to the photothrombotic stroke was assessed by vimentin immunolabelling in the brain sections. Vimentin is not normally expressed in cortical astroglia but is strongly upregulated in reactive astroglial cells following stroke (figure 3.3.17 A & B). Upregulation of vimentin expression is most marked within the peri-infarct tissue but can be detected even at distant regions within the ipsilateral cortex (figure 3.3.17 C).

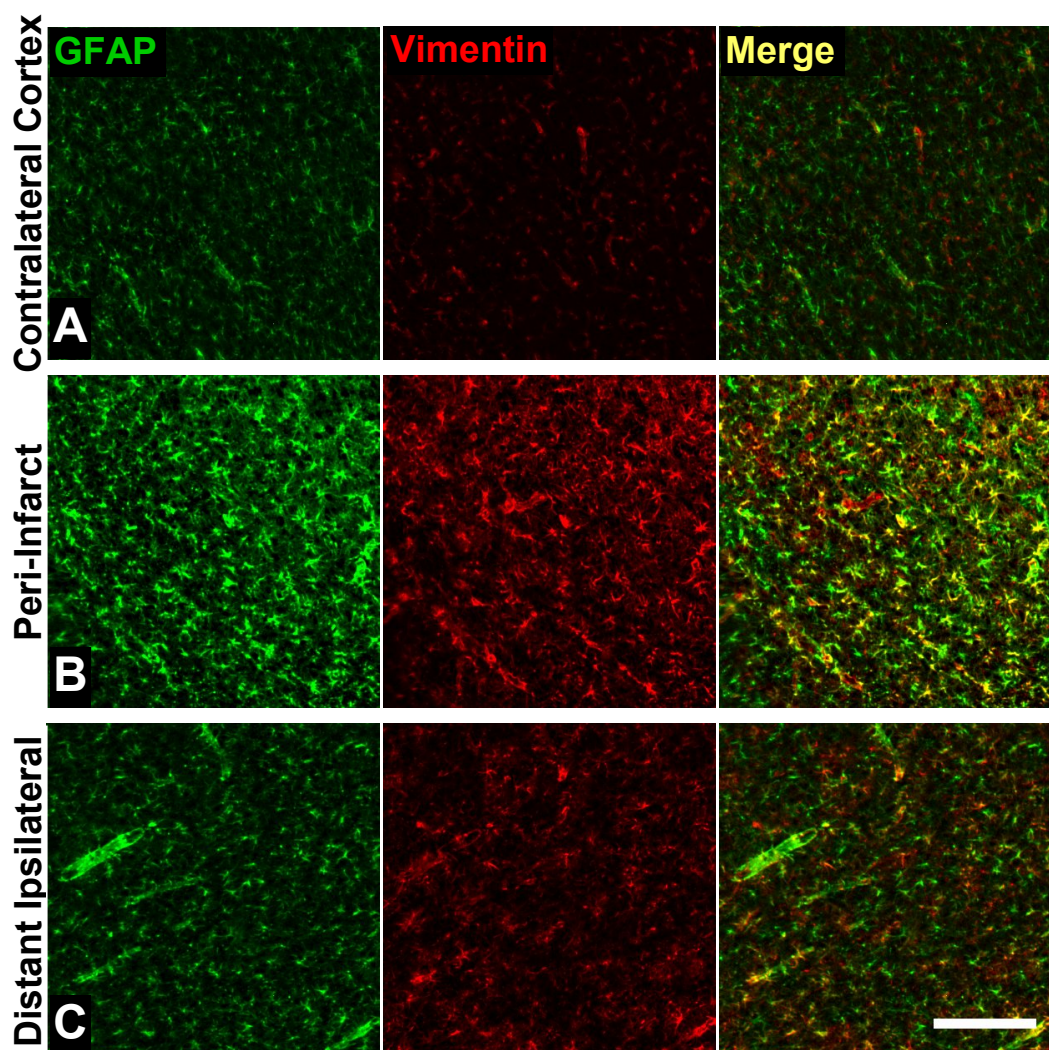


Figure 3.3.17 GFAP and vimentin expression at 3 days after stroke.

(A) Vimentin immunolabelling identifies only blood vessels within the contralateral cortex at 3 d after stroke. (B) Within the peri-infarct tissue vimentin is strongly upregulated and predominantly co-expressed with GFAP in reactive astroglial cells. (C) Within the ipsilateral cortex, vimentin expression can also be detected in astroglial cells in tissue regions that are distant from infarct (scale bar = 200 μ m).

Initial expression of vimentin was limited to the subcortical regions and to the blood vessels within the cortex. This was mostly unchanged at 3 and 24 h after stroke induction. By 2 d after stroke, there was a clear upregulation in vimentin expression in the peri-infarct and fluorescent labelling intensity increased further at 3 and 7 d after stroke (figure 3.3.14).

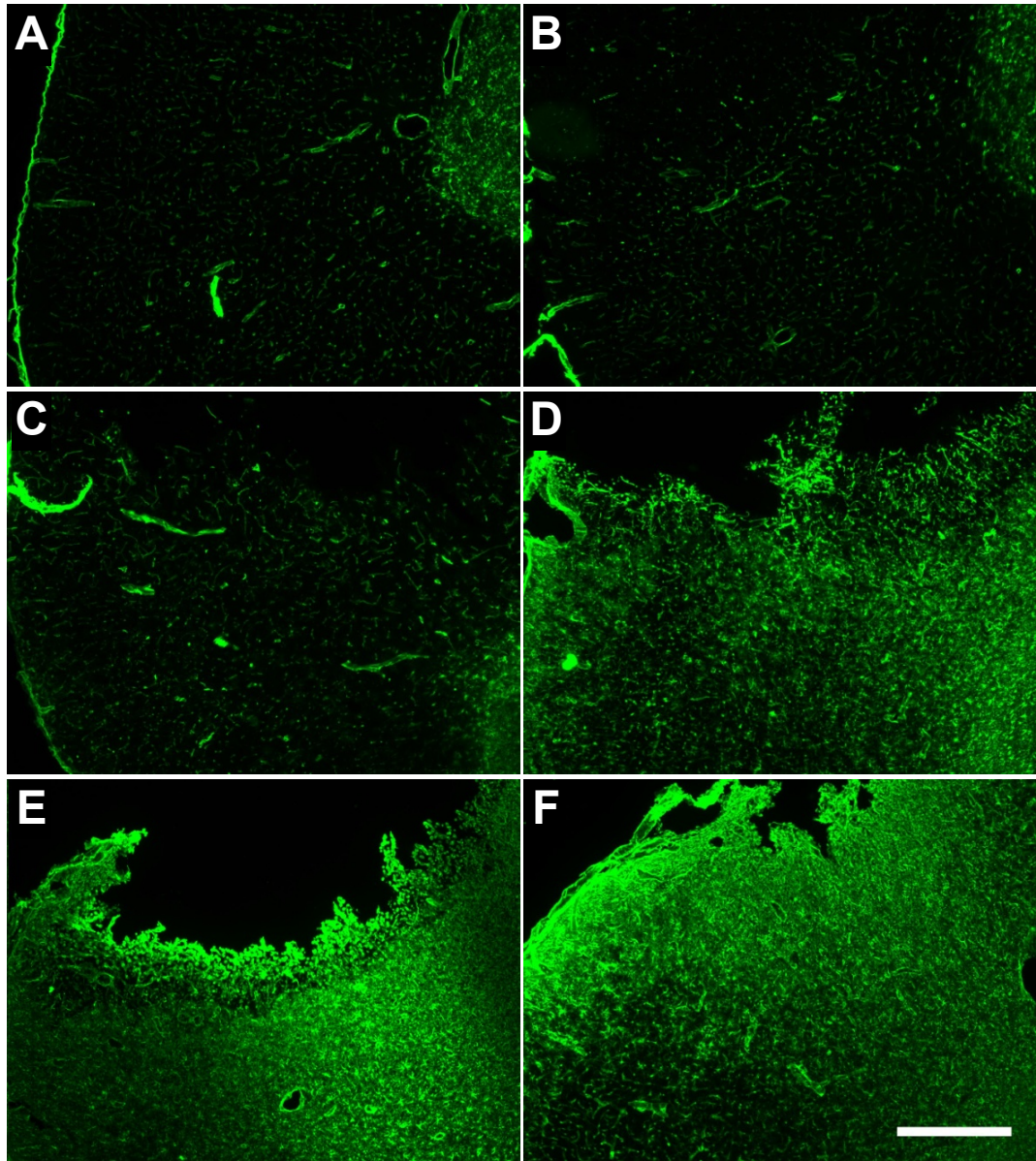


Figure 3.3.17 Representative fluorescence images of vimentin-immunolabelled sections at different time-points after stroke induction.

Images are shown for (A) Contralateral cortex at 3 h after stroke, (B, C) ipsilateral cortex at 3 and 24 h after stroke, and (D, E & F) ipsilateral cortex at 2, 3 and 7 d after stroke (scale bar = 500 μ m).

Vimentin area fraction was unaffected at 3 h but a small increase could be detected in the peri-infarct region at 24 h after stroke. Further marked increases were detected from 2 to 7 d after stroke (figure 3.3.15).

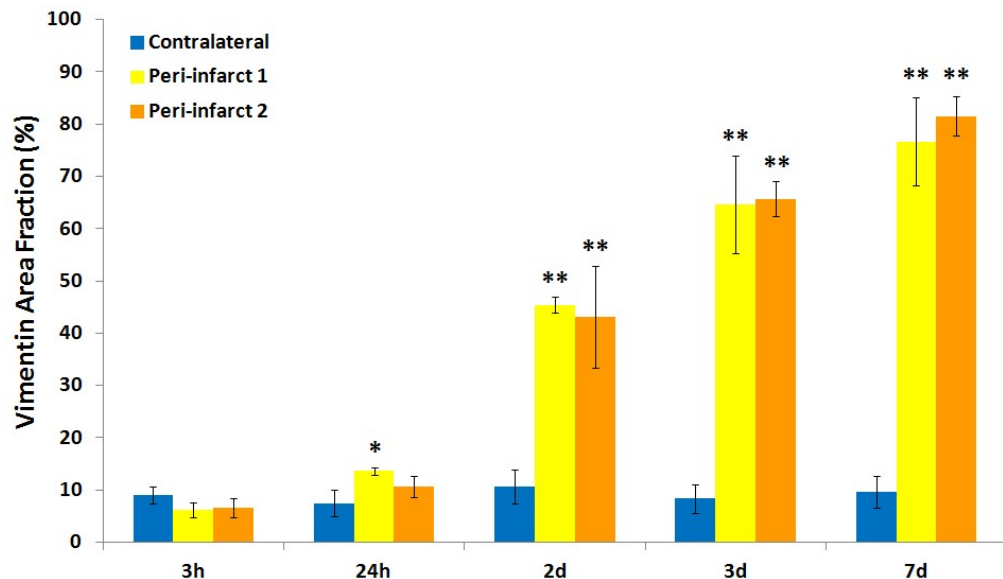


Figure 3.3.18 Increase in vimentin area fraction in the peri-infarct after stroke induction.

Vimentin area fraction in the peri-infarct regions were mostly unchanged between 3 and 24 h after stroke, but became significantly higher than the contralateral region by 2 d and continued to increase out to 7 d (* $p < 0.05$, ** $p < 0.01$ vs. *contralateral regions*, *One-way ANOVA with Tukey's HSD*). Values are shown as mean \pm SD (n = 4).

In agreement with the results from the vimentin area fraction analysis, Western blots for vimentin also revealed a striking increase in the density of the bands for the peri-infarct tissue samples at 3 d and 7 d after stroke (figure 3.3.18 A). Western blots for GFAP also showed a similar, albeit less marked increase over the same time period (figure 3.3.18 B)

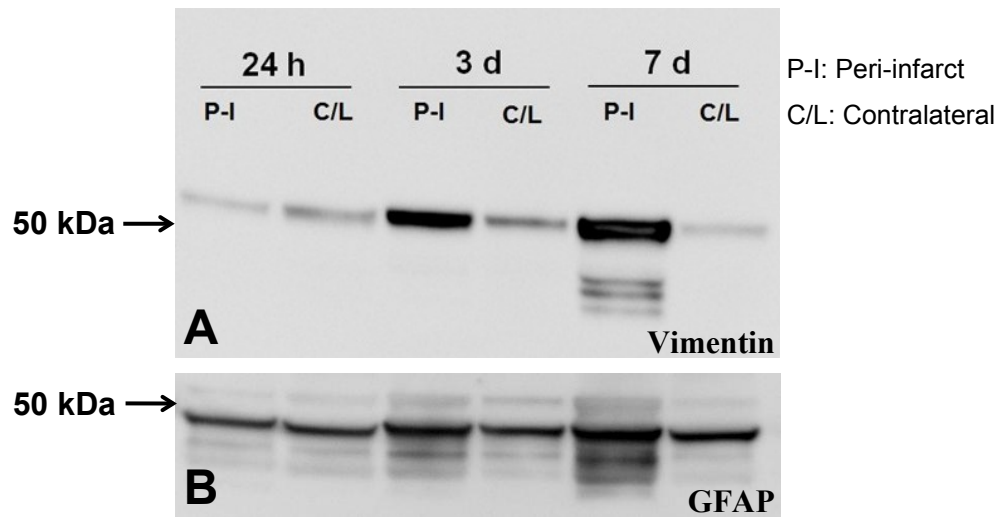


Figure 3.3.19 Western blots for Vimentin and GFAP following photothrombotic stroke.

Representative blots for (A) Vimentin, and (B) GFAP are shown for the peri-infarct and contralateral tissue from brain samples taken at 24 h, 3 d and 7 d after photothrombotic stroke. The blots reveal a progressive increase in the expression of both proteins within the peri-infarct tissue after stroke. The increase is especially marked for vimentin which is expressed at low levels within the contralateral tissue.

3.4 Discussion

There has in recent years been an increasing interest in understanding the nature of glial cell responses following stroke and their role in the facilitation of recovery. However, despite the widespread use of various animal models in the study of stroke in the previous decades, the glial cell responses in these models are still incompletely characterised. This is especially true of quantitative data that may be invaluable in the objective assessment of interventions targeting these responses.

In the present study, we have characterised the responses of microglia and astroglia following photothrombotic stroke using a quantitative approach that assessed changes in both morphology and cell numbers. Our characterisation of the microglial responses revealed a nearly 3-fold increase in the peri-infarct area fraction over the first 7 days and changes in circularity indicative of activation as early as 3 hours following stroke. These results were broadly consistent with previous studies that reported microglial activation within the first 1 – 2 days and subsequent increases in microglial cell density around the infarct (Li, H et al. 2014; Nowicka et al. 2008; Schroeter, Jander & Stoll 2002). However, using our quantitative approach, we were able to detect these changes at a much earlier time point. In addition, we have also detected a previously unreported loss in peri-infarct microglia at 24 hours following stroke.

As discussed in the introduction, the process of microglial activation involves a rapid and marked morphological shift from a highly ramified form to an amoeboid form. This change in cellular profile can be viewed as a shift from a less circular to a more circular shape and can be quantified in the form of the mathematical parameter circularity. The use of the circularity parameter, also termed “form factor”, as an approach to quantify microglial activation was described by Wilms, Hartmann and Sievers (1997) in a study investigating the effects of different growth substrates and conditioned media on microglial morphology. A variant of the method using the inverse of circularity, termed “transformation index”, was also described in other studies investigating changes in cultured microglial cells (Fujita et al. 1996; Szabo & Gulya 2013; Tanaka, J et al. 1998). However, these cell culture studies relied on sampling and analysis of individual cells and may be susceptible to observer bias.

More recently, Schmitz et al. (2014) utilised the circularity parameter to analyze changes in microglial morphology in a model of hyperoxia-induced white matter

injury in neonatal rats. In a very similar approach to our present study, the authors analyzed maximum projections of confocal image stacks taken from Iba1-immunolabelled brain sections using the ImageJ software. However, rather than directly analyzing the entire image field using the software, the authors have only used it to measure cell areas and perimeters in image segments and determined circularity values from these measurements. Regardless, using this approach, they were able to detect hyperoxia-induced microglia activation through increased circularity of microglial cells.

In our study, we have adapted the method to directly determine the average circularity of microglial cells within entire image fields using ImageJ. Using this approach, we observed that, as assessed by the circularity parameter, morphological changes in microglia can be detected as early as 3 hours, peaked by 24 hours, and persisted up to 7 days following stroke. Furthermore, transient changes in the morphology of microglia at distant regions were also detected at 24 hours based on the circularity measurement.

Additional analysis using Neurolucida, a different image analysis software, supported the results of the circularity analysis (see section 3.3.6). The additional analysis was based on alternative morphological parameters that are closely related to circularity. A decrease in cell perimeter reflects a loss or retraction of cell processes and correlates with an increase in circularity. In fact, this inverse relationship can be seen directly in the equation for circularity ($\text{circularity} = 4\pi \times \text{Area}/\text{Perimeter}^2$) (Wilms, Hartmann & Sievers 1997). Measurements of the microglial cell perimeter revealed a marked decrease (~ 41 %) in the peri-infarct region compared to the contralateral region at 24 hours and partial recovery at 7 days.

More interestingly, the analysis showed a contrasting shift in the total cell area and soma area at 24 hours. The total cell area reflected the total amount of space occupied by the entire microglial cell including both the cell soma and its associated processes. At 24 hours after stroke, microglial cells within the peri-infarct region exhibited, at the same time, an increased soma area and a decreased total cell area. These results suggested that, consistent with the known effects of activation on microglial morphology, there was hypertrophy of the soma together with the retraction of cell processes (see figure 1.4.3). At 7 days, the soma area had returned

to pre-hypertrophy values while the total cell area remained similar to that at 24 hours, suggesting that there was a partial re-extension of cell processes at this time. These results paralleled observations from the circularity analysis where the microglial cells exhibited peak circularity at 24 hours and partial recovery towards baseline levels at 7 days. This characteristic change in microglial soma size as a result of activation has in fact been utilised in a study by Kozłowski and Weimer (2012) to detect microglial activation in live animals using 2-photon microscopy.

Overall, the changes in the alternative parameters exhibited good agreement with the changes in circularity parameter and provided support for the interpretation that the circularity of microglial cells is closely correlated with the extent of de-ramification in these cells.

Other studies have also attempted to quantify the changes in microglial morphology during activation using more sophisticated morphometric approaches. These included fractal and Scholl analysis to determine morphological parameters such as fractal dimensions, lacunarity, convexity, solidity, ramification factor and branching density (Fumagalli et al. 2013; Hinwood et al. 2013; Karperien & Jelinek 2015; Soltys et al. 2005; Soltys et al. 2001).

Of particular interest is the study by Soltys et al. (2005) in which the authors investigated the effectiveness of different morphological parameters in evaluating the changes in microglial morphology induced in a global ischemia model in rats. In the study, microglial cells from different brain regions were randomly selected following global ischemia and grouped by visual inspection into four classes of morphologies associated with increasing degrees of activation. The authors then assessed the effectiveness of nine different morphological parameters, which included circularity (form factor), in distinguishing between the different classes of microglial cells. It was concluded from their analysis that circularity was the most effective amongst the parameters investigated.

Perhaps more relevant to our present investigations, a recent study by Morrison and Filosa (2013) utilised a “skeleton analysis” approach to measure the changes in microglial ramification in a mouse model of stroke. This method of analysis determines the extent of ramification in microglial cells by measuring the number of process end-points and total process length for each cell. The retraction of processes during microglial activation therefore results in decreases of the measured

ramification parameters. Indeed, the authors reported detection of significantly reduced microglial process end-points immediately upon the completion of the 60 minutes middle cerebral artery occlusion used as the stroke model. The effect of de-ramification was even more pronounced after 8 hours of reperfusion where significant reductions in the total process length were also detected. After 24 hours of reperfusion, the de-ramification process had spread to regions further away from the infarct.

It is interesting to note that we have in our present study achieved largely similar results to that reported by Morrison and Filosa (2013) despite using an arguably simpler approach for the analysis of microglial morphology. There was however a minor difference in that they also reported the detection of hyper-ramification of the microglial cells in the peri-infarct regions immediately adjacent to the infarct at the earliest time-point investigated. Although we have not detected a similar change (*i.e.* decrease in circularity) in our results, it is possible that this was due to differences in the stroke model used (middle cerebral artery occlusion *vs.* photothrombotic stroke) and the earliest time-point investigated (1 h *vs.* 3 h). In addition, the Morrison and Filosa study also used a different approach to define their peri-infarct regions. Based on the images supplied in their report, the regions nearest to the infarct, defined as regions 1 and 2 in their study, would have been identified in our study as part of the infarct core using our criterion of the loss of NeuN immunoreactivity.

In addition to morphological measures relating to microglial ramification, we have also quantified the microglial area fraction. The cellular area fraction is a measure combining the effects of cell size and numbers, both of which are influenced by the microglial activation responses of cellular hypertrophy, proliferation and migration. Area fraction analysis of Iba1 immunolabelling revealed a progressive increase within the peri-infarct tissue along the infarct border over 3 to 7 days following stroke. This is again consistent with observations from previous studies and extends these observations by quantifying the changes over the investigated time frame. An approximately 31-35% increase in Iba1 particle count at 3 days suggests that the increase in area fraction is due, at least partly, to an actual increase in microglial cell numbers rather than cellular hypertrophy alone. Co-localisation of the proliferation marker, Ki67, with microglial marker, Iba1, within the peri-infarct tissue (see figure 3.3.13) suggested that the increase in microglial cell numbers was due, at least in part, to *in situ* proliferation, in addition to cell migration into the region.

We detected from the area fraction data a previously unreported loss in peri-infarct microglia at 24 hours after stroke. A marked decrease (~33%) in Iba1 particle counts at this time suggested that the decrease in microglial area fraction was due primarily to a loss in microglial cell numbers. Although some oedema was evident, as can be seen in the cresyl violet stained sections (see figure 3.3.1 insets & figure 3.3.4), it is unlikely that the extent of tissue swelling within the peri-infarct tissue would be sufficient to completely account for the decrease in microglial density. Rather, it is highly probable that microglial migration into the infarct core and cell death were both significant factors in the observed loss. Tissue injury can trigger significant release of ATP and it has been shown that ischemic conditions can induce a large increase in ATP efflux from affected brain tissue (Dale & Frenguelli 2009; Frenguelli et al. 2007; Juranyi, Sperlagh & Vizi 1999; Melani et al. 2005). Given that microglial cells have been demonstrated to be susceptible to P₂X₇ receptor mediated cell death triggered by extracellular ATP (Eyo et al. 2013; Ferrari et al. 1997; Ferrari et al. 1999; Hao et al. 2013; Jeong et al. 2010), it is likely that the decrease in peri-infarct microglial cell numbers was at least partially due to cell death.

In our study, Iba1 was used as the primary marker for identifying microglial cells and quantifying their responses to stroke. Blood-derived macrophages that are recruited to the site of infarction following stroke also express Iba1 and are therefore a component of the microglial responses quantified using the measures of circularity and area fraction. However as discussed previously (see section 1.4.2.3) evidence from other studies have suggested that infiltration by the blood-derived macrophages is mostly localised to the infarct core and their numbers remained minimal at up to 3 days after stroke. Furthermore, even at peak infiltration, macrophages only contributed to a small fraction of the Iba1-immunolabelled cells within the peri-infarct tissue following photothrombotic stroke (Li, T et al. 2013). Given that the Iba1-based measures were used only in tissue regions outside of the infarct core, it is reasonable therefore to expect that changes in these measures are representative of changes in the microglial response following stroke.

Astrogliosis is probably the better characterised glial cell response in the stroke peri-infarct tissue. Upregulation in the expression of intermediate filaments, in particular the prototypical astroglial marker GFAP, as well as vimentin and nestin have long been observed in animal models of stroke (Duggal, Schmidt-Kastner & Hakim 1997; Li, Y & Chopp 1999; Petit et al. 1990). However, most of the earlier studies have

only attempted to describe qualitatively the changes in these markers using immunohistochemical staining or *in situ* hybridisation (Bidmon et al. 1997; Duggal, Schmidt-Kastner & Hakim 1997; Garcia et al. 1993; Nowicka et al. 2008; Schroeter et al. 1995). Others have attempted to semi-quantitatively characterise the astroglial changes using immunoblots but these studies were generally unable to distinguish between responses within the infarct core and peri-infarct tissue and they had only investigated these changes at limited time points (Imhof et al. 2006; Li, Q et al. 2009; Li, Y & Chopp 1999).

Two studies however stand out as early attempts to both quantitatively and spatio-temporally characterise changes in astroglial expression of GFAP (Chen, H et al. 1993; Li, Y et al. 1995). These studies measured the changes in area fraction of GFAP immunolabelling following stroke in a similar approach to our present investigation using vimentin immunolabelling. Using this method, the authors characterised the changes in GFAP area fraction within the infarct core and peri-infarct regions in brain sections over the first 7 days after stroke and reported early decreases within the core and large increases within the peri-infarct tissue from 2 days onwards. These results are in general agreement with our data using vimentin immunolabelling. However, it should be noted that unlike our study, both of the earlier studies have used fixed thresholding values that do not account for variations in background staining levels and furthermore, they have apparently sampled from fixed positions within the brain sections. In contrast, we have used a thresholding algorithm to determine the appropriate threshold value for each sampled image and we have also used NeuN immunolabelling in order to consistently identify the peri-infarct regions for sampling.

More recent examples of the use of area fraction analysis can be found in the studies by Brunkhorst et al. (2013) and Lopez-Valdes et al. (2014). The effects of drug interventions on astrogliosis in photothrombotic stroke models were investigated using area fraction analysis of GFAP immunolabelling in both studies. Although the investigators reported successful detection of changes in peri-infarct GFAP area fraction in both studies, they have not attempted to characterise these changes over time. Furthermore, neither group have reported the use of any method, such as NeuN immunolabelling, to consistently distinguish between the infarct and peri-infarct tissue.

We have chosen to use vimentin as the marker of astrogliosis for our study because, unlike GFAP, it is not normally expressed in cortical astroglia but becomes highly expressed in these cells following stroke (Schroeter et al. 1995). Although vimentin expression following stroke has been investigated in previous studies (Claus et al. 2013; Korzhhevskii et al. 2008; Schroeter et al. 1995), there have been no attempts to characterise the changes using a quantitative approach.

By measuring vimentin area fraction, we detected only a minor increase in the peri-infarct astroglial response 24 hours after stroke. The increase in area fraction became marked at 2 days and increased progressively out to 7 days after stroke. These results were corroborated by corresponding marked increases in immunoblots for GFAP and vimentin over the same time period, and are generally consistent with previous studies. However, while Schroeter et al. (1995) reported that vimentin expression was not detected in remote ipsilateral cortical regions, our investigations revealed that vimentin expression could be detected essentially across the entire ipsilateral cortex by 3 days after stroke (see figure 3.3.17).

A host of different tests of sensorimotor function have been used to assess functional deficits in studies of animal models of stroke, including adhesive removal, pole, rotarod, ladder or rung walking, foot fault, staircase and many others (Andersen, Andersen & Finger 1991; Barth, Jones & Schallert 1990; Kleim, Boychuk & Adkins 2007; Li, H et al. 2014; Whishaw & Kolb 2005). However, most of these tests are less useful for the present study as the stroke model used created a smaller lesion than most other models and is targeted at the forelimb motor cortical region which produced a relatively subtle functional deficit. Other studies that have utilised a similar model of stroke have very often used functional tests such as the cylinder test and the skilled reaching task (Alaverdashvili & Whishaw 2013; Shanina et al. 2006). However, while these tests have been reported to be effective at assessing the induced motor deficits, subsequent spontaneous recovery and the effects of various interventions, they are time consuming and analysis of the result is complicated.

In our characterisation of the stroke model, we have employed a simple forelimb placing test that is particularly sensitive to the induced functional deficit. The placing test assesses the sensorimotor reflex of the rat to reach out with its forepaw when its vibrissae are brushed against a platform (Madinier et al. 2014; Schallert et al. 2000; Schallert & Woodlee 2005). This method of assessing the functional effects of the

stroke has the advantage of not requiring pre-training of the animals and is straightforward to analyze. Animals exhibited marked impairments, in many cases near complete abolishment, of the placing reflex of their contralateral forelimb by 3 hours after stroke. This deficit remained marked at 2 days and only exhibited partial recovery by 7 days after stroke.

Studies investigating glial cell responses in various stroke models have mostly used cresyl violet or other forms of Nissl staining to define the infarct. Similarly, we have also used the cresyl violet staining method to assess the changes in infarct volume following stroke induction. Using this approach, we observed a rapid development of the lesion that followed a similar time course to that previously reported in studies using the photothrombotic stroke model (Grome et al. 1988; Li, H et al. 2014). The lesion was detectible as early as 3 hours after stroke, reached maximum volume by 24 hours, and contracted significantly at 7 days.

Although it was possible to visualise the infarct using the cresyl violet stain at all the time points examined in our study, it was not reliable as a method to identify the infarct boundary. At the earliest time point it was difficult to define the boundary between the infarct and peri-infarct tissue using cresyl violet staining as the decrease in staining intensity within the developing lesion was subtle and graded. At later time points, accumulation of microglia and other cell types along the boundary and their infiltration into the infarct started to obscure the infarct boundary (see figure 3.3.1 insets and figure 3.3.2). As a result of this ambiguity, it is possible that events occurring within the infarct core may be misidentified to be occurring in the peri-infarct tissue if cresyl violet or other Nissl stains were used as the method distinguish between the two regions.

NeuN and other neuronal markers have been used in various studies as indicators of viable neurons in models of focal (Badan et al. 2003; Bidmon et al. 1997; Davoli et al. 2002; Ito et al. 2001) and global ischemia (Bendel et al. 2005) as well as neurotoxicity (Collombet et al. 2006). Results from a previous study in our laboratory have further suggested that the loss of immunoreactivity to NeuN, an antigen specific to neurons, is an early predictor of neuronal loss in stroke (Lee et al. 2003). In fact, Collombet et al. (2006) reached a similar conclusion in a later study where they investigated the loss of neurons due to soman poisoning in mice over a 60

day period by comparing NeuN immunolabelling with two other markers of neuronal damage.

In the present study, we have investigated the effectiveness of using the loss of NeuN immunoreactivity as an approach to visualise the infarct core and to delineate the boundary between the infarct and peri-infarct tissue. NeuN-immunolabelled sections were counterstained with NeuroTrace™, a fluorescent Nissl stain, at different time points after photothrombotic stroke. NeuroTrace fluorescence revealed a very similar picture to cresyl violet staining with a similar difficulty of identifying the infarct boundary at early and late time points. In comparison, the infarct boundary is clearly demarcated by near complete loss of NeuN immunoreactivity within the core and strong NeuN signal in viable neurons within the peri-infarct tissue across the time points investigated. Consequently, we have used NeuN co-labelling with markers for microglia and astroglia in order to identify and study the changes in these cells within the peri-infarct tissue.

As discussed previously (see section 1.4.2), there has in recent years been increasing use of the concept of M1 and M2 activation in studies of microglial activation. This concept is based on observations from studies of peripheral macrophages that activation of these cells, far from being a stereotyped response, can lead to either the classical pro-inflammatory phenotype (M1) or an alternative anti-inflammatory phenotype (M2). Indeed, it is now evident that activated microglia are not all of a uniformly deleterious phenotype and exhibit far more diversity than the oversimplified M1 and M2 classification (Biber, Owens & Boddeke 2014; Colton & Wilcock 2010; Gertig & Hanisch 2014; Hanisch 2013).

The methods that we have adopted in this study have assessed microglial activation based on two parameters that facilitated the quantification of the physical changes in microglial cells during activation. The parameter of circularity assessed morphological changes that are rapid and not dependent on protein expression, but rather are mainly a result of the re-organisation of cytoskeletal proteins (Christensen et al. 2006; Cross & Woodroffe 1999; Hall et al. 2009). In contrast, area fraction is a parameter that measured the aggregated factors of hypertrophy, migration, cell death and proliferation. These responses depend at least in part on changes in gene expression that are slower to develop than the rapid cytoskeletal changes affecting cell morphology. Although the use of suitable M1 and M2 markers will likely

provide additional valuable information on the activation states of microglia, there are currently many difficulties involved in the implementation of this approach. Many of the markers, in particular cytokines like IL-1 β , are small soluble molecules that are poorly retained in the tissue during processing for immunohistochemistry. Approaches based on immunoblotting are unable to distinguish between expression of markers within the infarct core and the peri-infarct tissue. Furthermore, many of the markers, such as Cox-2, iNOS and various interleukins are also expressed in cell types other than microglia.

There is at present a long list of putative M1 and M2 markers, many of which are transiently expressed or slow to develop, and very few that are well characterised in microglial cells. Although some studies have attempted to investigate the expression of these markers in the post-stroke brain, these have mostly only looked at the infarct core or at limited time points and most of the characterisations have only been done at the level of RNA transcription rather than protein expression (Fumagalli et al. 2013; Hu et al. 2012; Perego, Fumagalli & De Simoni 2011; Xu, Y et al. 2012; Zarruk et al. 2012). Of the studies cited above, the works of Hu et al. (2012) and Zarruk et al. (2012) stand out in the fact that the authors have assessed the changes in protein expression, in addition to the mRNA, of M1 and M2 markers.

Hu et al. (2012) investigated the changes in the protein expression of an M1 marker (CD16/32) and an M2 marker (CD206) using immunolabelling over several time points out to 14 days after stroke. However, the authors have only looked at these changes within the infarct rather than the peri-infarct tissue. In contrast, Zarruk et al. (2012) investigated the changes in protein expression of several M1 and M2 markers but only at 24 hours after stroke. Although the authors have reportedly looked at the changes within the peri-infarct tissue by dissecting out only the region of tissue immediately surrounding the ischemic core, it may be difficult to routinely use this approach without contaminating the sample with tissue from within the infarct.

Overall, there is still very little that is currently known about microglial expression of the M1 and M2 markers in relation to the post-stroke peri-infarct tissue and their implications on neuronal plasticity. Further studies to investigate the roles that the different microglial phenotypes play in the post-stroke brain will be required to enable the identification of M1 and M2 markers that are relevant to the processes involved in functional recovery after stroke.

3.5 Conclusion

In the present study, we have characterised the changes in microglial and astroglial cells within the peri-infarct tissue as early as 3 hours and out to as far as 7 days following stroke. This was achieved using approaches that allowed the quantification of key aspects of these changes in immunohistochemically labelled brain sections that allowed the distinction of responses occurring within the peri-infarct tissue from those occurring within the infarct.

Analysis of the circularity of peri-infarct microglial cells using the ImageJ software revealed changes that were indicative of the morphological transformation associated with activation in these cells. Furthermore, analysis of alternative morphological parameters using a different software, Neurolucida, yielded additional information that supported the results of the circularity measurements. The circularity measurements provided a sensitive quantitative approach to characterise microglial activation and was able to detect these changes as early as 3 hours after stroke.

Area fraction analysis provided further quantification of the microglial responses that is a composite measure of cellular hypertrophy, migration, proliferation and death. These are all responses that are induced in microglia following an insult or injury such as stroke. The characterisation of microglial responses using area fraction revealed a previously unreported loss in peri-infarct microglial cells at 24 hours that preceded a rapid increase over the subsequent 6 days after stroke.

Furthermore, using area fraction analysis on the expression of vimentin, we have been able to quantify a key aspect of the astroglial response within the peri-infarct region over the first 7 days following stroke.

The spatiotemporal characterisation of the microglial and astroglial responses within the peri-infarct represents an important first step for further studies to investigate the effects of manipulating these responses within this critical region and their influence on the neuroplastic processes underlying functional recovery after stroke.

CHAPTER 4
***EFFECTS OF TREATMENT USING
MINOCYCLINE ON POST-STROKE GLIAL
CELL RESPONSES AND FUNCTIONAL
RECOVERY***

4.1 Introduction

Spontaneous partial recovery of function is commonly observed over the weeks to months following stroke. There is now increasing evidence that this recovery is due, at least in part, to the establishment of new connections by surviving neurons within the tissue adjacent to the infarct that take over some of the functions of neurons that were lost in the infarct (Dancause & Nudo 2011; Li, S et al. 2010; Li, Y, Jiang, et al. 1998; Murphy, TH & Corbett 2009) (see also section 1.3).

Occurring within the same regions of the peri-infarct tissue are striking changes in glial cell responses, in particular microglial activation and astrogliosis, that can be detected starting within hours of infarction and persisting out to weeks resulting in the eventual formation of a glial scar. It has long been observed that the glial scar presents a barrier to recovery due to its inhibition of axonal regeneration in spinal cord injuries (Silver & Miller 2004; Yiu & He 2006). However, studies over the recent decade have revealed that there are various aspects of the process of astrogliosis leading up to glial scar formation that are in fact protective and beneficial to recovery (Li, L et al. 2008; Liu, Z & Chopp 2015; Shimada et al. 2011; Sofroniew 2015) (see also section 1.4.1).

Microglial activation has often been viewed to be detrimental to the stroke outcome (Hailer 2008; Yenari, Kauppinen & Swanson 2010). In particular, activated microglia has been thought to exacerbate the injury caused by CNS trauma or ischemia based on the results of studies using drugs that reportedly suppressed microglial activation in animal models of injury (Lopez-Vales et al. 2005; Ng et al. 2012; Wakita et al. 1995; Yrjanheikki et al. 1998; Yrjanheikki et al. 1999). However, conflicting results have been reported in some studies that suggested a neuroprotective role for microglia during the acute stages of stroke (Girard et al. 2013; Lambertsen et al. 2009).

The role of activated microglia during the post-acute phase of stroke is no less confusing. Some studies have suggested that activated microglia can induce axonal retraction through direct contact (Horn et al. 2008; Kitayama et al. 2011) or induce conditions unfavourable to neuroplasticity through release of pro-inflammatory cytokines, ROS and NO (Liguz-Leczner & Kossut 2013; Munch et al. 2003). However, others have observed that activated microglia are a source of trophic factors that may promote neuroplasticity (Batchelor et al. 2002; Lai & Todd 2008;

Madinier et al. 2009; Yang, H et al. 2012) (see also section 1.4.2.1). In addition, the early activation of microglia is likely to play an important role in the induction and modulation of the astroglial responses via the production of various cytokines (Chen, SH et al. 2015; Liu, W, Tang & Feng 2011; Zhang, D et al. 2010).

Although it is evident that these glial cell responses can exert a significant influence on the processes underlying post-stroke functional recovery, the exact nature of their interactions and influence on neuronal plasticity is unclear at present. In order to develop therapies that can enhance these neuroplastic processes, it is therefore of great importance to increase our understanding of the interactions between the microglial and astroglial responses and how the modification of these responses may influence functional recovery.

Minocycline is an antibiotic that has been reported to be effective in suppressing microglial activation in various CNS diseases and injuries including stroke (Hailer 2008; Yrjanheikki et al. 1998; Yrjanheikki et al. 1999) (see also section 1.5.1). In our present study, we used a time-targeted minocycline treatment as an approach to modulate microglial activation during the early phase of stroke and investigated the subsequent effects on the development of astrogliosis within the peri-infarct tissue and functional recovery in a photothrombotic model of stroke in rats. We hypothesised that the treatment should result in the suppression of the changes in microglial circularity and area fraction that were characterised in the previous chapter. The decreased activation of microglia should lead to subsequent reduction of peri-infarct astroglial reactivity and improved functional recovery.

As was observed from the characterisation study, the microglial response was well developed by 3 days after photothrombotic stroke (see sections 3.3.3 & 3.3.4). In order to target the early microglial responses, we treated the stroke-affected animals using an early short-course minocycline treatment. The effect of the treatment was evaluated by assessment of the forelimb function as well as changes in microglial and astroglial markers in immunohistochemically stained brain sections and western blots at various time points up to 7 days following stroke.

Surprisingly, although the dosage (*i.e.* 50 mg/kg) used in our short-course treatment was comparable to other studies reporting suppression of microglial activation (Cardoso et al. 2013; Franco et al. 2012; Yenari et al. 2006; Yrjanheikki et al. 1999), we did not detect significant changes in the microglial response following stroke.

The astroglial response was similarly unaffected by the treatment. However, despite the lack of measurable effects on the glial cell responses and infarct volume, minocycline-treated animals performed better in the functional assessment compared to vehicle-treated controls at 3 days after stroke.

Due to the limited effects of treatment observed in the initial experiments, we used a higher dosage treatment regimen, comparable to that used by Kim, BJ et al. (2009) and Chu et al. (2010), in subsequent investigations in order to achieve clearer treatment effects. However, the treatment only resulted in modest changes in microglial area fraction but no changes in morphology within the peri-infarct tissue. Despite the modest effects on the microglial response, the treatment resulted in significant improvement in functional recovery that persisted out to 28 days after stroke. Surprisingly, although functional recovery was enhanced, astroglial reactivity as assessed by Western blots for GFAP and vimentin was significantly increased within the ipsilateral cortex.

Our present findings suggest that although minocycline treatment may promote functional recovery after stroke, the beneficial effects may not be the result of a direct suppression of early microglial activation. Furthermore, the enhanced functional recovery is associated with an increased astroglial response, in agreement with previous studies that have suggested a beneficial role for the astroglial responses that precede scar formation.

4.2 Materials and Methods

The common materials and methods used in the experiments in this chapter have been described in Chapter 2. Additional details, modifications and methods specific to this part of the study are provided in the following sections.

4.2.1 Initial Investigations of Treatment Using Minocycline

In the initial investigations into the effects of minocycline treatment after stroke, the rats were administered via intraperitoneal injections 50 mg/kg minocycline (10 mg/mL Minocycline Hydrochloride in PBS, pH 7.4) or equivalent volume of vehicle (PBS) at 1 h and 24 after stroke. The treatment regimen used here was similar to other studies that have reported significant effects in suppressing microglial activation following stroke (Cardoso et al. 2013; Franco et al. 2012; Yenari et al. 2006; Yrjanheikki et al. 1999). Rats that were sacrificed at 24 h only received the first injection at 1 h after stroke. This treatment regimen will be subsequently referred to as "low dose minocycline treatment". The rats were randomly pre-assigned to either minocycline or vehicle treatment and all functional assessments, image and data analyses were performed by investigators blinded to the treatment.

The effects of the treatment on infarct volume and microglial responses were assessed using cresyl violet staining and immunohistochemical labelling at 24 h, 3 d and 7 d after stroke. The effects of the treatment on the astroglial responses were assessed using immunohistochemical labelling and Western blots at 7 d. The animals were assessed for effects on functional recovery by forelimb placing assessment at 24 h and again just before sacrifice. A timeline of the experimental procedures is shown in figure 4.2.1.

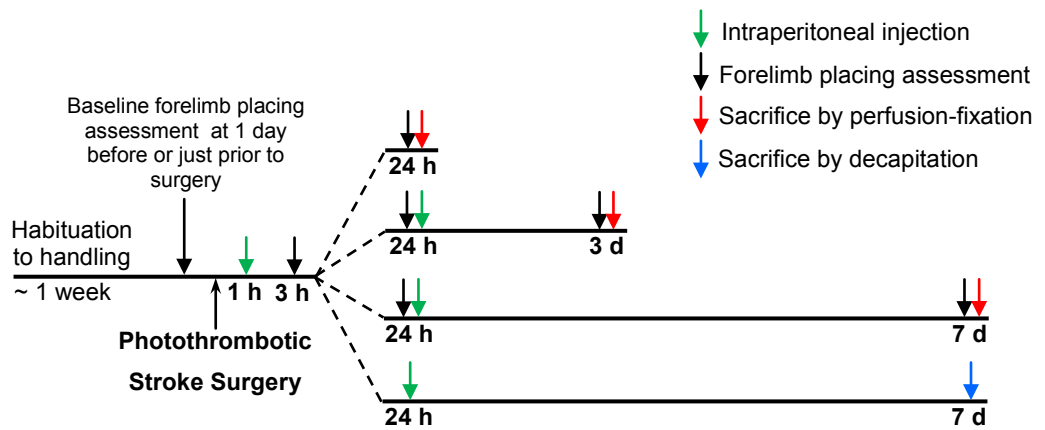


Figure 4.2.1 Experimental timeline for the investigation of the effects of low dose minocycline treatment following photothrombotic stroke.

Four groups of animals were used in this part of the study. One group sacrificed at each time point of 24 h, 3 d and 7 d by perfusion-fixation for cresyl violet staining and immunohistochemical labelling. The final group was sacrificed at 7 d by decapitation and the brains were extracted for Western blots. All animals were habituated to handling during the week before surgery. Baseline forelimb placing scores were assessed either on the day before surgery or just prior to surgery. Following surgery, the rats were assessed for inclusion at 3 h by forelimb placing scores (≤ 15). Treatment with minocycline or vehicle was administered by intraperitoneal injections at 1 h and 24 h following stroke, except for animals sacrificed at 24 h that only received the first injection. Forelimb placing scores were assessed again at 24 h and just before sacrifice, except for animals used in Western blots.

All animals were habituated (section 2.3.1) to handling during the week before photothrombotic stroke surgery in 10 min sessions on 3 separate days. Baseline forelimb placing scores of the rats were assessed (section 2.3.2) either on the day before surgery or just before the surgery. Following stroke surgery (section 2.3.3), the rats were treated at 1 h with either minocycline or vehicle according to their pre-assigned treatment group. At 3 h after stroke, the rats were assessed for inclusion by the forelimb placing assessment. Only rats that scored 15 or less at this time were included in the study. For the rats that were sacrificed at 24 h, no further treatments were administered. Other rats that were sacrificed at 3 d and 7 d received a second injection at 24 h. Functional recovery was assessed in all animals for forelimb placing assessed at 24 h and just before sacrifice, except for animals assigned for use in Western blots.

At 24 h, 3 d and 7 d after stroke, following forelimb placing assessments, animals were sacrificed by perfusion-fixation (section 2.3.4). The brains were then extracted and processed for cryosectioning (sections 2.3.5 & 2.3.6). The brain sections were then used for cresyl violet staining and immunohistochemical labelling.

The infarct volumes were determined from the cresyl violet stained sections (section 2.3.7). Brain sections were immunolabelled for Iba1 and vimentin to assess the effects of treatment on the microglial and astroglial responses following photothrombotic stroke as described in sections 2.3.8, 2.3.9 and 2.3.10. For this part of the study, the effects of treatment on microglial responses were only assessed at the peri-infarct region, "Ipsi01A", and the corresponding contralateral region, "Contra01". These regions were referred to respectively as "Peri-infarct" and "Contralateral" in the results section.

Animals were also sacrificed by decapitation at 7 d and their brains were extracted for Western blots to assess the effects of treatment on the astroglial expression of vimentin and neurocan (section 2.3.11).

4.2.2 High Dose Minocycline Treatment

In a subsequent series of experiments, a higher dosage treatment regimen similar to that used in the studies by Kim, BJ et al. (2009) and Chu et al. (2010), was used in order to achieve clearer effects of minocycline treatment. In this treatment regimen, subsequently referred to as "high dose minocycline treatment", minocycline (10 mg/mL Minocycline Hydrochloride in PBS, pH 7.4) or equivalent volume of vehicle (PBS) was administered via intraperitoneal injections at 1 h post-stroke at 90 mg/kg, then at 12, 24, 36 and 48 h at 50 mg/kg. The rats were randomly pre-assigned to minocycline or vehicle treatment and all functional assessments, image and data analyses were performed by investigators blinded to the treatment.

The effects of the treatment on infarct volume and microglial responses were assessed using cresyl violet staining and immunohistochemical labelling at 3 d after stroke. The effects of the treatment on astroglial responses were assessed using Western blots at 7 d after stroke. For this part of the study, forelimb placing scores were assessed starting at 24 h, then weekly at 7, 14, 21 and 28 d in order to evaluate

the effects of the treatment on long term functional recovery. A timeline of the experimental procedures is shown in figure 4.2.2.

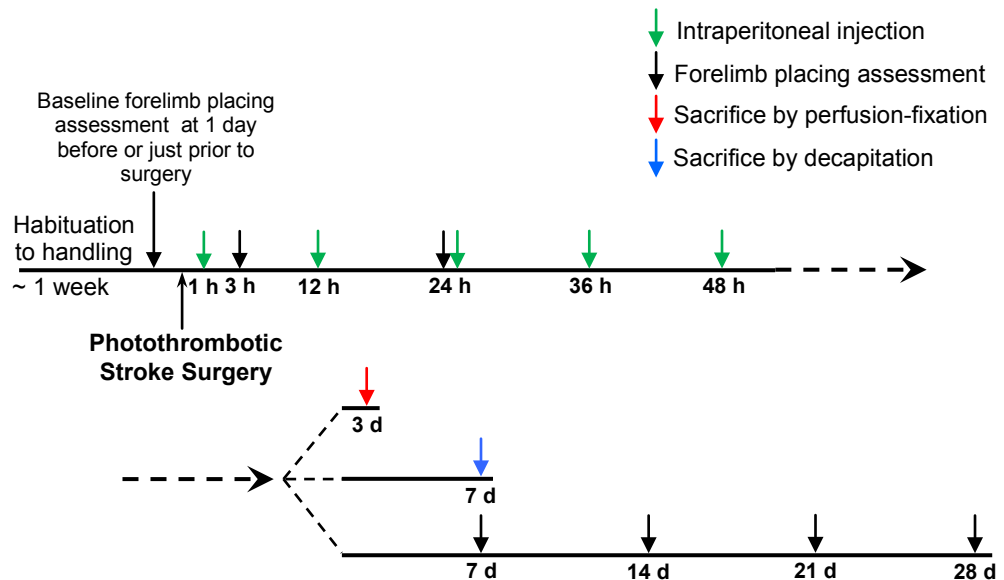


Figure 4.2.2 Experimental timeline for the investigation of the effects of high dose minocycline treatment following photothrombotic stroke.

Three groups of animals were used for this part of the study. One group was sacrificed at 3 d by perfusion-fixation for cresyl violet staining and immunohistochemical labelling. Another group was sacrificed at 7 d by decapitation and the brains were extracted for western blots. The final group were used for the evaluation of functional recovery by forelimb placing assessment at 24 h, 7 d, 14 d, 21 d and 28 d. All animals used in the experiments were habituated to handling during the week before photothrombotic stroke surgery. Baseline forelimb placing scores were assessed either on the day before surgery or just prior to surgery. Following surgery, the rats were assessed for inclusion at 3 h by the forelimb placing assessment (≤ 5). Treatment with minocycline or vehicle was administered by intraperitoneal injections at 1, 12, 24, 36 and 48 h following stroke.

All animals were prepared for photothrombotic stroke surgery as described in the previous section (section 4.2.1) but with two modifications aimed at improving consistency in the injury and functional deficits induced in the model. The first modification was to control the light intensity to between 160,000 and 170,000 lux for stroke induction during surgery. The second modification was the use of a more stringent inclusion criterion. Animals were included to the study only if they scored 5 or less in the forelimb placing assessment at 3 h after stroke induction.

Following surgery, the animals were treated with either minocycline or vehicle according to the "high dose minocycline treatment" regime as described at the beginning of this section. Three groups of animals were used for this part of the study. The first group was sacrificed at 3 d by perfusion-fixation. The second group was sacrificed at 7 d by decapitation for Western blots. The last group was assessed for functional recovery by forelimb placing assessment at 24 h and 7, 14, 21 and 28 d after stroke.

Brain samples from perfusion-fixed animals at 3 d were processed for cryosectioning and the brain sections were used for cresyl violet staining and immunohistochemical labelling. The infarct volumes were determined from the cresyl violet stained sections. The effects of the treatment on microglial responses were assessed brain sections immunolabelled for Iba1. Similar to the initial investigations using low dose minocycline treatment, the effects of the high dose treatment were only assessed at the peri-infarct region, "Ipsi01A" and contralateral region, "Contra01". For this part of the study, ED1 was used as an additional marker of the microglial response. The analysis of ED1 immunolabelled brain sections is described below in section 4.2.3.

The effects of the treatment on astroglial responses were assessed by Western blots for the expression of GFAP, vimentin and neurocan, using the brain samples from the animals sacrificed at 7 d after stroke.

4.2.3 Image Acquisition and Analysis for ED1-Immunolabelled Sections

ED1 is a marker of phagocytic activity in activated microglia and macrophages. The expression of ED1 was used as an additional marker of the microglial response in the high dose minocycline treatment experiments. Brain sections were co-labelled with NeuN to identify the infarct boundary and images were acquired on an Olympus AX70 microscope (Olympus Australia Pty Ltd, NSW, Australia) using the 10× objective lens.

Images were taken from the peri-infarct tissue along the infarct boundary and at a corresponding region in the contralateral cortex as shown in figure 4.2.3. The images were then analysed using ImageJ to count the number of ED1⁺ particles within the peri-infarct tissue and corresponding contralateral region. The images for the ED1 fluorescence channel were processed to reduce background noise using the "subtract background noise" function with "rolling ball radius" set at 100 pixels and the sliding paraboloid box checked. The images were then thresholded using the built-in thresholding algorithm "triangle". Using NeuN-immunolabelling to identify the infarct boundary, areas within the images were selected for analysis using the "specify" function as shown in figure 4.2.4.

The selected areas were analysed using the "Analyze Particles" function, with the particle size set to a lower limit of 30 pixel units. The particle counts from the 3 yellow boxes were summed and recorded as the "Peri-infarct" counts. The particle counts from the magenta rectangle selection were recorded separately as "Peri-infarct + 0.3 mm" counts. The ED1⁺ particle counts for the contralateral region were determined using the same procedure as for the peri-infarct. Two brain sections from each brain sample were analysed and the results were averaged.

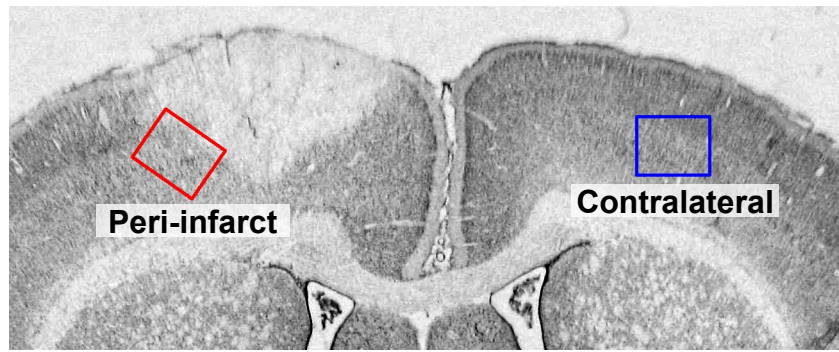


Figure 4.2.3 Location of images acquired for analysis of ED1 expression.

The boxes ($854 \times 683 \mu\text{m}$) show the positions of the images taken using the $10\times$ objective lens within the peri-infarct tissue and corresponding contralateral region.

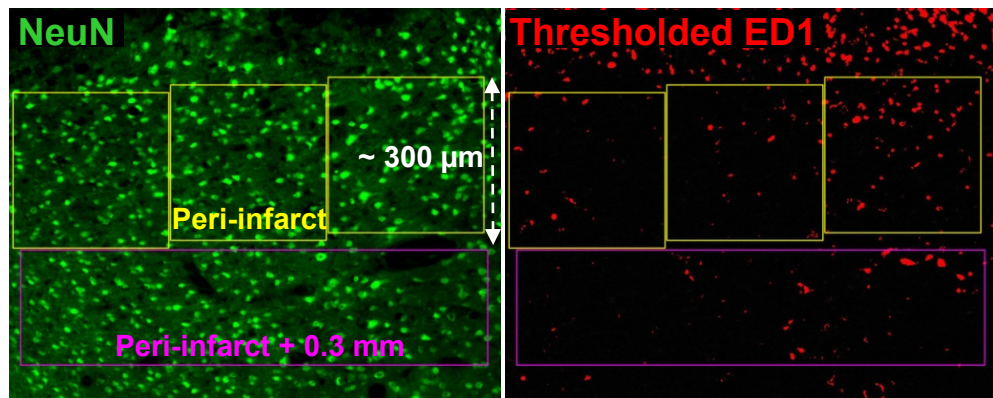


Figure 4.2.3 Area selection for analysis of ED1^+ particles.

The images shown ($854 \times 683 \mu\text{m}$) are representative images from the "Peri-infarct" position in figure 4.2.2. Using the image in the NeuN fluorescence channel, 3 boxes (yellow) of 270 by $270 \mu\text{m}$ in size were selected so that they lined up along the infarct boundary. A rectangular selection (magenta) 810 by $200 \mu\text{m}$ in size was selected approximately $300 \mu\text{m}$ behind the box on the leading edge of the infarct. The thresholded ED1 image was analysed then using the areas selected as shown.

4.3 Results

4.3.1 Initial Investigations of Treatment Using Minocycline

Initial investigations were conducted using low dose minocycline treatment. This was at a dosage that was similar to those used in other studies that reported changes in post-stroke microglial responses (see section 4.2.1), except that here a short-course treatment was used to target only the early glial cell responses. Microglial responses were examined at 24 h, 3 d and 7 d and astroglial responses at 7 d post-stroke. Functional recovery was assessed by the forelimb placing test starting at 3 h and up to 7 d post -stroke.

4.3.1.1 Infarct Volume

As previously observed in the characterisation experiments, infarct volume peaked at 24 h post-stroke and subsequently decreased, reflecting a contraction of the lesion over time. However, there were no effects of low dose minocycline treatment on the infarct volume at any of the time points investigated (figure 4.3.1).

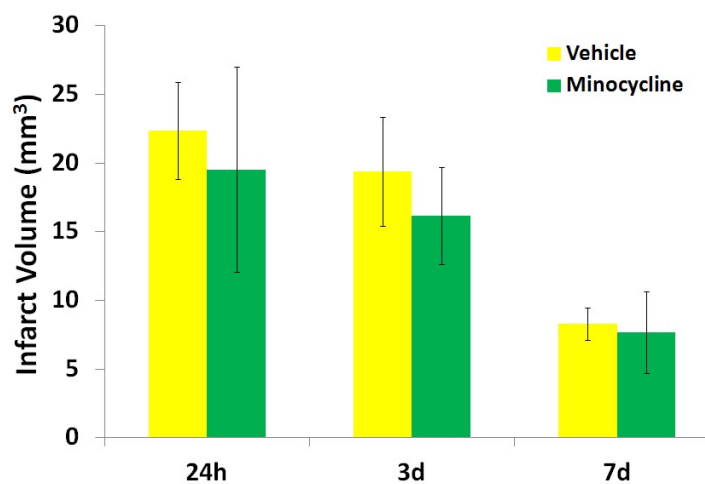


Figure 4.3.1 Infarct volume in animals treated with low dose minocycline or vehicle following stroke.

Two-way analysis of variance revealed no effects of treatment and a highly significant effect of time on infarct volume ($p < 0.01$). The infarct volume decreased over time following stroke for both treatment groups and became significantly smaller at 7 d compared to the earlier time points ($p < 0.01$, Tukey's HSD post-hoc test). Values are shown as mean \pm SD (n = 4 – 8 per group).

4.3.1.2 Forelimb Placing Reflex

Recovery of function was analysed for three separate groups of animals that were sacrificed for analyses at 24 h, 3 d or 7 d after stroke. The forelimb placing reflex of all animals was assessed at 3 h and 24 h after stroke. Additionally, animals sacrificed at 3 d and 7 d were assessed again just before sacrifice. Pooled data from all three groups of animals are shown in figure 4.3.2. The recovery of forelimb function of low dose minocycline-treated animals at 3 d after stroke was improved compared to vehicle-treated animals. Although there was a tendency for the minocycline-treated animals to perform better than the vehicle-treated counterparts at 7 d, the differences did not reach statistical significance.

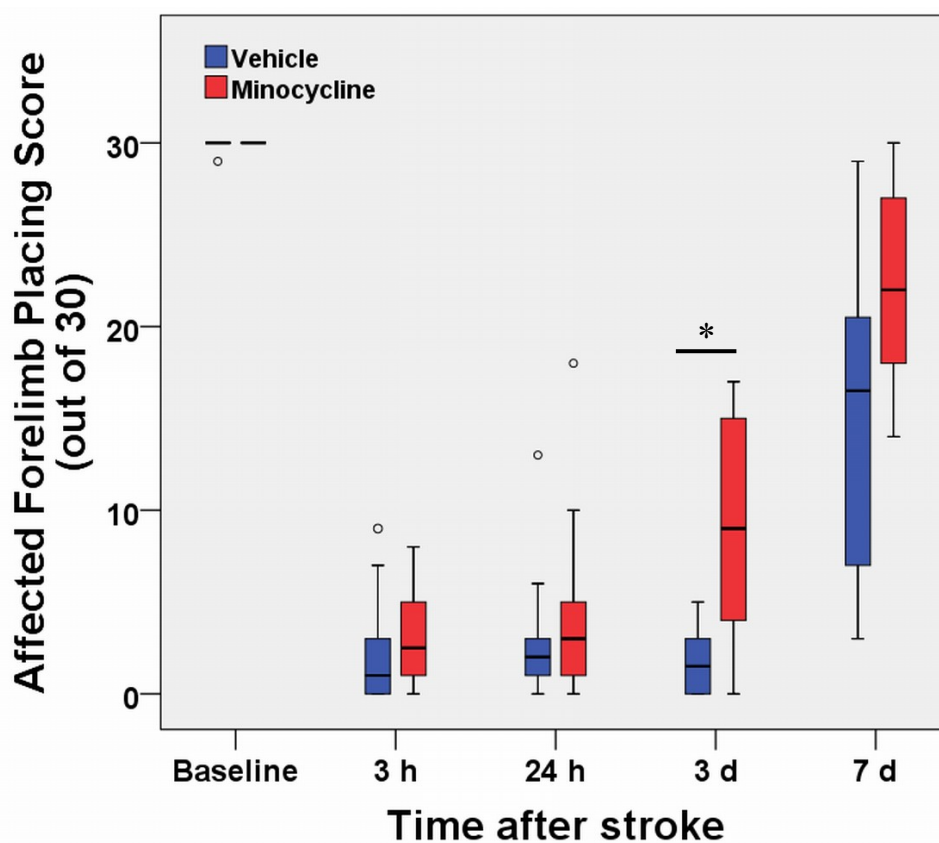


Figure 4.3.2 Forelimb placing score of the affected forelimb of animals treated with low dose minocycline or vehicle at baseline and up to 7 days after stroke.

The minocycline-treated animals exhibited an increased rate of recovery in their forelimb placing reflex compared with vehicle-treated controls over the first 3 days as assessed by the area under the curve of placing scores between 3 h and 3 d after stroke ($*p < 0.05$, Vehicle vs. Minocycline, Mann-Whitney *U* test). The data is presented in a box plot with outliers shown in open circles ($n \geq 6$ per group).

4.3.1.3 Microglial Morphology – Circularity

The microglial circularity measurements here confirmed the findings from the characterisation experiments (see section 2.3.3) where stroke induction resulted in a marked increase in peri-infarct microglial circularity at 24 h post-stroke for animals in both treatment groups. Similarly, this increase in circularity persisted at 3 d and started to decrease by 7 d but remained significantly higher than microglia in the contralateral cortex (figure 4.3.3).

Microglial morphology as assessed by circularity within both the contralateral and peri-infarct tissue was not significantly affected by low dose minocycline treatment at any of the time points investigated. Not surprisingly, the treatment also had no measurable effects on microglial circularity at regions further away from the infarct (data not shown).

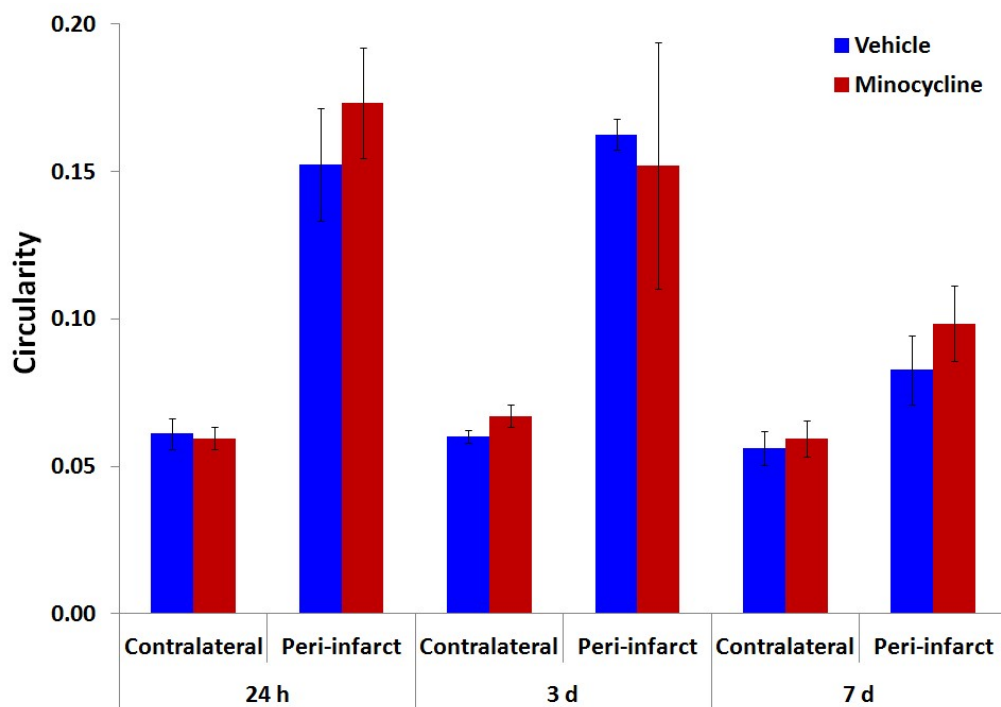


Figure 4.3.3 Circularity of microglial cells in the contralateral cortex and peri-infarct tissue of animals treated with low dose minocycline or vehicle.

Two-way analysis of variance revealed no effects of treatment but a highly significant difference in the circularity of microglial cells between the contralateral and peri-infarct tissue ($p < 0.001$). No significant interactions between the two factors were detected. Values are shown as mean \pm SD (n = 4 – 8 per group).

4.3.1.4 Microglial Area Fraction

Similar to the data for microglial circularity, the results for microglial area fraction in this part of the study also confirmed the observations of the characterisation experiments (see section 3.3.4). The loss of peri-infarct microglial cells at 24 h post-stroke was more clearly demonstrated in showing a significant difference between the area fractions in the contralateral (figure 4.3.4).

However, low dose minocycline treatment did not have any effect on the area fraction of microglial cells within the peri-infarct tissue at any of the time points investigated. Similarly, there were also no effects detected at regions further away from the infarct (data not shown).

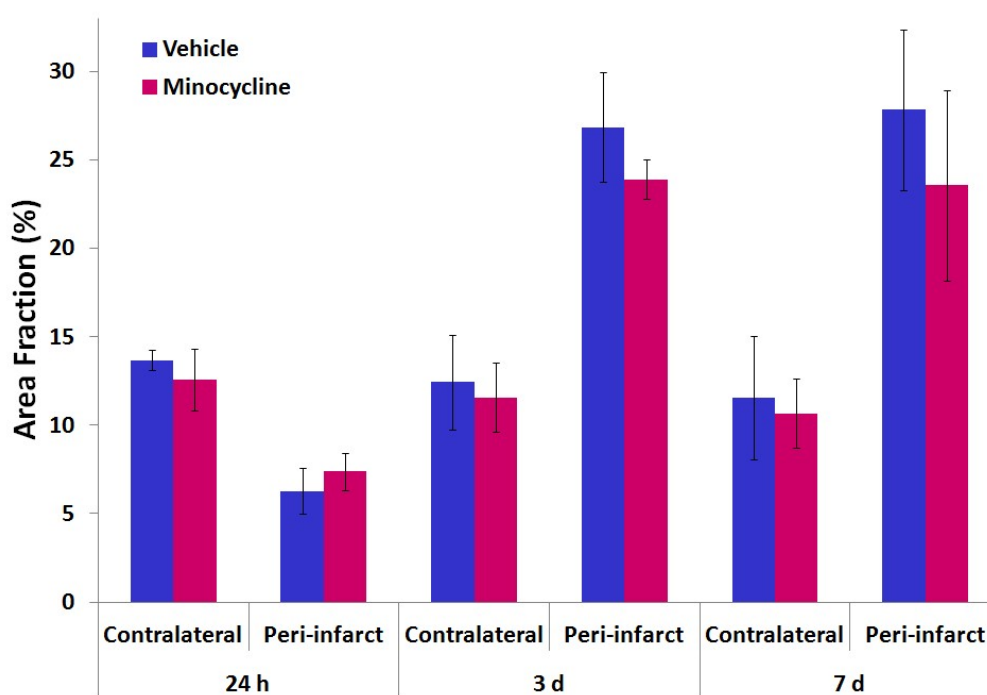


Figure 4.3.4 Area fraction of microglial cells in the contralateral cortex and peri-infarct tissue of animals treated with low dose minocycline or vehicle.

Two-way analysis of variance revealed no effects of treatment but a highly significant difference in the area fraction of microglial cells between the contralateral and peri-infarct tissue ($p < 0.001$). No significant interactions between the two factors were detected. Values are shown as mean \pm SD ($n = 4 - 8$ per group).

4.3.1.5 Astroglial Responses - Vimentin Area Fraction

Similar to observations from the characterisation experiments, the area fraction of vimentin immunolabelling within the peri-infarct tissue had increased markedly by 7 d after stroke compared to corresponding contralateral regions. However, low dose minocycline treatment did not have any measurable effects on vimentin area fraction in either tissue regions (figure 4.3.5).

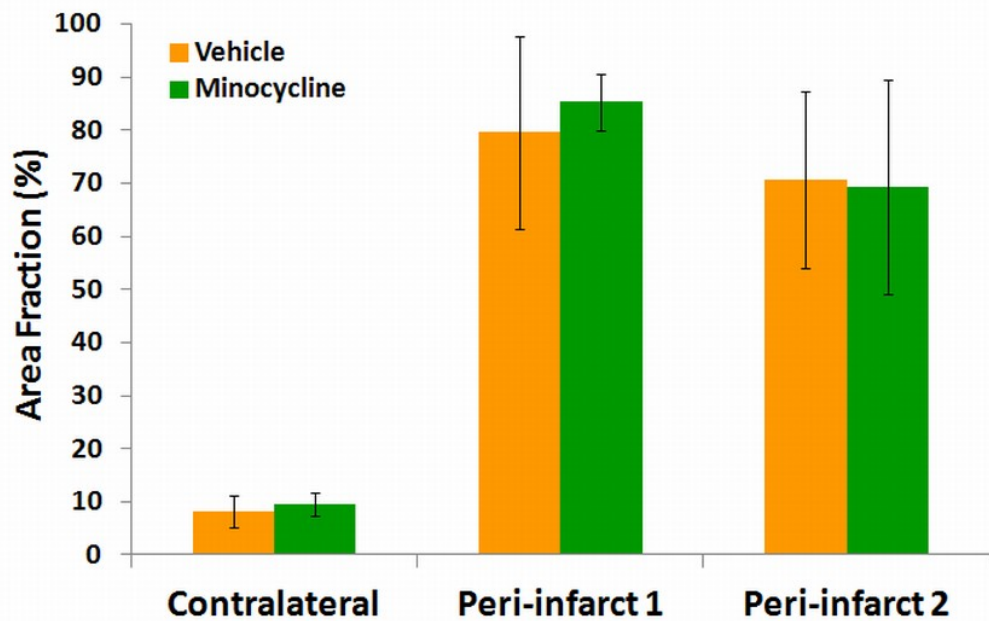


Figure 4.3.5 Area fraction of vimentin immunolabelling in the peri-infarct tissue and contralateral cortex of animals treated with low dose minocycline at 7 days after stroke. Two-way analysis of variance revealed no effects of treatment and a highly significant effect of tissue region on the area fraction of vimentin immunolabelling ($p < 0.001$, "Contralateral" vs. "Peri-infarct1" & "Peri-infarct2"). No significant interactions between the two factors were detected. Values are shown as mean \pm SD (n = 5 per group).

4.3.1.5 Astroglial Responses - Western Blots

Dissected peri-infarct brain tissue samples were analysed using western blotting and densitometry to determine the relative expression of proteins that are characteristic of astrogliosis. In addition to vimentin, a widely used marker of astrogliosis, neurocan expression was also investigated here as it is a CSPG expressed by astroglia that is known to be inhibitory to axonal regrowth.

Densitometric analysis on the Western blots for vimentin confirmed the observations from the area fraction analysis that low dose minocycline did not result in significant changes in the expression of vimentin (figure 4.3.6). The vimentin band intensities were normalised to total protein in the respective lanes on the PVDF membranes. The membrane protein content was determined using the stain-free gel method as previously reported Colella et al. (2012).

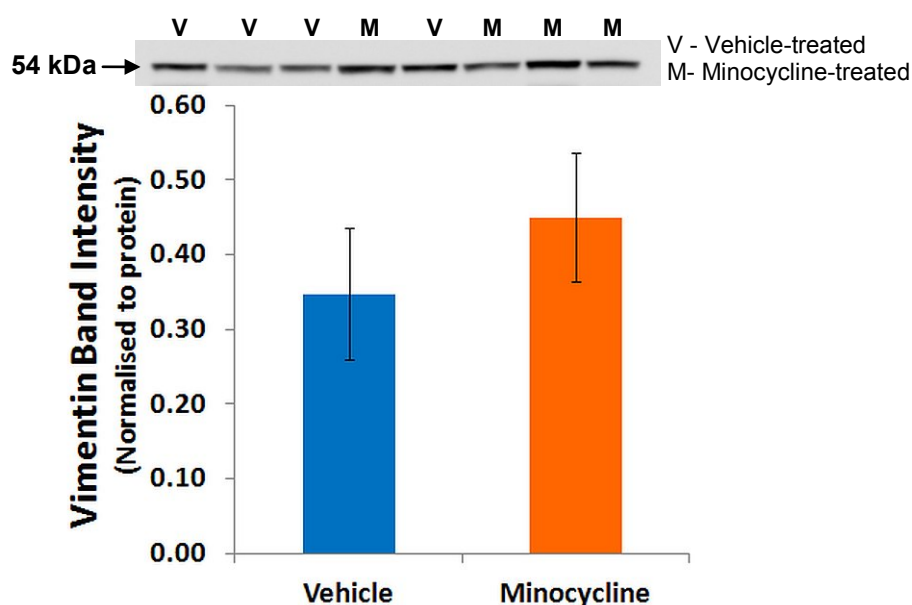


Figure 4.3.6 Densitometric analysis of western blots of vimentin expression in the peri-infarct tissue of animals treated with low dose minocycline at 7 days after stroke.

Blotting for vimentin reveals a single band at 54 kDa. Analysis using Student's t-test on the normalised band intensities revealed no effects of treatment on the expression of vimentin. Values are shown as mean \pm SD (n = 4).

Neurocan is normally present only in its truncated forms in the intact adult brain (Matsui *et al.* 1994). However, following injuries such as stroke and trauma, the full length form is rapidly upregulated in the ipsilateral cortex whereas the expression of the truncated forms remain relatively unchanged (Asher *et al.* 2000; Deguchi *et al.* 2005). In the present study, similar to the observations by Asher and co-workers and Deguchi and co-workers, Western blots of tissue samples from the uninjured contralateral cortex revealed only low or undetectable levels of the full length neurocan protein (data not shown).

The ratio of the expression of the full length neurocan to the truncated form was used as a measure of the effects of treatment on the astroglial response to stroke (figure 4.3.7). As with the results obtained for vimentin expression, low dose minocycline treatment did not have significant effects on the relative expression of the full length and truncated neurocan proteins within the peri-infarct tissue at 7 d.

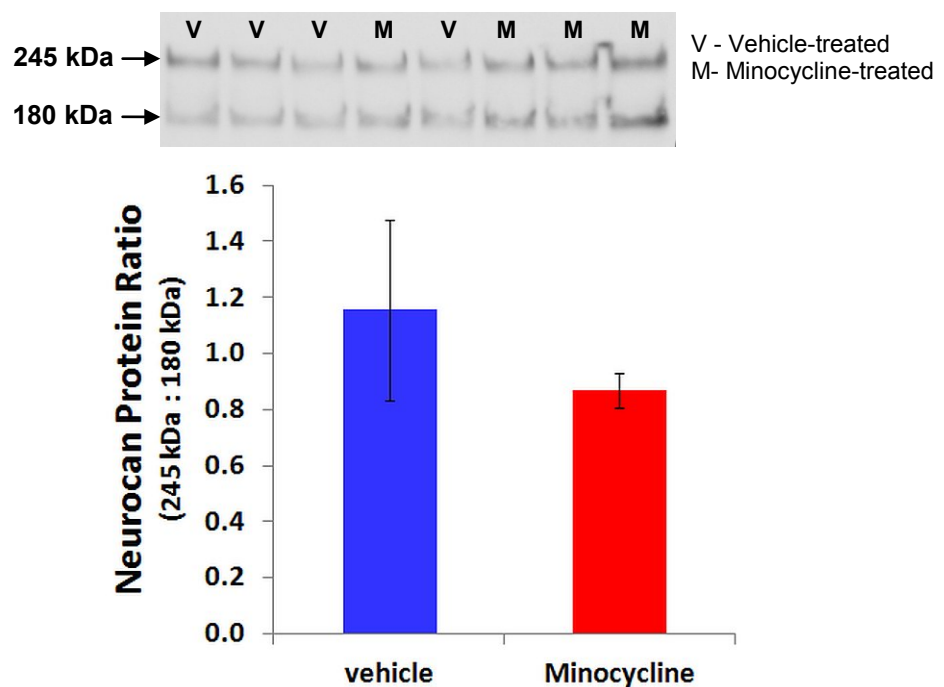


Figure 4.3.7 Densitometric analysis of western blots of neurocan expression in the peri-infarct tissue of animals treated with low dose minocycline at 7 days after stroke.

Blotting for neurocan reveals two bands, one at 245 kDa representing the full length protein and the other at 180 kDa representing the truncated form. Analysis using Student's t-test revealed no effects of treatment on the relative expression of the two forms of neurocan. Values are shown as mean \pm SD (n = 4).

4.3.2 High Dose Minocycline Treatment

The initial studies using low dose minocycline treatment resulted in a transient improvement in functional recovery but there were no measurable changes in the glial cell responses. Further experiments were attempted using a more intense, high dose minocycline treatment (see section 4.2.2), in order to investigate if it would result in more persistent improvements in functional recovery and significant changes to the glial cell responses.

Infarct volume and the microglial responses were assessed at 3 d and the effects on downstream astroglial changes were evaluated at 7 d post-stroke. The time points were chosen as minocycline treatment was completed at 2 d after stroke. Any effects of the treatment on the infarct volume and microglial responses were most likely to be detectable at 3 d, whereas changes to the astroglial responses downstream of the microglial responses should be well developed by 7 d after stroke.

Forelimb placing reflex was tested at 3 and 24 hours and thereafter weekly starting at 7 days to 28 days post-stroke to monitor the effects of the treatment on long-term functional recovery.

4.3.2.1 Infarct Volume

Analysis using Student's t-test revealed no significant effect of high dose minocycline treatment at 3 d post-stroke (17.20 ± 4.88 vs. 18.56 ± 5.26 mm³, mean \pm SD, $n = 6 - 7$, vehicle vs. minocycline).

4.3.2.2 Forelimb Placing Reflex

A more stringent inclusion criterion of a placing score of 5 or less in the affected forelimb at 3 h post-stroke was used here and in the subsequent parts of the study, in contrast to the previous characterisation experiments (see section 2.3.2). Here, the rats exhibited a similar marked deficit in the placing response of their affected forelimbs as observed during characterisation. However, the revised inclusion criterion achieved a more consistent deficit that persisted for a longer duration.

The placing scores of the affected forelimb of animals treated with either high dose minocycline or vehicle are displayed in figure 4.3.8. Analysis of the area under the curve revealed that the high dose minocycline treatment resulted in enhanced recovery of forelimb function over the first 28 days after stroke compared to vehicle-treated controls. The differences in forelimb placing performance were greatest at 7 and 14 d after stroke.

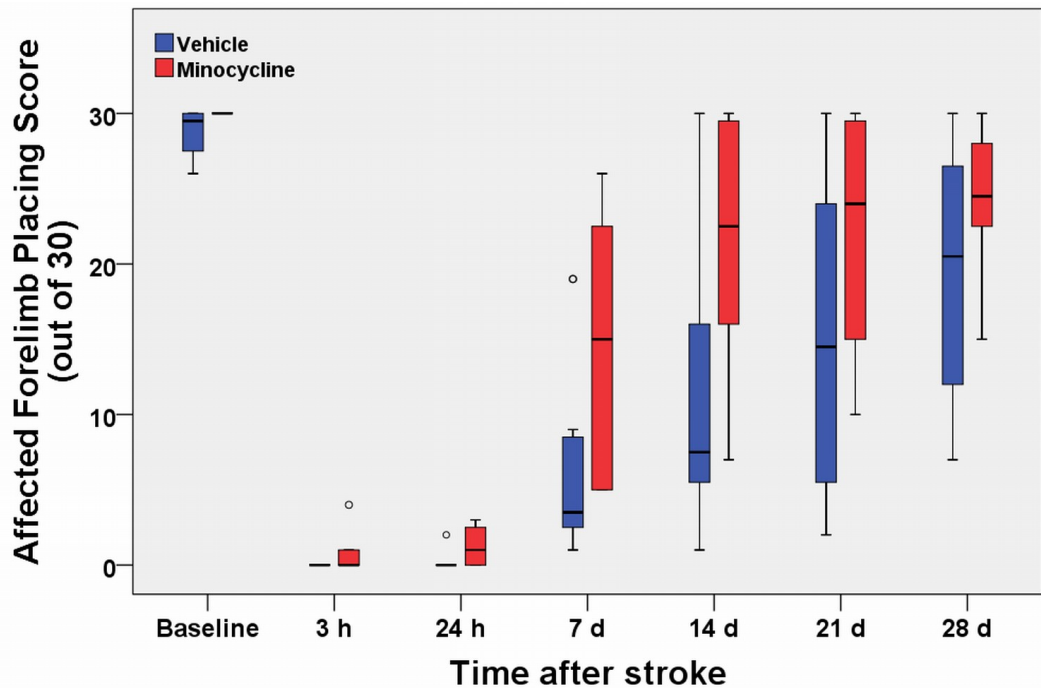


Figure 4.3.8 Forelimb placing score of the affected forelimb of animals treated with high dose minocycline or vehicle at baseline and up to 7 days after stroke.

High dose minocycline-treated animals exhibited improved recovery in their forelimb placing reflex over the first 28 days after stroke compared to vehicle-treated controls as assessed by area under the curve between 3 h and 28 d post-stroke ($p < 0.05$, *Vehicle vs. Minocycline, Mann-Whitney U test*). The data is presented in a box plot with outliers shown in open circles ($n = 8$ per group).

4.3.2.3 Microglial Morphology – Circularity

Microglial circularity at 3 d post-stroke was not affected by high dose minocycline treatment (figure 4.3.9). The circularity of microglial cells for both high dose minocycline- and vehicle-treated animals exhibited similar values to those observed in the characterisation and low dose minocycline treatment experiments at the same time point.

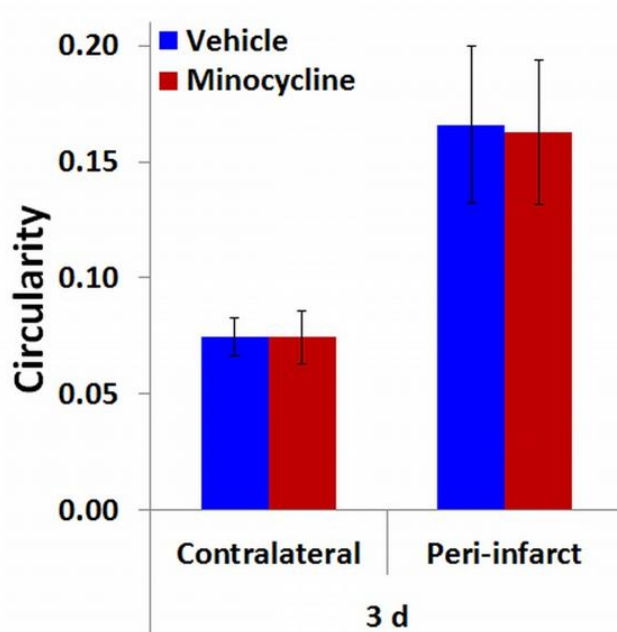


Figure 4.3.9 Circularity of microglial cells in the contralateral cortex and peri-infarct tissue of animals treated with high dose minocycline or vehicle.

Two-way analysis of variance revealed no significant effects of treatment and a highly significant effect of tissue region on the circularity of microglial cells at 3 d after stroke ($p < 0.01$, "Contralateral" vs. "Peri-infarct"). No significant interactions between the two factors were detected. Values are shown as mean \pm SD (n = 6 – 7 per group).

4.3.2.4 Microglial Area Fraction

The values for microglial area fraction for vehicle-treated animals were similar to those observed in the characterisation and low dose minocycline treatment experiments at the same time point. In contrast to the low dose treatment, high dose minocycline treatment had a small but significant effect in reducing in the microglial area fraction. This was detected in both the contralateral and peri-infarct regions at 3 d post-stroke (figure 4.3.10).

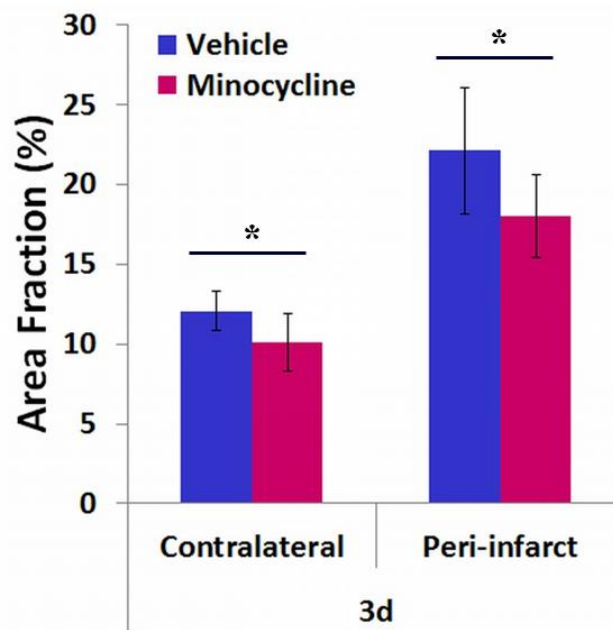


Figure 4.3.10 Area fraction of microglial cells in the contralateral cortex and peri-infarct tissue of animals treated with high dose minocycline or vehicle.

Two-way analysis of variance revealed a significant effect of treatment ($*p < 0.05$, "Vehicle" vs. "Minocycline") and a highly significant effect of tissue region ($p < 0.01$, "Contralateral" vs. "Peri-infarct") on the area fraction of microglial cells at 3 d after stroke. No significant interactions between the two factors were detected. Values are shown as mean \pm SD (n = 6 – 7 per group).

4.3.2.5 ED1⁺ Particle Count

As the effects of minocycline treatment on post-stroke microglial responses had been small so far, an additional measure of microglial activity, the expression of the phagocytic marker ED1, was investigated. At 3 d after stroke, expression of ED1 was mostly localised within the infarct (figure 4.3.11). Distribution of ED1⁺ cells within the peri-infarct tissue were restricted to within a short distance of the infarct boundary. This is evident from the marked decrease in ED1⁺ particle density at 0.3 mm away from the infarct boundary as seen in figure 4.3.12.

ED1-positive particles were counted within the peri-infarct and corresponding contralateral regions of ED1-immunolabelled brain sections (figure 4.3.12). High dose minocycline treatment strongly suppressed the expression of ED1 within the peri-infarct tissue compared to vehicle-treated controls, reducing the ED1⁺ particle density by more than half.

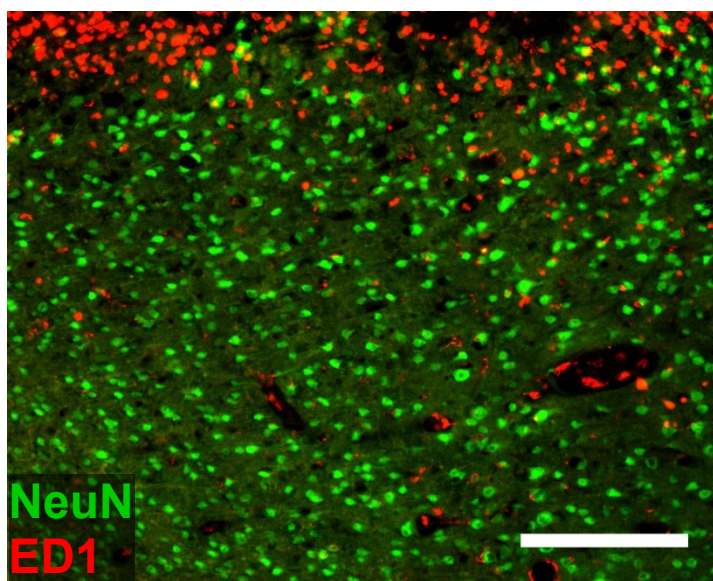


Figure 4.3.11 ED1-immunolabelling within the peri-infarct tissue at 3 days after stroke.

A representative image taken at the "Peri-infarct" position from a 3 d brain section of a vehicle-treated animal is shown. The infarct can be identified by the loss of NeuN-immunolabelling (green) along the top edge of the image. ED1 expressing cells (red) can be seen to accumulate in large numbers within the infarct and extended only a short distance into the peri-infarct tissue (scale bar = 200 μ m).

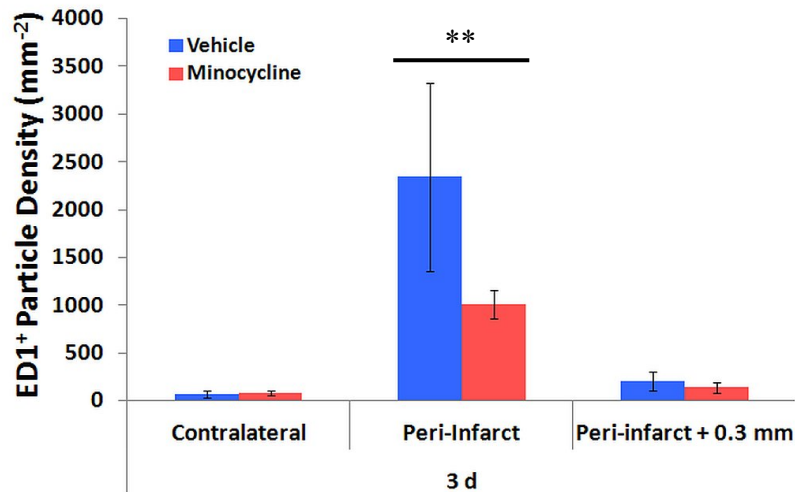


Figure 4.3.12 ED1⁺ particle density in the contralateral cortex and peri-infarct tissue of animals treated with high dose minocycline or vehicle.

Two-way analysis of variance revealed highly significant effects of both treatment ($p < 0.01$) and tissue region ($p < 0.001$) on ED1⁺ particle density at 3 d after stroke. There was also a strong interaction detected between the two factors ($p < 0.001$). Within the peri-infarct tissue immediately bordering the infarct, minocycline treatment resulted in a significant decrease in ED1⁺ particle density compared to vehicle-treated animals (** $p < 0.01$). Values are shown as mean \pm SD (n = 6 – 7 per group).

4.3.2.6 Astroglial Responses – Western Blots

Vimentin area fraction analysis was used for the low dose minocycline treatment experiments as it was an effective approach for the characterisation of the changes in vimentin expression following stroke (section 3.3.7). However, as the area fractions for vimentin were near saturation (~ 80%) at 7 d after stroke, it may potentially be less sensitive to treatment effects that promote further increases to its expression. Therefore, only Western blotting was used for this part of the study.

Densitometric analysis of western blots for vimentin and GFAP revealed that expression of both of these cytoskeletal proteins were significantly upregulated in the peri-infarct tissue of animals treated with high dose minocycline compared to vehicle-treated animals (figure 4.3.13).

However, in contrast to the marked changes observed for vimentin and GFAP expression, the relative ratio of the full length to truncated neurocan protein within the peri-infarct tissue was unaffected by the treatment (figure 4.3.14).

4.4 Discussion

In the present study, we have investigated the effects of a time-targeted minocycline treatment aimed at modulating the early microglial responses following photothrombotic stroke in rats. Early short-course treatment using minocycline resulted in significant improvements in functional recovery as assessed by the placing response of the affected forelimbs of the animals after stroke. Crucially, unlike most other studies investigating minocycline treatment in stroke, the improved recovery in our study was not associated with changes in infarct volume that are indicative of neuroprotection.

Low dose minocycline treatment resulted in a transient but significant improvement in forelimb function. However, there were no significant changes detected in any of the measures of microglial and astroglial responses within the peri-infarct tissue.

High dose minocycline treatment achieved a more lasting improvement in functional recovery. There was also a small but significant decrease in the area fraction of microglia in both the contralateral cortex and peri-infarct tissue. Similar to the low dose treatment, there were no changes in the circularity of microglial cells.

The area fraction is a composite measure that reflects cellular proliferation, migration and hypertrophy that are the consequences of changes in the expression of many genes. The sensitivity of area fraction as a measure of the microglial response was demonstrated in our earlier experiments where we detected a previously unreported transient loss in microglial cells within the peri-infarct tissue at 24 hours that was followed by large increases at 3 and 7 days (see sections 3.3.4 & 4.3.1.4). In the present study, the limited effect on microglial area fraction by minocycline strongly suggested that suppression of microglial activation may not be the primary mechanism underlying the effects of the treatment under the conditions used in the experiments. Furthermore, the small decrease in area fraction within the peri-infarct tissue was also observed in the contralateral cortex indicating a non-specific decrease in microglial activity that was not related to the infarction.

Surprisingly, the improved functional recovery was associated with increased astroglial reactivity as measured by GFAP and vimentin expression. This is contrary to expectations as improved functional recovery is usually associated with a reduced

astroglial response in other studies investigating pharmacological interventions after stroke (Brunkhorst et al. 2013; Lopez-Valdes et al. 2014; Schabitz et al. 2004).

Of the studies that have reported long-term functional improvements as a result of minocycline treatment after stroke, most have either initiated treatment early or used a delayed but prolonged treatment (Chu et al. 2010; Hayakawa et al. 2008; Hewlett & Corbett 2006; Liu, Z et al. 2007). Studies using early treatments have generally reported decreased infarct volumes indicative of neuroprotective effects while prolonged treatments may have effects on multiple pathways in different cell types. Both situations can complicate the investigation of the mechanisms underlying functional recovery. Unlike other studies, the early treatment used in our study did not result in changes in the infarct volume as we have utilised a stroke model that was resistant to the neuroprotective effects of minocycline. The timing and duration of the treatment was also targeted to coincide with the period after stroke where most of the microglial changes were observed to be occurring in our earlier characterisation experiments. Although we detected only minor changes to the microglial response as a result of the treatment, we have nonetheless observed substantial improvements in functional recovery after stroke.

Our results stand in contrast to other studies that have attributed the observed beneficial effects of minocycline treatment to the suppression of microglial activation (Chu et al. 2010; Hayakawa et al. 2008; Yang, Y et al. 2015; Yrjanheikki et al. 1999). In particular, the often cited study by Yrjanheikki et al. (1999) reported that minocycline treatment prevented the morphological changes triggered in microglial cells following stroke and suggested that microglial activation was strongly inhibited as a result of the treatment. However, the primary evidence provided in support of the claim was non-quantified images of CD11b-immunolabelled microglial cells from brain sections of animals pre-treated with minocycline 12 hours before stroke induction. Their results are in contrast with our study where minocycline treatment was initiated after stroke and did not result in suppression of the changes in microglial morphology as measured by circularity. Indeed, direct evidence for minocycline inhibition of microglial activation have mostly only been obtained from *in vitro* studies that have used conditions that are not appropriate for the study of stroke (see section 5.4 for a detailed discussion).

It has been observed that, in general, the magnitude of the microglial response is dependent on the severity of the injury (Abeysinghe et al. 2014; Kato et al. 1995; Streit 2000). Most of the studies that have reported that minocycline treatment suppressed microglial activation following stroke, including the study by Yrjanheikki et al. (1999), have also reported reductions in infarct volumes. Therefore, the suppression of the microglial response in these studies should not be considered as evidence of a direct effect of the minocycline treatment.

Although minocycline is generally regarded to be an anti-inflammatory agent and microglial cells are the presumed target in most stroke studies, results from the present study as well as from others suggest that other cell types may play a more prominent role.

In our study, we have used ED1 as an additional marker of activated microglia to evaluate the effect of minocycline treatment on microglial activation within the peri-infarct tissue. We detected a marked reduction in ED1 expression within the peri-infarct tissue as a result of minocycline treatment. This finding was broadly consistent with the results of studies by Liebigt et al. (2012) and Liu, Z et al. (2007) that used lower doses but more prolonged minocycline treatment regimens. Furthermore, we also observed that the ED1 expression was strongly localised to the infarct core and extended only a short distance into the peri-infarct tissue along the infarct boundary.

Interestingly, two studies that have also investigated the effects of minocycline-treatment on different aspects of the microglial response following stroke have also observed changes that were also localised to the infarct core. Chu et al. (2010) observed a decrease in the expression of 5-lipoxygenase (5-LOX), a key enzyme in the mediation of inflammatory responses, in microglial cells within the infarct core of minocycline-treated animals following stroke. Similarly, Hayakawa et al. (2008) observed that minocycline treatment resulted in reduced expression within the infarct core, of high mobility group box-1 (HMGB1), another protein that is also involved in the mediation of inflammation. Interestingly, the authors also reported a corresponding decrease in HMGB1 levels in the plasma. This is a finding that mirrored the decrease in plasma levels of pro-inflammatory molecules as a result of minocycline treatment reported in the study by Fox et al. (2005) that is discussed below.

Given that it has been observed that infiltrating macrophages from the circulation remained mostly within the infarct core and only invaded the peri-infarct tissue in limited numbers (see section 1.4.2.3), the pattern of changes induced in the expression of ED1, 5-LOX and HMGB1 by minocycline treatment would suggest a stronger effect on the infiltrating cells than the brain resident microglial cells. This would also be consistent with the observations in our study of a limited effect on the peri-infarct microglial responses.

Evidence in support of the view that minocycline has a stronger influence on the peripheral immune cells than the brain resident microglial cells in the treatment of stroke can be found in a study by Fox et al. (2005). In the study, 7 day old rat pups were treated using a single peritoneal injection of 45 mg/kg minocycline at 2 hours after reperfusion following temporary MCAo. Effects of the treatment were assessed by measuring the concentrations of cytokines in blood plasma and homogenised brain tissue using a cytokine assay kit. The authors reported that the stroke induced by MCAo resulted in a marked increase in the concentrations of the pro-inflammatory cytokines IL-1 β , CINC-1, IL-18 and MCP-1 in the plasma and ipsilateral brain hemisphere at 24 hours after reperfusion. Plasma concentrations of IL-1 β and CINC-1 were significantly decreased by minocycline treatment, but the concentrations of all four reported cytokines remained unchanged within the brain tissue. The use of neonatal rats in the study is of particular note as their immature blood brain barrier would be more permeable to minocycline than in adult rats and therefore more likely to result in higher minocycline concentrations in the CNS.

Although the evidence from the studies discussed so far points towards a primarily systemic effect, the marked reduction of ED1 expression within the peri-infarct tissue observed in the present study and others suggest the possibility that minocycline may also be modulating aspects of the microglial response that are not reflected in the measures of circularity and area fraction. This possibility has been demonstrated in principle by studies involving other disease models (Burke et al. 2014; Kobayashi et al. 2013). However, there is at present a lack of similar studies using stroke models.

A recent study by Yang, Y et al. (2015) reported that minocycline treatment following stroke suppressed the expression of M1 markers and promoted the expression of M2 markers in peri-infarct microglial cells. In the study, a single

intravenous injection of 3 mg/kg minocycline was administered immediately on reperfusion following temporary MCA occlusion in rats. The authors reported that the treatment significantly reduced the expression of M1 markers, TNF- α and IL-1 β , and increased the expression of M2 markers, TGF- β , IL-10 and YM1, at four weeks after stroke. However, the early treatment resulted in reduced infarct volumes and there was also a long time interval between the treatment and measurement of the markers. Consequently, the study did not provide evidence of a direct effect of minocycline in modifying the expression of M1 and M2 markers in microglial cells.

We have also attempted to address the current gap in knowledge regarding the effect of minocycline treatment on the activated microglial phenotype following stroke. Arginase-1 is an M2 marker that has been reported to be expressed by activated microglia following stroke and is associated with neuroplasticity and functional recovery (Hu et al. 2012; Lange et al. 2004; Quirie et al. 2013; Xia et al. 2015). Expression of arginase-1 has also been reported to be increased in microglial cells by treatments that improved functional recovery after stroke (Brifault et al. 2015; Verma et al. 2014), suggesting that it may be a suitable marker for our present investigations. However, preliminary experiments using arginase-1 immunolabelling in our stroke model have detected expression mainly in non-microglial cells at 3 d after stroke (data not shown). As discussed previously (see section 1.4.2.2), the expression of the M1 and M2 markers in microglia is not well characterised and their involvement in the facilitation of recovery following stroke is poorly understood at present. Further investigations are clearly needed to identify markers that may be useful in the evaluation of stroke treatments.

There is currently little, if any, evidence in the literature to suggest that minocycline may have direct effects on the astroglial response to stroke. However, the results from our study show that astroglial reactivity as indicated by the expression of GFAP and vimentin was upregulated downstream of the minocycline treatment. Astroglial reactivity is usually associated with inhibition of recovery due to the expression of CSPGs, such as neurocan, that have been demonstrated to inhibit axonal regeneration (Asher et al. 2000; Deguchi et al. 2005; Galtrey & Fawcett 2007; Siebert, Conta Steencken & Osterhout 2014). In our study, we observed improved functional recovery despite an increase in the astroglial response. Furthermore, the increased astroglial reactivity was not accompanied with a significant increase in neurocan expression. Although this is contrary to our initial hypothesis, other studies have also

reported treatments that led to both improved functional recovery and increased astroglial response after stroke.

Keiner et al. (2008) observed that rehabilitative training following photothrombotic stroke in rats resulted in improved functional recovery that was associated with enhanced survival of newly proliferated astroglial cells within the peri-infarct tissue. Using a similar model, Liebigt et al. (2012) further observed that combined rehabilitative training and treatment with either minocycline or indometacin, an anti-inflammatory drug, resulted in further improvements in functional recovery over rehabilitative training alone. The improved functional recovery was again associated with increased survival of newly proliferated astroglial cells. Interestingly, in both the above studies, there was a corresponding decrease in the survival of newly proliferated ED1-positive cells that paralleled our observations of a reduction in ED1-positive cells within the peri-infarct tissue of minocycline-treated animals.

Although astroglial expression of CSPGs may be detrimental to post-stroke functional recovery, the reactive astroglia is also a source of various factors that can improve the stroke outcome by promoting neuroplasticity (see section 1.4.1). Furthermore, astroglial cells may also play important roles in modulating the peripheral immune response after stroke (Sofroniew 2015). In particular, studies using transgenic mice to conditionally ablate proliferating astroglial cells in a stab wound model (Bush et al. 1999) and permanent MCA occlusion (Shimada et al. 2011) revealed an important role for astroglial cells in regulating the recruitment and infiltration of peripheral immune cells following injury. Ablation of proliferating astroglial cells in both studies resulted in large increases in the number of peripheral immune cells infiltrating into the peri-lesional tissue. These observations suggest a possible link between the increased astroglial response and decreased ED1-positive cells within the peri-infarct tissue in our study and the studies by Keiner et al. (2008) and Liebigt et al. (2012). An increased astroglial reactivity may potentially inhibit the infiltration of peripheral immune cells into the peri-infarct tissue.

It is possible that effects of minocycline treatment on other neural cell types may also contribute to the improved functional outcome. Some studies have suggested that minocycline treatment may promote the survival of newborn neurons arising from enhanced neurogenesis following stroke (Marlier et al. 2015; Thored et al. 2006; Yamashita, T et al. 2006). Although this is likely to contribute to the beneficial

effects of minocycline treatment observed in some studies employing prolonged treatment regimens (Liebig et al. 2012; Liu, Z et al. 2007), it is less likely to be a factor in the present study due to the early initiation and short duration of treatment.

In our study, we have used minocycline treatment as an approach for modulating microglial activation in order to investigate the influence of glial cell responses in the peri-infarct tissue on the neurorestorative processes underlying functional recovery following stroke. However, the molecular mechanisms underlying the effects of minocycline treatment are still unclear. Two studies utilising genomic (Crack et al. 2009) and proteomic (Agrawal et al. 2015) approaches have observed that the expression of many inflammatory and immune-related genes and proteins were modulated following minocycline treatment. Although the results from these studies do suggest the possibility that minocycline may strongly influence the responses of microglia and macrophages, they do not preclude the possibility that the genomic and proteomic changes observed were an indirect result of neuroprotection. Furthermore, it is also unclear if the immune responses elicited in the disease models used in the studies, traumatic brain injury and cypermethrin-induced neurodegeneration, are comparable to stroke models. In contrast to previous studies, our results do provide evidence that minocycline treatment may have an influence on the immune responses following stroke that are not related to neuroprotection. Furthermore, the treatment resulted in enhanced functional recovery, suggesting that the subsequent changes in the peri-infarct glial responses provided a microenvironment that was more favourable to neurorestorative processes.

4.5 Conclusion

The present study demonstrated that early post-stroke treatment with minocycline can improve the functional outcome via non-neuroprotective mechanisms. However, the exact mechanisms and cell types that are targeted by the treatment are unclear at present.

Minocycline has been demonstrated to have a strong influence on the activation response of both the peripheral immune cells and microglial cells. However, current evidence suggest that minocycline treatment, at least at the dosages used in the current and other similar studies, may only have a minor effect on microglial activation within the peri-infarct tissue. Instead, its primary effect may be in the modulation of the systemic immune response and recruitment of the peripheral immune cells to the infarct. Furthermore, minocycline may also be modifying the activated phenotype of microglial and peripheral immune cells to anti-inflammatory or pro-regenerative forms.

It was also observed that minocycline treatment led to a subsequent increase in the astroglial response within the peri-infarct tissue. Although astrogliosis is generally associated with impaired functional recovery, the evidence from our study suggest that there are beneficial aspects of the response that may be enhanced as an indirect effect of minocycline treatment likely as a result of modulation of the early immune cell responses.

Overall, the results of the study suggests that there are aspects of the early immune responses, involving both the peripheral immune and peri-infarct microglial cell populations, that may be important factors in the processes that underlie functional recovery during the later stages of stroke.

CHAPTER 5
A CELL CULTURE MODEL OF THE
PERI-INFARCT TISSUE

5.1 Introduction

Glial cell activation including astrogliosis and microglial activation are part of the natural responses of the CNS to challenges such as those posed by toxic insults, infections, trauma and disease. These responses serve to mobilise the innate defense mechanisms of the CNS to limit the spread of injury and to promote resolution and recovery.

As discussed previously (see section 1.4), the activation of astroglial cells is termed astrogliosis and is characterised by cellular hypertrophy and upregulation of cytoskeletal proteins including GFAP, vimentin and nestin. The process of astrogliosis develops over days to weeks following an insult and in severe injuries, such as those caused by stroke or trauma, eventually leads to the formation of a glial scar that serves to isolate the necrotic tissue from the healthy CNS.

Microglial activation on the other hand develops within hours with a marked morphological shift and upregulation of various inflammatory mediators (see section 1.4.2). The microglia appear ramified under normal conditions exhibiting a small cell body with several long, thin and highly branched processes. However, when exposed to an insult, microglia respond by retracting their processes and assuming a more amoeboid form (see figure 1.4.3). Within days, microglial migration and proliferation lead to greatly increased cell numbers around the site of injury.

The activated microglia are a source of many pro-inflammatory cytokines including IL1 β , IL6, IL10, TNF α and reactive oxygen species such as NO that have been identified to trigger or regulate various aspects of astrogliosis (Balasingam et al. 1996; Balasingam et al. 1994; Gao, Z et al. 2013; Giulian & Baker 1985; Zhang, D et al. 2010). These observations together with the observation that microglial activation tends to precede overt signs of astrogliosis has led to the suggestion that the process of astrogliosis is triggered by or is highly dependent on microglial activation.

It has long been recognised that the glial scar presents a barrier to axonal regeneration and is an impediment to functional recovery (see section 1.4.1). However, the processes leading up to its formation including microglial activation and astrogliosis involves complex mechanisms and cross-interactions that are incompletely understood at the present time, especially in the peri-infarct tissue in stroke. The results from various studies attempting to uncover the nature of these

processes have indicated that interfering with these post-stroke processes can have both beneficial and detrimental consequences at different time points after stroke. An improved understanding of the nature of these processes would therefore be critical in the development of therapies aimed at enhancing their beneficial aspects while minimising or avoiding the detrimental effects.

5.1.1 Studying Glial Cell Activation in Cell Cultures

Despite the large number of studies that have utilised cell culture models in the investigation of neurological disorders and injuries, there have been few that were designed to mimic focal insults such as those seen in focal stroke.

The aim of the present study was to develop a cell culture model of focal cell death that can simulate the conditions of the peri-infarct tissue in focal stroke. Such a model would be a useful tool for the investigation of peri-infarct astroglial-microglial interactions and their influence on the development of astrogliosis. It could also serve as a useful platform to investigate interventions to modulate the process of astrogliosis.

The successful culturing of dissociated mammalian brain cells by Booher and Sensenbrenner (1972) has contributed greatly to our current understanding of the basic cellular functions of the different cell types that make up the CNS. For example, the use of primary astroglia in cultures has been indispensable in the study of their receptor functions (Hosli & Hosli 1993; McCarthy & de Vellis 1980) and their role in the regulation of extracellular pH & ion concentrations (Hertz & Schousboe 1975; Schousboe, Fosmark & Formby 1976).

In many instances, the use of cell cultures has also been critical in the understanding of the role of different cell types within the CNS and their interactions in the development of diseases and injuries (Craig, Graf & Linhoff 2006; Hansson & Thorlin 1999; McMillian et al. 1994; Murphy, EJ & Horrocks 1993; Wu & Schwartz 1998). This is due to several key advantages they offer over the use of animal models. For example, the cellular composition of a culture can be manipulated to enrich certain cell types so that their specific functions and interactions can be studied without the interference of other cell types. Furthermore, the culture system allows direct access to the cells that permits manipulation of the cellular environment

to reproduce conditions that mimic specific aspects of the disease. Monitoring of the changes induced in the cells in response to the applied conditions is also far easier in cultures compared to animal models.

Various cell culture models have been devised to investigate different aspects of ischemic stroke in the brain. For example neuronal, glial and mixed cortical cultures have been used to study the mechanisms of cell death during the initial stages of stroke (Almeida et al. 2002; Bruno et al. 1994; Chock & Giffard 2005; Goldberg, WJ, Kadingo & Barrett 1986) and glial cell cultures have been used to investigate the mechanisms involved in glial cell activation and astrogliosis (Bohatschek et al. 2001; Wanner et al. 2008; Yu, Lee & Eng 1993).

The prevalent model of ischemic stroke in cell culture is the oxygen-glucose deprivation (OGD) model that was first reported by Goldberg, WJ, Kadingo and Barrett (1986) in a study that focused on the effects of ischemia on neurons. The model has since been applied to the investigation of astroglial responses and has been demonstrated to replicate some of the features of astrogliosis including upregulation of GFAP, neurocan and inhibition of neurite outgrowth in co-cultured neurons (Wang, R et al. 2012). However, a prolonged period of OGD was required to induce the observed responses; far longer than is normally required in animal models. Furthermore, the fact that the OGD insult had to be applied to the entire culture rather than a focused region meant that the model was more appropriate as a model of the ischemic core or as a model of global ischemia than of the peri-infarct tissue.

Other models that have been used in the study of astrogliosis included the scratch wound model, in which the insult is induced by physical scoring of the culture surface with a pipette tip, and chemical insults such as excess potassium and elevated glutamate concentrations (Murphy, EJ & Horrocks 1993; Petito, Juurlink & Hertz 1991; Yu, Lee & Eng 1993). Despite the fact that the models utilising chemical insults all had some degree of success at reproducing aspects of astrogliosis, they share the same weakness as the OGD model in that the entire culture was exposed to the insult. Although the scratch wound model does in fact introduce a localised area of insult, it was more a process that removed cells from the culture surface than one that created an injury associated with cell death.

Most of the models described above have also been applied to the study of various aspects of microglial activation including morphological changes, cytokine

expression and production of ROS. However, very few studies have examined in detail the interactions between microglia and astroglia and the influence of microglial activation on astrogliosis especially in the context of a focal insult.

5.1.2 Inducing Focal Injury in Cell Cultures

In 2004, Yu and co-workers described a method of triggering astrogliosis in astroglial cultures by inducing low temperature trauma with a liquid nitrogen pre-cooled copper pipe (Yu et al. 2004). Although it was proposed by the authors to be a model of cryo-surgery or cryo-injury, the model produced a focus of cell death defined by the contact area of the copper pipe with the culture dish. This focal lesion is surrounded by surviving cells that is reminiscent of the stroke infarct core and peri-infarct tissue.

The authors reported a rapid upregulation of various immediate early gene (IEG) proteins and the 70 kDa heat shock proteins (HSP70) in the peri-lesional cells within hours of lesion induction and increased GFAP expression after 6 days; a response that was similar to that reported in various animal models of stroke and cell culture models of astrogliosis (de Freitas et al. 2002; Gass et al. 1992; Iwata, Masago & Yamada 1997; Liu, HM 1995). However, characterisation of the model in the study was limited to qualitative descriptions and lacked quantitative data.

Despite the lack of detailed characterisation, the similarities in the focal nature of the induced cell death and the responses of the peri-lesional cells to those seen in animal models of focal ischemia suggested that this could be a suitable model for investigating cellular responses in the peri-infarct tissue after stroke.

5.1.3 A Cell Culture Model of the Peri-infarct Tissue after Stroke

In the present study, we evaluated the effectiveness of the approach of inducing focal cell death based on a significant adaptation of the method of Yu et al. (2004) (hereafter referred to as the "cryo-lesion" method, or "cryo-lesioning") as a model of the peri-infarct tissue after stroke. Modifications were made to the method by using a solid copper rod rather than a copper pipe to ensure uniform cooling within the entire

lesion area, and to have one end of the copper rod immersed into a liquid nitrogen filled box to ensure that a constant temperature was maintained throughout the experiments. In addition, the surface temperature of the cell cultures were monitored during the cooling process with an infrared thermometer to ensure a consistent temperature was achieved over the course of the experiments.

We have also used primary mixed glial cultures in our model to enable the study of microglial-astroglial interactions. Although it is acknowledged that microglia in culture exhibit signs of being in a more activated state than in intact brain tissue, they can be induced to undergo further distinct activation by insults (Glenn et al. 1992; Graeber et al. 1989).

We first characterised the responses of microglial and astroglial cells to cryo-lesioning within the peri-lesional regions up to 48 hours after cryo-lesioning. The microglial responses were characterised on the basis of the induced morphological changes by quantifying the relative proportions of ramified and amoeboid microglia. Changes in the microglial distribution due to proliferation and migration were also characterised by determining the microglial cell density within the peri-lesional regions. Astroglial responses were characterised by observing the morphological changes in GFAP-immunolabelled cells along the edge of the lesion as well as the changes in the labelling intensity of nestin in the peri-lesional regions.

We then performed an initial investigation into the nature of microglial-astroglial interactions within the post-stroke peri-infarct tissue by studying the effects of modulating microglial influence on the astroglial changes after cryo-lesioning. Microglial activity was manipulated by two different approaches. The first approach was treatment with minocycline, an antibiotic with anti-inflammatory properties that has been reported in many animal and cell culture studies to suppress microglial activation. The second was the more direct approach of abolishing microglial activity by depleting them from the cultures.

5.2 Materials and Methods

5.2.1 Primary Mixed Glial Cell Culture

Cell cultures were prepared based on the method as previously described by Muyderman et al. (2010), with significant modifications to both expand the microglial population and enhance the degree of ramification of microglial cells. These modifications were based on preliminary investigations and included an increase in the initial seeding density and changes in the feeding protocol. The increased seeding density resulted in an increased proportion of microglial cells within the cultures as the astroglial cells reached confluence earlier and stopped dividing. The feeding frequency was reduced from 3 times to 2 times per week and the medium used for feeding was changed from fresh culture medium to a 1:1 mixture with glial conditioned medium.

Primary mixed glial cultures were established using Sprague-Dawley rat pups up to 2 days old. The brains were removed following decapitation and carefully dissected free of the meninges and any visible blood vessels. The cortices were then separated from the rest of the brain and passed through an 80 µm nylon mesh into culture medium consisting of low glucose Dulbecco's modified Eagle's medium (DMEM) supplemented with 10 % fetal bovine serum and 1 % penicillin-streptomycin (10,000 U/mL). The cortical cell suspension was further dissociated by gentle trituration with a 10 mL serological pipette (86.1254.001; Sarsted Australia Pty Ltd, SA, Australia). The final cell suspension was diluted to a final volume in culture medium depending on the age of the pup: 15 mL per cortex for pups up to 1 day old and 20 mL per cortex for pups between 1 and 2 days old.

The final cell suspension was seeded onto poly-L-lysine-coated coverslips (see section 5.2.3) in 35 mm cell culture dishes (83.1800.003; Sarstedt Australia Pty Ltd, SA, Australia) at a volume of 0.5 mL per dish. The culture medium in each dish was then topped up to a final volume of 2 mL. The cultures were grown in a humidified atmosphere of 5.5 % CO₂ in air at 37 °C (subsequently referred to as “normal conditions”) and the culture medium was replaced with fresh culture medium (FCM) at 4 days after initial seeding (4 DIV – days *in vitro*).

At 7 DIV and thereafter, the cells were fed twice per week. The medium from all the dishes was first collected and pooled (glia-conditioned medium – GCM) then mixed

at a 1:1 ratio with FCM (GCM:FCM). The mixture of conditioned and fresh culture medium was then fed back to the cells using 2 mL per dish. This feeding procedure was used at 7 DIV and onwards. Maintained under these conditions, the cultures typically reach confluence at between 8 and 10 DIV. Initial investigations revealed that disturbances in the culture medium due to feeding resulted in de-ramification of microglial cells. In order to maximise ramification of microglial cells, the cultures were only used for experiments at least 3 days after the last feeding when confluence is reached. These conditions were typically satisfied at 14 DIV. Microglial cells constituted 28.69 ± 2.75 % (mean \pm SD, n = 6) of the total cell population within the cultures at 14 DIV. For microglial depletion experiments additional treatments were performed as described in section 5.2.3.

5.2.3 Coating of Coverslips with Poly-L-lysine

Coating of the coverslips (No.1, 30 mm diameter; Menzel-Gläser, Braunschweig, Germany) with poly-L-lysine was done at least one day in advance of the seeding. The coverslips were placed into the cell culture dishes and incubated in 0.01 % poly-L-Lysine for 15 min at room temperature. Poly-L-lysine was dissolved in double-distilled water and sterilised by filtration through a 0.20 μ m syringe filter (16534K ; Sartorius Stedim Australia Pty Ltd, VIC, Australia) before use. Following incubation in poly-L-lysine, the coverslips were rinsed twice in sterile filtered double-distilled water. The culture dishes with the poly-L-lysine-coated coverslips were then dried overnight at 37 °C before cell seeding.

5.2.3 Depletion of Microglial Cells from Mixed Glial Cultures

Microglial cells were depleted from the mixed glial cultures using cytosine β -D-arabinofuranoside (Ara-C) and L-leucine methyl ester (LME) treatment based on the method described by Hamby et al. (2006).

Cultures to be used for the microglial depletion experiments were treated for 3 days with 8 μ M Ara-C dissolved in GCM:FCM at 11 DIV after they have become confluent. Ara-C treatment is toxic to actively dividing cells such as microglia but does not affect astroglia that are contact-inhibited and stop dividing after reaching confluence.

Following Ara-C treatment, at 14 DIV, LME treatment was used to eliminate the remaining microglia. LME is a lysosomotropic agent that is selectively toxic to cells, such as microglia, that are enriched in lysosomes (Thiele, Kurosaka & Lipsky 1983). LME was prepared at a concentration of 50 mM in DMEM and pH adjusted to 7.4. Cultures were incubated in 1 mL of 50 mM LME for 60 minutes under normal culture conditions. Following LME treatment, the cultures were rinsed twice in DMEM and maintained under normal culture conditions in GCM:FCM for 2 days, then fed once again with GCM:FCM and cultured for a further 3 days before being used in the microglial depletion experiments.

5.2.4 Minocycline Treatment

For the minocycline treatment experiments, the cultures were pre-treated with 10 μ M minocycline. The treatment concentration was selected based on other cell culture studies that have reported inhibition of microglial activation using minocycline treatment (Huang et al. 2010; Kremlev, Roberts & Palmer 2004; Silva Bastos et al. 2011; Suk 2004). A stock solution of 1 mM minocycline was prepared in DMEM and sterile filtered by passing through a 0.20 μ m syringe filter. The stock solution was then added to the cultures at 1:100 dilution and the cultures were incubated under normal conditions for 30 min before cryo-lesion induction.

5.2.5 Induction of Cryo-lesion

Cryo-lesion was induced in cultures by means of a brief contact with a liquid-nitrogen-cooled copper rod (figure 5.2.1). The solid copper rod was cooled by insertion into a liquid nitrogen filled polystyrene foam box through a hole in the lid. The upper face of the rod (10 mm diameter) protruded slightly above the lid and its temperature was allowed to equilibrate for at least 15 min before the start of experiments. During cryo-lesion induction, the temperature of the cell culture surface was monitored using an infrared thermometer (IR-77L; CEM, Shenzhen Everbest Machinery Industry Co. Ltd, Guangdong Province, China) positioned directly above the copper rod.

The culture medium was first removed by pipetting from the culture dish and retained in a sterile 15 mL tube. Then the underside of the dish was pressed firmly

against the exposed face of the rod for several seconds while the temperature of the cell culture surface was monitored. As soon as the temperature decreased to 5°C, which typically took between 6 to 8 s in this experimental set-up, the culture dish was removed from contact with the rod and the culture medium was returned to the culture dish. The temperature of 5 °C was determined in preliminary investigations to consistently induce near complete cell death within the contact area by 2 h after cryo-lesion.

For unlesioned controls, the culture medium was first removed and retained in a sterile tube, similar to the process for cryo-lesion induction. However, instead of contacting the copper rod, the cultures were simply exposed to air for 15 s, which was the approximate duration that the cultures were deprived of medium during the cryo-lesion induction process. The culture medium was then returned to the dishes.

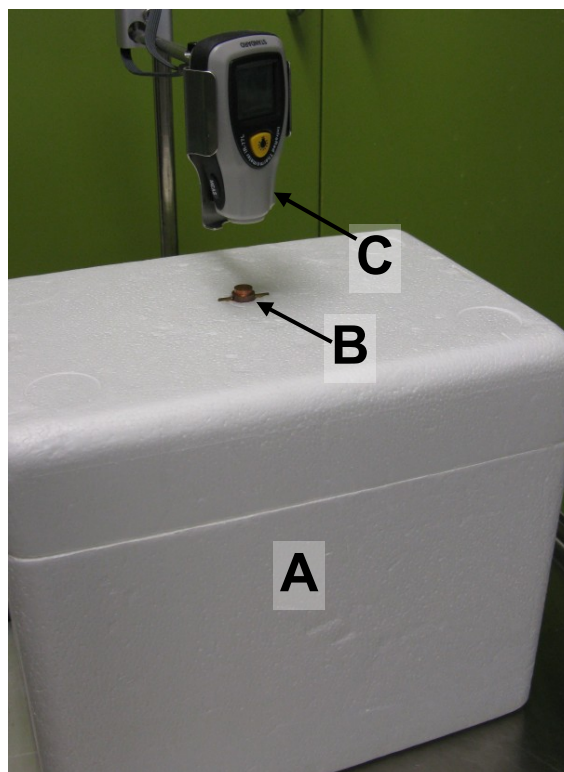


Figure 5.2.1 Experimental set-up for induction of cryo-lesion in cell cultures.

The experimental set-up consists of a liquid nitrogen filled polystyrene foam box (A) with a solid copper rod (B) inserted through a hole in the lid. An infrared thermometer (C) mounted on a retort stand is positioned above the copper rod to monitor temperature changes during cryo-lesion induction.

Cold-treated cultures were included in the experiments as a control for the possible effects of cold exposure alone as experienced by cells outside of the immediate contact region of the copper rod (see figure 5.3.1). For cold-treated cultures the culture medium was removed and retained in a sterile tube and 1 mL of DMEM pre-chilled to 16 - 17 °C was added to the cultures. After 10 s, the pre-chilled DMEM was removed and the culture medium was returned to the culture dish.

All treatment conditions were performed in duplicates and the data reported for each experiment were the averaged values of the duplicates. The cultures were maintained under normal conditions following treatment until they were used for assessment of cell death and viability or immunocytochemistry.

For the characterisation experiments, the cultures were processed for immunocytochemistry at 2, 6, 24 and 48 h after cryo-lesioning. Assessment of cell death and viability was performed using cultures at 2 and 6 h after cryo-lesioning.

For the assessment of microglial changes in the minocycline experiments, the cultures were processed for immunocytochemistry at 24 h after cryo-lesioning. Assessment of the astroglial changes in the minocycline and microglia depletion experiments was performed using the cultures at 48 h after cryo-lesioning

5.2.6 Thermal imaging of cell culture surfaces during Cryo-lesion induction

The change in the surface temperatures of the cultures during cryo-lesion induction was visualised using a thermal imaging camera (ThermoVision™ A40M; FLIR systems Australia, VIC, Australia).

5.2.7 Assessment of Cell Death and Viability Following Cryo-lesioning

Cell death induced in the cultures by cryo-lesioning was assessed by staining with calcein acetoylmethyl ester (Calcein AM) and propidium iodide (PI). All cell nuclei were counterstained with Hoechst 33258. Cell cultures were washed twice in HEPES-buffered salt solution (HBSS; 137 mM NaCl, 5.4 mM KCl, 0.41 mM MgSO₄, 0.49 mM MgCl₂, 1.26 mM CaCl₂, 0.64 mM KH₂PO₄, 3 mM NaHCO₃, 5.5 mM D-glucose, 20 mM HEPES, pH 7.4) then incubated for 20 min under normal conditions in 1 mL each of 1 μM Calcein AM, 25 μM PI and Hoechst (1:1000

dilution) dissolved in HBSS (pH 7.4). Cells were visualised using fluorescence microscopy (Olympus IX71) immediately following incubation. Cultures were assessed for cell death and viability at 2 and 6 h following cryo-lesion.

Calcein AM is lipophilic and crosses cell membranes into live cells where it is hydrolysed by nonspecific esterases into a fluorescent and less lipophilic form that is retained within the cell. In contrast, PI is excluded from viable cells and only binds with the nuclei of dead or dying cells with disrupted cell membranes. Hence, live cells exhibit strong fluorescence within their cell bodies from calcein accumulation and exclude PI from their nuclei, whereas dead or dying cells exhibit PI fluorescence in their nuclei and do not accumulate calcein.

5.2.8 Immunocytochemistry

A list of primary and secondary antibodies, dilutions used, and the suppliers are provided in the Table 5.2.1. In addition, all cell nuclei were counterstained with Hoechst 33258 (1:1000 dilution).

Table 5.2.1 List of antibodies and dilutions used in immunocytochemistry

Primary Antibodies			
Description	Dilution	Product No.	Supplier
Mouse monoclonal anti-CD11b/c [Clone OX-42]	1:400	MR6200	ThermoFisher / Invitrogen™
Mouse monoclonal anti-Nestin [Clone 2Q178]	1:400	ab6142	Abcam
Rabbit polyclonal anti-GFAP	1:500	G4546	Sigma-Aldrich
Rabbit polyclonal anti-iNOS	1:200	ab3523	Abcam
Secondary Antibodies			
Description	Dilution	Product No.	Supplier
Donkey anti-Rabbit IgG (H+L) Alexa Fluor® 488 conjugate	1:500	A-21206	ThermoFisher / Invitrogen™
Donkey anti-Goat IgG (H+L) Alexa Fluor® 647 conjugate	1:500	A-31571	ThermoFisher / Invitrogen™

Cultures were rinsed in Tris-buffered saline (TBS; 0.9 % NaCl in 0.1 M Tris, pH 7.4) then fixed in 4 % paraformaldehyde in 0.1 M sodium phosphate buffer for 15 min at room temperature and then rinsed again in TBS. Next, the cultures were blocked and permeabilised in blocking buffer (1 % BSA, 0.5 % Triton-X in TBS, pH 7.4) for 1 h at room temperature.

For the characterisation experiments, double immunolabelling was performed using antibodies for CD11b/c and GFAP. For the minocycline treatment and microglial depletion experiments, two combinations of double immunolabelling were used – CD11b/c with iNOS, and GFAP with nestin. Following blocking and permeabilisation, the cultures were incubated overnight at 4 °C with the primary antibodies diluted in blocking buffer.

After incubation with primary antibodies, the cultures were washed 3 times in TBST (0.5 % Triton-X100 in TBS, pH 7.4) for 5 min each time at room temperature. Then the cultures were incubated with secondary antibodies and Hoechst 33258 diluted in TBS for 2 h at room temperature on an orbital shaker (Bioline orbital shaker, BL8136; Bioline Global Pty Ltd, NSW, Australia).

Finally, the cultures were washed 3 times in TBS for 5 minutes at room temperature, and then the coverslips were mounted on glass slides (76 × 26 mm, HD 41808 1P0; HD Scientific Supplies Pty Ltd, NSW, Australia) in ProLong® Gold antifade reagent. The antifade reagent was allowed to cure overnight before the edges of the coverslips were sealed with clear nail polish. The cells in the cultures were then visualised using conventional fluorescence microscopy except for the minocycline treatment experiments where confocal microscopy was used for CD11b/c and iNOS-immunolabelled cells.

5.2.9 Image Acquisition

Fluorescence images were acquired using an Olympus IX71 inverted microscope (Olympus Australia Pty Ltd, NSW, Australia). The microscope was also equipped with a custom-fitted calibrated stage. For quantitative analyses, images were acquired using the 10× objective lens at the ROIs (approximately 898 × 671 μm image fields) for each coverslip as shown in figure 5.2.2. Identical camera exposure settings were used to capture all the GFAP immunofluorescence images from all ROIs in all the cultures used for the analysis of astroglial responses. Exposure settings were similarly fixed for all the nestin immunofluorescence images that were captured.

For the minocycline treatment experiments, cells that were immunolabelled for CD11b/c and iNOS were scanned using confocal microscopy at the same locations using a Leica TCS SP5 confocal microscope (Leica Microsystems Pty Ltd, NSW,

Australia). Images were taken in a 10 μm stack at 1 μm steps (11 images per stack) using the 20 \times objective lens, corresponding to an image field of 775 by 775 μm area.

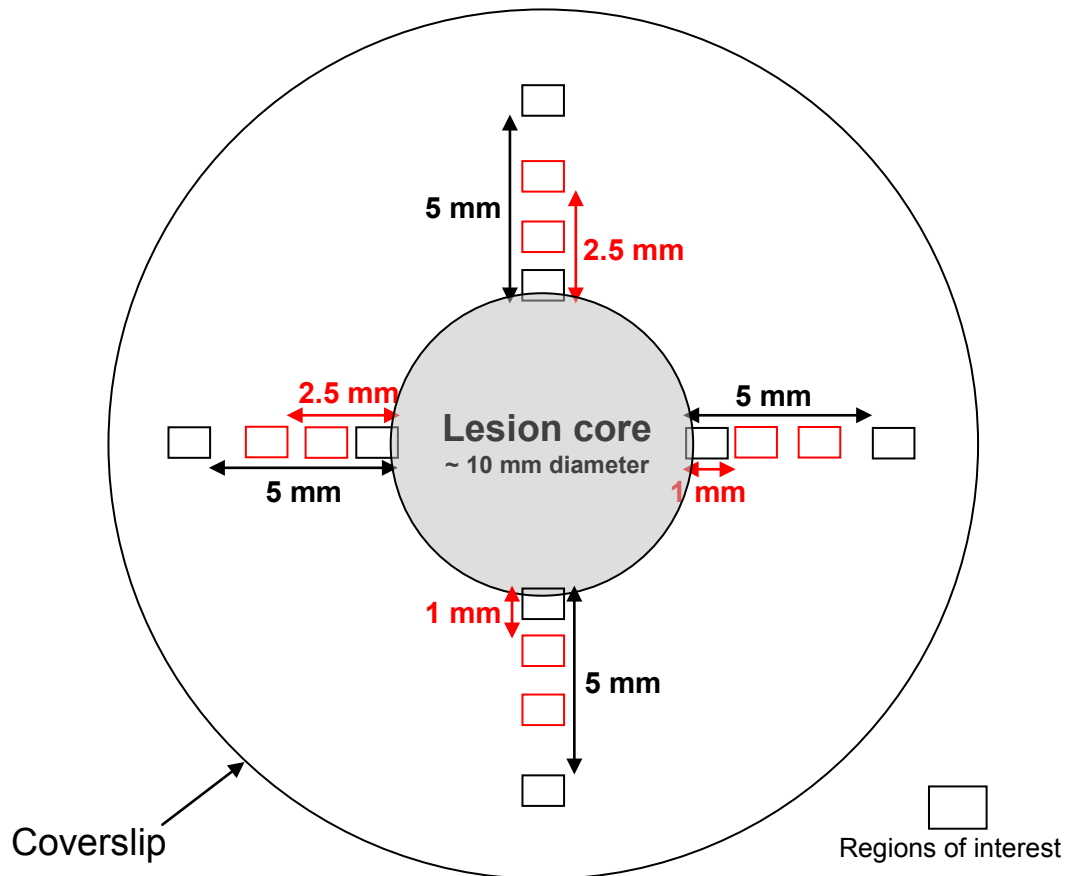


Figure 5.2.2 Diagram illustrating regions of interest for image acquisition on each coverslip.

Fluorescence images were acquired for CD11b/c immunofluorescence at the 8 positions as shown by the black boxes in the diagram above. Four images were acquired along the lesion border at the top and bottom, left and right edges of the lesion, and a further four were acquired at a distance of 5 mm away from the first four images. Images acquired using the 10 \times objective lens covered image fields with an area of approximately 898 by 671 μm . For GFAP and nestin immunofluorescence, in addition to the ROIs indicated by the black boxes, images were also acquired at 1 and 2.5 mm as shown by the red boxes. For the later experiments to modify glial responses, images were acquired for CD11b/c and iNOS immunofluorescence by confocal microscopy at the same positions indicated by the black boxes using the 20 \times objective lens. This captured image fields of 775 by 775 μm .

5.2.10 Image Analysis

5.2.10.1 Characterisation of Microglial Responses to Cryo-lesion

Manual cell counting was performed for the experiments to characterise the microglial responses to cryo-lesion. Cell counts were determined from 200 by 200 μm crops of each of the 8 ROIs (as shown in figure 5.2.2). Counting was performed using the “Cell counter” plugin in the image analysis software "ImageJ" (Schneider, Rasband & Eliceiri 2012).

Total cell density was determined from counts of Hoechst-stained cell nuclei and microglial cell density from counts of CD11b/c⁺ cells. Ramified and amoeboid microglia were identified based on morphological criteria and expressed as a percentage of the total microglial cell population. Ramified microglia were defined as having a small cell body with at least two long and thin processes, and one or more of the processes exhibiting secondary branching. Amoeboid microglia were defined as being either round and devoid of processes, or have an enlarged cell body with only short and thick processes. Cells with intermediate morphologies that did not match the definitions for either ramified or amoeboid microglia were included in the total count but not separately reported.

5.2.10.2 Measuring Changes in Microglial Responses to Cryo-lesion and Minocycline Treatment

i. Changes in Circularity & Area Fraction

For the minocycline treatment experiments, microglial circularity and area fraction were analyzed using a similar approach to that described for the animal studies (see section 2.3.10). A “sum of slices” projection of the CD11b/c image stacks was used here rather than the maximum projection as used for the animal studies as it provided a better contrast of the cell profiles and suppression of the background in the fluorescence images of the cell cultures. The “sum of slices” projection generated 32-bit images that were then converted to 8-bit. The images were then processed using the “Subtract Background” function with a 100 pixel rolling ball radius and sliding paraboloid option. The “De-speckle” function was then applied to the images to remove speckling noise.

A manual thresholding method was used to determine the threshold level to be used to identify the cell profiles. The average background fluorescence in each image was determined by sampling the fluorescence at 5 locations within the image that were devoid of cells. The threshold level was set at twice the average background fluorescence intensity rounded down to the nearest integer. The "specify" function was then used to select an area of $500 \times 500 \mu\text{m}$ for analysis. The selected area was then analysed for circularity and area fraction using the "Analyze Particles" function with particle size set to a lower limit of 200 pixel units.

ii. Changes in iNOS expression

For the analysis of changes in iNOS expression, the iNOS image stacks were processed in the same way as the CD11b/c image stacks except for the following changes. The built-in "triangle" thresholding algorithm was used instead of manual thresholding. The lower limit for particle size in "Analyze Particles" was set at 50 pixel units.

5.2.10.3 *Measuring Changes in Astroglial Responses to Cryo-lesion*

The changes in astroglial expression of GFAP and nestin were quantified for the minocycline treatment and microglial depletion experiments. The unprocessed fluorescence images were opened in ImageJ and an area $500 \times 500 \mu\text{m}$ was selected using the "Specify" function. The mean fluorescence intensity within the selected area was determined using the "Measure" function. The values at each position were then normalised to the averaged fluorescence intensity of the unlesioned and untreated controls in each experiment in order to account for the variability in immunolabelling and imaging conditions between experiments.

5.2.11 Measuring Nitrite Content Using the Griess Reaction

Nitrite accumulation in the cultures was assessed as an additional measure of the glial cell response to cryo-lesion and the effects of minocycline treatment. 120 μL of the cell culture medium was sampled from each dish before cryo-lesion. At 24 h after cryo-lesion, half of the dishes were processed for immunocytochemistry and all the culture medium from these dishes were collected and stored. At 48 h, the remaining dishes were also processed for immunocytochemistry and the culture medium from these dishes were similarly collected and stored. The medium samples were stored at $-80\text{ }^{\circ}\text{C}$ until they were assayed for nitrite content using the Griess Reaction (Bryan & Grisham 2007; Tsikas 2007).

The samples were thawed then centrifuged at 1000 RCF for 5 min at $4\text{ }^{\circ}\text{C}$ (Sigma 1-15K; SciQuip Ltd, Shropshire, UK). 50 μL of the supernatants and nitrite standards were pipetted in duplicates into 96 well plates (Item No: 655001; Greiner Bio-One GmbH, Kremsmünster, Austria). The nitrite standards were prepared at concentrations of 0, 0.5, 1, 2, 4, 8, 12 and 20 μM using sodium nitrite dissolved in double-distilled water. An equal volume of Griess reagent was pipetted into each well and the reaction was allowed to develop for 15 min. The absorbance at 540 nm was measured on a plate reader (Victor™ X4 Multilabel Plate Reader, Product No. 2030-0050; PerkinElmer Inc, MA, USA). The change in nitrite content over the 24 or 48 h duration after cryo-lesion was calculated by subtracting the corresponding baseline values.

5.3 Results

5.3.1 Characterisation of the Cell Culture Model

5.3.1.1 Surface Temperatures of Cell Cultures during Induction of Cell Death by Rapid Cooling

Preliminary investigations using different contact times monitored with an infrared thermometer indicated that approximately 7 s of contact with the cooled copper rod was sufficient to produce a decrease in the surface temperature of confluent cultures to between 0 and 5 °C and appeared to induce near complete cell death within the core region (figure 5.3.1).

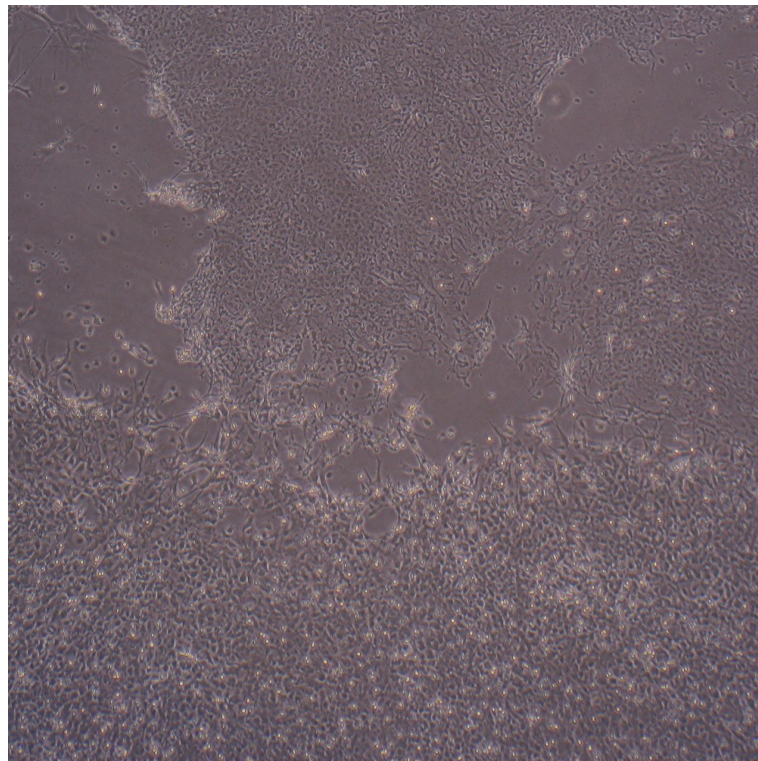


Figure 5.3.1 Unfixed primary mixed glial culture 24 hours after 7 seconds contact with liquid nitrogen cooled copper rod.

A representative dark field microscope image is shown. The core region that was in contact with the copper rod is located in the upper half of the image. Cell bodies within the contact region appeared shrunken and disrupted in comparison to the cells outside the region.

In order to investigate the extent of the cooling on the regions outside of the immediate core region of the copper rod, the surface temperatures of cell cultures ($n = 2$) were mapped using a thermal imaging camera during induction of the cryo-lesion. These images revealed that while the entire core region in direct contact with the copper rod fell to below $10\text{ }^{\circ}\text{C}$ after 7 s of contact, regions outside of the immediate core of the copper rod stayed mostly above $20\text{ }^{\circ}\text{C}$ (figure 5.3.2). These results suggested that the effect of rapid cooling by brief contact with the copper rod was highly localised and cells outside of the immediate core region were not subjected to major temperature changes. However, the possible effects of this milder temperature decrease were taken into account by including cold-treated controls in the subsequent characterisation experiments.

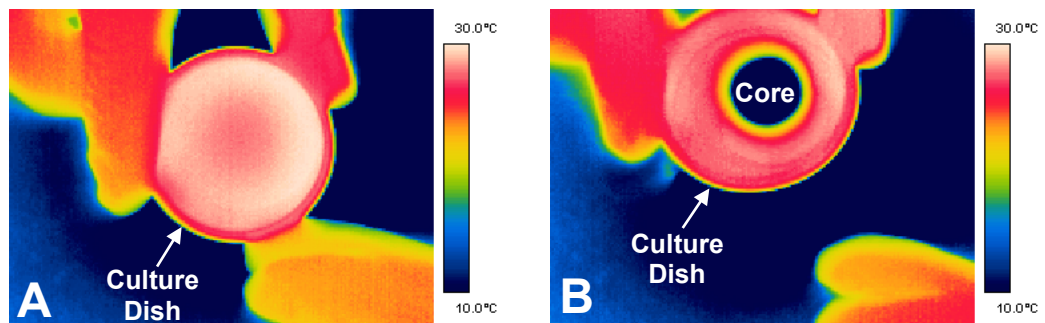


Figure 5.3.2 Thermal images of cell culture surface before and immediately after induction of cryo-lesion.

The images show the surface temperatures of a primary mixed glial culture grown on a coverslip in a cell culture dish (35 mm diameter) during cryo-lesion induction. (A) The cell culture surface temperatures were mostly at or near $30\text{ }^{\circ}\text{C}$ after removal of the culture medium and before contact with the copper rod. (B) After contact with the liquid nitrogen cooled copper rod for 7 s, the regions outside of the area of contact with the core of the copper rod remained mostly above $20\text{ }^{\circ}\text{C}$.

5.3.1.2 Cold Induced Cell Death in the Core Region

Unfixed cultures were incubated with calcein and propidium iodide (PI) at between 2 and 6 h after cryo-lesion in order to visualise the induction of cell death. Dying cells with compromised cell membranes were unable to retain the green fluorescent calcein dye within the cytoplasm while allowing the entry of PI to stain the nucleus. Conversely, intact cells exhibited green fluorescence in the cell bodies and nuclei unstained by PI. The experiments ($n = 4$) revealed essentially complete cell death within the core while at the border region there was a sharp transition from complete cell death inside the core to fully intact, viable cells outside the core (figure 5.3.3).

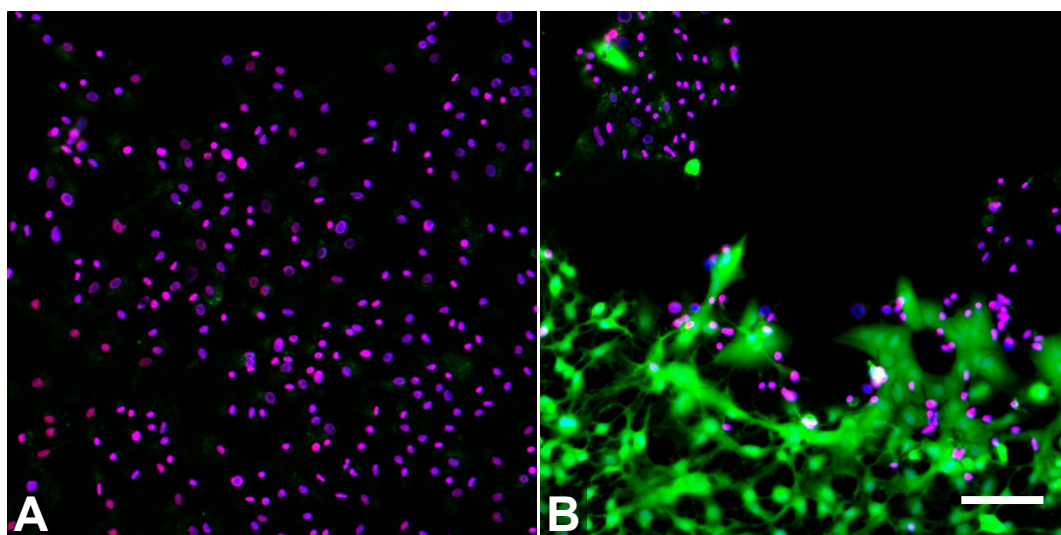


Figure 5.3.3 Fluorescence images of live cultures stained with calcein and propidium iodide at 2 hours after cryo-lesion.

(A) All cells within the core region exhibited nuclei stained with propidium iodide (red/magenta) while only weakly staining for calcein (green). (B) The image, taken along the lesion boundary, revealed a sharp and distinct transition from near complete cell death within the lesion (top half of image) to fully viable cells outside of the lesion (bottom half). Cells outside of the core region exhibit intense staining for calcein and exclude propidium iodide from their nuclei. Some void areas can also be seen within the core region where cells have detached as a result of the cryo-lesion treatment (scale bar = 100 μm).

5.3.1.3 Effects of Cryo-lesion on Microglial Morphology and Distribution around the Lesion

i. Morphological Changes

Under the culture conditions used for the current model, control cultures consisted of microglia in varying states of activation based on morphological criteria (see section 5.2.10.1), including ramified and amoeboid microglia as well as microglia in intermediate states. Figure 5.3.4 provides a representative image showing the difference morphologies of microglia immunolabelled for CD11b/c in a control culture.

Based on the criteria adopted for this study, the microglial population in a typical control culture consisted of approximately 50% amoeboid microglia and between 10 to 15 % ramified microglia.

However, this proportion changed rapidly after cryo-lesion with a complete disappearance of ramified microglia and a near complete shift to the amoeboid form along the lesion border by 2 h after lesion (figure 5.3.5).

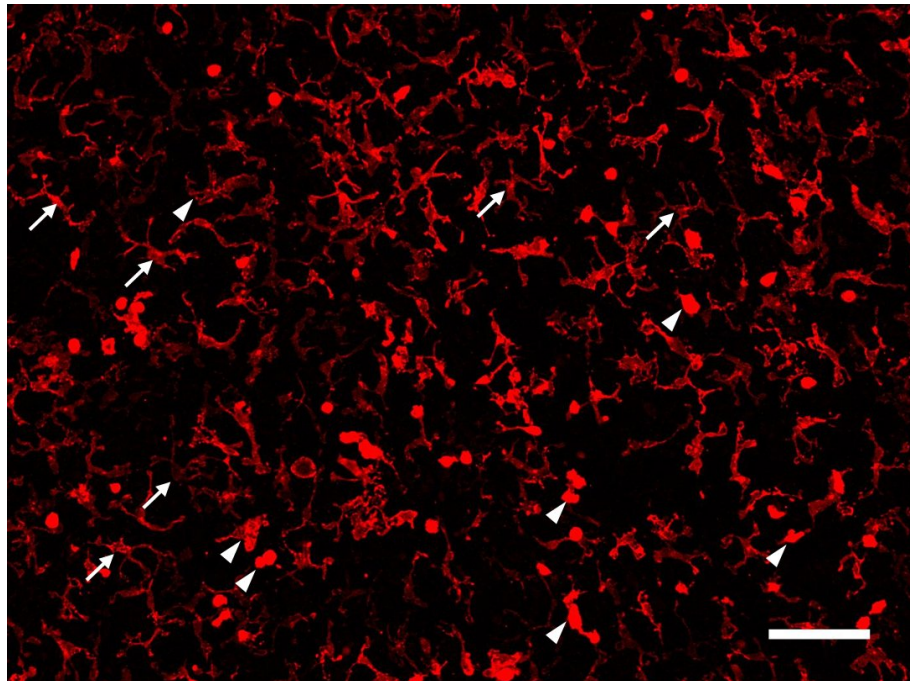


Figure 5.3.4 Microglial cells in control cultures at 14 DIV.

Microglia immunolabelled for CD11b/c in control cultures exhibit varying morphological states ranging from ramified through intermediate to amoeboid. Examples of ramified (arrows) and amoeboid (arrowheads) microglia are highlighted (scale bar = 100 μ m).

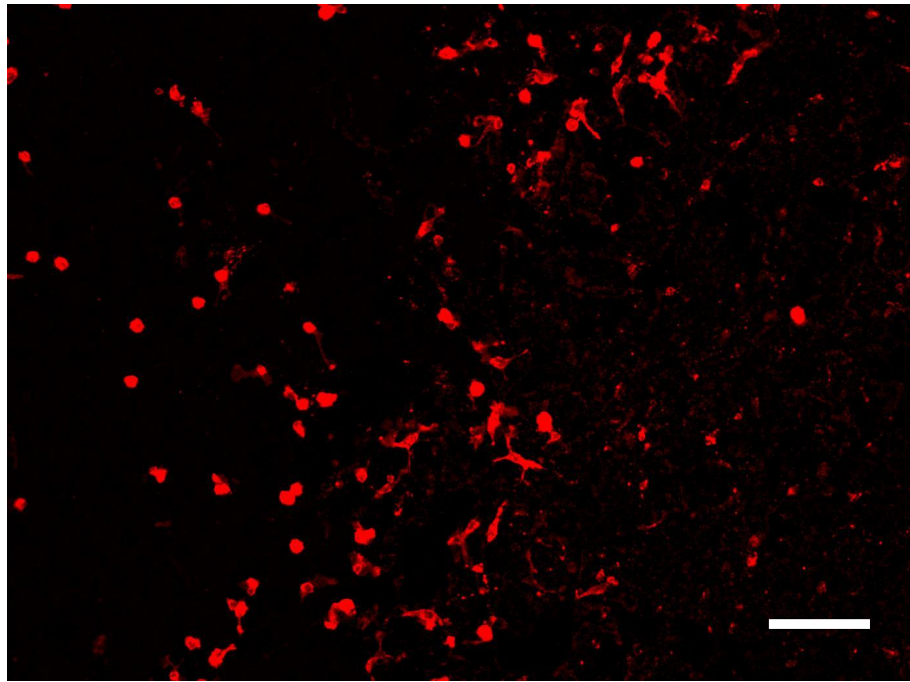


Figure 5.3.5 Microglial cells along the lesion border at 2 hours after cryo-lesion.

Microglia along the lesion border were essentially all in the amoeboid form at 2 h after cryo-lesion (scale bar = 100 μ m).

ii. Changes in Distribution

Figure 5.3.6 shows a series of montages generated from images for microglia immunolabelled for CD11b/c taken around the lesion boundary over the first 48 hours following cryo-lesion. These montages provided a qualitative overview of the changes in microglial distribution around the lesion boundary as well as within the lesion core as a result of the cryo-lesion.

It can be seen that at 2 h after lesion, there was a marked decrease in microglia along the lesion boundary and near complete absence within the lesion core. Few microglia were observed with processes and almost none were ramified.

At 6 h, microglia can be seen to be accumulating along the lesion boundary. Although more process-bearing microglia can be seen at this time, very few met the criteria for the ramified form. The increase in microglial density can most likely be attributed to migration from regions further away from the lesion due to the earlier observation that essentially all cells would have died as a result of the cryo-lesion by 2 h and the duration was too short for significant proliferation to have occurred *in situ* 6 h after cryo-lesioning.

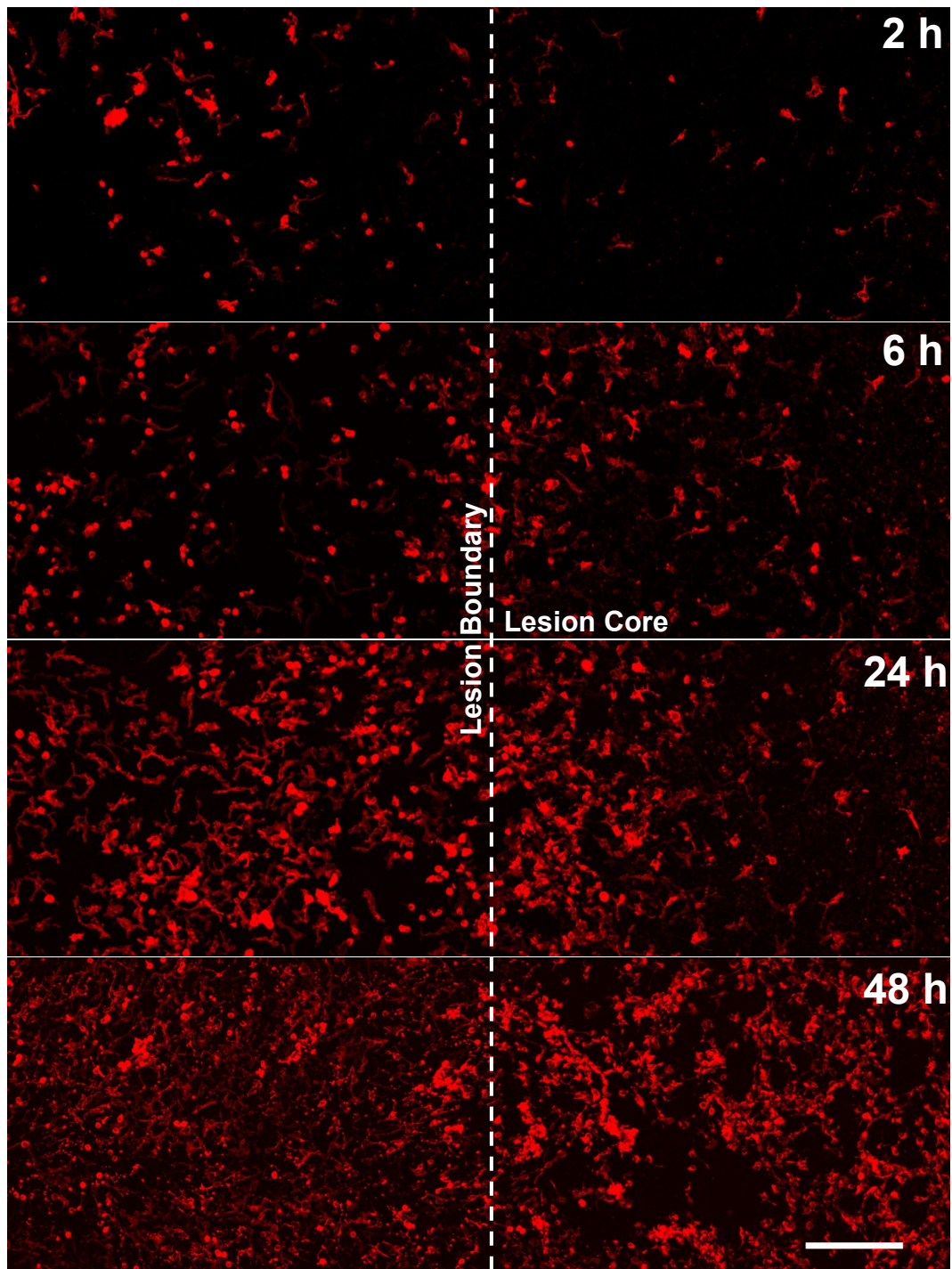


Figure 5.3.6 Infiltration of microglia into the lesion core over time.

Microglia migrated towards the lesion from the outer regions of the culture and gradually infiltrated the core of the lesion over the course of 48 h following cryo-lesion. There was also a marked shift in the morphological state of the microglial cells in the region along the border of the lesion over the same time course (scale bar = 200 μm).

At 24 h, although there was increased accumulation of microglia along the boundary, most of the microglial cells have only infiltrated a short distance into the lesion core. Outside the core, microglial density appeared to be near the level of control cultures, but the bulk of the cells still remained amoeboid in form.

Finally, at 48 h, microglial cells can be found throughout the core of the lesion and the microglial density became higher than that of control cultures before the lesion. By this time, there was a clear shift in the morphology of the cells outside of the core towards a more ramified form.

These changes in cell densities and microglial morphology were quantified at the lesion border as well as 5 mm away and the results are presented in sections 5.3.1.4 and 5.3.1.5.

5.3.1.4 Effects of Cryo-lesion on Cell Densities

i. At Lesion Border

Following cryo-lesioning, there was a rapid and marked decrease (~ 39 %) in microglial cell density along the lesion border compared to unlesioned controls at 2 h (figure 5.3.7 B). This decrease in microglial cell density remained significant at 6 h and recovered by 24 h.

In contrast, there were no significant changes in total cell density within the same region at 2 h following cryo-lesioning (figure 5.3.7 A). However, although there was no further decrease in microglial cell density between 2 h and 6 h after cryo-lesioning, there was a significant decrease in total cell density at 6 h. The relative changes in total and microglial cell densities suggested that there was an initial rapid loss of microglial cells along the lesion border at 2 h that was followed by a delayed loss of astroglial cells at 6 h within the same region.

Within the control cultures, the microglial cell density increased by approximately 36 % between 2 h and 48 h. In comparison, along the lesion border of cryo-lesioned cultures, the microglial cell density increased by 89 % over the same time period.

Cold treatment did not result in changes to total cell density and microglial cell density.

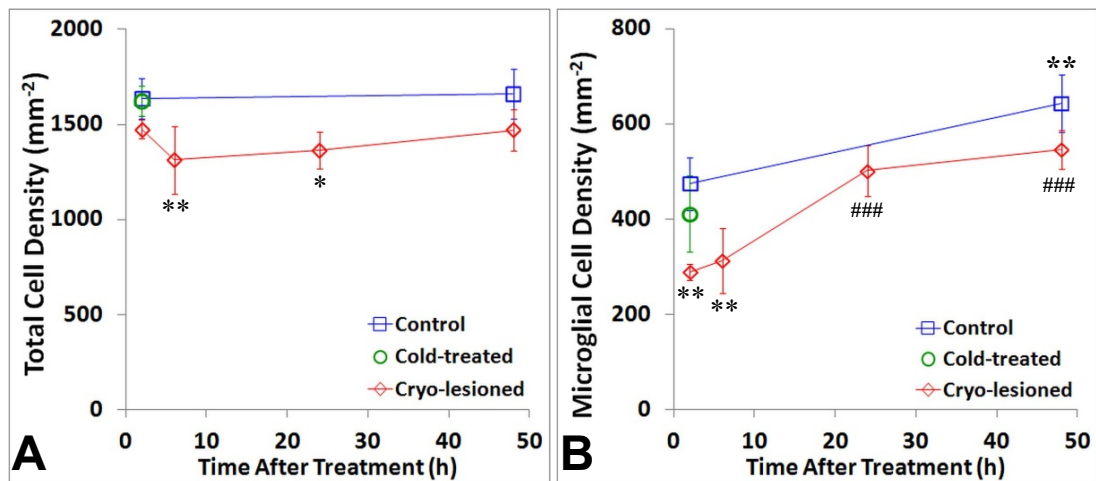


Figure 5.3.7 Changes in total and microglial cell densities along the lesion border following cryo-lesioning.

The charts show the changes in the (A) total cell density and (B) microglial cell density along the lesion border in cryo-lesioned cultures and within the corresponding regions of unlesioned and cold-treated controls. One-way analysis of variance detected highly significant effects of treatment and time on total cell density ($p < 0.01$) and microglial cell density ($p < 0.001$). Total cell density in cryo-lesioned cultures at 6 h and 24 h were significantly decreased compared to control cultures at 2 h ($*p < 0.05$, $**p < 0.01$, vs. "Control" at 2 h, Tukey's HSD). Microglial cell density in cryo-lesioned cultures at 2 h and 6 h were significantly decreased compared to control cultures at 2 h ($**p < 0.01$, vs. "Control" at 2 h, Tukey's HSD). In control cultures, the microglial cell density increased significantly between 2 h and 48 h ($**p < 0.01$, vs. "Control" at 2 h, Tukey's HSD). Cryo-lesioned cultures exhibited marked increases in microglial cell density over the same time period ($###p < 0.001$, vs. "Cryo-lesioned" at 2 h, Tukey's HSD). Values are shown as mean \pm SD (n = 3 – 7 per group).

ii. At 5 mm from Lesion Border

There were initially no significant changes to the cell densities following cryo-lesion at 5 mm away from the lesion border (figure 5.3.8). The microglial cell densities increased over time in both control and cryo-lesioned cultures between 2 h and 48 h. Over this period of time, the microglial cell density in the control cultures increased by approximately 56 %. In comparison, the microglial cell density in the cryo-lesioned cultures increased by 149 % over the same duration.

The large increase in microglial cell numbers in the cryo-lesioned cultures contributed to a significant increase in total cell density whereas in control cultures the total cell density was not significantly changed.

Similar to observations at the lesion border, cold treatment did not result in changes to total cell density and microglial cell density.

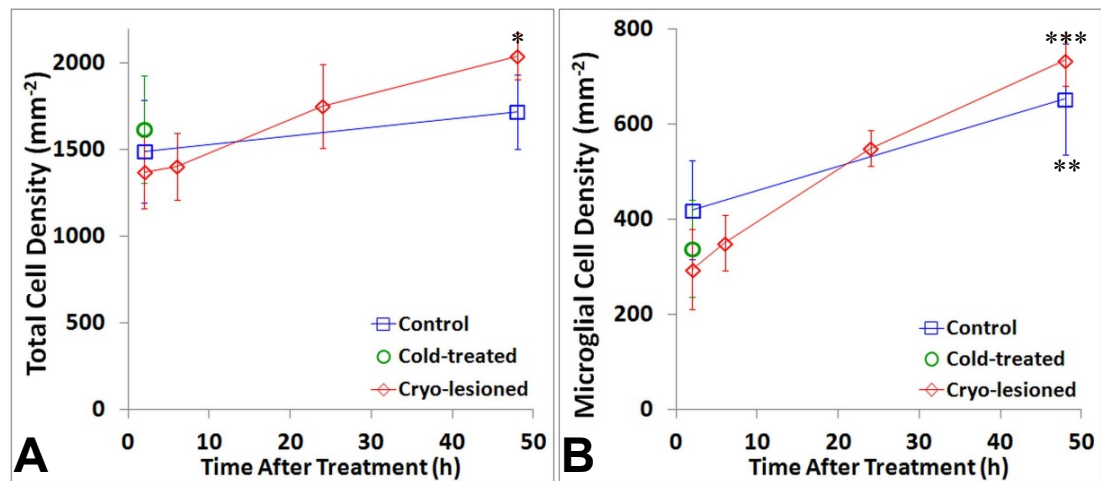


Figure 5.3.8 Changes in total and microglial cell densities at 5 mm from the lesion border following cryo-lesioning.

The charts show the changes in the (A) total cell density and (B) microglial cell density at 5 mm from the lesion border in cryo-lesioned cultures and within the corresponding regions of unlesioned and cold-treated controls. One-way analysis of variance detected significant effects of treatment and time on total cell densities ($p < 0.05$) and microglial cell densities ($p < 0.001$). Total cell density in cryo-lesioned cultures at 48 h was significantly increased compared to control cultures at 2 h ($*p < 0.05$, vs. "Control" at 2 h, Tukey's HSD). Microglial cell density in both cryo-lesioned and control cultures were significantly increased at 48 h compared to control cultures at 2 h ($**p < 0.01$, $***p < 0.001$, vs. "Control" at 2 h, Tukey's HSD). Values are shown as mean \pm SD (n = 3 – 7 per group).

5.3.1.5 Quantifying the Effects of Cryo-lesion on Microglial Morphology

The proportions of ramified and amoeboid microglia under each of the treatment conditions were determined based on morphological criteria as detailed in section 5.2.10.1. The proportions were expressed as a percentage of the total microglial population at each of the time points at the lesion border and at 5 mm away.

i. At Lesion Border

Cryo-lesion treatment induced a marked and rapid shift in microglial morphology towards a more amoeboid form that was evident by 2 h after lesion (figure 5.3.9). These changes persisted for up to 24 h after lesion and started to return towards control proportions at 48 h. Microglial morphology was unaffected in cold-treated and control cultures at 2 h after treatment and remained unchanged in control cultures at 48 h.

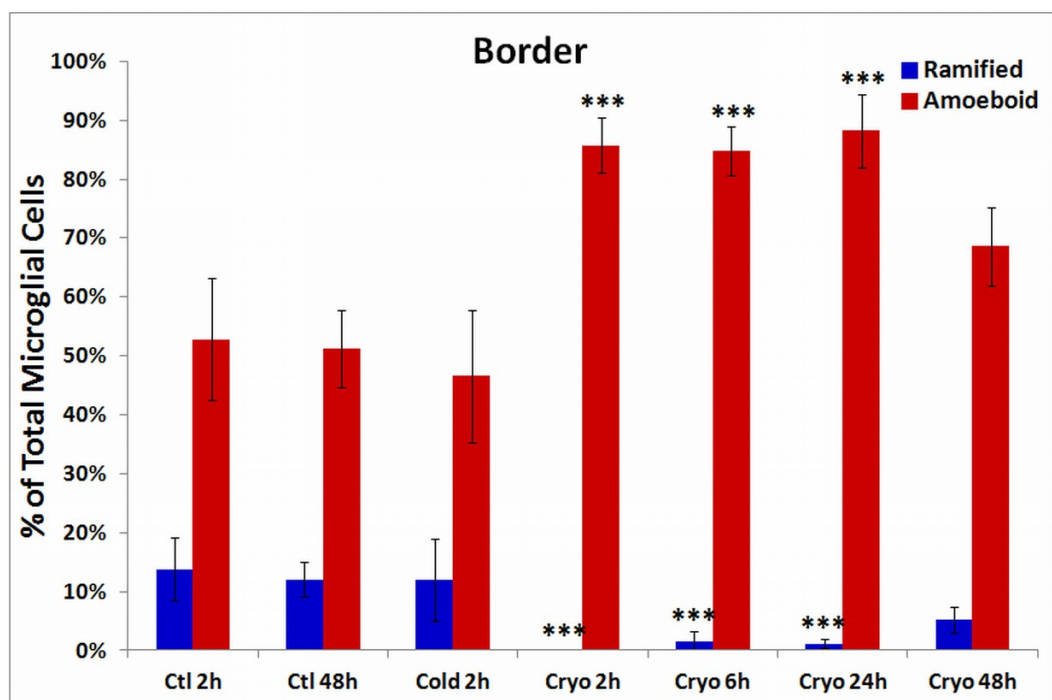


Figure 5.3.9 Changes in the proportions of ramified and amoeboid microglia along the lesion border following cryo-lesioning.

One-way analysis of variance detected highly significant effects of treatment and time on the percentages of ramified ($p < 0.001$) and amoeboid ($p < 0.001$) microglia at the lesion border. Induction of cryo-lesion resulted in marked and rapid shift in microglial morphology towards a more amoeboid form that persisted out to 24 h after lesion ($***p < 0.001$, vs. "Ctl 2h", Tukey's HSD). Cold treatment did not result in significant changes to either the ramified or amoeboid microglial fraction at 2 h. Values are shown as mean \pm SD ($n = 3 - 7$ per group).

ii. 5 mm from Lesion Border

Similar to the lesion border, at 5 mm from the lesion border there was also a shift in microglial morphology towards a more amoeboid form (figure 5.3.10). However, these changes were less marked. The differences only became statistically significant at 6 h but remained detectable at 48 h.

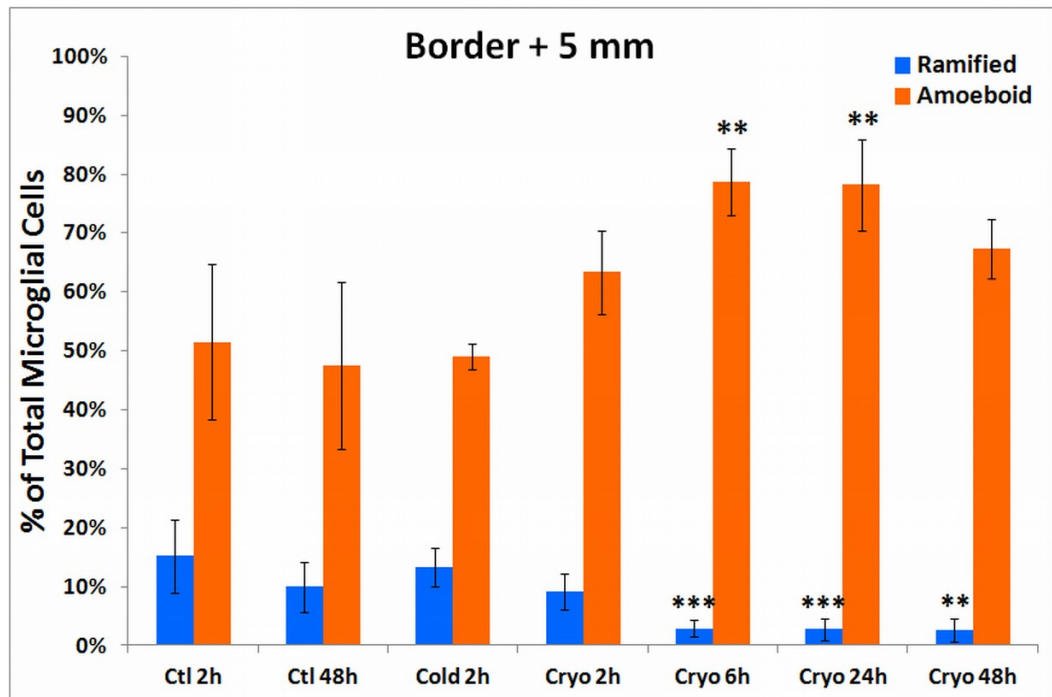


Figure 5.3.10 Changes in the proportions of ramified and amoeboid microglia at 5 mm from the lesion border following cryo-lesioning.

One-way analysis of variance detected highly significant effects of treatment and time on the percentages of ramified ($p < 0.001$) and amoeboid ($p < 0.001$) microglia at 5 mm from the lesion border. Induction of cryo-lesion resulted in a delayed shift in microglial morphology that reached significance at 6 hours after cryo-lesion ($**p < 0.01$, $***p < 0.001$, vs. "Ctl 2h", Tukey's HSD). While the amoeboid fraction started to return to control levels by 48 h, the ramified fraction remained depressed even at that time. Cold treatment did not result in significant changes to either the ramified or amoeboid microglial fraction at 2 h. Values are shown as mean \pm SD (n = 3 – 7 per group).

iii. Effects of Distance on the Microglial Response to Cryo-lesioning

Further analysis was performed on the changes in the ramified microglial fraction in cryo-lesioned cultures using 2-way ANOVA to determine if distance from the lesion had an influence on the time progression of changes in microglial morphology. The analysis revealed that there were significant effects of both distance ($p < 0.01$) and time ($p < 0.05$), as well as highly significant interactions between the two factors ($p < 0.001$). The analysis indicated that the time progression of changes in the morphology of microglial cells as a result of cryo-lesioning at the lesion border is different from the changes occurring at 5 mm away. Taken together with the results in the previous sections (sections 5.3.1.5 i & ii), these results suggested that there was a propagation of activation signals outwards from the lesion core that manifested as a time delayed decrease in the ramified microglial fraction following cryo-lesioning.

5.3.1.6 Effects of Cryo-lesion on Astroglia around the Lesion

Astroglial responses to cryo-lesion was investigated by immunolabelling the cultures for GFAP and nestin – two of the intermediate filament proteins found in astroglia. Both GFAP and nestin have been found to be highly expressed in reactive astroglial cells in the injured and diseased CNS (see section 1.4).

i. GFAP Expression

Figure 5.3.11 shows the typical expression of GFAP in a control culture at 14 DIV. The GFAP fibrils appear to be aligned around the nuclei of the astroglial cells without any overall order or organisation with the neighbouring cells.

Following cryo-lesion, cells within the lesion core exhibited intense GFAP staining along with highly disrupted cellular structures (figure 5.3.12). However there were very little changes in GFAP expression along the lesion border outside the core for the first 6 hours after lesion. By 24 h, the astroglial cells have started extending processes directed towards the lesion core with the GFAP organised into elongated fibrils within the processes. At 48 h, GFAP expression within astroglial cells near the lesion border were almost entirely organised into long fibrillar processes. In addition, the cells nearest to the lesion edge had all extended processes well into the lesion core by this time.

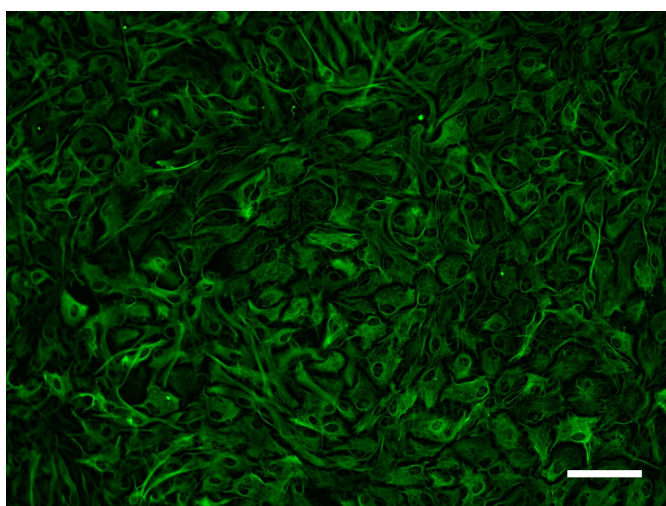


Figure 5.3.11 GFAP expression in control cultures at 14 DIV.

Astroglia stained for GFAP in control cultures appear flat and rounded with very few long processes (scale bar = 100 μ m).

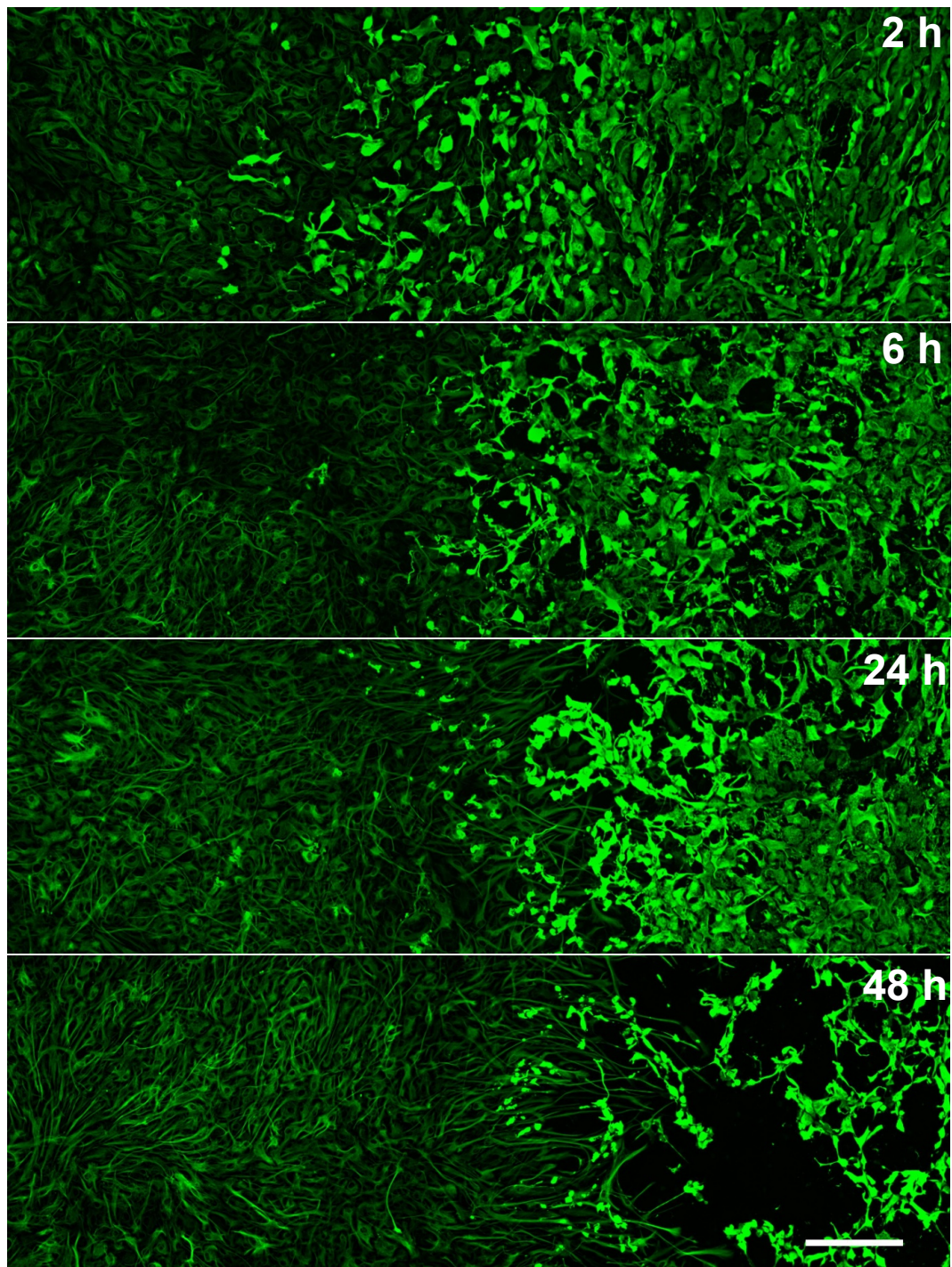


Figure 5.3.12 Changes in astroglial GFAP expression along lesion border following cryo-lesioning.

Cryo-lesion induction resulted in an intense GFAP staining of the astroglia in the lesion core. Changes in GFAP expression along the lesion border were unremarkable over the first 6 h after lesion. However, by 24 h, GFAP expression was concentrated in elongated processes that extended noticeably into the lesion core. The fibrillar organisation and process extension became more pronounced at 48 h (scale bar = 200 μ m).

ii. Nestin Expression

Nestin expression in control cultures showed a similar pattern to that of GFAP, although the intensity was much weaker. At 48 h cryo-lesioning, the nestin molecules exhibited a similar reorganisation into long fibrils that extended towards and into the core of the lesion. Unlike GFAP however, the intensity of nestin immunolabelling is increased markedly along the lesion border (Figure 5.3.13).

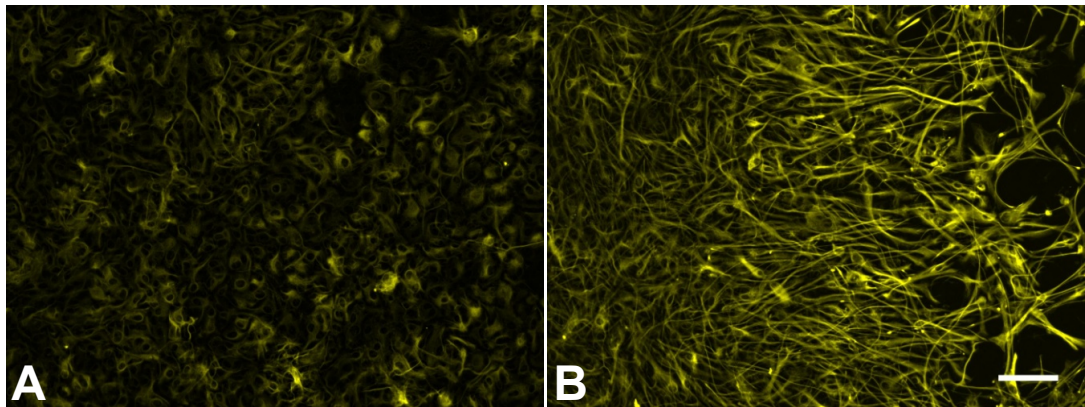


Figure 5.3.13 Changes in nestin expression in astroglia along lesion border following cryo-lesioning.

The pattern of nestin expression in (A) control cultures appeared to be very similar to that observed for GFAP (figure 5.3.10). (B) At 48 h after cryo-lesioning, astroglial processes along the lesion border exhibited greatly increased immunoreactivity for nestin (scale bar = 100 μ m).

5.3.2 Modifying Glial Responses to Cold-Induced Focal Cell Death

The characterisation experiments revealed clear changes in morphology and evidence of increased proliferation in microglial cells following cryo-lesion that are characteristic of activation. These were also accompanied by changes in astroglial morphology as well as a striking increase in the intensity of nestin immunolabelling.

The next series of experiments investigated if it was possible to modify the microglial responses induced by cryo-lesion by treatment with minocycline, a tetracycline antibiotic that has been reported to suppress activation in other models (see sections 5.4 and 1.5.1). The experiments also investigated the influence of microglia on the development of astroglial responses following cryo-lesion by using minocycline treatment and depletion of microglia in the cultures.

5.3.2.1 Effects of Minocycline Treatment on Microglial Responses Following Cryo-lesion

The effects of minocycline treatment on microglial responses were investigated by assessing the changes in microglial morphology and cell density at 24 h after cryo-lesioning on cultures that were either untreated or pre-treated with 10 μ M minocycline.

Unlike the manual counting method used for the characterisation experiments, the microglial responses in this investigation were assessed by determining the parameters of microglial area fraction and circularity as identified by CD11b/c immunolabelling (see section 5.2.10.2). This is similar to the approach used for the *in vivo* studies described previously (section 2.3.10).

The parameter of area fraction is a composite function of cell number and average cell size and is therefore related to cell density. However, by incorporating the effect of cell size, the area fraction measurement should be sensitive to both the increased proliferation and cellular hypertrophy that is typical of activated microglial cells. The circularity of a microglial cell increases as its morphology changes from a ramified to an amoeboid form therefore changes in the circularity parameter is indicative of changes in the proportions of the ramified and amoeboid forms of microglial in the cultures. This approach of assessing microglial response has the additional advantage of being less observer dependent over manual cell counting as the quantification is

performed using an automated function within the image analysis software ImageJ (figure 5.3.14).

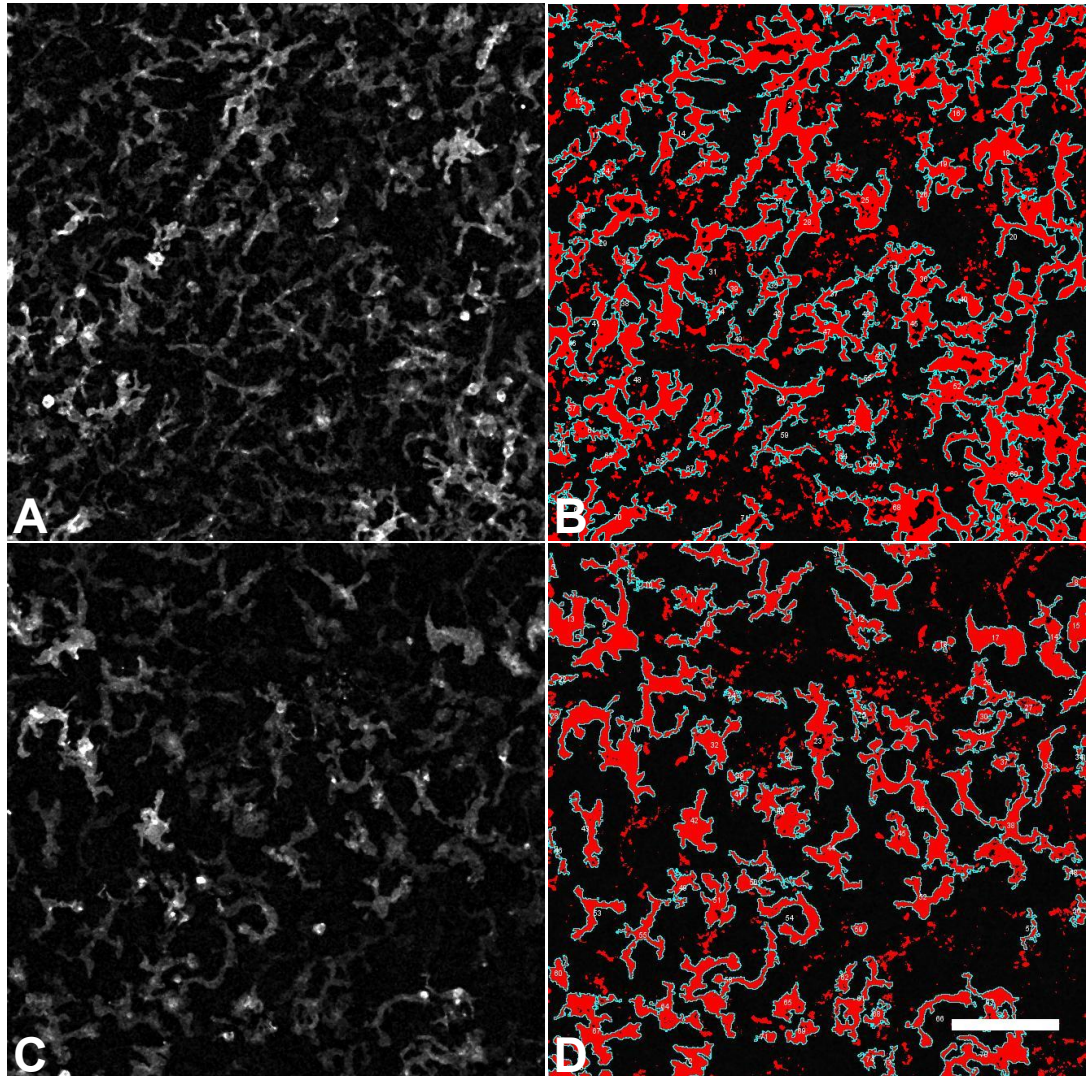


Figure 5.3.14 Quantification of microglial area fraction and circularity in control and cryo-lesioned cultures.

Microglia immunolabelled for CD11b/c in untreated control (A) and cryo-lesioned (C) cultures at 24 h after cryo-lesioning were processed by thresholding and particle analysis (B, D) in ImageJ to determine microglial area fraction and circularity. Thresholded pixels are highlighted in red and particles identified as microglial cells are outlined in cyan. The representative images shown here were taken along the lesion border in a cryo-lesioned culture and at a corresponding region in a control culture (scale bar = 100 μ m).

i. At Lesion Border

Consistent with the changes observed in microglial cell density in the characterisation experiments (sections 5.3.1.4), there was a decrease in microglial area fraction along the lesion border of cryo-lesioned cultures at 24 h (figure 5.3.15). There was only a small increase in microglial circularity, but this was expected as the fraction of ramified microglial cells was only approximately 13 % in control cultures (see figure 5.3.9). Furthermore, cultured microglia generally have less extensive ramification than microglia within the intact brain. Nonetheless, the shift in morphology could be detected from the changes in microglial circularity.

However, minocycline treatment did not have significant effects on microglial area fraction and circularity.

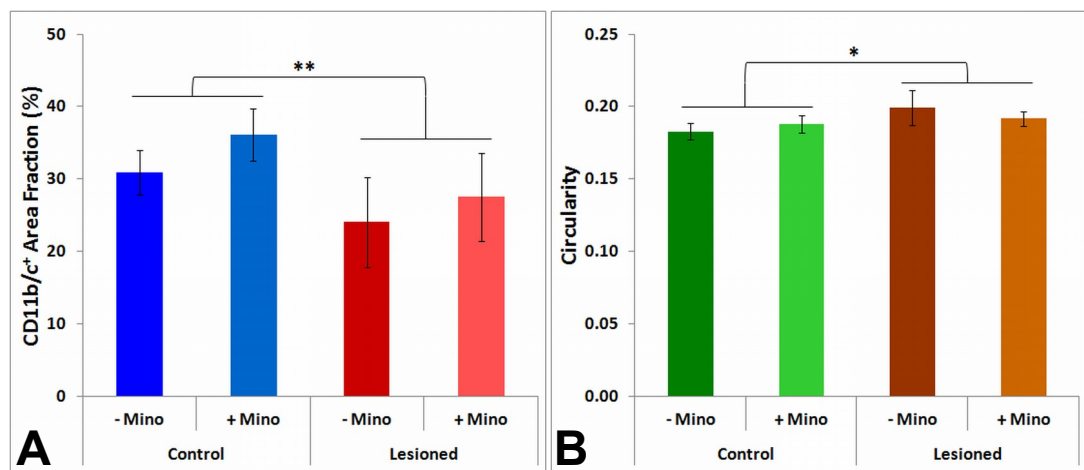


Figure 5.3.15 Effects of minocycline treatment on area fraction and circularity of microglial cells along the lesion border following cryo-lesioning.

Control and lesioned cultures were either untreated (- Mino) or pre-treated with 10 μ M minocycline (+ Mino). Two-way analysis of variance detected a highly significant effect of cryo-lesioning ($**p < 0.01$) but no effect of minocycline treatment on microglial (CD11b/c⁺) area fraction (A). Similarly, there was also a significant effect of cryo-lesioning ($*p < 0.05$) but no effect of minocycline treatment on microglial circularity (B). No significant interactions between cryo-lesioning and minocycline treatment were detected for both microglial area fraction and circularity. Values are shown as mean \pm SD (n = 4).

ii. 5 mm from Lesion Border

At 5 mm from the lesion border, cryo-lesioning did not result in changes to the microglial area fraction. This is again consistent with the earlier characterisation data. However, deviating from the earlier observations, there was also no apparent effect of cryo-lesion on microglial morphology at this distance when measured using the parameter of circularity (figure 5.3.16). This is perhaps unsurprising due to the less marked shift in the ramified and amoeboid microglial fractions in this region (see figure 5.3.10).

Minocycline treatment did not have a significant effect on microglial circularity but resulted in a small increase in microglial area fraction.

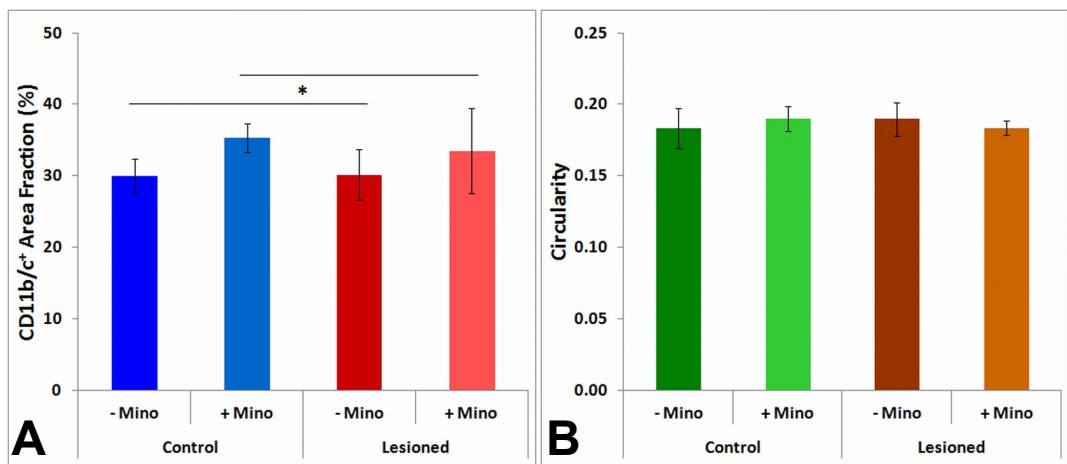


Figure 5.3.16 Effects of minocycline treatment on area fraction and circularity of microglial cells at 5 mm from the lesion border following cryo-lesioning.

Control and lesioned cultures were either untreated (- Mino) or pre-treated with 10 μ M minocycline (+ Mino). Two-way analysis of variance detected a significant effect of minocycline treatment but no effect of cryo-lesioning on microglial (CD11b/c⁺) area fraction (A). No effects of cryo-lesioning and minocycline treatment on microglial circularity (B) were detected. There were also no significant interactions between cryo-lesioning and minocycline treatment detected for both microglial area fraction and circularity. Values are shown as mean \pm SD (n = 4).

5.3.2.2 Effect of Minocycline Treatment on iNOS Expression and Nitrite Production

The effects of minocycline treatment on the glial cell responses were further investigated by assessing the changes in iNOS expression and nitrite production following cryo-lesion.

Changes in iNOS expression were assessed at 24 h after cryo-lesioning on cultures that were either untreated or pre-treated with 10 μ M minocycline (figure 5.3.17). No significant effects of cryo-lesioning and minocycline treatment on the expression of iNOS in the cultures were detected.

The nitrite content of the cell culture medium at 24 and 48 h was measured using the Griess reaction to assess possible changes in nitrite production as a result of cryo-lesioning and minocycline treatment (figure 5.3.18). There were significant increases in the nitrite content of the culture medium over time from 24 to 48 h in the experiment. However, consistent with the lack of effects on iNOS expression, there were no significant effects of cryo-lesioning and minocycline treatment on the production of nitrite in the cultures.

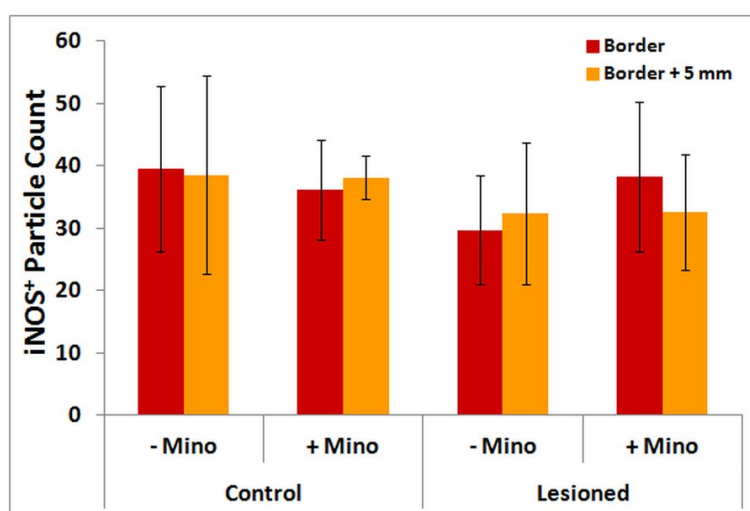


Figure 5.3.17 Particle count of iNOS-immunolabelled particles at the lesion border and 5 mm away 24 hours after cryo-lesioning.

Control and lesioned cultures were either untreated (- Mino) or pre-treated with 10 μ M minocycline (+ Mino). Two-way analysis of variance revealed no effects of minocycline treatment and no effects of cryo-lesioning on the number of iNOS-immunolabelled particles at the lesion border and 5 mm away from the border. Values are shown as mean \pm SD (n = 4).

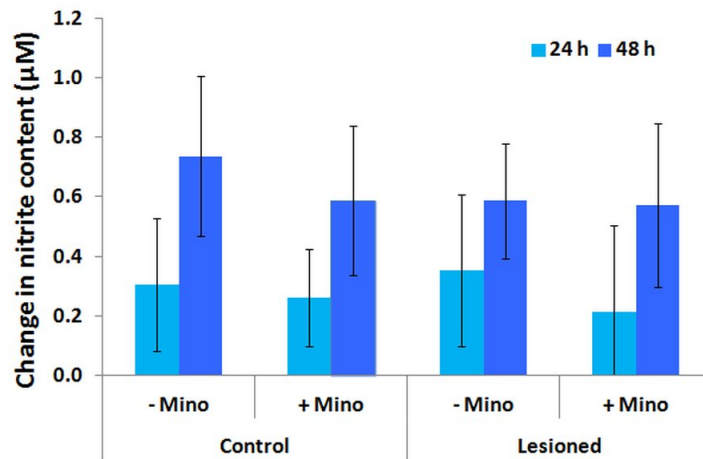


Figure 5.3.18 Increase in nitrite content at 24 and 48 hours after cryo-lesioning.

Control and lesioned cultures were either untreated (- Mino) or pre-treated with 10 µM minocycline (+ Mino). Three-way analysis of variance revealed a highly significant effect of time ($p < 0.01$) but neither minocycline treatment nor cryo-lesioning had any effects on nitrite production at 24 and 48 h. Values are shown as mean \pm SD ($n = 3 - 5$).

5.3.2.3 Effects of Modulating Microglial Activity on Astroglial Responses Following Cryo-Lesioning

As observed previously, cryo-lesion induction resulted in changes in the expression of GFAP and nestin in astroglial cells. The influence of microglia on astroglial responses was investigated by assessing the changes in the expression of these proteins following cryo-lesion when microglial activity was modulated with minocycline treatment or ablated by depleting microglial cells from the cultures.

i. Microglia Depletion

Preliminary trials using different incubation times and concentrations of Ara-C and LME were used to identify a suitable treatment regime to eliminate microglial cells from the cultures. The final conditions chosen was a 3 day treatment with 8 µM Ara-C followed by a 60 minute treatment with 50 mM LME that produced essentially microglia-free cultures. Cultures that were treated in this way were grown under standard conditions for a further 5 days before being used in the subsequent cryo-lesion experiments. The effectiveness of the microglia depletion treatment was assessed from CD11b/c immunolabelling of controls in these experiments.

Duplicate cultures from a total of 4 sets of microglia depletion treatments were assessed by sampling images at 8 different locations on each culture as described in section 5.2.9. In 63 of the 64 images sampled, the only detectable CD11b/c immunolabelling were cell debris and enucleated cell bodies (figure 5.3.19). It was in only 1 out of all the images sampled where 2 intact microglial cells were identified.

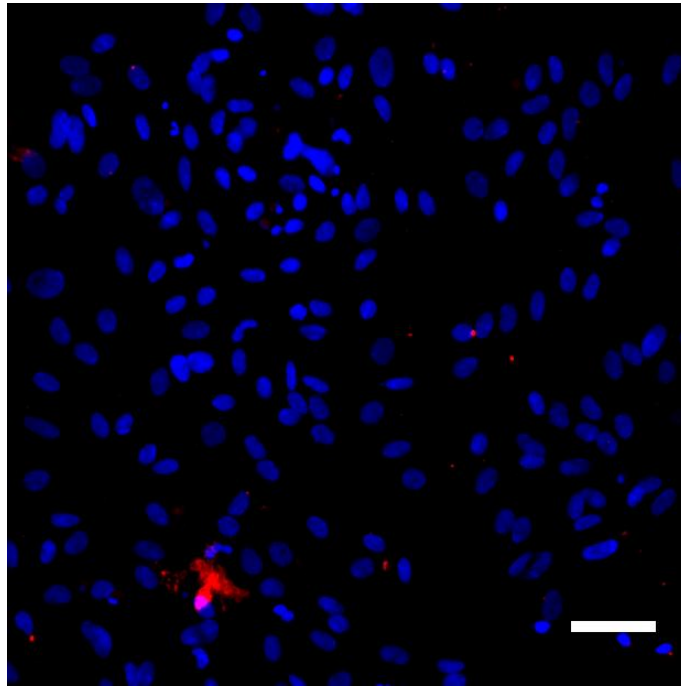


Figure 5.3.19 Primary mixed glial culture 6 days after microglia depletion treatment. A typical image field taken from a fluorescently labelled microglia depleted control culture is shown. Cell nuclei were stained with Hoechst 33258 (blue). Some microglial cell debris can be seen by CD11b/c immunolabelling (red) but no intact microglial cells can be detected. Note that the prominent CD11b/c⁺ cell body near the bottom left of the image does not co-localise with a nucleus (scale bar = 50 μ m).

ii. GFAP Expression

Although cryo-lesioning resulted in striking changes in the morphology of astroglial cells along the lesion border (see figure 5.3.12), GFAP expression as measured by fluorescence intensity in immunolabelled cultures was not significantly different compared to unlesioned controls at 48 h (figure 5.3.20). GFAP fluorescence intensity was also not affected by minocycline treatment and microglia depletion.

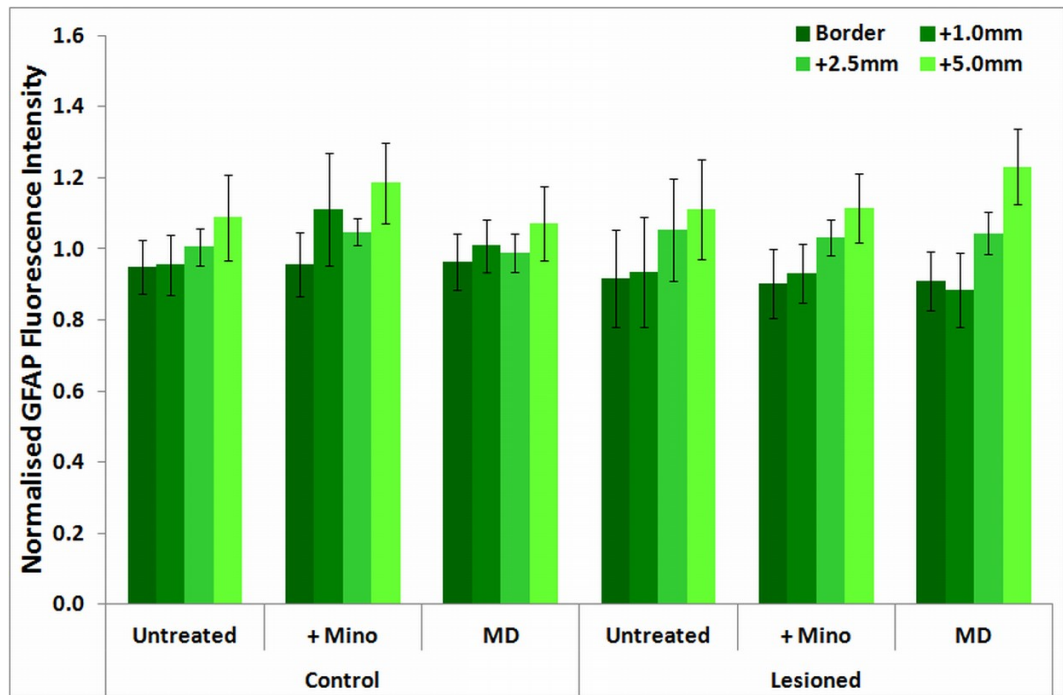


Figure 5.3.20 Normalised GFAP fluorescence intensity at 48 hours after cryo-lesioning.

Control and lesioned cultures were either untreated, pre-treated with 10 μ M minocycline (+ Mino), or depleted of microglia (MD). Fluorescence intensities at the lesion border, and 1 mm, 2.5 mm and 5 mm away are shown. Three-way analysis of variance detected no significant effects of cryo-lesioning, treatment and distance. Values are shown as mean \pm SD (n = 4 - 5).

iii. Nestin Expression

In contrast to GFAP expression, quantification of nestin expression in terms of fluorescence intensity revealed a large response in astroglial cells to cryo-lesioning (figure 5.3.21). This was consistent with the striking changes observed in the characterisation experiments (see figure 5.3.13). Cryo-lesioning resulted in an increased nestin expression in astroglia that was most marked along the border of the lesion.

Microglial depletion led to a further increase in nestin expression in the cryo-lesioned cultures. Interestingly, microglial depletion also resulted in a similar increase in nestin expression in the unlesioned cultures. These results suggested that microglia has an influence in regulating the basal level of nestin expression in

astroglial cells, but may not be involved in mediating the astroglial response to cryo-lesioning.

In contrast, minocycline treatment did not have any effect on the astroglial response, at least with respect to changes in nestin expression.

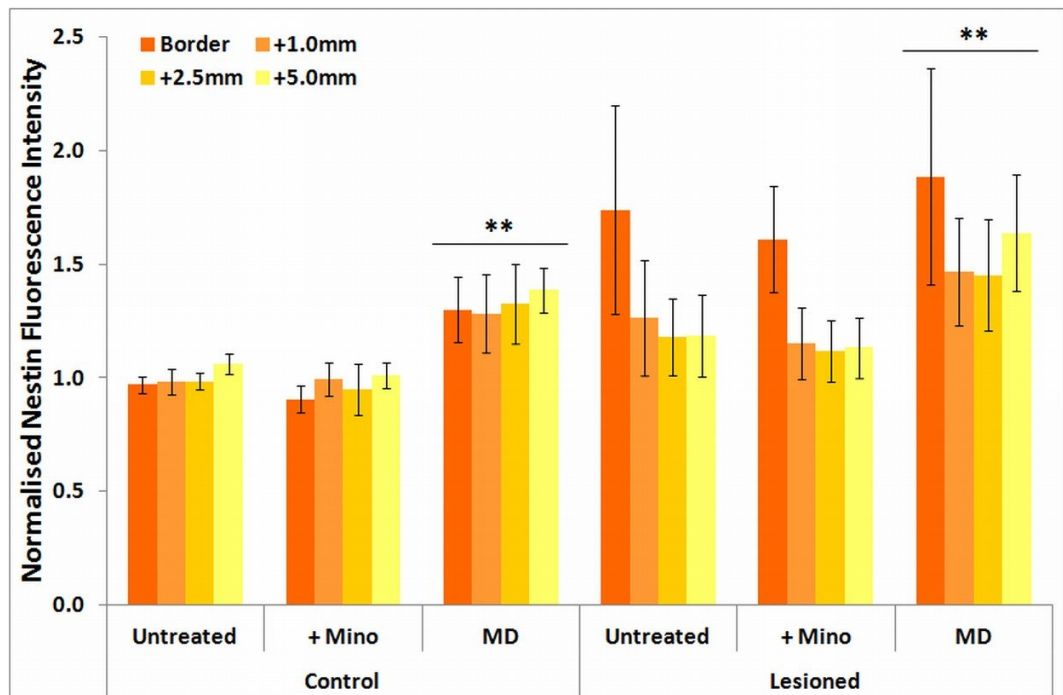


Figure 5.3.21. Normalised nestin fluorescence intensity at 48 hours after cryo-lesioning. Control and lesioned cultures were either untreated, pre-treated with 10 μ M minocycline (+ Mino), or depleted of microglia (MD). Fluorescence intensities at the lesion border, and 1 mm, 2.5 mm and 5 mm away are shown. Three-way analysis of variance detected highly significant effects of cryo-lesioning ($p < 0.001$), treatment ($p < 0.01$) and distance ($p < 0.01$). There was a highly significant interaction between cryo-lesioning and distance effects ($p < 0.001$). No other interactions between the factors were detected. Microglial depletion resulted in significant increases in nestin fluorescence intensity (** $p < 0.01$, vs. "Untreated" & "+Mino", Tukey's HSD). Values are shown as mean \pm SD (n = 4 - 5).

5.4 Discussion

This study demonstrates that brief exposure of mixed glial cultures to focal cooling generates a well demarcated lesion in which there is rapid death of all cells in the cooled region with preservation of essentially all other cells in the culture. More importantly, the formation of this lesion induces rapid morphological changes indicative of activation in neighbouring microglia that spread during the subsequent hours to distant parts of the culture. Microglia increased in numbers and accumulated along the lesion boundary, gradually migrating into the lesion core over time. Astroglial changes developed over a longer duration of time compared to microglial responses and included an increased expression of nestin and extension of processes into the lesion by cells along the lesion boundary.

The system for culturing primary mixed glial cells in the current study was based largely on the original work of Booher and Sensenbrenner (1972) that was adapted and refined by Hansson and co-workers (Hansson et al. 1982; Hansson et al. 1980). A detailed study of the cellular composition of such cultures by Hansson (1984) indicated that the cultures were primarily comprised of mixed glial cells, with astroglia constituting the majority of all cell types (~70%) and microglia making up approximately 10 % of the total cell population. This method was established in our laboratory and was the basis for several published works investigating astroglial cell function (Muyderman, Nilsson & Sims 2004; Muyderman et al. 2007; Muyderman et al. 2010; Wadey et al. 2009). Further modifications to the cell culture system were made in this study to promote microglial ramification as detailed in section 5.2.1 that also enriched the microglial fraction to approximately 25 – 30%.

The conditions for lesion induction involved a brief contact of the underside of the culture dish to a copper rod cooled by insertion into liquid nitrogen. In preliminary studies, contact for approximately seven seconds was observed to result in highly localised cooling and essentially complete cell death within the region of contact but little change in the temperature and viability of cells outside this region. The extent of temperature decrease outside of the contact region was unlikely to be responsible for the peri-lesional glial cell changes based on control experiments exposing cultures to medium cooled to a similar extent.

The rapid loss of cell viability and widespread incorporation of PI into cell nuclei indicated that necrosis was the major form of cell death induced in this model.

Again, this feature mimics the major role played by necrotic cell death in ischemic stroke in humans and in animal models (Back & Schuler 2004; Garcia et al. 1993; Grome et al. 1988; Li, Y, Powers, et al. 1998).

Thus, although the insult is clearly different to that producing tissue damage in cerebral ischemia, the cryo-lesion method closely mimics key features of ischemic stroke, including the focal aspect of the insult, the mode of cell death within the lesion and the glial cell responses outside of the lesion. The induction of these responses suggests the suitability of the cryo-lesion model as a platform for investigating peri-infarct glial cell responses after focal ischemic stroke.

Microglial activity can significantly influence the eventual outcome of stroke either by directly affecting the survival of neuronal cells during the development of ischemia or through modulation of the environment of the peri-infarct tissue to either facilitate or inhibit plasticity of the surviving neurons.

One of the pathways in which microglia may influence post-stroke recovery is through the modulation of astrogliosis within the peri-infarct tissue. Although the processes involved in the development of astrogliosis are not fully understood at present, it is known that certain aspects of the astroglial response, such as the secretion of CSPGs can be inhibitory to neuronal plasticity (Morgenstern, Asher & Fawcett 2002; Sandvig et al. 2004).

The possible role that microglia may play in astrogliosis was first raised by studies linking the presence of activated microglia and microglia-derived factors with astroglial responses to insults (Balasingam et al. 1996; Balasingam et al. 1994; Gao, Z et al. 2013; Giulian & Baker 1985; Zhang, D et al. 2010), leading to suggestions that the development of reactive gliosis is largely dependent on microglial activation (Liu, W, Tang & Feng 2011; McMillian et al. 1994; Wu & Schwartz 1998; Zhang, D et al. 2010).

The present cell culture model was devised as an approach to investigate glial cell responses and interactions within the peri-infarct tissue after stroke and to study the effects of manipulating these responses. We have used this model to specifically test the hypothesis that the development of astrogliosis in the peri-infarct tissue is primarily driven by microglial responses and can be suppressed by inhibiting microglial activation.

We have used two approaches in an attempt to investigate the effect of microglial activation on the development of astroglial changes within the peri-infarct tissue. The most direct approach was to deplete microglia from the cultures by treatment with Ara-C and LME using the method described by Hamby et al. (2006). This treatment resulted in the upregulation of the expression of nestin, a marker associated with astrogliosis, in astroglial cells. However, cryo-lesioning resulted in further increases in nestin expression that was unaffected by microglial depletion. This suggests that signals such as the loss of contact with other cells rather than those initiated by microglia might be more important in the development of peri-lesional astroglial responses.

In the second approach, minocycline was used due to previous reports that it was effective in inhibiting microglial activation (see section 1.5.1). In particular, it has been shown to be beneficial in animal models of stroke, with its effects mainly attributed to the suppression of microglial activation although evidence to support these claims were rarely presented (see sections 1.5.1 & 4.4). In contrast with these studies, the results from our study using the photothrombotic model of stroke did not reveal any evidence that minocycline treatment suppressed post-stroke microglial activation (see sections 4.3 & 4.4). In fact, almost all direct evidence of minocycline inhibition of microglial activation has been derived from cell culture studies.

In our cell culture model however, other than a subtle increase in the microglial area fraction, we did not detect any direct effects of minocycline treatment in suppressing microglial activation. Consistent with the lack of influence on microglial activity, we also did not detect any changes in astroglial responses to the focal lesion. These results contrasted with the findings from other studies that have used different cell culture models.

There are several key factors that may have contributed to this disparity between the results obtained in the present study and other studies investigating glial cell reactivity. Perhaps the most important factor in the resultant differences is the large number of cell culture studies that have used conditions that are not appropriate or inadequate for simulating the *in vivo* situation, especially in the context of focal ischemic stroke.

A large proportion of studies investigating microglial responses have used lipopolysaccharides (LPS) as the insult to induce activation in microglial cells

(Brahmachari, Fung & Pahan 2006; Chao et al. 1992; Drew & Chavis 2000; Munch et al. 2003; Zhou et al. 2009). LPS are a class of bacterial endotoxins that trigger a robust response in immune cells including microglia. However, LPS are molecules that are not normally encountered in the CNS except in bacterial infections and results of studies using LPS as a stimulus cannot be directly extrapolated to sterile pathologies such as stroke.

In fact, the importance of the use of an appropriate stimulus has been demonstrated in various studies that revealed critical differences in microglial responses to different activating stimuli (Bauer et al. 1997; Huang et al. 2010; Kobayashi et al. 2013; Lai et al. 2013; Nikodemova, Duncan & Watters 2006). Of particular relevance to the present study, the study by Huang et al. (2010) revealed that while LPS treatment strongly induced NO production in primary microglia, OGD treatment did not trigger a similar response. Consistent with these results, Kaushal and Schlichter (2008) also did not detect any increase in NO production in an OGD model. Similarly, Lai et al. (2013) observed that while LPS treatment triggered large increases in both NO and TNF- α production in microglia, ATP treatment only induced a mild response. Furthermore, Kobayashi et al. (2013) also demonstrated that LPS treatment triggered a predominantly pro-inflammatory response in microglia that is inhibited by minocycline treatment whereas IL-4 treatment resulted in anti-inflammatory responses that are not affected by minocycline treatment. As a final example of the importance of the stimuli in microglial activation, a study by Neumann et al. (2006) revealed, using a microglial cell line, that OGD-stimulated microglia provided neuroprotection when introduced to hippocampal slice culture challenged by OGD, whereas LPS-stimulated microglia did not exhibit any neuroprotective activity.

What is perhaps most relevant to the present study is the fact that the large majority of studies reporting significant effects of minocycline treatment in suppressing microglial activation in culture have used LPS treatment as the activating stimulus (Filipovic & Zecevic 2008; Fordyce et al. 2005; Gibbons & Dragunow 2006; Henry et al. 2008; Kremlev, Roberts & Palmer 2004; Liu, X et al. 2013). This is especially significant in light of the revelation by Kobayashi et al. (2013) that the effect of minocycline treatment on microglial activation is dependent on the nature of the insult.

In addition to the nature of the insult, the focal aspect of the insult is a specific consideration necessary in the modelling of the peri-infarct tissue in focal ischemic stroke. In focal ischemia, the insult initiating subsequent events is a deprivation of oxygen and metabolic substrates due to an interruption of blood supply which leads to pan-necrotic cell death within the affected brain tissue. This may appear to suggest that OGD treatment is the ideal stimulus to simulate the conditions of ischemic stroke in culture. However, in focal ischemia the bulk of the peri-infarct tissue is generally not directly affected by ischemia, but rather the cell responses within that tissue are triggered by signals arising from the dead and dying cells within the infarcted tissue.

In contrast, in OGD models, the entire culture is exposed to the insult and incomplete cell death is often induced even after exposure for periods greatly in excess of those causing damage *in vivo* (Goldberg, MP & Choi 1993; Yenari & Giffard 2001; Zhao, G & Flavin 2000). As a result, astrogliosis (Gao, Q et al. 2008; Wang, R et al. 2012) and microglial activation (Chock & Giffard 2005; Kong et al. 2014) induced by OGD are likely to be more relevant as models of glial cell responses to metabolic stress rather than peri-infarct responses to cell death within the infarct core.

Kaushal and Schlichter (2008) devised an indirect OGD model that they described as a model of the stroke penumbra. In the model, microglial cells cultured on Transwell inserts were exposed to OGD pre-treated neuronal-astroglial cultures to trigger microglial activation. Subsequently, the Transwell inserts with the activated microglia were transferred onto naïve neuronal-astroglial cultures. The authors then examined the influence of the activated microglia on neurotoxicity in the naïve cultures. However, as with the other OGD models, this model only induced partial cell death (~ 40 %). Glial cell responses to the insult were also poorly characterised in the model. Furthermore, the lack of direct contact between the microglial cells and the neuronal-astroglial cultures meant that an important signalling component is missing from the model.

More recently, Richard et al. (2010) reported a significantly improved OGD model in which focal OGD can be induced in a brain slice culture. The experimental set-up involved the immersion of an acutely prepared rat brain slice in a laminar flow bath of artificial cerebral spinal fluid (aCSF). Focal OGD was induced in a section of the brain slice by applying glucose and oxygen-free aCSF through a nozzle positioned

just above the brain slice. Despite the fact that this method more closely models the *in vivo* conditions of focal ischemia than most other cell culture models to date, the difficulties of maintaining brain slice cultures for extended periods *in vitro* very likely limits its usefulness in investigating peri-infarct processes that occur after the maturation of the infarct core. Although it would probably not be difficult to adapt the method for cell cultures, the complexity of the experimental set-up limits its effectiveness in routine use requiring larger sample sizes.

Amongst the other forms of insults that have been used in the study of glial cell reactivity, the scratch wound is one of the few that is capable creating a focal insult (Mandell, Gocan & Vandenberg 2001; Yu, Lee & Eng 1993). However, the process of creating the scratch wound is more a process of physical removal of the cells with only a minor component of injured cells along the edge of the scratch. In fact, in the original study of Yu, Lee and Eng (1993), extensive scoring of the culture surface in a grid pattern, which effectively negated the focal nature of the scratch wound, was required to induce measurable responses in astroglia.

Another key factor that may have contributed to the differences between the results obtained in our study and that reported by others is the nature of the cell culture system used in the models. The use of primary cultures or cell lines, and monotypic or mixed cultures has been demonstrated to be important determinants of cell responses to stimulus.

The convenience and ease of establishment and maintenance of microglial cell lines in culture compared to primary microglial cells have led to their widespread use in studies of microglial properties. However, the process of immortalising cells to create cell lines can significantly alter their properties. When challenged with an LPS insult, primary microglial cells exhibited significant differences in the expression of markers including Iba1, TNF- α , IL-1 β , IL-6, MCP-1, pERK 42/44 and nitrite production when compared to a rat (HAPI) and a mouse (BV-2) microglial cell line (Horvath et al. 2008). Roy et al. (2006) examined the expression of CD11b mRNA, a microglial marker, and nitrate production in LPS treated primary microglia and BV-2 cells. Although no direct comparisons were made in the study, the results clearly showed a much larger increase in CD11b mRNA expression and a more than 10-fold higher nitrite production in BV-2 cells in comparison to primary microglia. In addition, significant differences were also reported in the response of primary

microglia and BV-2 cells to minocycline treatment (Silva Bastos et al. 2011). Specifically, while Kim, SS et al. (2004) reported that minocycline treatment significantly decreased Cox-2 expression in LPS-challenged BV-2 cells, Silva Bastos et al. (2011) did not detect a similar response using primary microglia. The results of these studies strongly suggested that microglial cell lines do not accurately model microglia *in vivo* both in terms of their response to insults as well as to pharmacological treatments.

Many of the studies have also looked at microglial activity in monotypic cultures of microglial cells or have investigated the effects of conditioned medium from activated microglial cells in these cultures on other neural cell types. Although monocultures of microglia may be a useful system for studying their basic cell properties, their basal activity and responses to stimuli within the brain environment are strongly modulated by interactions with other neural cell types. In particular, astroglia have been shown to induce ramification in microglial cells (Schilling, T et al. 2001; Sievers, Parwaresch & Wottge 1994; Tanaka, J & Maeda 1996; Tanaka, J et al. 1999; Wilms, Hartmann & Sievers 1997; Wirjatijasa et al. 2002). The studies by Sievers, Parwaresch and Wottge (1994) and Wilms, Hartmann and Sievers (1997) identified the presence of both contact-dependent and diffusible factors from astroglial cells that induced ramification in microglial cells. More surprisingly, these studies also demonstrated that even peripheral macrophage can be induced to ramify by co-culture with astroglial cells, further highlighting the importance of astroglial modulation on microglial activity within the brain environment. Similar observations were made in a later study by Hailer et al. (2001) where the authors observed increased ramification of cultured microglia treated with astrocyte-conditioned medium.

Furthermore, other studies have also demonstrated astroglial modulation of microglial reactivity to insults. Vincent, Tilders and Van Dam (1997) observed that LPS-induced nitrite production in microglial cells was inhibited by astroglial cells in mixed glial cultures. Their observation of astroglial inhibition of microglia was further supported by the results of a later study by Tichauer, Saud and von Bernhardt (2007) in a model using IFN- γ -activated microglia. Acevedo et al. (2013) showed that astroglia inhibited both microglia and bone marrow derived cells from activation into a mature dendritic cell-like phenotype via a contact-dependent process following stimulation with granulocyte/monocyte colony-stimulating factor and LPS. Costello

et al. (2011) also demonstrated that contact signalling by astroglial cells via CD200-CD200R inhibits microglial production of inflammatory cytokines.

These studies suggest that astroglial cells play critical roles in maintaining microglia in a quiescent state under normal conditions in the brain, as well as modulating microglial reactivity and preventing over-activation in response to insults. As a result, studies using monotypic cultures of microglial cells are unlikely to be representative of their normal function and responses to insults in the brain (Biber, Owens & Boddeke 2014).

In our investigations, we have assessed microglial activation in the cryo-lesion model based on the physical changes (*i.e.* retraction of processes, hypertrophy and proliferation) that are stereotypical of their response to insult. In addition to these, we also attempted to detect changes in the expression of iNOS and nitrite production that have been widely used as indicators of microglial activation in cell culture studies. Although the cryo-lesion elicited marked physical changes that were consistent with microglial activation, there were no corresponding increases in iNOS expression or nitrite production detected (see section 5.3.2.2). This result stands in contrast to the studies that have used LPS as the stimulus, but is consistent with some of the studies that have used other types of stimulus as discussed previously. Furthermore, the presence of astroglial cells in the mixed glial cultures used in our model would have acted to further suppress the microglial response, including nitrite production, to the lesion. Nonetheless, it is important to note that those studies using stimulus other than LPS have also detected induction of markers such as TNF- α and IL-1 β that are suppressed by minocycline (Huang et al. 2010; Suk 2004). It will be necessary to look at these and other potential markers of microglial activation in future studies in order to fully characterise the changes induced by cryo-lesion and to detect effects of treatments.

The astroglial cells in our model responded to the cryo-lesion with marked increases in nestin expression along with a striking remodelling of the processes of the peri-lesional cells. Peri-lesional astroglia extended long processes arranged in parallel “palisading” arrays towards the lesion core (see figures 5.3.12 & 5.3.13) in a similar manner to that seen in our animal stroke model as well as in other animal studies (Katsman et al. 2003; Sun & Jakobs 2012). We did not detect significant increases in GFAP expression as a result of the cryo-lesion, but this is perhaps not surprising as

very few cell culture studies have reported measurable increases beyond the morphological changes. Studies that have reported quantifiable increases in GFAP expression have normally used insults that are more severe than the lesion induced in our model. For example, Yu, Lee and Eng (1993) managed to induce only 70-80% increase in GFAP expression after extensive scratch injury distributed across approximately 37% of the total culture surface. In contrast, the lesion induced in our model is limited to a focal area covering less than 10% of the culture surface. Although the effect of cryo-lesioning on GFAP expression was limited in our model, we can nonetheless readily detect changes in the astroglial response by measuring nestin expression that exhibited a much higher capacity for upregulation.

The lack of sensitivity of GFAP expression in response to insults in culture is also likely to be partially due to the high basal level of expression in astroglia as a result of the culture conditions as compared to the *in vivo* environment (McMillian et al. 1994; Wu & Schwartz 1998). Neuronal inhibition is an important factor regulating astroglial responses *in vivo* and has been demonstrated to downregulate many of the markers associated with astrogliosis in neuron-glia co-cultures (McMillian et al. 1994; Wu & Schwartz 1998). Although the mixed glial culture used in our study is an improvement over other studies that have used monotypic cultures, it still does not provide a complete picture of the peri-infarct glial responses. It will be important to investigate how the presence of neuronal cells affect the glial cell responses in future studies by using mixed cortical cultures or neuron-glia co-cultures. The addition of neurons to the cryo-lesion model will further extend the model to facilitate the investigation of neuronal plasticity in the peri-lesional regions, and how it may be influenced by manipulating glial responses.

A novel feature of the cryo-lesion model that has not been previously reported in other cell culture models of stroke is the propagation of microglial activation from the lesion boundary to distant regions over time. Astroglial gap junctions have been implicated in the facilitation of microglial signalling in ischemia (Baroja-Mazo, Barbera-Cremades & Pelegrin 2013; Bennett, MV et al. 2012; Dale & Frenguelli 2009) and could be the mechanism underlying the propagation of microglial activation signals in the cryo-lesion model. This suggests that the cryo-lesion model may also be a potential platform for investigating the role of gap junction signalling in the development of glial responses within the peri-infarct. This possibility could

be investigated in future studies by studying the effects of channel blockers such as carbenoxolone on the progression of microglial activation following cryo-lesion.

5.5 Conclusion

We have presented a cell culture model that recapitulates many of the features of peri-infarct glial cell responses following focal ischemia in animal models. These included readily detectible activation of microglia that spreads over time to regions distant from the infarct and subsequent astroglial responses including increased nestin expression and extension of processes into the lesion. The rapid induction of a focal lesion is the defining feature that makes the model more suitable for the investigation of processes involved in post-stroke recovery and plasticity, whereas other models are generally more appropriate for the study of the acute processes involved in neurotoxicity and neuronal survival.

The results of our initial investigations using the model suggest that the initiation of astroglial responses within the peri-infarct tissue may be largely independent of microglial activation, although certain aspects of the astroglial processes may be regulated by microglia activity. Further studies will be necessary to elucidate the nature of these interactions between astroglia and microglia.

We have also observed that the glial cell responses that have been characterised in this model were largely unaffected by minocycline treatment. Although our study does not preclude the possibility that minocycline may influence aspects of glial cell responses that were not measured in our experiments, it does suggest that caution needs to be applied to the interpretation of results obtained from cell culture studies. Most studies, especially those that have used LPS stimulus, cell lines or monotypic cultures are likely to trigger changes that are not representative of glial cell responses in the post-stroke peri-infarct tissue. Consequently, although minocycline may have therapeutic benefits in improving post-stroke recovery, it may not act through the pathways identified in those models.

CHAPTER 6
***GENERAL CONCLUSIONS AND
FUTURE DIRECTIONS***

In the studies presented in the thesis, we have quantitatively characterised the microglial and astroglial responses, as well as the recovery of function, over the first 7 days after photothrombotic stroke in rats. Using the quantitative approaches developed in this part of the studies, we have made the novel observation of a transient loss in peri-infarct microglial cells at 24 hours following photothrombotic stroke. We have also reported that the morphological changes associated with microglial activation can be detected quantitatively as early as 3 hours after stroke induction.

Using the characterised model, we investigated the consequences of modifying the early microglial responses using time-targeted treatment with minocycline, a widely reported inhibitor of microglial activation, on the development of astrogliosis and functional recovery after stroke. Although we have used dosages comparable with other studies that have reported strong inhibition of microglial activation, we have only observed limited effects of minocycline treatment on the microglial response in our investigations. Nonetheless, the treatment resulted in downstream changes to the astroglial response and subsequent improvements in functional recovery. Crucially, the improved functional recovery was not associated with changes in the infarct volume. Surprisingly, the changes observed in the astroglial response were upregulation in the expression of GFAP and vimentin. These changes were indicative of increased astrogliosis and are not usually associated with improved recovery of function after stroke.

The increase in astroglial response was unexpected as the reactive astroglia are a source of CSPGs that have been demonstrated to be inhibitory to neuro-regeneration. Interestingly, although the minocycline-treated animals exhibited increased astroglial expression of GFAP and vimentin, the expression of neurocan was not significantly affected. These results suggested that beneficial aspects of astrogliosis were selectively enhanced as a result of the minocycline treatment. These may include the increased astroglial production of various trophic factors or signalling molecules that promote or support the neuroplastic processes underlying functional recovery (as discussed in section 1.4.1). Future studies to identify and characterise the particular molecules that are involved will be useful in the development of treatment regimens to maximise the benefits of minocycline treatment after stroke.

The increased astrogliosis may also have had a further beneficial effect by presenting a heightened barrier that reduced the infiltration of peripheral immune cells into the peri-infarct tissue (see figure 1.4.2). Evidence that supported this possibility can be found in the results from ED1 immunolabelling as discussed below.

We have used immunolabelling for ED1 as an additional measure of the inflammatory response that may be modulated by minocycline treatment. In agreement with other studies that have also used this marker, we observed significant decreases in ED1 expression in minocycline treated animals following stroke. These results suggested that the effects of minocycline treatment may be mediated through the modification of the activated microglial phenotype rather than the direct suppression of activation. However, the expression of ED1 is highly localised to the infarct and only extends a short distance into the peri-infarct tissue. This is a pattern that is consistent with the infiltrating peripheral immune cells observed from studies using bone marrow chimeric and parabiotic animals (see section 1.4.2.3). The reduced expression of ED1 in the peri-infarct tissue therefore suggests that some of the beneficial effects of minocycline treatment may be attributed to the restriction of infiltration by the peripheral immune cells.

The results of these investigations revealed that early short-course minocycline treatment can improve functional recovery via non-neuroprotective mechanisms. However, the observations from our study suggested that microglia may not play a significant role in mediating the effects of the treatment. Taken together with the results from other studies, the current evidence suggests that minocycline treatment, at least at the commonly used dosages, may have a greater effect on the peripheral immune response than on the local microglia. However, the nature of the involvement of the two immune cell populations is unclear at present due to the difficulty in distinguishing between them in immunohistochemistry-based approaches.

The recent discovery of the microglia specific marker, TMEM119, provides a potentially powerful new tool in investigations regarding the role of microglial responses in the facilitation of recovery after stroke (Bennett, ML et al. 2016; Butovsky et al. 2014; Satoh et al. 2016). In particular, the use of antibodies against TMEM119 in immunolabelling studies will help to distinguish between the responses of infiltrating peripheral immune cells from locally recruited microglia

within the infarct and peri-infarct tissue. This will further assist in clarifying the relative influence of the two immune cell populations in the facilitation of recovery after stroke.

A further obstacle to the investigation of microglial responses and their involvement in the processes underlying post-stroke recovery is the lack of well characterised markers that are associated with the promotion or inhibition of neuroplasticity and regeneration. As discussed in section 1.4.2.2, the use of M1/M2 markers in such investigations is not likely to be useful at present. Very few such markers have been well characterised in stroke due, in part, to the difficulty in measuring the expression of these markers within the peri-infarct tissue. Even fewer have been demonstrated to have a clear role in the processes involved in recovery. For example, although M1 markers such as IL-6 and TNF- α are generally regarded to be indicative of a deleterious phenotype in microglia, some studies have shown that they may promote functional recovery during the later stages of stroke (see section 1.4.2.1). In general, there is insufficient knowledge at present regarding what constitutes a beneficial or detrimental phenotype at different times following stroke to apply the concept in a meaningful manner in investigations. This deficiency will need to be addressed in future studies designed to identify and characterise markers that are relevant to the processes involved in post-stroke recovery.

As discussed in section 2.4, an important distinction between our study and most other studies is the use of loss of NeuN immunolabelling as the method of identifying the infarct and demarcating the boundary of the peri-infarct tissue in brain sections. This is a crucial difference as most other studies have either not defined their method for delineating the infarct boundary, or have used Nissl staining that did not allow clear visualisation of the boundary between the infarct and peri-infarct regions. This may potentially have led to mis-identification of process occurring within the infarct, peri-infarct or even in regions distant from the infarct.

The study by Yrjanheikki et al. (1999) offers a particularly pertinent example. This is a study that has been very influential in attributing the beneficial effects of minocycline treatment to the suppression of microglial activation. In the study, the authors did not describe any method for identifying the infarct in immunolabelled brain sections. In fact, it appears that they have sampled images from identical brain regions in examining the effects of minocycline treatment on microglial activation.

However, given that the treatment resulted in marked reductions in infarct volume, such a sampling strategy would have resulted in images being sampled at different distances relative to the infarct in minocycline-treated and control animals. For example, the same region located in the peri-infarct tissue of a control animal would be located some distance away from the infarct in minocycline-treated animals due to the reduced infarct volume. In effect, the inhibitory effect on microglial activation attributed to minocycline treatment was probably an indirect result of neuroprotection.

In the final portion of this thesis, we reported on the development of a new model of the peri-infarct tissue based on a previously reported method of producing focal cell death in cultured cells. We have characterised this model of injury in primary mixed glial cultures and demonstrated that the peri-lesional glial cells recapitulated key features of the peri-infarct glial cell responses in stroke. Specifically, induction of the focal lesion led to rapid activation of peri-lesional microglial cells that spread to distant regions and accumulation of activated microglia along the lesion boundary that gradually migrated into the lesion. Changes consistent with astrogliosis developed over a longer period of time in peri-lesional astroglial cells with increased expression of nestin and gradual extension of processes into the lesion.

Furthermore, using the newly developed model, we investigated the role of microglial activation in the development of astrogliosis following focal cell death using two different approaches. The first approach was by pre-treating the cultures with minocycline and the second by depletion of microglial cells from the cultures by treatment with Ara-C and LME. Our results revealed that minocycline was not effective in suppressing microglial activation induced by focal cell death. Also, neither minocycline treatment nor microglial depletion had significant effects on the astroglial response to lesion induction. However, microglial depletion resulted in increased expression of nestin in both lesioned and unlesioned cultures. These results suggest that although astroglial reactivity may be influenced by microglial activity, it can be triggered directly by lesion induction and is not dependent on microglial activation.

The development of the cell culture model of the peri-infarct tissue provides a new platform for the investigation of the effects of drug treatments on the glial responses to focal lesions. For example, pharmacological manipulations of the mechanisms

underlying the propagation of microglial activation, such as gap junction signalling in astroglial cells, using the model may shed further light on the development of peri-infarct glial responses in stroke. Furthermore, there is also the potential of using the model for studying the effects of modifying glial cell responses on the development of neuroplastic processes by using primary cortical cultures or neuron-glia co-culture systems.

In the cell culture model, we observed a lack of effects of minocycline treatment on both the microglial activation and, unlike in the animal model, the astroglial response following lesion induction. It is expected that peripheral immune cells would be absent or only present in small numbers as contaminants in the cultures. Therefore, these observations would be consistent with the hypothesis that minocycline treatment primarily influenced the peripheral immune response in the animal model. This hypothesis can be investigated in future studies using the cell culture model by introducing peripheral immune cells into the cultures.

In conclusion, the outcome of the investigations in this thesis revealed that the early immune responses following stroke can significantly influence the stroke outcome through mechanisms that are not related to the development of infarction. Furthermore, the results from our studies suggests that effects of the immune response may, at least in part, be mediated through the modulation of the astroglial response that can influence the processes underlying recovery. Finally, the evidence from our studies as well as others suggested a greater involvement of the peripheral immune responses than the brain resident microglia in facilitating the beneficial effects of minocycline treatment following stroke.

BIBLIOGRAPHY

Abeysinghe, HC, Bokhari, L, Dusting, GJ & Roulston, CL 2014, 'Brain remodelling following endothelin-1 induced stroke in conscious rats', *PLoS One*, vol. 9, no. 5, p. e97007.

Acevedo, G, Padala, NK, Ni, L & Jonakait, GM 2013, 'Astrocytes inhibit microglial surface expression of dendritic cell-related co-stimulatory molecules through a contact-mediated process', *J Neurochem*, vol. 125, no. 4, pp. 575-87.

Agrawal, S, Singh, A, Tripathi, P, Mishra, M, Singh, PK & Singh, MP 2015, 'Cypermethrin-induced nigrostriatal dopaminergic neurodegeneration alters the mitochondrial function: a proteomics study', *Mol Neurobiol*, vol. 51, no. 2, pp. 448-65.

Alaverdashvili, M, Moon, SK, Beckman, CD, Virag, A & Whishaw, IQ 2008, 'Acute but not chronic differences in skilled reaching for food following motor cortex devascularization vs. photothrombotic stroke in the rat', *Neuroscience*, vol. 157, no. 2, pp. 297-308.

Alaverdashvili, M & Whishaw, IQ 2013, 'A behavioral method for identifying recovery and compensation: hand use in a preclinical stroke model using the single pellet reaching task', *Neurosci Biobehav Rev*, vol. 37, no. 5, pp. 950-67.

Aldskogius, H 2001, 'Microglia in neuroregeneration', *Microsc Res Tech*, vol. 54, no. 1, pp. 40-6.

Allred, RP, Kim, SY & Jones, TA 2014, 'Use it and/or lose it-experience effects on brain remodeling across time after stroke', *Front Hum Neurosci*, vol. 8, p. 379.

Almeida, A, Delgado-Esteban, M, Bolanos, JP & Medina, JM 2002, 'Oxygen and glucose deprivation induces mitochondrial dysfunction and oxidative stress in neurones but not in astrocytes in primary culture', *J Neurochem*, vol. 81, no. 2, pp. 207-17.

Alper, BS, Malone-Moses, M, McLellan, JS, Prasad, K & Manheimer, E 2015a, 'Authors' reply to Wardlaw and Berge', *BMJ*, vol. 350, p. h1795.

—— 2015b, 'Thrombolysis in acute ischaemic stroke: time for a rethink?', *BMJ*, vol. 350, p. h1075.

Amantea, D, Bagetta, G, Tassorelli, C, Mercuri, NB & Corasaniti, MT 2010, 'Identification of distinct cellular pools of interleukin-1beta during the evolution of the neuroinflammatory response induced by transient middle cerebral artery occlusion in the brain of rat', *Brain Res*, vol. 1313, pp. 259-69.

Amantea, D, Micieli, G, Tassorelli, C, Cuartero, MI, Ballesteros, I, Certo, M, Moro, MA, Lizasoain, I & Bagetta, G 2015, 'Rational modulation of the innate immune system for neuroprotection in ischemic stroke', *Frontiers in Neuroscience*, vol. 9.

Amor, S, Puentes, F, Baker, D & van der Valk, P 2010, 'Inflammation in neurodegenerative diseases', *Immunology*, vol. 129, no. 2, pp. 154-69.

Andersen, CS, Andersen, AB & Finger, S 1991, 'Neurological correlates of unilateral and bilateral "strokes" of the middle cerebral artery in the rat', *Physiol Behav*, vol. 50, no. 2, pp. 263-9.

Arnett, HA, Mason, J, Marino, M, Suzuki, K, Matsushima, GK & Ting, JP 2001, 'TNF alpha promotes proliferation of oligodendrocyte progenitors and remyelination', *Nat Neurosci*, vol. 4, no. 11, pp. 1116-22.

Asher, RA, Morgenstern, DA, Fidler, PS, Adcock, KH, Oohira, A, Braistead, JE, Levine, JM, Margolis, RU, Rogers, JH & Fawcett, JW 2000, 'Neurocan is upregulated in injured brain and in cytokine-treated astrocytes', *J Neurosci*, vol. 20, no. 7, pp. 2427-38.

Askvig, JM, Leiphon, LJ & Watt, JA 2012, 'Neuronal activity and axonal sprouting differentially regulate CNTF and CNTF receptor complex in the rat supraoptic nucleus', *Exp Neurol*, vol. 233, no. 1, pp. 243-52.

Bacigaluppi, M, Comi, G & Hermann, DM 2010a, 'Animal models of ischemic stroke. Part one: modeling risk factors', *Open Neurol J*, vol. 4, pp. 26-33.

—— 2010b, 'Animal models of ischemic stroke. Part two: modeling cerebral ischemia', *Open Neurol J*, vol. 4, pp. 34-8.

Back, T & Schuler, OG 2004, 'The natural course of lesion development in brain ischemia', *Acta Neurochir Suppl*, vol. 89, pp. 55-61.

Badan, I, Buchhold, B, Hamm, A, Gratz, M, Walker, LC, Platt, D, Kessler, C & Popa-Wagner, A 2003, 'Accelerated glial reactivity to stroke in aged rats correlates with reduced functional recovery', *J Cereb Blood Flow Metab*, vol. 23, no. 7, pp. 845-54.

Baird, AE, Benfield, A, Schlaug, G, Siewert, B, Lovblad, KO, Edelman, RR & Warach, S 1997, 'Enlargement of human cerebral ischemic lesion volumes measured by diffusion-weighted magnetic resonance imaging', *Ann Neurol*, vol. 41, no. 5, pp. 581-9.

Balami, JS, Sutherland, BA, Edmunds, LD, Grunwald, IQ, Neuhaus, AA, Hadley, G, Karbalai, H, Metcalf, KA, DeLuca, GC & Buchan, AM 2015, 'A systematic review and meta-analysis of randomized controlled trials of endovascular thrombectomy compared with best medical treatment for acute ischemic stroke', *Int J Stroke*, vol. 10, no. 8, pp. 1168-78.

Balasingam, V, Dickson, K, Brade, A & Yong, VW 1996, 'Astrocyte reactivity in neonatal mice: apparent dependence on the presence of reactive microglia/macrophages', *Glia*, vol. 18, no. 1, pp. 11-26.

Balasingam, V, Tejada-Berges, T, Wright, E, Bouckova, R & Yong, VW 1994, 'Reactive astrogliosis in the neonatal mouse brain and its modulation by cytokines', *J Neurosci*, vol. 14, no. 2, pp. 846-56.

Bandtlow, CE & Zimmermann, DR 2000, 'Proteoglycans in the developing brain: new conceptual insights for old proteins', *Physiol Rev*, vol. 80, no. 4, pp. 1267-90.

Barker, AJ & Ullian, EM 2010, 'Astrocytes and synaptic plasticity', *Neuroscientist*, vol. 16, no. 1, pp. 40-50.

Baroja-Mazo, A, Barbera-Cremades, M & Pelegrin, P 2013, 'The participation of plasma membrane hemichannels to purinergic signaling', *Biochim Biophys Acta*, vol. 1828, no. 1, pp. 79-93.

Barth, TM, Jones, TA & Schallert, T 1990, 'Functional subdivisions of the rat somatic sensorimotor cortex', *Behav Brain Res*, vol. 39, no. 1, pp. 73-95.

Batchelor, PE, Porritt, MJ, Martinello, P, Parish, CL, Liberatore, GT, Donnan, GA & Howells, DW 2002, 'Macrophages and Microglia Produce Local Trophic Gradients That Stimulate Axonal Sprouting Toward but Not beyond the Wound Edge', *Mol Cell Neurosci*, vol. 21, no. 3, pp. 436-53.

Bauer, MK, Lieb, K, Schulze-Osthoff, K, Berger, M, Gebicke-Haerter, PJ, Bauer, J & Fiebich, BL 1997, 'Expression and regulation of cyclooxygenase-2 in rat microglia', *Eur J Biochem*, vol. 243, no. 3, pp. 726-31.

Bejot, Y, Prigent-Tessier, A, Cachia, C, Giroud, M, Mossiat, C, Bertrand, N, Garnier, P & Marie, C 2011, 'Time-dependent contribution of non neuronal cells to BDNF production after ischemic stroke in rats', *Neurochem Int*, vol. 58, no. 1, pp. 102-11.

Bendel, O, Alkass, K, Bueters, T, von Euler, M & von Euler, G 2005, 'Reproducible loss of CA1 neurons following carotid artery occlusion combined with halothane-induced hypotension', *Brain Res*, vol. 1033, no. 2, pp. 135-42.

Bennett, ML, Bennett, FC, Liddel, SA, Ajami, B, Zamanian, JL, Fernhoff, NB, Mulinyawe, SB, Bohlen, CJ, Adil, A, Tucker, A, Weissman, IL, Chang, EF, Li, G, Grant, GA, Hayden Gephart, MG & Barres, BA 2016, 'New tools for studying microglia in the mouse and human CNS', *Proc Natl Acad Sci U S A*, vol. 113, no. 12, pp. E1738-46.

Bennett, MV, Garre, JM, Orellana, JA, Bukauskas, FF, Nedergaard, M & Saez, JC 2012, 'Connexin and pannexin hemichannels in inflammatory responses of glia and neurons', *Brain Res*, vol. 1487, pp. 3-15.

Bernardino, L, Agasse, F, Silva, B, Ferreira, R, Grade, S & Malva, JO 2008, 'Tumor necrosis factor-alpha modulates survival, proliferation, and neuronal differentiation in neonatal subventricular zone cell cultures', *Stem Cells*, vol. 26, no. 9, pp. 2361-71.

Biber, K, Owens, T & Boddeke, E 2014, 'What is microglia neurotoxicity (Not)?', *Glia*, vol. 62, no. 6, pp. 841-54.

Bidmon, HJ, Jancsik, V, Schleicher, A, Hagemann, G, Witte, OW, Woodhams, P & Zilles, K 1997, 'Structural alterations and changes in cytoskeletal proteins and proteoglycans after focal cortical ischemia', *Neuroscience*, vol. 82, no. 2, pp. 397-420.

Binder, DK & Scharfman, HE 2004, 'Brain-derived neurotrophic factor', *Growth Factors*, vol. 22, no. 3, pp. 123-31.

Bjorklund, A & Lindvall, O 2000, 'Cell replacement therapies for central nervous system disorders', *Nat Neurosci*, vol. 3, no. 6, pp. 537-44.

Boche, D, Perry, VH & Nicoll, JA 2013, 'Review: activation patterns of microglia and their identification in the human brain', *Neuropathol Appl Neurobiol*, vol. 39, no. 1, pp. 3-18.

Bogousslavsky, J, Van Melle, G & Regli, F 1988, 'The Lausanne Stroke Registry: analysis of 1,000 consecutive patients with first stroke', *Stroke*, vol. 19, no. 9, pp. 1083-92.

Bohatschek, M, Kloss, CU, Kalla, R & Raivich, G 2001, 'In vitro model of microglial deramification: ramified microglia transform into amoeboid phagocytes following addition of brain cell membranes to microglia-astrocyte cocultures', *J Neurosci Res*, vol. 64, no. 5, pp. 508-22.

Booher, J & Sensenbrenner, M 1972, 'Growth and cultivation of dissociated neurons and glial cells from embryonic chick, rat and human brain in flask cultures', *Neurobiology*, vol. 2, no. 3, pp. 97-105.

Bovolenta, P, Wandosell, F & Nieto-Sampedro, M 1991, 'Neurite outgrowth over resting and reactive astrocytes', *Restor Neurol Neurosci*, vol. 2, no. 4, pp. 221-8.

Brahmachari, S, Fung, YK & Pahan, K 2006, 'Induction of glial fibrillary acidic protein expression in astrocytes by nitric oxide', *J Neurosci*, vol. 26, no. 18, pp. 4930-9.

Brakebusch, C, Seidenbecher, CI, Asztely, F, Rauch, U, Matthies, H, Meyer, H, Krug, M, Bockers, TM, Zhou, X, Kreutz, MR, Montag, D, Gundelfinger, ED & Fassler, R 2002, 'Brevican-deficient mice display impaired hippocampal CA1 long-term potentiation but show no obvious deficits in learning and memory', *Mol Cell Biol*, vol. 22, no. 21, pp. 7417-27.

Brifault, C, Gras, M, Liot, D, May, V, Vaudry, D & Wurtz, O 2015, 'Delayed pituitary adenylate cyclase-activating polypeptide delivery after brain stroke improves functional recovery by inducing m2 microglia/macrophage polarization', *Stroke*, vol. 46, no. 2, pp. 520-8.

Brouns, R & De Deyn, PP 2009, 'The complexity of neurobiological processes in acute ischemic stroke', *Clin Neurol Neurosurg*, vol. 111, no. 6, pp. 483-95.

Brown, CE, Aminoltejari, K, Erb, H, Winship, IR & Murphy, TH 2009, 'In vivo voltage-sensitive dye imaging in adult mice reveals that somatosensory maps lost to stroke are replaced over weeks by new structural and functional circuits with prolonged modes of activation within both the peri-infarct zone and distant sites', *J Neurosci*, vol. 29, no. 6, pp. 1719-34.

Brown, CE, Boyd, JD & Murphy, TH 2010, 'Longitudinal in vivo imaging reveals balanced and branch-specific remodeling of mature cortical pyramidal dendritic arbors after stroke', *J Cereb Blood Flow Metab*, vol. 30, no. 4, pp. 783-91.

Brown, CE & Murphy, TH 2008, 'Livin' on the edge: imaging dendritic spine turnover in the peri-infarct zone during ischemic stroke and recovery', *Neuroscientist*, vol. 14, no. 2, pp. 139-46.

Brown, CE, Wong, C & Murphy, TH 2008, 'Rapid morphologic plasticity of peri-infarct dendritic spines after focal ischemic stroke', *Stroke*, vol. 39, no. 4, pp. 1286-91.

Brunkhorst, R, Kanaan, N, Koch, A, Ferreiros, N, Mirceska, A, Zeiner, P, Mittelbronn, M, Derouiche, A, Steinmetz, H, Foerch, C, Pfeilschifter, J & Pfeilschifter, W 2013, 'FTY720 treatment in the convalescence period improves functional recovery and reduces reactive astrogliosis in photothrombotic stroke', *PLoS One*, vol. 8, no. 7, p. e70124.

Bruno, VM, Goldberg, MP, Dugan, LL, Giffard, RG & Choi, DW 1994, 'Neuroprotective effect of hypothermia in cortical cultures exposed to oxygen-glucose deprivation or excitatory amino acids', *J Neurochem*, vol. 63, no. 4, pp. 1398-406.

Bryan, NS & Grisham, MB 2007, 'Methods to detect nitric oxide and its metabolites in biological samples', *Free Radic Biol Med*, vol. 43, no. 5, pp. 645-57.

Bukalo, O, Schachner, M & Dityatev, A 2001, 'Modification of extracellular matrix by enzymatic removal of chondroitin sulfate and by lack of tenascin-R differentially affects several forms of synaptic plasticity in the hippocampus', *Neuroscience*, vol. 104, no. 2, pp. 359-69.

Burda, JE & Sofroniew, MV 2014, 'Reactive gliosis and the multicellular response to CNS damage and disease', *Neuron*, vol. 81, no. 2, pp. 229-48.

Burke, NN, Kerr, DM, Moriarty, O, Finn, DP & Roche, M 2014, 'Minocycline modulates neuropathic pain behaviour and cortical M1-M2 microglial gene expression in a rat model of depression', *Brain Behav Immun*, vol. 42, pp. 147-56.

Bush, TG, Puvanachandra, N, Horner, CH, Polito, A, Ostefeld, T, Svendsen, CN, Mucke, L, Johnson, MH & Sofroniew, MV 1999, 'Leukocyte infiltration, neuronal degeneration, and neurite outgrowth after ablation of scar-forming, reactive astrocytes in adult transgenic mice', *Neuron*, vol. 23, no. 2, pp. 297-308.

Butefisch, CM, Kleiser, R, Korber, B, Muller, K, Wittsack, HJ, Homberg, V & Seitz, RJ 2005, 'Recruitment of contralesional motor cortex in stroke patients with recovery of hand function', *Neurology*, vol. 64, no. 6, pp. 1067-9.

Butovsky, O, Jedrychowski, MP, Moore, CS, Cialic, R, Lanser, AJ, Gabriely, G, Koeglsperger, T, Dake, B, Wu, PM, Doykan, CE, Fanek, Z, Liu, L, Chen, Z, Rothstein, JD, Ransohoff, RM, Gygi, SP, Antel, JP & Weiner, HL 2014, 'Identification of a unique TGF-beta-dependent molecular and functional signature in microglia', *Nat Neurosci*, vol. 17, no. 1, pp. 131-43.

Byrnes, KR & Faden, AI 2007, 'Role of cell cycle proteins in CNS injury', *Neurochem Res*, vol. 32, no. 10, pp. 1799-807.

Cadilhac, DA, Carter, R, Thrift, AG & Dewey, HM 2009, 'Estimating the long-term costs of ischemic and hemorrhagic stroke for Australia: new evidence derived from the North East Melbourne Stroke Incidence Study (NEMESIS)', *Stroke*, vol. 40, no. 3, pp. 915-21.

Canazza, A, Minati, L, Boffano, C, Parati, E & Binks, S 2014, 'Experimental models of brain ischemia: a review of techniques, magnetic resonance imaging, and investigational cell-based therapies', *Front Neurol*, vol. 5, p. 19.

Caplan, LR 2006, *Stroke*, Demos Medical Publishing, New York, <<http://flinders.ebib.com/patron/FullRecord.aspx?p=289786>>.

Cardoso, MM, Franco, EC, de Souza, CC, da Silva, MC, Gouveia, A & Gomes-Leal, W 2013, 'Minocycline treatment and bone marrow mononuclear cell transplantation after endothelin-1 induced striatal ischemia', *Inflammation*, vol. 36, no. 1, pp. 197-205.

Carmichael, ST 2003, 'Plasticity of cortical projections after stroke', *Neuroscientist*, vol. 9, no. 1, pp. 64-75.

— 2005, 'Rodent models of focal stroke: size, mechanism, and purpose', *NeuroRx*, vol. 2, no. 3, pp. 396-409.

— 2006, 'Cellular and molecular mechanisms of neural repair after stroke: making waves', *Ann Neurol*, vol. 59, no. 5, pp. 735-42.

Carmichael, ST, Archibeque, I, Luke, L, Nolan, T, Momiy, J & Li, S 2005, 'Growth-associated gene expression after stroke: evidence for a growth-promoting region in peri-infarct cortex', *Exp Neurol*, vol. 193, no. 2, pp. 291-311.

Cernak, I, Stoica, B, Byrnes, KR, Di Giovanni, S & Faden, AI 2005, 'Role of the cell cycle in the pathobiology of central nervous system trauma', *Cell Cycle*, vol. 4, no. 9, pp. 1286-93.

Chan, WY, Kohsaka, S & Rezaie, P 2007, 'The origin and cell lineage of microglia: new concepts', *Brain Res Rev*, vol. 53, no. 2, pp. 344-54.

Chao, CC, Hu, S, Molitor, TW, Shaskan, EG & Peterson, PK 1992, 'Activated microglia mediate neuronal cell injury via a nitric oxide mechanism', *J Immunol*, vol. 149, no. 8, pp. 2736-41.

Charnay, Y, Imhof, A, Vallet, PG, Kovari, E, Bouras, C & Giannakopoulos, P 2012, 'Clusterin in neurological disorders: molecular perspectives and clinical relevance', *Brain Res Bull*, vol. 88, no. 5, pp. 434-43.

Chen, CJ, Ding, D, Starke, RM, Mehndiratta, P, Crowley, RW, Liu, KC, Southerland, AM & Worrall, BB 2015, 'Endovascular vs medical management of acute ischemic stroke', *Neurology*, vol. 85, no. 22, pp. 1980-90.

Chen, F, Suzuki, Y, Nagai, N, Jin, L, Yu, J, Wang, H, Marchal, G & Ni, Y 2007, 'Rodent stroke induced by photochemical occlusion of proximal middle cerebral artery: evolution monitored with MR imaging and histopathology', *Eur J Radiol*, vol. 63, no. 1, pp. 68-75.

Chen, H, Chopp, M, Schultz, L, Bodzin, G & Garcia, JH 1993, 'Sequential neuronal and astrocytic changes after transient middle cerebral artery occlusion in the rat', *J Neurol Sci*, vol. 118, no. 2, pp. 109-6.

Chen, HH, Chien, CH & Liu, HM 1994, 'Correlation between angiogenesis and basic fibroblast growth factor expression in experimental brain infarct', *Stroke*, vol. 25, no. 8, pp. 1651-7.

Chen, J, Venkat, P, Zacharek, A & Chopp, M 2014, 'Neurorestorative therapy for stroke', *Front Hum Neurosci*, vol. 8, p. 382.

Chen, R, Cohen, LG & Hallett, M 2002, 'Nervous system reorganization following injury', *Neuroscience*, vol. 111, no. 4, pp. 761-73.

Chen, SH, Oyarzabal, EA, Sung, YF, Chu, CH, Wang, Q, Chen, SL, Lu, RB & Hong, JS 2015, 'Microglial regulation of immunological and neuroprotective functions of astroglia', *Glia*, vol. 63, no. 1, pp. 118-31.

Cherry, JD, Olschowka, JA & O'Banion, MK 2014, 'Neuroinflammation and M2 microglia: the good, the bad, and the inflamed', *J Neuroinflammation*, vol. 11, p. 98.

Chiamulera, C, Terron, A, Reggiani, A & Cristofori, P 1993, 'Qualitative and quantitative analysis of the progressive cerebral damage after middle cerebral artery occlusion in mice', *Brain Res*, vol. 606, no. 2, pp. 251-8.

Chock, VY & Giffard, RG 2005, 'Development of neonatal murine microglia in vitro: changes in response to lipopolysaccharide and ischemia-like injury', *Pediatr Res*, vol. 57, no. 4, pp. 475-80.

Chopp, M, Li, Y & Zhang, ZG 2009, 'Mechanisms underlying improved recovery of neurological function after stroke in the rodent after treatment with neurorestorative cell-based therapies', *Stroke*, vol. 40, no. 3 Suppl, pp. S143-5.

Chou, RH, Lu, CY, Wei, L, Fan, JR, Yu, YL & Shyu, WC 2014, 'The potential therapeutic applications of olfactory ensheathing cells in regenerative medicine', *Cell Transplant*, vol. 23, no. 4-5, pp. 567-71.

Christensen, RN, Ha, BK, Sun, F, Bresnahan, JC & Beattie, MS 2006, 'Kainate induces rapid redistribution of the actin cytoskeleton in amoeboid microglia', *J Neurosci Res*, vol. 84, no. 1, pp. 170-81.

Christopherson, KS, Ullian, EM, Stokes, CC, Mallowney, CE, Hell, JW, Agah, A, Lawler, J, Moshier, DF, Bornstein, P & Barres, BA 2005, 'Thrombospondins are astrocyte-secreted proteins that promote CNS synaptogenesis', *Cell*, vol. 120, no. 3, pp. 421-33.

Chu, LS, Fang, SH, Zhou, Y, Yin, YJ, Chen, WY, Li, JH, Sun, J, Wang, ML, Zhang, WP & Wei, EQ 2010, 'Minocycline inhibits 5-lipoxygenase expression and accelerates functional recovery in chronic phase of focal cerebral ischemia in rats', *Life Sci*, vol. 86, no. 5-6, pp. 170-7.

Clark, RK, Lee, EV, Fish, CJ, White, RF, Price, WJ, Jonak, ZL, Feuerstein, GZ & Barone, FC 1993, 'Development of tissue damage, inflammation and resolution following stroke: an immunohistochemical and quantitative planimetric study', *Brain Res Bull*, vol. 31, no. 5, pp. 565-72.

Clarkson, AN, Lopez-Valdes, HE, Overman, JJ, Charles, AC, Brennan, KC & Thomas Carmichael, S 2013, 'Multimodal examination of structural and functional remapping in the mouse photothrombotic stroke model', *J Cereb Blood Flow Metab*, vol. 33, no. 5, pp. 716-23.

Claus, HL, Walberer, M, Simard, ML, Emig, B, Muesken, SM, Rueger, MA, Fink, GR & Schroeter, M 2013, 'NG2 and NG2-positive cells delineate focal cerebral infarct demarcation in rats', *Neuropathology*, vol. 33, no. 1, pp. 30-8.

Clausen, BH, Lambertsen, KL, Meldgaard, M & Finsen, B 2005, 'A quantitative in situ hybridization and polymerase chain reaction study of microglial-macrophage expression of interleukin-1beta mRNA following permanent middle cerebral artery occlusion in mice', *Neuroscience*, vol. 132, no. 4, pp. 879-92.

Cobbs, CS, Chen, J, Greenberg, DA & Graham, SH 1998, 'Vascular endothelial growth factor expression in transient focal cerebral ischemia in the rat', *Neurosci Lett*, vol. 249, no. 2-3, pp. 79-82.

Colella, AD, Chegenii, N, Tea, MN, Gibbins, IL, Williams, KA & Chataway, TK 2012, 'Comparison of Stain-Free gels with traditional immunoblot loading control methodology', *Anal Biochem*, vol. 430, no. 2, pp. 108-110.

Collombet, JM, Masqueliez, C, Four, E, Burckhart, MF, Bernabe, D, Baubichon, D & Lallemand, G 2006, 'Early reduction of NeuN antigenicity induced by soman poisoning in mice can be used to predict delayed neuronal degeneration in the hippocampus', *Neurosci Lett*, vol. 398, no. 3, pp. 337-42.

Colton, C & Wilcock, DM 2010, 'Assessing activation states in microglia', *CNS Neurol Disord Drug Targets*, vol. 9, no. 2, pp. 174-91.

Costantini, C, Lorenzetto, E, Cellini, B, Buffelli, M, Rossi, F & Della-Bianca, V 2010, 'Astrocytes regulate the expression of insulin-like growth factor 1 receptor (IGF1-R) in primary cortical neurons during in vitro senescence', *J Mol Neurosci*, vol. 40, no. 3, pp. 342-52.

Costello, DA, Lyons, A, Denieffe, S, Browne, TC, Cox, FF & Lynch, MA 2011, 'Long term potentiation is impaired in membrane glycoprotein CD200-deficient mice: a role for Toll-like receptor activation', *J Biol Chem*, vol. 286, no. 40, pp. 34722-32.

Crack, PJ, Gould, J, Bye, N, Ross, S, Ali, U, Habgood, MD, Morganti-Kossmann, C, Saunders, NR, Hertzog, PJ & Victorian Neurotrauma Research, G 2009, 'The genomic profile of the cerebral cortex after closed head injury in mice: effects of minocycline', *J Neural Transm (Vienna)*, vol. 116, no. 1, pp. 1-12.

Craig, AM, Graf, ER & Linhoff, MW 2006, 'How to build a central synapse: clues from cell culture', *Trends Neurosci*, vol. 29, no. 1, pp. 8-20.

Cramer, SC 2008a, 'Repairing the human brain after stroke. II. Restorative therapies', *Ann Neurol*, vol. 63, no. 5, pp. 549-60.

—— 2008b, 'Repairing the human brain after stroke: I. Mechanisms of spontaneous recovery', *Ann Neurol*, vol. 63, no. 3, pp. 272-87.

Cross, AK & Woodroffe, MN 1999, 'Chemokines induce migration and changes in actin polymerization in adult rat brain microglia and a human fetal microglial cell line in vitro', *J Neurosci Res*, vol. 55, no. 1, pp. 17-23.

Cuadros, MA & Navascues, J 1998, 'The origin and differentiation of microglial cells during development', *Prog Neurobiol*, vol. 56, no. 2, pp. 173-89.

- Dale, N & Frenguelli, BG 2009, 'Release of adenosine and ATP during ischemia and epilepsy', *Curr Neuropharmacol*, vol. 7, no. 3, pp. 160-79.
- Dancause, N, Barbay, S, Frost, SB, Plautz, EJ, Chen, D, Zoubina, EV, Stowe, AM & Nudo, RJ 2005, 'Extensive cortical rewiring after brain injury', *J Neurosci*, vol. 25, no. 44, pp. 10167-79.
- Dancause, N & Nudo, RJ 2011, 'Shaping plasticity to enhance recovery after injury', *Prog Brain Res*, vol. 192, pp. 273-95.
- Davalos, D, Grutzendler, J, Yang, G, Kim, JV, Zuo, Y, Jung, S, Littman, DR, Dustin, ML & Gan, W-B 2005, 'ATP mediates rapid microglial response to local brain injury in vivo', *Nat Neurosci*, vol. 8, no. 6, pp. 752-8.
- Davoli, MA, Fourtounis, J, Tam, J, Xanthoudakis, S, Nicholson, D, Robertson, GS, Ng, GY & Xu, D 2002, 'Immunohistochemical and biochemical assessment of caspase-3 activation and DNA fragmentation following transient focal ischemia in the rat', *Neuroscience*, vol. 115, no. 1, pp. 125-36.
- de Freitas, MS, Spohr, TC, Benedito, AB, Caetano, MS, Margulis, B, Lopes, UG & Moura-Neto, V 2002, 'Neurite outgrowth is impaired on HSP70-positive astrocytes through a mechanism that requires NF-kappaB activation', *Brain Res*, vol. 958, no. 2, pp. 359-70.
- Deguchi, K, Takaishi, M, Hayashi, T, Oohira, A, Nagotani, S, Li, F, Jin, G, Nagano, I, Shoji, M, Miyazaki, M, Abe, K & Huh, NH 2005, 'Expression of neurocan after transient middle cerebral artery occlusion in adult rat brain', *Brain Res*, vol. 1037, no. 1-2, pp. 194-9.
- Dey, A, Allen, J & Hankey-Giblin, PA 2015, 'Ontogeny and polarization of macrophages in inflammation: blood monocytes versus tissue macrophages', *Front Immunol*, vol. 5, p. 683.
- Di Giovanni, S 2009, 'Molecular targets for axon regeneration: focus on the intrinsic pathways', *Expert Opin Ther Targets*, vol. 13, no. 12, pp. 1387-98.
- Di Giovanni, S, Movsesyan, V, Ahmed, F, Cernak, I, Schinelli, S, Stoica, B & Faden, AI 2005, 'Cell cycle inhibition provides neuroprotection and reduces glial proliferation and scar formation after traumatic brain injury', *Proc Natl Acad Sci U S A*, vol. 102, no. 23, pp. 8333-8.
- Dobolyi, A, Vincze, C, Pal, G & Lovas, G 2012, 'The neuroprotective functions of transforming growth factor beta proteins', *Int J Mol Sci*, vol. 13, no. 7, pp. 8219-58.
- Doyle, KP, Cekanaviciute, E, Mamer, LE & Buckwalter, MS 2010, 'TGFbeta signaling in the brain increases with aging and signals to astrocytes and innate immune cells in the weeks after stroke', *J Neuroinflammation*, vol. 7, p. 62.

- Doyle, KP, Simon, RP & Stenzel-Poore, MP 2008, 'Mechanisms of ischemic brain damage', *Neuropharmacology*, vol. 55, no. 3, pp. 310-8.
- Drew, PD & Chavis, JA 2000, 'Inhibition of microglial cell activation by cortisol', *Brain Res Bull*, vol. 52, no. 5, pp. 391-6.
- Dugan, LL & Kim-Han, JS 2004, 'Astrocyte mitochondria in in vitro models of ischemia', *J Bioenerg Biomembr*, vol. 36, no. 4, pp. 317-21.
- Duggal, N, Schmidt-Kastner, R & Hakim, AM 1997, 'Nestin expression in reactive astrocytes following focal cerebral ischemia in rats', *Brain Res*, vol. 768, no. 1-2, pp. 1-9.
- Eyo, UB, Miner, SA, Ahlers, KE, Wu, LJ & Dailey, ME 2013, 'P2X7 receptor activation regulates microglial cell death during oxygen-glucose deprivation', *Neuropharmacology*, vol. 73, pp. 311-9.
- Famakin, BM 2014, 'The Immune Response to Acute Focal Cerebral Ischemia and Associated Post-stroke Immunodepression: A Focused Review', *Aging Dis*, vol. 5, no. 5, pp. 307-26.
- Feigin, VL, Forouzanfar, MH, Krishnamurthi, R, Mensah, GA, Connor, M, Bennett, DA, Moran, AE, Sacco, RL, Anderson, L, Truelsen, T, O'Donnell, M, Venketasubramanian, N, Barker-Collo, S, Lawes, CM, Wang, W, Shinohara, Y, Witt, E, Ezzati, M, Naghavi, M, Murray, C, Global Burden of Diseases, I, Risk Factors, S & the, GBDSEG 2014, 'Global and regional burden of stroke during 1990-2010: findings from the Global Burden of Disease Study 2010', *Lancet*, vol. 383, no. 9913, pp. 245-54.
- Feigin, VL, Krishnamurthi, RV, Parmar, P, Norrving, B, Mensah, GA, Bennett, DA, Barker-Collo, S, Moran, AE, Sacco, RL, Truelsen, T, Davis, S, Pandian, JD, Naghavi, M, Forouzanfar, MH, Nguyen, G, Johnson, CO, Vos, T, Meretoja, A, Murray, CJ, Roth, GA, Group, GBDW & Group, GBDSPE 2015, 'Update on the Global Burden of Ischemic and Hemorrhagic Stroke in 1990-2013: The GBD 2013 Study', *Neuroepidemiology*, vol. 45, no. 3, pp. 161-76.
- Ferrari, D, Chiozzi, P, Falzoni, S, Dal Susino, M, Collo, G, Buell, G & Di Virgilio, F 1997, 'ATP-mediated cytotoxicity in microglial cells', *Neuropharmacology*, vol. 36, no. 9, pp. 1295-301.
- Ferrari, D, Los, M, Bauer, MK, Vandenabeele, P, Wesselborg, S & Schulze-Osthoff, K 1999, 'P2Z purinoreceptor ligation induces activation of caspases with distinct roles in apoptotic and necrotic alterations of cell death', *FEBS Lett*, vol. 447, no. 1, pp. 71-5.
- Filipovic, R & Zecevic, N 2008, 'Neuroprotective role of minocycline in co-cultures of human fetal neurons and microglia', *Exp Neurol*, vol. 211, no. 1, pp. 41-51.

Fitch, MT & Silver, J 1997, 'Glial cell extracellular matrix: boundaries for axon growth in development and regeneration', *Cell Tissue Res*, vol. 290, no. 2, pp. 379-84.

— 2008, 'CNS injury, glial scars, and inflammation: Inhibitory extracellular matrices and regeneration failure', *Exp Neurol*, vol. 209, no. 2, pp. 294-301.

Fluri, F, Schuhmann, MK & Kleinschnitz, C 2015, 'Animal models of ischemic stroke and their application in clinical research', *Drug Des Devel Ther*, vol. 9, pp. 3445-54.

Flynn, RW, MacWalter, RS & Doney, AS 2008, 'The cost of cerebral ischaemia', *Neuropharmacology*, vol. 55, no. 3, pp. 250-6.

Fordyce, CB, Jagasia, R, Zhu, X & Schlichter, LC 2005, 'Microglia Kv1.3 channels contribute to their ability to kill neurons', *J Neurosci*, vol. 25, no. 31, pp. 7139-49.

Fox, C, Dingman, A, Derugin, N, Wendland, MF, Manabat, C, Ji, S, Ferriero, DM & Vexler, ZS 2005, 'Minocycline confers early but transient protection in the immature brain following focal cerebral ischemia-reperfusion', *J Cereb Blood Flow Metab*, vol. 25, no. 9, pp. 1138-49.

Franco, EC, Cardoso, MM, Gouveia, A, Pereira, A & Gomes-Leal, W 2012, 'Modulation of microglial activation enhances neuroprotection and functional recovery derived from bone marrow mononuclear cell transplantation after cortical ischemia', *Neurosci Res*, vol. 73, no. 2, pp. 122-32.

Freguelli, BG, Wigmore, G, Llaudet, E & Dale, N 2007, 'Temporal and mechanistic dissociation of ATP and adenosine release during ischaemia in the mammalian hippocampus', *J Neurochem*, vol. 101, no. 5, pp. 1400-13.

Fujita, H, Tanaka, J, Toku, K, Tateishi, N, Suzuki, Y, Matsuda, S, Sakanaka, M & Maeda, N 1996, 'Effects of GM-CSF and ordinary supplements on the ramification of microglia in culture: a morphometrical study', *Glia*, vol. 18, no. 4, pp. 269-81.

Fumagalli, S, Perego, C, Ortolano, F & De Simoni, MG 2013, 'CX3CR1 deficiency induces an early protective inflammatory environment in ischemic mice', *Glia*, vol. 61, no. 6, pp. 827-42.

Gahwiler, BH, Capogna, M, Debanne, D, McKinney, RA & Thompson, SM 1997, 'Organotypic slice cultures: a technique has come of age', *Trends Neurosci*, vol. 20, no. 10, pp. 471-7.

Galtrey, CM & Fawcett, JW 2007, 'The role of chondroitin sulfate proteoglycans in regeneration and plasticity in the central nervous system', *Brain Res Rev*, vol. 54, no. 1, pp. 1-18.

Gao, Q, Li, Y, Shen, L, Zhang, J, Zheng, X, Qu, R, Liu, Z & Chopp, M 2008, 'Bone marrow stromal cells reduce ischemia-induced astrocytic activation in vitro', *Neuroscience*, vol. 152, no. 3, pp. 646-55.

Gao, Z, Zhu, Q, Zhang, Y, Zhao, Y, Cai, L, Shields, CB & Cai, J 2013, 'Reciprocal modulation between microglia and astrocyte in reactive gliosis following the CNS injury', *Mol Neurobiol*, vol. 48, no. 3, pp. 690-701.

Garcia, JH, Yoshida, Y, Chen, H, Li, Y, Zhang, ZG, Lian, J, Chen, S & Chopp, M 1993, 'Progression from ischemic injury to infarct following middle cerebral artery occlusion in the rat', *Am J Pathol*, vol. 142, no. 2, pp. 623-35.

Garrido-Mesa, N, Zarzuelo, A & Galvez, J 2013a, 'Minocycline: far beyond an antibiotic', *Br J Pharmacol*, vol. 169, no. 2, pp. 337-52.

—— 2013b, 'What is behind the non-antibiotic properties of minocycline?', *Pharmacol Res*, vol. 67, no. 1, pp. 18-30.

Gass, P, Spranger, M, Herdegen, T, Bravo, R, Kock, P, Hacke, W & Kiessling, M 1992, 'Induction of FOS and JUN proteins after focal ischemia in the rat: differential effect of the N-methyl-D-aspartate receptor antagonist MK-801', *Acta Neuropathol*, vol. 84, no. 5, pp. 545-53.

Gerloff, C, Bushara, K, Sailer, A, Wassermann, EM, Chen, R, Matsuoka, T, Waldvogel, D, Wittenberg, GF, Ishii, K, Cohen, LG & Hallett, M 2006, 'Multimodal imaging of brain reorganization in motor areas of the contralesional hemisphere of well recovered patients after capsular stroke', *Brain*, vol. 129, no. Pt 3, pp. 791-808.

Gertig, U & Hanisch, UK 2014, 'Microglial diversity by responses and responders', *Front Cell Neurosci*, vol. 8, p. 101.

Gertz, K, Kronenberg, G, Kalin, RE, Baldinger, T, Werner, C, Balkaya, M, Eom, GD, Hellmann-Regen, J, Krober, J, Miller, KR, Lindauer, U, Laufs, U, Dirnagl, U, Heppner, FL & Endres, M 2012, 'Essential role of interleukin-6 in post-stroke angiogenesis', *Brain*, vol. 135, no. Pt 6, pp. 1964-80.

Gibbons, HM & Dragunow, M 2006, 'Microglia induce neural cell death via a proximity-dependent mechanism involving nitric oxide', *Brain Res*, vol. 1084, no. 1, pp. 1-15.

Giffard, RG & Swanson, RA 2005, 'Ischemia-induced programmed cell death in astrocytes', *Glia*, vol. 50, no. 4, pp. 299-306.

Ginhoux, F, Lim, S, Hoeffel, G, Low, D & Huber, T 2013, 'Origin and differentiation of microglia', *Front Cell Neurosci*, vol. 7, p. 45.

Ginsberg, MD 2008, 'Neuroprotection for ischemic stroke: past, present and future', *Neuropharmacology*, vol. 55, no. 3, pp. 363-89.

—— 2009, 'Current status of neuroprotection for cerebral ischemia: synoptic overview', *Stroke*, vol. 40, no. 3 Suppl, pp. S111-4.

Girard, S, Brough, D, Lopez-Castejon, G, Giles, J, Rothwell, NJ & Allan, SM 2013, 'Microglia and macrophages differentially modulate cell death after brain injury caused by oxygen-glucose deprivation in organotypic brain slices', *Glia*, vol. 61, no. 5, pp. 813-24.

Giulian, D & Baker, TJ 1985, 'Peptides released by ameboid microglia regulate astroglial proliferation', *J Cell Biol*, vol. 101, no. 6, pp. 2411-5.

Glenn, JA, Ward, SA, Stone, CR, Booth, PL & Thomas, WE 1992, 'Characterisation of ramified microglial cells: detailed morphology, morphological plasticity and proliferative capability', *J Anat*, vol. 180 (Pt 1), pp. 109-18.

Gloede, TD, Halbach, SM, Thrift, AG, Dewey, HM, Pfaff, H & Cadilhac, DA 2014, 'Long-term costs of stroke using 10-year longitudinal data from the North East Melbourne Stroke Incidence Study', *Stroke*, vol. 45, no. 11, pp. 3389-94.

Goldberg, MP & Choi, DW 1993, 'Combined oxygen and glucose deprivation in cortical cell culture: calcium-dependent and calcium-independent mechanisms of neuronal injury', *J Neurosci*, vol. 13, no. 8, pp. 3510-24.

Goldberg, WJ, Kadingo, RM & Barrett, JN 1986, 'Effects of ischemia-like conditions on cultured neurons: protection by low Na⁺, low Ca²⁺ solutions', *J Neurosci*, vol. 6, no. 11, pp. 3144-51.

Goldmacher, GV, Nasser, R, Lee, DY, Yigit, S, Rosenwasser, R & Iacovitti, L 2013, 'Tracking transplanted bone marrow stem cells and their effects in the rat MCAO stroke model', *PLoS One*, vol. 8, no. 3, p. e60049.

Goyal, M, Yu, AY, Menon, BK, Dippel, DW, Hacke, W, Davis, SM, Fisher, M, Yavagal, DR, Turjman, F, Ross, J, Yoshimura, S, Miao, Z, Bhatia, R, Almekhlafi, M, Murayama, Y, Sohn, SI, Saver, JL, Demchuk, AM & Hill, MD 2016, 'Endovascular Therapy in Acute Ischemic Stroke: Challenges and Transition From Trials to Bedside', *Stroke*, vol. 47, no. 2, pp. 548-53.

Graeber, MB, Banati, RB, Streit, WJ & Kreutzberg, GW 1989, 'Immunophenotypic characterization of rat brain macrophages in culture', *Neurosci Lett*, vol. 103, no. 3, pp. 241-6.

Graeber, MB & Streit, WJ 2010, 'Microglia: biology and pathology', *Acta Neuropathol*, vol. 119, no. 1, pp. 89-105.

Greenberg, DA & Jin, K 2013, 'Vascular endothelial growth factors (VEGFs) and stroke', *Cell Mol Life Sci*, vol. 70, no. 10, pp. 1753-61.

Gregersen, R, Lambertsen, K & Finsen, B 2000, 'Microglia and macrophages are the major source of tumor necrosis factor in permanent middle cerebral artery occlusion in mice', *J Cereb Blood Flow Metab*, vol. 20, no. 1, pp. 53-65.

Grome, JJ, Gojowczyk, G, Hofmann, W & Graham, DI 1988, 'Quantitation of photochemically induced focal cerebral ischemia in the rat', *J Cereb Blood Flow Metab*, vol. 8, no. 1, pp. 89-95.

Guillemin, GJ & Brew, BJ 2004, 'Microglia, macrophages, perivascular macrophages, and pericytes: a review of function and identification', *J Leukoc Biol*, vol. 75, no. 3, pp. 388-97.

Guthrie, KM, Woods, AG, Nguyen, T & Gall, CM 1997, 'Astroglial ciliary neurotrophic factor mRNA expression is increased in fields of axonal sprouting in deafferented hippocampus', *J Comp Neurol*, vol. 386, no. 1, pp. 137-48.

Hailer, NP 2008, 'Immunosuppression after traumatic or ischemic CNS damage: it is neuroprotective and illuminates the role of microglial cells', *Prog Neurobiol*, vol. 84, no. 3, pp. 211-33.

Hailer, NP, Wirjatijasa, F, Roser, N, Hischebeth, GT, Korf, HW & Dehghani, F 2001, 'Astrocytic factors protect neuronal integrity and reduce microglial activation in an in vitro model of N-methyl-D-aspartate-induced excitotoxic injury in organotypic hippocampal slice cultures', *Eur J Neurosci*, vol. 14, no. 2, pp. 315-26.

Hall, AA, Herrera, Y, Ajmo, CT, Jr., Cuevas, J & Pennypacker, KR 2009, 'Sigma receptors suppress multiple aspects of microglial activation', *Glia*, vol. 57, no. 7, pp. 744-54.

Hallenbeck, JM 2002, 'The many faces of tumor necrosis factor in stroke', *Nat Med*, vol. 8, no. 12, pp. 1363-8.

Hallett, M 2001, 'Plasticity of the human motor cortex and recovery from stroke', *Brain Res Brain Res Rev*, vol. 36, no. 2-3, pp. 169-74.

Hamby, ME, Uliasz, TF, Hewett, SJ & Hewett, JA 2006, 'Characterization of an improved procedure for the removal of microglia from confluent monolayers of primary astrocytes', *J Neurosci Methods*, vol. 150, no. 1, pp. 128-37.

Hanisch, UK 2013, 'Functional diversity of microglia - how heterogeneous are they to begin with?', *Front Cell Neurosci*, vol. 7, p. 65.

Hanisch, UK & Kettenmann, H 2007, 'Microglia: active sensor and versatile effector cells in the normal and pathologic brain', *Nat Neurosci*, vol. 10, no. 11, pp. 1387-94.

Hansson, E 1984, 'Cellular composition of a cerebral hemisphere primary culture', *Neurochem Res*, vol. 9, no. 2, pp. 153-72.

Hansson, E, Ronnback, L, Lowenthal, A, Noppe, M, Alling, C, Karlsson, B & Sellstrom, A 1982, 'Brain primary culture-- a characterization (part II)', *Brain Res*, vol. 231, no. 1, pp. 173-83.

Hansson, E, Sellstrom, A, Persson, LI & Ronnback, L 1980, 'Brain primary culture - a characterization', *Brain Res*, vol. 188, no. 1, pp. 233-46.

Hansson, E & Thorlin, T 1999, 'Brain primary cultures and vibrodissociated cells as tools for the study of astroglial properties and functions', *Dev Neurosci*, vol. 21, no. 1, pp. 1-11.

Hao, F, Zhang, NN, Zhang, DM, Bai, HY, Piao, H, Yuan, B, Zhu, HY, Yu, H, Xiao, CS & Li, AP 2013, 'Chemokine fractalkine attenuates overactivation and apoptosis of BV-2 microglial cells induced by extracellular ATP', *Neurochem Res*, vol. 38, no. 5, pp. 1002-12.

Harrison, TC, Silasi, G, Boyd, JD & Murphy, TH 2013, 'Displacement of sensory maps and disorganization of motor cortex after targeted stroke in mice', *Stroke*, vol. 44, no. 8, pp. 2300-6.

Hayakawa, K, Mishima, K, Nozako, M, Hazekawa, M, Mishima, S, Fujioka, M, Orito, K, Egashira, N, Iwasaki, K & Fujiwara, M 2008, 'Delayed treatment with minocycline ameliorates neurologic impairment through activated microglia expressing a high-mobility group box1-inhibiting mechanism', *Stroke*, vol. 39, no. 3, pp. 951-8.

Hayakawa, K, Nakano, T, Irie, K, Higuchi, S, Fujioka, M, Orito, K, Iwasaki, K, Jin, G, Lo, EH, Mishima, K & Fujiwara, M 2010, 'Inhibition of reactive astrocytes with fluorocitrate retards neurovascular remodeling and recovery after focal cerebral ischemia in mice', *J Cereb Blood Flow Metab*, vol. 30, no. 4, pp. 871-82.

Hayashi, N, Tatsumi, K, Okuda, H, Yoshikawa, M, Ishizaka, S, Miyata, S, Manabe, T & Wanaka, A 2007, 'DACS, novel matrix structure composed of chondroitin sulfate proteoglycan in the brain', *Biochem Biophys Res Commun*, vol. 364, no. 2, pp. 410-5.

Heldmann, U, Thored, P, Claasen, JH, Arvidsson, A, Kokaia, Z & Lindvall, O 2005, 'TNF-alpha antibody infusion impairs survival of stroke-generated neuroblasts in adult rat brain', *Exp Neurol*, vol. 196, no. 1, pp. 204-8.

Hellwig, S, Heinrich, A & Biber, K 2013, 'The brain's best friend: microglial neurotoxicity revisited', *Front Cell Neurosci*, vol. 7, p. 71.

Henry, CJ, Huang, Y, Wynne, A, Hanke, M, Himler, J, Bailey, MT, Sheridan, JF & Godbout, JP 2008, 'Minocycline attenuates lipopolysaccharide (LPS)-induced neuroinflammation, sickness behavior, and anhedonia', *J Neuroinflammation*, vol. 5, p. 15.

Hermann, DM & Zechariah, A 2009, 'Implications of vascular endothelial growth factor for postischemic neurovascular remodeling', *J Cereb Blood Flow Metab*, vol. 29, no. 10, pp. 1620-43.

Hertz, L & Schousboe, A 1975, 'Ion and energy metabolism of the brain at the cellular level', *Int Rev Neurobiol*, vol. 18, pp. 141-211.

Hewlett, KA & Corbett, D 2006, 'Delayed minocycline treatment reduces long-term functional deficits and histological injury in a rodent model of focal ischemia', *Neuroscience*, vol. 141, no. 1, pp. 27-33.

Hinman, JD, Rasband, MN & Carmichael, ST 2013, 'Remodeling of the axon initial segment after focal cortical and white matter stroke', *Stroke*, vol. 44, no. 1, pp. 182-9.

Hinwood, M, Tynan, RJ, Charnley, JL, Beynon, SB, Day, TA & Walker, FR 2013, 'Chronic stress induced remodeling of the prefrontal cortex: structural reorganization of microglia and the inhibitory effect of minocycline', *Cereb Cortex*, vol. 23, no. 8, pp. 1784-97.

Hol, EM & Pekny, M 2015, 'Glial fibrillary acidic protein (GFAP) and the astrocyte intermediate filament system in diseases of the central nervous system', *Curr Opin Cell Biol*, vol. 32, pp. 121-30.

Horinouchi, K, Ikeda, S, Harada, K, Ohwatashi, A, Kamikawa, Y, Yoshida, A, Nomoto, Y, Etoh, S & Kawahira, K 2007, 'Functional recovery and expression of GDNF seen in photochemically induced cerebral infarction', *Int J Neurosci*, vol. 117, no. 3, pp. 315-26.

Horn, KP, Busch, SA, Hawthorne, AL, van Rooijen, N & Silver, J 2008, 'Another barrier to regeneration in the CNS: activated macrophages induce extensive retraction of dystrophic axons through direct physical interactions', *J Neurosci*, vol. 28, no. 38, pp. 9330-41.

Horvath, RJ, Nutile-McMenemy, N, Alkaitis, MS & Deleo, JA 2008, 'Differential migration, LPS-induced cytokine, chemokine, and NO expression in immortalized BV-2 and HAPI cell lines and primary microglial cultures', *J Neurochem*, vol. 107, no. 2, pp. 557-69.

Hosli, E & Hosli, L 1993, 'Receptors for neurotransmitters on astrocytes in the mammalian central nervous system', *Prog Neurobiol*, vol. 40, no. 4, pp. 477-506.

Hossmann, KA 2008, 'Cerebral ischemia: models, methods and outcomes', *Neuropharmacology*, vol. 55, no. 3, pp. 257-70.

—— 2009, 'Pathophysiological basis of translational stroke research', *Folia Neuropathol*, vol. 47, no. 3, pp. 213-27.

—— 2012, 'The two pathophysiologies of focal brain ischemia: implications for translational stroke research', *J Cereb Blood Flow Metab*, vol. 32, no. 7, pp. 1310-6.

Hu, X, Leak, RK, Shi, Y, Suenaga, J, Gao, Y, Zheng, P & Chen, J 2015, 'Microglial and macrophage polarization-new prospects for brain repair', *Nat Rev Neurol*, vol. 11, no. 1, pp. 56-64.

Hu, X, Li, P, Guo, Y, Wang, H, Leak, RK, Chen, S, Gao, Y & Chen, J 2012, 'Microglia/macrophage polarization dynamics reveal novel mechanism of injury expansion after focal cerebral ischemia', *Stroke*, vol. 43, no. 11, pp. 3063-70.

Huang, WC, Qiao, Y, Xu, L, Kacimi, R, Sun, X, Giffard, RG & Yenari, MA 2010, 'Direct protection of cultured neurons from ischemia-like injury by minocycline', *Anat Cell Biol*, vol. 43, no. 4, pp. 325-31.

Iadecola, C & Anrather, J 2011, 'The immunology of stroke: from mechanisms to translation', *Nat Med*, vol. 17, no. 7, pp. 796-808.

Imhof, A, Charnay, Y, Vallet, PG, Aronow, B, Kovari, E, French, LE, Bouras, C & Giannakopoulos, P 2006, 'Sustained astrocytic clusterin expression improves remodeling after brain ischemia', *Neurobiol Dis*, vol. 22, no. 2, pp. 274-83.

Issa, R, AlQteishat, A, Mitsios, N, Saka, M, Krupinski, J, Tarkowski, E, Gaffney, J, Slevin, M, Kumar, S & Kumar, P 2005, 'Expression of basic fibroblast growth factor mRNA and protein in the human brain following ischaemic stroke', *Angiogenesis*, vol. 8, no. 1, pp. 53-62.

Ito, D, Tanaka, K, Suzuki, S, Dembo, T & Fukuuchi, Y 2001, 'Enhanced expression of Iba1, ionized calcium-binding adapter molecule 1, after transient focal cerebral ischemia in rat brain', *Stroke*, vol. 32, no. 5, pp. 1208-15.

Iwata, A, Masago, A & Yamada, K 1997, 'Expression of basic fibroblast growth factor mRNA after transient focal ischemia: comparison with expression of c-fos, c-jun, and hsp 70 mRNA', *J Neurotrauma*, vol. 14, no. 4, pp. 201-10.

Jablonka, JA, Burnat, K, Witte, OW & Kossut, M 2010, 'Remapping of the somatosensory cortex after a photothrombotic stroke: dynamics of the compensatory reorganization', *Neuroscience*, vol. 165, no. 1, pp. 90-100.

Jablonka, JA, Kossut, M, Witte, OW & Liguz-Leczna, M 2012, 'Experience-dependent brain plasticity after stroke: effect of ibuprofen and poststroke delay', *Eur J Neurosci*, vol. 36, no. 5, pp. 2632-9.

Jaillard, A, Martin, CD, Garambois, K, Lebas, JF & Hommel, M 2005, 'Vicarious function within the human primary motor cortex? A longitudinal fMRI stroke study', *Brain*, vol. 128, no. Pt 5, pp. 1122-38.

Jander, S, Kraemer, M, Schroeter, M, Witte, OW & Stoll, G 1995, 'Lymphocytic infiltration and expression of intercellular adhesion molecule-1 in photochemically induced ischemia of the rat cortex', *J Cereb Blood Flow Metab*, vol. 15, no. 1, pp. 42-51.

Jeong, HK, Ji, KM, Kim, B, Kim, J, Jou, I & Joe, EH 2010, 'Inflammatory responses are not sufficient to cause delayed neuronal death in ATP-induced acute brain injury', *PLoS One*, vol. 5, no. 10, p. e13756.

Jha, MK, Kim, JH & Suk, K 2014, 'Proteome of brain glia: the molecular basis of diverse glial phenotypes', *Proteomics*, vol. 14, no. 4-5, pp. 378-98.

Jin, Q, Cheng, J, Liu, Y, Wu, J, Wang, X, Wei, S, Zhou, X, Qin, Z, Jia, J & Zhen, X 2014, 'Improvement of functional recovery by chronic metformin treatment is associated with enhanced alternative activation of microglia/macrophages and increased angiogenesis and neurogenesis following experimental stroke', *Brain Behav Immun*, vol. 40, pp. 131-42.

Johnston, DG, Denizet, M, Mostany, R & Portera-Cailliau, C 2013, 'Chronic in vivo imaging shows no evidence of dendritic plasticity or functional remapping in the contralesional cortex after stroke', *Cereb Cortex*, vol. 23, no. 4, pp. 751-62.

Jordan, J, Segura, T, Brea, D, Galindo, MF & Castillo, J 2008, 'Inflammation as therapeutic objective in stroke', *Curr Pharm Des*, vol. 14, no. 33, pp. 3549-64.

Juranyi, Z, Sperlagh, B & Vizi, ES 1999, 'Involvement of P2 purinoceptors and the nitric oxide pathway in [3H]purine outflow evoked by short-term hypoxia and hypoglycemia in rat hippocampal slices', *Brain Res*, vol. 823, no. 1-2, pp. 183-90.

Kang, SS, Keasey, MP, Cai, J & Hagg, T 2012, 'Loss of neuron-astroglial interaction rapidly induces protective CNTF expression after stroke in mice', *J Neurosci*, vol. 32, no. 27, pp. 9277-87.

Karonen, JO, Liu, Y, Vanninen, RL, Ostergaard, L, Kaarina Partanen, PL, Vainio, PA, Vanninen, EJ, Nuutinen, J, Roivainen, R, Soimakallio, S, Kuikka, JT & Aronen, HJ 2000, 'Combined perfusion- and diffusion-weighted MR imaging in acute ischemic stroke during the 1st week: a longitudinal study', *Radiology*, vol. 217, no. 3, pp. 886-94.

Karperien, A & Jelinek, H 2015, 'Fractal, Multifractal, and Lacunarity Analysis of Microglia in Tissue Engineering', *Frontiers in Bioengineering and Biotechnology*, vol. 3.

Kato, H, Kogure, K, Araki, T & Itoyama, Y 1995, 'Graded expression of immunomolecules on activated microglia in the hippocampus following ischemia in a rat model of ischemic tolerance', *Brain Res*, vol. 694, no. 1-2, pp. 85-93.

Katsman, D, Zheng, J, Spinelli, K & Carmichael, ST 2003, 'Tissue microenvironments within functional cortical subdivisions adjacent to focal stroke', *J Cereb Blood Flow Metab*, vol. 23, no. 9, pp. 997-1009.

Katsumoto, A, Lu, H, Miranda, AS & Ransohoff, RM 2014, 'Ontogeny and functions of central nervous system macrophages', *J Immunol*, vol. 193, no. 6, pp. 2615-21.

Kaushal, V & Schlichter, LC 2008, 'Mechanisms of microglia-mediated neurotoxicity in a new model of the stroke penumbra', *J Neurosci*, vol. 28, no. 9, pp. 2221-30.

Kawamata, T, Dietrich, WD, Schallert, T, Gotts, JE, Cocke, RR, Benowitz, LI & Finklestein, SP 1997, 'Intracisternal basic fibroblast growth factor enhances functional recovery and up-regulates the expression of a molecular marker of neuronal sprouting following focal cerebral infarction', *Proc Natl Acad Sci U S A*, vol. 94, no. 15, pp. 8179-84.

Kawano, H, Kimura-Kuroda, J, Komuta, Y, Yoshioka, N, Li, HP, Kawamura, K, Li, Y & Raisman, G 2012, 'Role of the lesion scar in the response to damage and repair of the central nervous system', *Cell Tissue Res*, vol. 349, no. 1, pp. 169-80.

Keiner, S, Wurm, F, Kunze, A, Witte, OW & Redecker, C 2008, 'Rehabilitative therapies differentially alter proliferation and survival of glial cell populations in the perilesional zone of cortical infarcts', *Glia*, vol. 56, no. 5, pp. 516-27.

Kettenmann, H, Hanisch, UK, Noda, M & Verkhratsky, A 2011, 'Physiology of microglia', *Physiol Rev*, vol. 91, no. 2, pp. 461-553.

Kigerl, KA, de Rivero Vaccari, JP, Dietrich, WD, Popovich, PG & Keane, RW 2014, 'Pattern recognition receptors and central nervous system repair', *Exp Neurol*, vol. 258, pp. 5-16.

Kim, BJ, Kim, MJ, Park, JM, Lee, SH, Kim, YJ, Ryu, S, Kim, YH & Yoon, BW 2009, 'Reduced neurogenesis after suppressed inflammation by minocycline in transient cerebral ischemia in rat', *J Neurol Sci*, vol. 279, no. 1-2, pp. 70-5.

Kim, JY, Kawabori, M & Yenari, MA 2014, 'Innate inflammatory responses in stroke: mechanisms and potential therapeutic targets', *Curr Med Chem*, vol. 21, no. 18, pp. 2076-97.

Kim, JY, Kim, N & Yenari, MA 2015, 'Mechanisms and potential therapeutic applications of microglial activation after brain injury', *CNS Neurosci Ther*, vol. 21, no. 4, pp. 309-19.

Kim, SS, Kong, PJ, Kim, BS, Sheen, DH, Nam, SY & Chun, W 2004, 'Inhibitory action of minocycline on lipopolysaccharide-induced release of nitric oxide and prostaglandin E2 in BV2 microglial cells', *Arch Pharm Res*, vol. 27, no. 3, pp. 314-8.

Kitamura, Y, Takata, K, Inden, M, Tsuchiya, D, Yanagisawa, D, Nakata, J & Taniguchi, T 2004, 'Intracerebroventricular injection of microglia protects against focal brain ischemia', *J Pharmacol Sci*, vol. 94, no. 2, pp. 203-6.

Kitamura, Y, Yanagisawa, D, Inden, M, Takata, K, Tsuchiya, D, Kawasaki, T, Taniguchi, T & Shimohama, S 2005, 'Recovery of focal brain ischemia-induced behavioral dysfunction by intracerebroventricular injection of microglia', *J Pharmacol Sci*, vol. 97, no. 2, pp. 289-93.

Kitayama, M, Ueno, M, Itakura, T & Yamashita, T 2011, 'Activated Microglia Inhibit Axonal Growth through RGMa', *PLoS One*, vol. 6, no. 9, p. e25234.

Kleim, JA, Boychuk, JA & Adkins, DL 2007, 'Rat models of upper extremity impairment in stroke', *ILAR J*, vol. 48, no. 4, pp. 374-84.

Kobayashi, K, Imagama, S, Ohgomori, T, Hirano, K, Uchimura, K, Sakamoto, K, Hirakawa, A, Takeuchi, H, Suzumura, A, Ishiguro, N & Kadomatsu, K 2013, 'Minocycline selectively inhibits M1 polarization of microglia', *Cell Death Dis*, vol. 4, p. e525.

Komitova, M, Mattsson, B, Johansson, BB & Eriksson, PS 2005, 'Enriched environment increases neural stem/progenitor cell proliferation and neurogenesis in the subventricular zone of stroke-lesioned adult rats', *Stroke*, vol. 36, no. 6, pp. 1278-82.

Komitova, M, Perfilieva, E, Mattsson, B, Eriksson, PS & Johansson, BB 2006, 'Enriched environment after focal cortical ischemia enhances the generation of astroglia and NG2 positive polydendrocytes in adult rat neocortex', *Exp Neurol*, vol. 199, no. 1, pp. 113-21.

Kong, H, Omran, A, Ashhab, MU, Gan, N, Peng, J, He, F, Wu, L, Deng, X & Yin, F 2014, 'Changes in microglial inflammation-related and brain-enriched MicroRNAs expressions in response to in vitro oxygen-glucose deprivation', *Neurochem Res*, vol. 39, no. 2, pp. 233-43.

Korzhevskii, DE, Lentsman, MV, Kirik, OV & Otellin, VA 2008, 'Vimentin-immunopositive cells in the rat telencephalon after experimental ischemic stroke', *Neurosci Behav Physiol*, vol. 38, no. 8, pp. 845-8.

Kotila, M, Waltimo, O, Niemi, ML, Laaksonen, R & Lempinen, M 1984, 'The profile of recovery from stroke and factors influencing outcome', *Stroke*, vol. 15, no. 6, pp. 1039-44.

Kozlowski, C & Weimer, RM 2012, 'An automated method to quantify microglia morphology and application to monitor activation state longitudinally in vivo', *PLoS One*, vol. 7, no. 2, p. e31814.

Kremlev, SG, Roberts, RL & Palmer, C 2004, 'Differential expression of chemokines and chemokine receptors during microglial activation and inhibition', *J Neuroimmunol*, vol. 149, no. 1-2, pp. 1-9.

- Kriz, J 2006, 'Inflammation in ischemic brain injury: timing is important', *Crit Rev Neurobiol*, vol. 18, no. 1-2, pp. 145-57.
- Kriz, J & Lalancette-Hebert, M 2009, 'Inflammation, plasticity and real-time imaging after cerebral ischemia', *Acta Neuropathol*, vol. 117, no. 5, pp. 497-509.
- Kuric, E, Wieloch, T & Ruscher, K 2013, 'Dopamine receptor activation increases glial cell line-derived neurotrophic factor in experimental stroke', *Exp Neurol*, vol. 247, pp. 202-8.
- Lai, AY, Dibal, CD, Armitage, GA, Winship, IR & Todd, KG 2013, 'Distinct activation profiles in microglia of different ages: a systematic study in isolated embryonic to aged microglial cultures', *Neuroscience*, vol. 254, pp. 185-95.
- Lai, AY & Todd, KG 2008, 'Differential regulation of trophic and proinflammatory microglial effectors is dependent on severity of neuronal injury', *Glia*, vol. 56, no. 3, pp. 259-70.
- Lalancette-Hebert, M, Gowing, G, Simard, A, Weng, YC & Kriz, J 2007, 'Selective ablation of proliferating microglial cells exacerbates ischemic injury in the brain', *J Neurosci*, vol. 27, no. 10, pp. 2596-605.
- Lambertsen, KL, Biber, K & Finsen, B 2012, 'Inflammatory cytokines in experimental and human stroke', *J Cereb Blood Flow Metab*, vol. 32, no. 9, pp. 1677-98.
- Lambertsen, KL, Clausen, BH, Babcock, AA, Gregersen, R, Fenger, C, Nielsen, HH, Haugaard, LS, Wirenfeldt, M, Nielsen, M, Dagnaes-Hansen, F, Bluethmann, H, Faergeman, NJ, Meldgaard, M, Deierborg, T & Finsen, B 2009, 'Microglia protect neurons against ischemia by synthesis of tumor necrosis factor', *J Neurosci*, vol. 29, no. 5, pp. 1319-30.
- Lambertsen, KL, Meldgaard, M, Ladeby, R & Finsen, B 2005, 'A quantitative study of microglial-macrophage synthesis of tumor necrosis factor during acute and late focal cerebral ischemia in mice', *J Cereb Blood Flow Metab*, vol. 25, no. 1, pp. 119-35.
- Langan, TJ & Slater, MC 1991, 'Quiescent astroglia in long-term primary cultures re-enter the cell cycle and require a non-sterol isoprenoid in late G1', *Brain Res*, vol. 548, no. 1-2, pp. 9-17.
- Lange, PS, Langley, B, Lu, P & Ratan, RR 2004, 'Novel roles for arginase in cell survival, regeneration, and translation in the central nervous system', *J Nutr*, vol. 134, no. 10 Suppl, pp. 2812S-7S; discussion 8S-9S.
- Lee, DR, Helps, SC, Gibbins, IL, Nilsson, M & Sims, NR 2003, 'Losses of NG2 and NeuN immunoreactivity but not astrocytic markers during early reperfusion following severe focal cerebral ischemia', *Brain Res*, vol. 989, no. 2, pp. 221-30.

Lehrmann, E, Kiefer, R, Christensen, T, Toyka, KV, Zimmer, J, Diemer, NH, Hartung, HP & Finsen, B 1998, 'Microglia and macrophages are major sources of locally produced transforming growth factor-beta1 after transient middle cerebral artery occlusion in rats', *Glia*, vol. 24, no. 4, pp. 437-48.

Leong, WK, Henshall, TL, Arthur, A, Kremer, KL, Lewis, MD, Helps, SC, Field, J, Hamilton-Bruce, MA, Warming, S, Manavis, J, Vink, R, Gronthos, S & Koblar, SA 2012, 'Human adult dental pulp stem cells enhance poststroke functional recovery through non-neural replacement mechanisms', *Stem Cells Transl Med*, vol. 1, no. 3, pp. 177-87.

Levine, SR & Brott, TG 1992, 'Thrombolytic therapy in cerebrovascular disorders', *Prog Cardiovasc Dis*, vol. 34, no. 4, pp. 235-62.

Levy, AD, Omar, MH & Koleske, AJ 2014, 'Extracellular matrix control of dendritic spine and synapse structure and plasticity in adulthood', *Front Neuroanat*, vol. 8, p. 116.

Li, H, Zhang, N, Lin, HY, Yu, Y, Cai, QY, Ma, L & Ding, S 2014, 'Histological, cellular and behavioral assessments of stroke outcomes after photothrombosis-induced ischemia in adult mice', *BMC Neurosci*, vol. 15, p. 58.

Li, L, Lundkvist, A, Andersson, D, Wilhelmsson, U, Nagai, N, Pardo, AC, Nodin, C, Stahlberg, A, Aprico, K, Larsson, K, Yabe, T, Moons, L, Fotheringham, A, Davies, I, Carmeliet, P, Schwartz, JP, Pekna, M, Kubista, M, Blomstrand, F, Maragakis, N, Nilsson, M & Pekny, M 2008, 'Protective role of reactive astrocytes in brain ischemia', *J Cereb Blood Flow Metab*, vol. 28, no. 3, pp. 468-81.

Li, Q, Zhang, R, Guo, YL & Mei, YW 2009, 'Effect of neuregulin on apoptosis and expressions of STAT3 and GFAP in rats following cerebral ischemic reperfusion', *J Mol Neurosci*, vol. 37, no. 1, pp. 67-73.

Li, S, Overman, JJ, Katsman, D, Kozlov, SV, Donnelly, CJ, Twiss, JL, Giger, RJ, Coppola, G, Geschwind, DH & Carmichael, ST 2010, 'An age-related sprouting transcriptome provides molecular control of axonal sprouting after stroke', *Nat Neurosci*, vol. 13, no. 12, pp. 1496-504.

Li, T, Pang, S, Yu, Y, Wu, X, Guo, J & Zhang, S 2013, 'Proliferation of parenchymal microglia is the main source of microgliosis after ischaemic stroke', *Brain*, vol. 136, no. Pt 12, pp. 3578-88.

Li, Y, Chen, J, Zhang, CL, Wang, L, Lu, D, Katakowski, M, Gao, Q, Shen, LH, Zhang, J, Lu, M & Chopp, M 2005, 'Gliosis and brain remodeling after treatment of stroke in rats with marrow stromal cells', *Glia*, vol. 49, no. 3, pp. 407-17.

Li, Y & Chopp, M 1999, 'Temporal profile of nestin expression after focal cerebral ischemia in adult rat', *Brain Res*, vol. 838, no. 1-2, pp. 1-10.

Li, Y, Chopp, M, Zhang, ZG & Zhang, RL 1995, 'Expression of glial fibrillary acidic protein in areas of focal cerebral ischemia accompanies neuronal expression of 72-kDa heat shock protein', *J Neurol Sci*, vol. 128, no. 2, pp. 134-42.

Li, Y, Jiang, N, Powers, C & Chopp, M 1998, 'Neuronal damage and plasticity identified by microtubule-associated protein 2, growth-associated protein 43, and cyclin D1 immunoreactivity after focal cerebral ischemia in rats', *Stroke*, vol. 29, no. 9, pp. 1972-80; discussion 80-1.

Li, Y, Li, D, Ibrahim, A & Raisman, G 2012, 'Repair involves all three surfaces of the glial cell', *Prog Brain Res*, vol. 201, pp. 199-218.

Li, Y, Powers, C, Jiang, N & Chopp, M 1998, 'Intact, injured, necrotic and apoptotic cells after focal cerebral ischemia in the rat', *J Neurol Sci*, vol. 156, no. 2, pp. 119-32.

Liauw, J, Hoang, S, Choi, M, Eroglu, C, Choi, M, Sun, GH, Percy, M, Wildman-Tobriner, B, Bliss, T, Guzman, RG, Barres, BA & Steinberg, GK 2008, 'Thrombospondins 1 and 2 are necessary for synaptic plasticity and functional recovery after stroke', *J Cereb Blood Flow Metab*, vol. 28, no. 10, pp. 1722-32.

Liberto, CM, Albrecht, PJ, Herx, LM, Yong, VW & Levison, SW 2004, 'Pro-regenerative properties of cytokine-activated astrocytes', *J Neurochem*, vol. 89, no. 5, pp. 1092-100.

Liebigt, S, Schlegel, N, Oberland, J, Witte, OW, Redecker, C & Keiner, S 2012, 'Effects of rehabilitative training and anti-inflammatory treatment on functional recovery and cellular reorganization following stroke', *Exp Neurol*, vol. 233, no. 2, pp. 776-82.

Liguz-Lecznar, M & Kossut, M 2013, 'Influence of inflammation on poststroke plasticity', *Neural Plast*, vol. 2013, p. 258582.

Lin, TN, Wang, PY, Chi, SI & Kuo, JS 1998, 'Differential regulation of ciliary neurotrophic factor (CNTF) and CNTF receptor alpha (CNTFR alpha) expression following focal cerebral ischemia', *Brain Res Mol Brain Res*, vol. 55, no. 1, pp. 71-80.

Lippoldt, A, Moenning, U & Reichel, A 2005, 'Progress in the identification of stroke-related genes: emerging new possibilities to develop concepts in stroke therapy', *CNS Drugs*, vol. 19, no. 10, p. 821+.

Lipton, P 1999, 'Ischemic cell death in brain neurons', *Physiol Rev*, vol. 79, no. 4, pp. 1431-568.

Liu, F, Schafer, DP & McCullough, LD 2009, 'TTC, fluoro-Jade B and NeuN staining confirm evolving phases of infarction induced by middle cerebral artery occlusion', *J Neurosci Methods*, vol. 179, no. 1, pp. 1-8.

Liu, HM 1995, 'Correlation between proto-oncogene, fibroblast growth factor and adaptive response in brain infarct', *Prog Brain Res*, vol. 105, pp. 239-44.

Liu, W, Tang, Y & Feng, J 2011, 'Cross talk between activation of microglia and astrocytes in pathological conditions in the central nervous system', *Life Sci*, vol. 89, no. 5-6, pp. 141-6.

Liu, X, Su, H, Chu, TH, Guo, A & Wu, W 2013, 'Minocycline inhibited the pro-apoptotic effect of microglia on neural progenitor cells and protected their neuronal differentiation in vitro', *Neurosci Lett*, vol. 542, pp. 30-6.

Liu, Z & Chopp, M 2015, 'Astrocytes, therapeutic targets for neuroprotection and neurorestoration in ischemic stroke', *Prog Neurobiol*.

Liu, Z, Chopp, M, Ding, X, Cui, Y & Li, Y 2013, 'Axonal remodeling of the corticospinal tract in the spinal cord contributes to voluntary motor recovery after stroke in adult mice', *Stroke*, vol. 44, no. 7, pp. 1951-6.

Liu, Z, Fan, Y, Won, SJ, Neumann, M, Hu, D, Zhou, L, Weinstein, PR & Liu, J 2007, 'Chronic treatment with minocycline preserves adult new neurons and reduces functional impairment after focal cerebral ischemia', *Stroke*, vol. 38, no. 1, pp. 146-52.

Liu, Z, Li, Y, Cui, Y, Roberts, C, Lu, M, Wilhelmsson, U, Pekny, M & Chopp, M 2014, 'Beneficial effects of gfap/vimentin reactive astrocytes for axonal remodeling and motor behavioral recovery in mice after stroke', *Glia*, vol. 62, no. 12, pp. 2022-33.

Liu, Z, Li, Y, Zhang, ZG, Cui, X, Cui, Y, Lu, M, Savant-Bhonsale, S & Chopp, M 2010, 'Bone marrow stromal cells enhance inter- and intracortical axonal connections after ischemic stroke in adult rats', *J Cereb Blood Flow Metab*, vol. 30, no. 7, pp. 1288-95.

Liu, Z, Xin, H & Chopp, M 2014, 'Reactive astrocytes promote axonal remodeling and neurological recovery after stroke', *Neural Regen Res*, vol. 9, no. 21, pp. 1874-5.

Lloyd-Burton, SM, York, EM, Anwar, MA, Vincent, AJ & Roskams, AJ 2013, 'SPARC regulates microgliosis and functional recovery following cortical ischemia', *J Neurosci*, vol. 33, no. 10, pp. 4468-81.

Lopez-Valdes, HE, Clarkson, AN, Ao, Y, Charles, AC, Carmichael, ST, Sofroniew, MV & Brennan, KC 2014, 'Memantine enhances recovery from stroke', *Stroke*, vol. 45, no. 7, pp. 2093-100.

Lopez-Vales, R, Garcia-Alias, G, Fores, J, Udina, E, Gold, BG, Navarro, X & Verdu, E 2005, 'FK 506 reduces tissue damage and prevents functional deficit after spinal cord injury in the rat', *J Neurosci Res*, vol. 81, no. 6, pp. 827-36.

Lozano, R, Naghavi, M, Foreman, K, Lim, S, Shibuya, K, Aboyans, V, Abraham, J, Adair, T, Aggarwal, R, Ahn, SY, Alvarado, M, Anderson, HR, Anderson, LM, Andrews, KG, Atkinson, C, Baddour, LM, Barker-Collo, S, Bartels, DH, Bell, ML, Benjamin, EJ, Bennett, D, Bhalla, K, Bikbov, B, Bin Abdulhak, A, Birbeck, G, Blyth, F, Bolliger, I, Boufous, S, Bucello, C, Burch, M, Burney, P, Carapetis, J, Chen, H, Chou, D, Chugh, SS, Coffeng, LE, Colan, SD, Colquhoun, S, Colson, KE, Condon, J, Connor, MD, Cooper, LT, Corriere, M, Cortinovis, M, de Vaccaro, KC, Couser, W, Cowie, BC, Criqui, MH, Cross, M, Dabhadkar, KC, Dahodwala, N, De Leo, D, Degenhardt, L, Delossantos, A, Denenberg, J, Des Jarlais, DC, Dharmaratne, SD, Dorsey, ER, Driscoll, T, Duber, H, Ebel, B, Erwin, PJ, Espindola, P, Ezzati, M, Feigin, V, Flaxman, AD, Forouzanfar, MH, Fowkes, FG, Franklin, R, Fransen, M, Freeman, MK, Gabriel, SE, Gakidou, E, Gaspari, F, Gillum, RF, Gonzalez-Medina, D, Halasa, YA, Haring, D, Harrison, JE, Havmoeller, R, Hay, RJ, Hoen, B, Hotez, PJ, Hoy, D, Jacobsen, KH, James, SL, Jasrasaria, R, Jayaraman, S, Johns, N, Karthikeyan, G, Kassebaum, N, Keren, A, Khoo, JP, Knowlton, LM, Kobusingye, O, Koranteng, A, Krishnamurthi, R, Lipnick, M, Lipshultz, SE, Ohno, SL, Mabweijano, J, MacIntyre, MF, Mallinger, L, March, L, Marks, GB, Marks, R, Matsumori, A, Matzopoulos, R, Mayosi, BM, McAnulty, JH, McDermott, MM, McGrath, J, Mensah, GA, Merriman, TR, Michaud, C, Miller, M, Miller, TR, Mock, C, Mocumbi, AO, Mokdad, AA, Moran, A, Mulholland, K, Nair, MN, Naldi, L, Narayan, KM, Nasser, K, Norman, P, O'Donnell, M, Omer, SB, Ortblad, K, Osborne, R, Ozgediz, D, Pahari, B, Pandian, JD, Rivero, AP, Padilla, RP, Perez-Ruiz, F, Perico, N, Phillips, D, Pierce, K, Pope, CA, 3rd, Porrini, E, Pourmalek, F, Raju, M, Ranganathan, D, Rehm, JT, Rein, DB, Remuzzi, G, Rivara, FP, Roberts, T, De Leon, FR, Rosenfeld, LC, Rushton, L, Sacco, RL, Salomon, JA, Sampson, U, Sanman, E, Schwebel, DC, Segui-Gomez, M, Shepard, DS, Singh, D, Singleton, J, Sliwa, K, Smith, E, Steer, A, Taylor, JA, Thomas, B, Tleyjeh, IM, Towbin, JA, Truelsen, T, Undurraga, EA, Venketasubramanian, N, Vijayakumar, L, Vos, T, Wagner, GR, Wang, M, Wang, W, Watt, K, Weinstock, MA, Weintraub, R, Wilkinson, JD, Woolf, AD, Wulf, S, Yeh, PH, Yip, P, Zabetian, A, Zheng, ZJ, Lopez, AD, Murray, CJ, AlMazroa, MA & Memish, ZA 2012, 'Global and regional mortality from 235 causes of death for 20 age groups in 1990 and 2010: a systematic analysis for the Global Burden of Disease Study 2010', *Lancet*, vol. 380, no. 9859, pp. 2095-128.

Macrae, IM 2011, 'Preclinical stroke research--advantages and disadvantages of the most common rodent models of focal ischaemia', *Br J Pharmacol*, vol. 164, no. 4, pp. 1062-78.

Madinier, A, Bertrand, N, Mossiat, C, Prigent-Tessier, A, Beley, A, Marie, C & Garnier, P 2009, 'Microglial involvement in neuroplastic changes following focal brain ischemia in rats', *PLoS One*, vol. 4, no. 12, p. e8101.

Madinier, A, Bertrand, N, Rodier, M, Quirie, A, Mossiat, C, Prigent-Tessier, A, Marie, C & Garnier, P 2013, 'Ipsilateral versus contralateral spontaneous post-stroke neuroplastic changes: involvement of BDNF?', *Neuroscience*, vol. 231, pp. 169-81.

Madinier, A, Quattromani, MJ, Sjolund, C, Ruscher, K & Wieloch, T 2014, 'Enriched housing enhances recovery of limb placement ability and reduces aggrecan-containing perineuronal nets in the rat somatosensory cortex after experimental stroke', *PLoS One*, vol. 9, no. 3, p. e93121.

Mandell, JW, Gocan, NC & Vandenberg, SR 2001, 'Mechanical trauma induces rapid astroglial activation of ERK/MAP kinase: Evidence for a paracrine signal', *Glia*, vol. 34, no. 4, pp. 283-95.

Mantovani, A, Biswas, SK, Galdiero, MR, Sica, A & Locati, M 2013, 'Macrophage plasticity and polarization in tissue repair and remodelling', *J Pathol*, vol. 229, no. 2, pp. 176-85.

Margaritescu, O, Pirici, D & Margaritescu, C 2011, 'VEGF expression in human brain tissue after acute ischemic stroke', *Rom J Morphol Embryol*, vol. 52, no. 4, pp. 1283-92.

Marlier, Q, Verteneuil, S, Vandebosch, R & Malgrange, B 2015, 'Mechanisms and Functional Significance of Stroke-Induced Neurogenesis', *Front Neurosci*, vol. 9, p. 458.

Matsumoto, H, Kumon, Y, Watanabe, H, Ohnishi, T, Shudou, M, Ii, C, Takahashi, H, Imai, Y & Tanaka, J 2007, 'Antibodies to CD11b, CD68, and lectin label neutrophils rather than microglia in traumatic and ischemic brain lesions', *J Neurosci Res*, vol. 85, no. 5, pp. 994-1009.

McCarthy, KD & de Vellis, J 1980, 'Preparation of separate astroglial and oligodendroglial cell cultures from rat cerebral tissue', *J Cell Biol*, vol. 85, no. 3, pp. 890-902.

McKeon, RJ, Juryneec, MJ & Buck, CR 1999, 'The chondroitin sulfate proteoglycans neurocan and phosphacan are expressed by reactive astrocytes in the chronic CNS glial scar', *J Neurosci*, vol. 19, no. 24, pp. 10778-88.

McMillian, MK, Thai, L, Hong, JS, O'Callaghan, JP & Pennypacker, KR 1994, 'Brain injury in a dish: a model for reactive gliosis', *Trends Neurosci*, vol. 17, no. 4, pp. 138-42.

Melani, A, Turchi, D, Vannucchi, MG, Cipriani, S, Gianfriddo, M & Pedata, F 2005, 'ATP extracellular concentrations are increased in the rat striatum during in vivo ischemia', *Neurochem Int*, vol. 47, no. 6, pp. 442-8.

Minnerup, J, Sutherland, BA, Buchan, AM & Kleinschnitz, C 2012, 'Neuroprotection for stroke: current status and future perspectives', *Int J Mol Sci*, vol. 13, no. 9, pp. 11753-72.

Minnerup, J, Wersching, H, Schilling, M & Schabitz, WR 2014, 'Analysis of early phase and subsequent phase III stroke studies of neuroprotectants: outcomes and predictors for success', *Exp Transl Stroke Med*, vol. 6, no. 1, p. 2.

Montero, M, Gonzalez, B & Zimmer, J 2009, 'Immunotoxic depletion of microglia in mouse hippocampal slice cultures enhances ischemia-like neurodegeneration', *Brain Res*, vol. 1291, pp. 140-52.

Morancho, A, Rosell, A, Garcia-Bonilla, L & Montaner, J 2010, 'Metalloproteinase and stroke infarct size: role for anti-inflammatory treatment?', *Ann N Y Acad Sci*, vol. 1207, pp. 123-33.

Moretti, A, Ferrari, F & Villa, RF 2015, 'Neuroprotection for ischaemic stroke: current status and challenges', *Pharmacol Ther*, vol. 146, pp. 23-34.

Morgenstern, DA, Asher, RA & Fawcett, JW 2002, 'Chondroitin sulphate proteoglycans in the CNS injury response', *Prog Brain Res*, vol. 137, pp. 313-32.

Morris, DC, Chopp, M, Zhang, L, Lu, M & Zhang, ZG 2010, 'Thymosin beta4 improves functional neurological outcome in a rat model of embolic stroke', *Neuroscience*, vol. 169, no. 2, pp. 674-82.

Morrison, HW & Filosa, JA 2013, 'A quantitative spatiotemporal analysis of microglia morphology during ischemic stroke and reperfusion', *J Neuroinflammation*, vol. 10, p. 4.

Mosser, DM & Edwards, JP 2008, 'Exploring the full spectrum of macrophage activation', *Nat Rev Immunol*, vol. 8, no. 12, pp. 958-69.

Munch, G, Gasic-Milenkovic, J, Dukic-Stefanovic, S, Kuhla, B, Heinrich, K, Riederer, P, Huttunen, HJ, Founds, H & Sajithlal, G 2003, 'Microglial activation induces cell death, inhibits neurite outgrowth and causes neurite retraction of differentiated neuroblastoma cells', *Exp Brain Res*, vol. 150, no. 1, pp. 1-8.

Murphy, EJ & Horrocks, LA 1993, 'Mechanisms of hypoxic and ischemic injury. Use of cell culture models', *Mol Chem Neuropathol*, vol. 19, no. 1-2, pp. 95-106.

Murphy, TH & Corbett, D 2009, 'Plasticity during stroke recovery: from synapse to behaviour', *Nat Rev Neurosci*, vol. 10, no. 12, pp. 861-72.

Murray, CJ, Vos, T, Lozano, R, Naghavi, M, Flaxman, AD, Michaud, C, Ezzati, M, Shibuya, K, Salomon, JA, Abdalla, S, Aboyans, V, Abraham, J, Ackerman, I, Aggarwal, R, Ahn, SY, Ali, MK, Alvarado, M, Anderson, HR, Anderson, LM, Andrews, KG, Atkinson, C, Baddour, LM, Bahalim, AN, Barker-Collo, S, Barrero, LH, Bartels, DH, Basanez, MG, Baxter, A, Bell, ML, Benjamin, EJ, Bennett, D, Bernabe, E, Bhalla, K, Bhandari, B, Bikbov, B, Bin Abdulhak, A, Birbeck, G, Black, JA, Blencowe, H, Blore, JD, Blyth, F, Bolliger, I, Bonaventure, A, Boufous, S, Bourne, R, Boussinesq, M, Braithwaite, T, Brayne, C, Bridgett, L, Brooker, S, Brooks, P, Brugha, TS, Bryan-Hancock, C, Bucello, C, Buchbinder, R, Buckle, G, Budke, CM, Burch, M, Burney, P, Burstein, R, Calabria, B, Campbell, B, Canter, CE, Carabin, H, Carapetis, J, Carmona, L, Cella, C, Charlson, F, Chen, H, Cheng, AT, Chou, D, Chugh, SS, Coffeng, LE, Colan, SD, Colquhoun, S, Colson, KE, Condon, J, Connor, MD, Cooper, LT, Corriere, M, Cortinovis, M, de Vaccaro, KC, Couser, W, Cowie, BC, Criqui, MH, Cross, M, Dabhadkar, KC, Dahiya, M, Dahodwala, N, Damsere-Derry, J, Danaei, G, Davis, A, De Leo, D, Degenhardt, L, Dellavalle, R, Delossantos, A, Denenberg, J, Derrett, S, Des Jarlais, DC, Dharmaratne, SD, Dherani, M, Diaz-Torne, C, Dolk, H, Dorsey, ER, Driscoll, T, Duber, H, Ebel, B, Edmond, K, Elbaz, A,

Ali, SE, Erskine, H, Erwin, PJ, Espindola, P, Ewoigbokhan, SE, Farzadfar, F, Feigin, V, Felson, DT, Ferrari, A, Ferri, CP, Fevre, EM, Finucane, MM, Flaxman, S, Flood, L, Foreman, K, Forouzanfar, MH, Fowkes, FG, Fransen, M, Freeman, MK, Gabbe, BJ, Gabriel, SE, Gakidou, E, Ganatra, HA, Garcia, B, Gaspari, F, Gillum, RF, Gmel, G, Gonzalez-Medina, D, Gosselin, R, Grainger, R, Grant, B, Groeger, J, Guillemin, F, Gunnell, D, Gupta, R, Haagsma, J, Hagan, H, Halasa, YA, Hall, W, Haring, D, Haro, JM, Harrison, JE, Havmoeller, R, Hay, RJ, Higashi, H, Hill, C, Hoen, B, Hoffman, H, Hotez, PJ, Hoy, D, Huang, JJ, Ibeanusi, SE, Jacobsen, KH, James, SL, Jarvis, D, Jirasaria, R, Jayaraman, S, Johns, N, Jonas, JB, Karthikeyan, G, Kassebaum, N, Kawakami, N, Keren, A, Khoo, JP, King, CH, Knowlton, LM, Kobusingye, O, Koranteng, A, Krishnamurthi, R, Laden, F, Lalloo, R, Laslett, LL, Lathlean, T, Leasher, JL, Lee, YY, Leigh, J, Levinson, D, Lim, SS, Limb, E, Lin, JK, Lipnick, M, Lipshultz, SE, Liu, W, Loane, M, Ohno, SL, Lyons, R, Mabweijano, J, MacIntyre, MF, Malekzadeh, R, Mallinger, L, Manivannan, S, Marcenes, W, March, L, Margolis, DJ, Marks, GB, Marks, R, Matsumori, A, Matzopoulos, R, Mayosi, BM, McAnulty, JH, McDermott, MM, McGill, N, McGrath, J, Medina-Mora, ME, Meltzer, M, Mensah, GA, Merriman, TR, Meyer, AC, Miglioli, V, Miller, M, Miller, TR, Mitchell, PB, Mock, C, Mocumbi, AO, Moffitt, TE, Mokdad, AA, Monasta, L, Montico, M, Moradi-Lakeh, M, Moran, A, Morawska, L, Mori, R, Murdoch, ME, Mwaniki, MK, Naidoo, K, Nair, MN, Naldi, L, Narayan, KM, Nelson, PK, Nelson, RG, Nevitt, MC, Newton, CR, Nolte, S, Norman, P, Norman, R, O'Donnell, M, O'Hanlon, S, Olives, C, Omer, SB, Ortblad, K, Osborne, R, Ozgediz, D, Page, A, Pahari, B, Pandian, JD, Rivero, AP, Patten, SB, Pearce, N, Padilla, RP, Perez-Ruiz, F, Perico, N, Pesudovs, K, Phillips, D, Phillips, MR, Pierce, K, Pion, S, Polanczyk, GV, Polinder, S, Pope, CA, 3rd, Popova, S, Porrini, E, Pourmalek, F, Prince, M, Pullan, RL, Ramaiah, KD, Ranganathan, D, Razavi, H, Regan, M, Rehm, JT, Rein, DB, Remuzzi, G, Richardson, K, Rivara, FP, Roberts, T, Robinson, C, De Leon, FR, Ronfani, L, Room, R, Rosenfeld, LC, Rushton, L, Sacco, RL, Saha, S, Sampson, U, Sanchez-Riera, L, Sanman, E, Schwebel, DC, Scott, JG, Segui-Gomez, M, Shahraz, S, Shepard, DS, Shin, H, Shivakoti, R, Singh, D, Singh, GM, Singh, JA, Singleton, J, Sleet, DA, Sliwa, K, Smith, E, Smith, JL, Stapelberg, NJ, Steer, A, Steiner, T, Stolk, WA, Stovner, LJ, Sudfeld, C, Syed, S, Tamburlini, G, Tavakkoli, M, Taylor, HR, Taylor, JA, Taylor, WJ, Thomas, B, Thomson, WM, Thurston, GD, Tleyjeh, IM, Tonelli, M, Towbin, JA, Truelsen, T, Tsilimbaris, MK, Ubeda, C, Undurraga, EA, van der Werf, MJ, van Os, J, Vavilala, MS, Venketasubramanian, N, Wang, M, Wang, W, Watt, K, Weatherall, DJ, Weinstock, MA, Weintraub, R, Weisskopf, MG, Weissman, MM, White, RA, Whiteford, H, Wiebe, N, Wiersma, ST, Wilkinson, JD, Williams, HC, Williams, SR, Witt, E, Wolfe, F, Woolf, AD, Wulf, S, Yeh, PH, Zaidi, AK, Zheng, ZJ, Zonies, D, Lopez, AD, AlMazroa, MA & Memish, ZA 2012, 'Disability-adjusted life years (DALYs) for 291 diseases and injuries in 21 regions, 1990-2010: a systematic analysis for the Global Burden of Disease Study 2010', *Lancet*, vol. 380, no. 9859, pp. 2197-223.

Muyderman, H, Nilsson, M & Sims, NR 2004, 'Highly selective and prolonged depletion of mitochondrial glutathione in astrocytes markedly increases sensitivity to peroxynitrite', *J Neurosci*, vol. 24, no. 37, pp. 8019-28.

Muyderman, H, Wadey, AL, Nilsson, M & Sims, NR 2007, 'Mitochondrial glutathione protects against cell death induced by oxidative and nitrative stress in astrocytes', *J Neurochem*, vol. 102, no. 4, pp. 1369-82.

Muyderman, H, Yew, WP, Homkajorn, B & Sims, NR 2010, 'Astrocytic responses to DNA delivery using nucleofection', *Neurochem Res*, vol. 35, no. 11, pp. 1771-9.

- Napoli, I & Neumann, H 2009, 'Microglial clearance function in health and disease', *Neuroscience*, vol. 158, no. 3, pp. 1030-8.
- Neumann, J, Gunzer, M, Gutzeit, HO, Ullrich, O, Reymann, KG & Dinkel, K 2006, 'Microglia provide neuroprotection after ischemia', *FASEB J*, vol. 20, no. 6, pp. 714-6.
- Neumann, J, Sauerzweig, S, Ronicke, R, Gunzer, F, Dinkel, K, Ullrich, O, Gunzer, M & Reymann, KG 2008, 'Microglia cells protect neurons by direct engulfment of invading neutrophil granulocytes: a new mechanism of CNS immune privilege', *J Neurosci*, vol. 28, no. 23, pp. 5965-75.
- Newman, EA 2003, 'New roles for astrocytes: regulation of synaptic transmission', *Trends Neurosci*, vol. 26, no. 10, pp. 536-42.
- Ng, SY, Semple, BD, Morganti-Kossmann, MC & Bye, N 2012, 'Attenuation of microglial activation with minocycline is not associated with changes in neurogenesis after focal traumatic brain injury in adult mice', *J Neurotrauma*, vol. 29, no. 7, pp. 1410-25.
- Nikodemova, M, Duncan, ID & Watters, JJ 2006, 'Minocycline exerts inhibitory effects on multiple mitogen-activated protein kinases and IkappaBalpha degradation in a stimulus-specific manner in microglia', *J Neurochem*, vol. 96, no. 2, pp. 314-23.
- Nimmerjahn, A, Kirchhoff, F & Helmchen, F 2005, 'Resting Microglial Cells Are Highly Dynamic Surveillants of Brain Parenchyma in Vivo', *Science*, vol. 308, no. 5726, pp. 1314-8.
- Noraberg, J, Poulsen, FR, Blaabjerg, M, Kristensen, BW, Bonde, C, Montero, M, Meyer, M, Gramsbergen, JB & Zimmer, J 2005, 'Organotypic hippocampal slice cultures for studies of brain damage, neuroprotection and neurorepair', *Curr Drug Targets CNS Neurol Disord*, vol. 4, no. 4, pp. 435-52.
- Nowicka, D, Rogozinska, K, Aleksy, M, Witte, OW & Skangiel-Kramaska, J 2008, 'Spatiotemporal dynamics of astroglial and microglial responses after photothrombotic stroke in the rat brain', *Acta Neurobiol Exp (Wars)*, vol. 68, no. 2, pp. 155-68.
- Nudo, RJ 2007, 'Postinfarct cortical plasticity and behavioral recovery', *Stroke*, vol. 38, no. 2 Suppl, pp. 840-5.
- O'Hare, M, Wang, F & Park, DS 2002, 'Cyclin-dependent kinases as potential targets to improve stroke outcome', *Pharmacol Ther*, vol. 93, no. 2-3, pp. 135-43.
- Ohtaki, H, Ylostalo, JH, Foraker, JE, Robinson, AP, Reger, RL, Shioda, S & Prockop, DJ 2008, 'Stem/progenitor cells from bone marrow decrease neuronal death in global ischemia by modulation of inflammatory/immune responses', *Proc Natl Acad Sci U S A*, vol. 105, no. 38, pp. 14638-43.

Olsen, TS, Skriver, EB & Herning, M 1985, 'Cause of cerebral infarction in the carotid territory. Its relation to the size and the location of the infarct and to the underlying vascular lesion', *Stroke*, vol. 16, no. 3, pp. 459-66.

Oshima, T, Lee, S, Sato, A, Oda, S, Hirasawa, H & Yamashita, T 2009, 'TNF-alpha contributes to axonal sprouting and functional recovery following traumatic brain injury', *Brain Res*, vol. 1290, pp. 102-10.

Osuga, H, Osuga, S, Wang, F, Fetni, R, Hogan, MJ, Slack, RS, Hakim, AM, Ikeda, JE & Park, DS 2000, 'Cyclin-dependent kinases as a therapeutic target for stroke', *Proc Natl Acad Sci U S A*, vol. 97, no. 18, pp. 10254-9.

Pal, G, Vincze, C, Renner, E, Wappler, EA, Nagy, Z, Lovas, G & Dobolyi, A 2012, 'Time course, distribution and cell types of induction of transforming growth factor betas following middle cerebral artery occlusion in the rat brain', *PLoS One*, vol. 7, no. 10, p. e46731.

Palaniswami, M & Yan, B 2015, 'Mechanical Thrombectomy Is Now the Gold Standard for Acute Ischemic Stroke: Implications for Routine Clinical Practice', *Interv Neurol*, vol. 4, no. 1-2, pp. 18-29.

Patel, AR, Ritzel, R, McCullough, LD & Liu, F 2013, 'Microglia and ischemic stroke: a double-edged sword', *Int J Physiol Pathophysiol Pharmacol*, vol. 5, no. 2, pp. 73-90.

Pekny, M, Johansson, CB, Eliasson, C, Stakeberg, J, Wallen, A, Perlmann, T, Lendahl, U, Betsholtz, C, Berthold, CH & Frisen, J 1999, 'Abnormal reaction to central nervous system injury in mice lacking glial fibrillary acidic protein and vimentin', *J Cell Biol*, vol. 145, no. 3, pp. 503-14.

Pekny, M & Pekna, M 2014, 'Astrocyte reactivity and reactive astrogliosis: costs and benefits', *Physiol Rev*, vol. 94, no. 4, pp. 1077-98.

Perego, C, Fumagalli, S & De Simoni, MG 2011, 'Temporal pattern of expression and colocalization of microglia/macrophage phenotype markers following brain ischemic injury in mice', *J Neuroinflammation*, vol. 8, p. 174.

Peruzzotti-Jametti, L, Donega, M, Giusto, E, Mallucci, G, Marchetti, B & Pluchino, S 2014, 'The role of the immune system in central nervous system plasticity after acute injury', *Neuroscience*, vol. 283, pp. 210-21.

Petito, CK, Juurlink, BH & Hertz, L 1991, 'In vitro models differentiating between direct and indirect effects of ischemia on astrocytes', *Exp Neurol*, vol. 113, no. 3, pp. 364-72.

Petito, CK, Morgello, S, Felix, JC & Lesser, ML 1990, 'The two patterns of reactive astrocytosis in postischemic rat brain', *J Cereb Blood Flow Metab*, vol. 10, no. 6, pp. 850-9.

Phillips, LL, Chan, JL, Doperalski, AE & Reeves, TM 2014, 'Time dependent integration of matrix metalloproteinases and their targeted substrates directs axonal sprouting and synaptogenesis following central nervous system injury', *Neural Regen Res*, vol. 9, no. 4, pp. 362-76.

Planas, AM, Gorina, R & Chamorro, A 2006, 'Signalling pathways mediating inflammatory responses in brain ischaemia', *Biochem Soc Trans*, vol. 34, no. Pt 6, pp. 1267-70.

Przybylowski, CJ, Ding, D, Starke, RM, Durst, CR, Crowley, RW & Liu, KC 2014, 'Evolution of endovascular mechanical thrombectomy for acute ischemic stroke', *World J Clin Cases*, vol. 2, no. 11, pp. 614-22.

Quirie, A, Demougeot, C, Bertrand, N, Mossiat, C, Garnier, P, Marie, C & Prigent-Tessier, A 2013, 'Effect of stroke on arginase expression and localization in the rat brain', *Eur J Neurosci*, vol. 37, no. 7, pp. 1193-202.

Ramos-Cabrer, P, Justicia, C, Wiedermann, D & Hoehn, M 2010, 'Stem cell mediation of functional recovery after stroke in the rat', *PLoS One*, vol. 5, no. 9, p. e12779.

Reitmeir, R, Kilic, E, Reinboth, BS, Guo, Z, ElAli, A, Zechariah, A, Kilic, U & Hermann, DM 2012, 'Vascular endothelial growth factor induces contralesional corticobulbar plasticity and functional neurological recovery in the ischemic brain', *Acta Neuropathol*, vol. 123, no. 2, pp. 273-84.

Richard, MJ, Saleh, TM, El Bahh, B & Zidichouski, JA 2010, 'A novel method for inducing focal ischemia in vitro', *J Neurosci Methods*, vol. 190, no. 1, pp. 20-7.

Ridet, JL, Malhotra, SK, Privat, A & Gage, FH 1997, 'Reactive astrocytes: cellular and molecular cues to biological function', *Trends Neurosci*, vol. 20, no. 12, pp. 570-7.

Riecker, A, Groschel, K, Ackermann, H, Schnaudigel, S, Kassubek, J & Kastrup, A 2010, 'The role of the unaffected hemisphere in motor recovery after stroke', *Hum Brain Mapp*, vol. 31, no. 7, pp. 1017-29.

Roitberg, B 2004, 'Transplantation for stroke', *Neurol Res*, vol. 26, no. 3, pp. 256-64.

Rosell, A & Lo, EH 2008, 'Multiphasic roles for matrix metalloproteinases after stroke', *Curr Opin Pharmacol*, vol. 8, no. 1, pp. 82-9.

Roy, A, Fung, YK, Liu, X & Pahan, K 2006, 'Up-regulation of microglial CD11b expression by nitric oxide', *J Biol Chem*, vol. 281, no. 21, pp. 14971-80.

Rupalla, K, Allegrini, PR, Sauer, D & Wiessner, C 1998, 'Time course of microglia activation and apoptosis in various brain regions after permanent focal cerebral ischemia in mice', *Acta Neuropathol*, vol. 96, no. 2, pp. 172-8.

Sandvig, A, Berry, M, Barrett, LB, Butt, A & Logan, A 2004, 'Myelin-, reactive glia-, and scar-derived CNS axon growth inhibitors: expression, receptor signaling, and correlation with axon regeneration', *Glia*, vol. 46, no. 3, pp. 225-51.

Satoh, J, Kino, Y, Asahina, N, Takitani, M, Miyoshi, J, Ishida, T & Saito, Y 2016, 'TMEM119 marks a subset of microglia in the human brain', *Neuropathology*, vol. 36, no. 1, pp. 39-49.

Savage, CD, Lopez-Castejon, G, Denes, A & Brough, D 2012, 'NLRP3-inflammasome activating DAMPs stimulate an inflammatory response in glia in the absence of priming which contributes to brain inflammation after injury', *Frontiers in Immunology*, vol. 3.

Schabitz, WR, Berger, C, Kollmar, R, Seitz, M, Tanay, E, Kiessling, M, Schwab, S & Sommer, C 2004, 'Effect of brain-derived neurotrophic factor treatment and forced arm use on functional motor recovery after small cortical ischemia', *Stroke*, vol. 35, no. 4, pp. 992-7.

Schallert, T, Fleming, SM, Leasure, JL, Tillerson, JL & Bland, ST 2000, 'CNS plasticity and assessment of forelimb sensorimotor outcome in unilateral rat models of stroke, cortical ablation, parkinsonism and spinal cord injury', *Neuropharmacology*, vol. 39, no. 5, pp. 777-87.

Schallert, T & Woodlee, MT 2005, 'Orienting and Placing', in IQ Whishaw & B Kolb (eds), *The Behavior of the Laboratory Rat*, Oxford University Press, Oxford ; New York, pp. 129 - 40.

Schilling, M, Besselmann, M, Leonhard, C, Mueller, M, Ringelstein, EB & Kiefer, R 2003, 'Microglial activation precedes and predominates over macrophage infiltration in transient focal cerebral ischemia: a study in green fluorescent protein transgenic bone marrow chimeric mice', *Exp Neurol*, vol. 183, no. 1, pp. 25-33.

Schilling, M, Besselmann, M, Muller, M, Strecker, JK, Ringelstein, EB & Kiefer, R 2005, 'Predominant phagocytic activity of resident microglia over hematogenous macrophages following transient focal cerebral ischemia: an investigation using green fluorescent protein transgenic bone marrow chimeric mice', *Exp Neurol*, vol. 196, no. 2, pp. 290-7.

Schilling, T, Nitsch, R, Heinemann, U, Haas, D & Eder, C 2001, 'Astrocyte-released cytokines induce ramification and outward K⁺ channel expression in microglia via distinct signalling pathways', *Eur J Neurosci*, vol. 14, no. 3, pp. 463-73.

Schmitz, T, Krabbe, G, Weikert, G, Scheuer, T, Matheus, F, Wang, Y, Mueller, S, Kettenmann, H, Matyash, V, Buhner, C & Endesfelder, S 2014, 'Minocycline protects the immature white matter against hyperoxia', *Exp Neurol*, vol. 254, pp. 153-65.

Schneider, CA, Rasband, WS & Eliceiri, KW 2012, 'NIH Image to ImageJ: 25 years of image analysis', *Nat Methods*, vol. 9, no. 7, pp. 671-5.

Schousboe, A, Fosmark, H & Formby, B 1976, 'Effect of serum withdrawal on Na⁺-K⁺ ATPase activity in astrocytes cultured from dissociated brain hemispheres', *J Neurochem*, vol. 26, no. 5, pp. 1052-5.

Schroeter, M, Jander, S, Huitinga, I, Witte, OW & Stoll, G 1997, 'Phagocytic response in photochemically induced infarction of rat cerebral cortex. The role of resident microglia', *Stroke*, vol. 28, no. 2, pp. 382-6.

Schroeter, M, Jander, S & Stoll, G 2002, 'Non-invasive induction of focal cerebral ischemia in mice by photothrombosis of cortical microvessels: characterization of inflammatory responses', *J Neurosci Methods*, vol. 117, no. 1, pp. 43-9.

Schroeter, M, Jander, S, Witte, OW & Stoll, G 1994, 'Local immune responses in the rat cerebral cortex after middle cerebral artery occlusion', *J Neuroimmunol*, vol. 55, no. 2, pp. 195-203.

Schroeter, M, Schiene, K, Kraemer, M, Hagemann, G, Weigel, H, Eysel, UT, Witte, OW & Stoll, G 1995, 'Astroglial responses in photochemically induced focal ischemia of the rat cortex', *Exp Brain Res*, vol. 106, no. 1, pp. 1-6.

Shanina, EV, Schallert, T, Witte, OW & Redecker, C 2006, 'Behavioral recovery from unilateral photothrombotic infarcts of the forelimb sensorimotor cortex in rats: role of the contralateral cortex', *Neuroscience*, vol. 139, no. 4, pp. 1495-506.

Sharma, K, Selzer, ME & Li, S 2012, 'Scar-mediated inhibition and CSPG receptors in the CNS', *Exp Neurol*, vol. 237, no. 2, pp. 370-8.

Shearer, MC & Fawcett, JW 2001, 'The astrocyte/meningeal cell interface--a barrier to successful nerve regeneration?', *Cell Tissue Res*, vol. 305, no. 2, pp. 267-73.

Shen, LH, Li, Y, Chen, J, Cui, Y, Zhang, C, Kapke, A, Lu, M, Savant-Bhonsale, S & Chopp, M 2007, 'One-year follow-up after bone marrow stromal cell treatment in middle-aged female rats with stroke', *Stroke*, vol. 38, no. 7, pp. 2150-6.

Shen, LH, Li, Y, Chen, J, Zacharek, A, Gao, Q, Kapke, A, Lu, M, Raginski, K, Vanguri, P, Smith, A & Chopp, M 2007, 'Therapeutic benefit of bone marrow stromal cells administered 1 month after stroke', *J Cereb Blood Flow Metab*, vol. 27, no. 1, pp. 6-13.

Shen, LH, Li, Y & Chopp, M 2010, 'Astrocytic endogenous glial cell derived neurotrophic factor production is enhanced by bone marrow stromal cell

- transplantation in the ischemic boundary zone after stroke in adult rats', *Glia*, vol. 58, no. 9, pp. 1074-81.
- Shen, LH, Li, Y, Gao, Q, Savant-Bhonsale, S & Chopp, M 2008, 'Down-regulation of neurocan expression in reactive astrocytes promotes axonal regeneration and facilitates the neurorestorative effects of bone marrow stromal cells in the ischemic rat brain', *Glia*, vol. 56, no. 16, pp. 1747-54.
- Shimada, IS, Borders, A, Aronshtam, A & Spees, JL 2011, 'Proliferating reactive astrocytes are regulated by Notch-1 in the peri-infarct area after stroke', *Stroke*, vol. 42, no. 11, pp. 3231-7.
- Shy, BD 2014, 'Implications of ECASS III error on emergency department treatment of ischemic stroke', *J Emerg Med*, vol. 46, no. 3, pp. 385-6.
- Siebert, JR, Conta Steencken, A & Osterhout, DJ 2014, 'Chondroitin sulfate proteoglycans in the nervous system: inhibitors to repair', *Biomed Res Int*, vol. 2014, p. 845323.
- Sievers, J, Parwaresch, R & Wottge, HU 1994, 'Blood monocytes and spleen macrophages differentiate into microglia-like cells on monolayers of astrocytes: morphology', *Glia*, vol. 12, no. 4, pp. 245-58.
- Sigler, A & Murphy, TH 2010, 'In vivo 2-photon imaging of fine structure in the rodent brain: before, during, and after stroke', *Stroke*, vol. 41, no. 10 Suppl, pp. S117-23.
- Silva Bastos, LF, Pinheiro de Oliveira, AC, Magnus Schlachetzki, JC & Fiebich, BL 2011, 'Minocycline reduces prostaglandin E synthase expression and 8-isoprostane formation in LPS-activated primary rat microglia', *Immunopharmacol Immunotoxicol*, vol. 33, no. 3, pp. 576-80.
- Silver, J & Miller, JH 2004, 'Regeneration beyond the glial scar', *Nat Rev Neurosci*, vol. 5, no. 2, pp. 146-56.
- Sist, B, Fouad, K & Winship, IR 2014, 'Plasticity beyond peri-infarct cortex: spinal up regulation of structural plasticity, neurotrophins, and inflammatory cytokines during recovery from cortical stroke', *Exp Neurol*, vol. 252, pp. 47-56.
- Skilbeck, CE, Wade, DT, Hewer, RL & Wood, VA 1983, 'Recovery after stroke', *J Neurol Neurosurg Psychiatry*, vol. 46, no. 1, pp. 5-8.
- Sofroniew, MV 2005, 'Reactive astrocytes in neural repair and protection', *Neuroscientist*, vol. 11, no. 5, pp. 400-7.
- 2009, 'Molecular dissection of reactive astrogliosis and glial scar formation', *Trends Neurosci*, vol. 32, no. 12, pp. 638-47.

— 2015, 'Astrocyte barriers to neurotoxic inflammation', *Nat Rev Neurosci*, vol. 16, no. 5, pp. 249-63.

Sofroniew, MV & Vinters, HV 2010, 'Astrocytes: biology and pathology', *Acta Neuropathol*, vol. 119, no. 1, pp. 7-35.

Soltys, Z, Orzyłowska-Sliwiska, O, Zaremba, M, Orlowski, D, Piechota, M, Fiedorowicz, A, Janeczko, K & Oderfeld-Nowak, B 2005, 'Quantitative morphological study of microglial cells in the ischemic rat brain using principal component analysis', *J Neurosci Methods*, vol. 146, no. 1, pp. 50-60.

Soltys, Z, Ziaja, M, Pawlinski, R, Setkowicz, Z & Janeczko, K 2001, 'Morphology of reactive microglia in the injured cerebral cortex. Fractal analysis and complementary quantitative methods', *J Neurosci Res*, vol. 63, no. 1, pp. 90-7.

Sood, RR, Taheri, S, Candelario-Jalil, E, Estrada, EY & Rosenberg, GA 2008, 'Early beneficial effect of matrix metalloproteinase inhibition on blood-brain barrier permeability as measured by magnetic resonance imaging countered by impaired long-term recovery after stroke in rat brain', *J Cereb Blood Flow Metab*, vol. 28, no. 2, pp. 431-8.

Starkey, ML, Bleul, C, Zorner, B, Lindau, NT, Mueggler, T, Rudin, M & Schwab, ME 2012, 'Back seat driving: hindlimb corticospinal neurons assume forelimb control following ischaemic stroke', *Brain*, vol. 135, no. Pt 11, pp. 3265-81.

Starkey, ML & Schwab, ME 2014, 'How Plastic Is the Brain after a Stroke?', *Neuroscientist*, vol. 20, no. 4, pp. 359-71.

Stoll, G, Jander, S & Schroeter, M 1998, 'Inflammation and glial responses in ischemic brain lesions', *Prog Neurobiol*, vol. 56, no. 2, pp. 149-71.

— 2002, 'Detrimental and beneficial effects of injury-induced inflammation and cytokine expression in the nervous system', *Adv Exp Med Biol*, vol. 513, pp. 87-113.

Streit, WJ 2000, 'Microglial response to brain injury: a brief synopsis', *Toxicol Pathol*, vol. 28, no. 1, pp. 28-30.

Stroemer, RP, Kent, TA & Hulsebosch, CE 1995, 'Neocortical neural sprouting, synaptogenesis, and behavioral recovery after neocortical infarction in rats', *Stroke*, vol. 26, no. 11, pp. 2135-44.

Suk, K 2004, 'Minocycline suppresses hypoxic activation of rodent microglia in culture', *Neurosci Lett*, vol. 366, no. 2, pp. 167-71.

Sun, D & Jakobs, TC 2012, 'Structural remodeling of astrocytes in the injured CNS', *Neuroscientist*, vol. 18, no. 6, pp. 567-88.

Sutherland, BA, Minnerup, J, Balami, JS, Arba, F, Buchan, AM & Kleinschnitz, C 2012, 'Neuroprotection for ischaemic stroke: translation from the bench to the bedside', *Int J Stroke*, vol. 7, no. 5, pp. 407-18.

Suzuki, S, Tanaka, K, Nogawa, S, Nagata, E, Ito, D, Dembo, T & Fukuuchi, Y 1999, 'Temporal profile and cellular localization of interleukin-6 protein after focal cerebral ischemia in rats', *J Cereb Blood Flow Metab*, vol. 19, no. 11, pp. 1256-62.

Suzuki, S, Tanaka, K & Suzuki, N 2009, 'Ambivalent aspects of interleukin-6 in cerebral ischemia: inflammatory versus neurotrophic aspects', *J Cereb Blood Flow Metab*, vol. 29, no. 3, pp. 464-79.

Swartz, KR, Liu, F, Sewell, D, Schochet, T, Campbell, I, Sandor, M & Fabry, Z 2001, 'Interleukin-6 promotes post-traumatic healing in the central nervous system', *Brain Res*, vol. 896, no. 1-2, pp. 86-95.

Szabo, M & Gulya, K 2013, 'Development of the microglial phenotype in culture', *Neuroscience*, vol. 241, pp. 280-95.

Szalay, G, Martinecz, B, Lenart, N, Kornyei, Z, Orsolits, B, Judak, L, Csaszar, E, Fekete, R, West, BL, Katona, G, Rozsa, B & Denes, A 2016, 'Microglia protect against brain injury and their selective elimination dysregulates neuronal network activity after stroke', *Nat Commun*, vol. 7, p. 11499.

Takatsuru, Y, Nabekura, J & Koibuchi, N 2014, 'Contribution of neuronal and glial circuit in intact hemisphere for functional remodeling after focal ischemia', *Neurosci Res*, vol. 78, pp. 38-44.

Tanaka, J & Maeda, N 1996, 'Microglial ramification requires nondiffusible factors derived from astrocytes', *Exp Neurol*, vol. 137, no. 2, pp. 367-75.

Tanaka, J, Toku, K, Matsuda, S, Sudo, S, Fujita, H, Sakanaka, M & Maeda, N 1998, 'Induction of resting microglia in culture medium devoid of glycine and serine', *Glia*, vol. 24, no. 2, pp. 198-215.

Tanaka, J, Toku, K, Sakanaka, M & Maeda, N 1999, 'Morphological differentiation of microglial cells in culture: involvement of insoluble factors derived from astrocytes', *Neurosci Res*, vol. 34, no. 4, pp. 207-15.

Tanaka, R, Komine-Kobayashi, M, Mochizuki, H, Yamada, M, Furuya, T, Migita, M, Shimada, T, Mizuno, Y & Urabe, T 2003, 'Migration of enhanced green fluorescent protein expressing bone marrow-derived microglia/macrophage into the mouse brain following permanent focal ischemia', *Neuroscience*, vol. 117, no. 3, pp. 531-9.

Taylor, RA & Sansing, LH 2013, 'Microglial responses after ischemic stroke and intracerebral hemorrhage', *Clin Dev Immunol*, vol. 2013, p. 746068.

Thiele, DL, Kurosaka, M & Lipsky, PE 1983, 'Phenotype of the accessory cell necessary for mitogen-stimulated T and B cell responses in human peripheral blood: delineation by its sensitivity to the lysosomotropic agent, L-leucine methyl ester', *J Immunol*, vol. 131, no. 5, pp. 2282-90.

Thored, P, Arvidsson, A, Cacci, E, Ahlenius, H, Kallur, T, Darsalia, V, Ekdahl, CT, Kokaia, Z & Lindvall, O 2006, 'Persistent production of neurons from adult brain stem cells during recovery after stroke', *Stem Cells*, vol. 24, no. 3, pp. 739-47.

Tian, DS, Yu, ZY, Xie, MJ, Bu, BT, Witte, OW & Wang, W 2006, 'Suppression of astroglial scar formation and enhanced axonal regeneration associated with functional recovery in a spinal cord injury rat model by the cell cycle inhibitor olomoucine', *J Neurosci Res*, vol. 84, no. 5, pp. 1053-63.

Tichauer, J, Saud, K & von Bernhardt, R 2007, 'Modulation by astrocytes of microglial cell-mediated neuroinflammation: effect on the activation of microglial signaling pathways', *Neuroimmunomodulation*, vol. 14, no. 3-4, pp. 168-74.

Tikka, T, Fiebich, BL, Goldsteins, G, Keinanen, R & Koistinaho, J 2001, 'Minocycline, a tetracycline derivative, is neuroprotective against excitotoxicity by inhibiting activation and proliferation of microglia', *J Neurosci*, vol. 21, no. 8, pp. 2580-8.

'Tissue plasminogen activator for acute ischemic stroke. The National Institute of Neurological Disorders and Stroke rt-PA Stroke Study Group', 1995, *N Engl J Med*, vol. 333, no. 24, pp. 1581-7.

Traystman, RJ 2003, 'Animal models of focal and global cerebral ischemia', *ILAR J*, vol. 44, no. 2, pp. 85-95.

Tremblay, ME, Stevens, B, Sierra, A, Wake, H, Bessis, A & Nimmerjahn, A 2011, 'The role of microglia in the healthy brain', *J Neurosci*, vol. 31, no. 45, pp. 16064-9.

Tsikas, D 2007, 'Analysis of nitrite and nitrate in biological fluids by assays based on the Griess reaction: appraisal of the Griess reaction in the L-arginine/nitric oxide area of research', *J Chromatogr B Analyt Technol Biomed Life Sci*, vol. 851, no. 1-2, pp. 51-70.

Tsivgoulis, G, Katsanos, AH & Alexandrov, AV 2014, 'Reperfusion therapies of acute ischemic stroke: potentials and failures', *Front Neurol*, vol. 5, p. 215.

Turner, RC, Dodson, SC, Rosen, CL & Huber, JD 2013, 'The science of cerebral ischemia and the quest for neuroprotection: navigating past failure to future success', *J Neurosurg*, vol. 118, no. 5, pp. 1072-85.

Tuttolomondo, A, Di Raimondo, D, di Sciacca, R, Pinto, A & Licata, G 2008, 'Inflammatory cytokines in acute ischemic stroke', *Curr Pharm Des*, vol. 14, no. 33, pp. 3574-89.

Tuttolomondo, A, Pecoraro, R & Pinto, A 2014, 'Studies of selective TNF inhibitors in the treatment of brain injury from stroke and trauma: a review of the evidence to date', *Drug Des Devel Ther*, vol. 8, pp. 2221-38.

Ueno, Y, Chopp, M, Zhang, L, Buller, B, Liu, Z, Lehman, NL, Liu, XS, Zhang, Y, Roberts, C & Zhang, ZG 2012, 'Axonal outgrowth and dendritic plasticity in the cortical peri-infarct area after experimental stroke', *Stroke*, vol. 43, no. 8, pp. 2221-8.

van der Zijden, JP, van der Toorn, A, van der Marel, K & Dijkhuizen, RM 2008, 'Longitudinal in vivo MRI of alterations in perilesional tissue after transient ischemic stroke in rats', *Exp Neurol*, vol. 212, no. 1, pp. 207-12.

Vartiainen, N, Pyykonen, I, Hokfelt, T & Koistinaho, J 1996, 'Induction of thymosin beta(4) mRNA following focal brain ischemia', *Neuroreport*, vol. 7, no. 10, pp. 1613-6.

Verma, R, Friedler, BD, Harris, NM & McCullough, LD 2014, 'Pair housing reverses post-stroke depressive behavior in mice', *Behav Brain Res*, vol. 269, pp. 155-63.

Vincent, VA, Tilders, FJ & Van Dam, AM 1997, 'Inhibition of endotoxin-induced nitric oxide synthase production in microglial cells by the presence of astroglial cells: a role for transforming growth factor beta', *Glia*, vol. 19, no. 3, pp. 190-8.

Wadey, AL, Muyderman, H, Kwek, PT & Sims, NR 2009, 'Mitochondrial glutathione uptake: characterization in isolated brain mitochondria and astrocytes in culture', *J Neurochem*, vol. 109 Suppl 1, pp. 101-8.

Wake, H, Moorhouse, AJ, Jinno, S, Kohsaka, S & Nabekura, J 2009, 'Resting Microglia Directly Monitor the Functional State of Synapses In Vivo and Determine the Fate of Ischemic Terminals', *The Journal of Neuroscience*, vol. 29, no. 13, pp. 3974-80.

Wakita, H, Tomimoto, H, Akiguchi, I & Kimura, J 1995, 'Protective effect of cyclosporin A on white matter changes in the rat brain after chronic cerebral hypoperfusion', *Stroke*, vol. 26, no. 8, pp. 1415-22.

Wang, R, Zhang, X, Zhang, J, Fan, Y, Shen, Y, Hu, W & Chen, Z 2012, 'Oxygen-glucose deprivation induced glial scar-like change in astrocytes', *PLoS One*, vol. 7, no. 5, p. e37574.

Wang, W, Redecker, C, Yu, ZY, Xie, MJ, Tian, DS, Zhang, L, Bu, BT & Witte, OW 2008, 'Rat focal cerebral ischemia induced astrocyte proliferation and delayed neuronal death are attenuated by cyclin-dependent kinase inhibition', *J Clin Neurosci*, vol. 15, no. 3, pp. 278-85.

Wanner, IB, Anderson, MA, Song, B, Levine, J, Fernandez, A, Gray-Thompson, Z, Ao, Y & Sofroniew, MV 2013, 'Glial scar borders are formed by newly proliferated,

elongated astrocytes that interact to corral inflammatory and fibrotic cells via STAT3-dependent mechanisms after spinal cord injury', *J Neurosci*, vol. 33, no. 31, pp. 12870-86.

Wanner, IB, Deik, A, Torres, M, Rosendahl, A, Neary, JT, Lemmon, VP & Bixby, JL 2008, 'A new in vitro model of the glial scar inhibits axon growth', *Glia*, vol. 56, no. 15, pp. 1691-709.

Wardlaw, J & Berge, E 2015, 'Cochrane reviewers' response to Alper and colleagues' analysis of thrombolysis in acute ischaemic stroke', *BMJ*, vol. 350, p. h1790.

Wardlaw, JM, Murray, V, Berge, E & del Zoppo, GJ 2014, 'Thrombolysis for acute ischaemic stroke', *Cochrane Database Syst Rev*, no. 7, p. CD000213.

Watson, BD, Dietrich, WD, Busto, R, Wachtel, MS & Ginsberg, MD 1985, 'Induction of reproducible brain infarction by photochemically initiated thrombosis', *Ann Neurol*, vol. 17, no. 5, pp. 497-504.

Wei, G, Wu, G & Cao, X 2000, 'Dynamic expression of glial cell line-derived neurotrophic factor after cerebral ischemia', *Neuroreport*, vol. 11, no. 6, pp. 1177-83.

Whishaw, IQ & Kolb, B 2005, *The behavior of the laboratory rat : a handbook with tests*, Oxford University Press, Oxford ; New York.

Wiese, S, Karus, M & Faissner, A 2012, 'Astrocytes as a source for extracellular matrix molecules and cytokines', *Front Pharmacol*, vol. 3, p. 120.

Wilhelmi, E, Schoder, UH, Benabdallah, A, Sieg, F, Breder, J & Reymann, KG 2002, 'Organotypic brain-slice cultures from adult rats: approaches for a prolonged culture time', *Altern Lab Anim*, vol. 30, no. 3, pp. 275-83.

Wilhelmsson, U, Li, L, Pekna, M, Berthold, CH, Blom, S, Eliasson, C, Renner, O, Bushong, E, Ellisman, M, Morgan, TE & Pekny, M 2004, 'Absence of glial fibrillary acidic protein and vimentin prevents hypertrophy of astrocytic processes and improves post-traumatic regeneration', *J Neurosci*, vol. 24, no. 21, pp. 5016-21.

Wilms, H, Hartmann, D & Sievers, J 1997, 'Ramification of microglia, monocytes and macrophages in vitro: influences of various epithelial and mesenchymal cells and their conditioned media', *Cell Tissue Res*, vol. 287, no. 3, pp. 447-58.

Winship, IR & Murphy, TH 2009, 'Remapping the somatosensory cortex after stroke: insight from imaging the synapse to network', *Neuroscientist*, vol. 15, no. 5, pp. 507-24.

Wirjatijasa, F, Dehghani, F, Blaheta, RA, Korf, HW & Hailer, NP 2002, 'Interleukin-4, interleukin-10, and interleukin-1-receptor antagonist but not transforming growth

factor-beta induce ramification and reduce adhesion molecule expression of rat microglial cells', *J Neurosci Res*, vol. 68, no. 5, pp. 579-87.

Wu, VW & Schwartz, JP 1998, 'Cell culture models for reactive gliosis: new perspectives', *J Neurosci Res*, vol. 51, no. 6, pp. 675-81.

Xerri, C, Merzenich, MM, Peterson, BE & Jenkins, W 1998, 'Plasticity of primary somatosensory cortex paralleling sensorimotor skill recovery from stroke in adult monkeys', *J Neurophysiol*, vol. 79, no. 4, pp. 2119-48.

Xia, CY, Zhang, S, Gao, Y, Wang, ZZ & Chen, NH 2015, 'Selective modulation of microglia polarization to M2 phenotype for stroke treatment', *Int Immunopharmacol*, vol. 25, no. 2, pp. 377-82.

Xin, H, Li, Y, Shen, LH, Liu, X, Hozeska-Solgot, A, Zhang, RL, Zhang, ZG & Chopp, M 2011, 'Multipotent mesenchymal stromal cells increase tPA expression and concomitantly decrease PAI-1 expression in astrocytes through the sonic hedgehog signaling pathway after stroke (in vitro study)', *J Cereb Blood Flow Metab*, vol. 31, no. 11, pp. 2181-8.

Xu, SY & Pan, SY 2013, 'The failure of animal models of neuroprotection in acute ischemic stroke to translate to clinical efficacy', *Med Sci Monit Basic Res*, vol. 19, pp. 37-45.

Xu, Y, Qian, L, Zong, G, Ma, K, Zhu, X, Zhang, H, Li, N, Yang, Q, Bai, H, Ben, J, Li, X, Xu, Y & Chen, Q 2012, 'Class A scavenger receptor promotes cerebral ischemic injury by pivoting microglia/macrophage polarization', *Neuroscience*, vol. 218, pp. 35-48.

Yamashita, K, Gerken, U, Vogel, P, Hossmann, K & Wiessner, C 1999, 'Biphasic expression of TGF-beta1 mRNA in the rat brain following permanent occlusion of the middle cerebral artery', *Brain Res*, vol. 836, no. 1-2, pp. 139-45.

Yamashita, T, Ninomiya, M, Hernandez Acosta, P, Garcia-Verdugo, JM, Sunabori, T, Sakaguchi, M, Adachi, K, Kojima, T, Hirota, Y, Kawase, T, Araki, N, Abe, K, Okano, H & Sawamoto, K 2006, 'Subventricular zone-derived neuroblasts migrate and differentiate into mature neurons in the post-stroke adult striatum', *J Neurosci*, vol. 26, no. 24, pp. 6627-36.

Yang, H, Feng, GD, Liang, Z, Vitale, A, Jiao, XY, Ju, G & You, SW 2012, 'In vitro beneficial activation of microglial cells by mechanically-injured astrocytes enhances the synthesis and secretion of BDNF through p38MAPK', *Neurochem Int*, vol. 61, no. 2, pp. 175-86.

Yang, Y & Herrup, K 2007, 'Cell division in the CNS: protective response or lethal event in post-mitotic neurons?', *Biochim Biophys Acta*, vol. 1772, no. 4, pp. 457-66.

Yang, Y, Salayandia, VM, Thompson, JF, Yang, LY, Estrada, EY & Yang, Y 2015, 'Attenuation of acute stroke injury in rat brain by minocycline promotes blood-brain barrier remodeling and alternative microglia/macrophage activation during recovery', *J Neuroinflammation*, vol. 12, p. 26.

Yenari, MA & Giffard, RG 2001, 'Ischemic vulnerability of primary murine microglial cultures', *Neurosci Lett*, vol. 298, no. 1, pp. 5-8.

Yenari, MA, Kauppinen, TM & Swanson, RA 2010, 'Microglial activation in stroke: therapeutic targets', *Neurotherapeutics*, vol. 7, no. 4, pp. 378-91.

Yenari, MA, Xu, L, Tang, XN, Qiao, Y & Giffard, RG 2006, 'Microglia potentiate damage to blood-brain barrier constituents: improvement by minocycline in vivo and in vitro', *Stroke*, vol. 37, no. 4, pp. 1087-93.

Yiu, G & He, Z 2006, 'Glial inhibition of CNS axon regeneration', *Nat Rev Neurosci*, vol. 7, no. 8, pp. 617-27.

Yrjanheikki, J, Keinanen, R, Pellikka, M, Hokfelt, T & Koistinaho, J 1998, 'Tetracyclines inhibit microglial activation and are neuroprotective in global brain ischemia', *Proc Natl Acad Sci U S A*, vol. 95, no. 26, pp. 15769-74.

Yrjanheikki, J, Tikka, T, Keinanen, R, Goldsteins, G, Chan, PH & Koistinaho, J 1999, 'A tetracycline derivative, minocycline, reduces inflammation and protects against focal cerebral ischemia with a wide therapeutic window', *Proc Natl Acad Sci U S A*, vol. 96, no. 23, pp. 13496-500.

Yu, AC, Lee, YL & Eng, LF 1993, 'Astrogliosis in culture: I. The model and the effect of antisense oligonucleotides on glial fibrillary acidic protein synthesis', *J Neurosci Res*, vol. 34, no. 3, pp. 295-303.

Yu, AC, Wu, BY, Liu, RY, Li, Q, Li, YX, Wong, PF, Liu, S, Lau, LT & Fung, YW 2004, 'A model to induce low temperature trauma for in vitro astrogliosis study', *Neurochem Res*, vol. 29, no. 11, pp. 2171-6.

Yuan, T, Liao, W, Feng, NH, Lou, YL, Niu, X, Zhang, AJ, Wang, Y & Deng, ZF 2013, 'Human induced pluripotent stem cell-derived neural stem cells survive, migrate, differentiate, and improve neurologic function in a rat model of middle cerebral artery occlusion', *Stem Cell Res Ther*, vol. 4, no. 3, p. 73.

Zacharek, A, Chen, J, Cui, X, Li, A, Li, Y, Roberts, C, Feng, Y, Gao, Q & Chopp, M 2007, 'Angiopoietin1/Tie2 and VEGF/Fik1 induced by MSC treatment amplifies angiogenesis and vascular stabilization after stroke', *J Cereb Blood Flow Metab*, vol. 27, no. 10, pp. 1684-91.

Zamanian, JL, Xu, L, Foo, LC, Nouri, N, Zhou, L, Giffard, RG & Barres, BA 2012, 'Genomic analysis of reactive astrogliosis', *J Neurosci*, vol. 32, no. 18, pp. 6391-410.

Zanier, ER, Pischiutta, F, Riganti, L, Marchesi, F, Turola, E, Fumagalli, S, Perego, C, Parotto, E, Vinci, P, Veglianese, P, D'Amico, G, Verderio, C & De Simoni, MG 2014, 'Bone marrow mesenchymal stromal cells drive protective M2 microglia polarization after brain trauma', *Neurotherapeutics*, vol. 11, no. 3, pp. 679-95.

Zarruk, JG, Fernandez-Lopez, D, Garcia-Yebenes, I, Garcia-Gutierrez, MS, Vivancos, J, Nombela, F, Torres, M, Burguete, MC, Manzanares, J, Lizasoain, I & Moro, MA 2012, 'Cannabinoid type 2 receptor activation downregulates stroke-induced classic and alternative brain macrophage/microglial activation concomitant to neuroprotection', *Stroke*, vol. 43, no. 1, pp. 211-9.

Zhang, C, Li, Y, Chen, J, Gao, Q, Zacharek, A, Kapke, A & Chopp, M 2006, 'Bone marrow stromal cells upregulate expression of bone morphogenetic proteins 2 and 4, gap junction protein connexin-43 and synaptophysin after stroke in rats', *Neuroscience*, vol. 141, no. 2, pp. 687-95.

Zhang, D, Hu, X, Qian, L, O'Callaghan, JP & Hong, JS 2010, 'Astrogliosis in CNS pathologies: is there a role for microglia?', *Mol Neurobiol*, vol. 41, no. 2-3, pp. 232-41.

Zhang, L, Li, Y, Zhang, C, Chopp, M, Gosiewska, A & Hong, K 2011, 'Delayed administration of human umbilical tissue-derived cells improved neurological functional recovery in a rodent model of focal ischemia', *Stroke*, vol. 42, no. 5, pp. 1437-44.

Zhang, Q, Chen, C, Lu, J, Xie, M, Pan, D, Luo, X, Yu, Z, Dong, Q & Wang, W 2009, 'Cell cycle inhibition attenuates microglial proliferation and production of IL-1beta, MIP-1alpha, and NO after focal cerebral ischemia in the rat', *Glia*, vol. 57, no. 8, pp. 908-20.

Zhang, X, Tong, F, Li, CX, Yan, Y, Kempf, D, Nair, G, Wang, S, Muly, EC, Zola, S & Howell, L 2015, 'Temporal evolution of ischemic lesions in nonhuman primates: a diffusion and perfusion MRI study', *PLoS One*, vol. 10, no. 2, p. e0117290.

Zhao, BQ, Wang, S, Kim, HY, Storrie, H, Rosen, BR, Mooney, DJ, Wang, X & Lo, EH 2006, 'Role of matrix metalloproteinases in delayed cortical responses after stroke', *Nat Med*, vol. 12, no. 4, pp. 441-5.

Zhao, G & Flavin, MP 2000, 'Differential sensitivity of rat hippocampal and cortical astrocytes to oxygen-glucose deprivation injury', *Neurosci Lett*, vol. 285, no. 3, pp. 177-80.

Zhao, Y & Rempe, DA 2010, 'Targeting astrocytes for stroke therapy', *Neurotherapeutics*, vol. 7, no. 4, pp. 439-51.

Zhou, C, Zhang, C, Chi, S, Xu, Y, Teng, J, Wang, H, Song, Y & Zhao, R 2009, 'Effects of human marrow stromal cells on activation of microglial cells and production of inflammatory factors induced by lipopolysaccharide', *Brain Res*, vol. 1269, pp. 23-30.

Zhu, Z, Zhang, Q, Yu, Z, Zhang, L, Tian, D, Zhu, S, Bu, B, Xie, M & Wang, W 2007, 'Inhibiting cell cycle progression reduces reactive astrogliosis initiated by scratch injury in vitro and by cerebral ischemia in vivo', *Glia*, vol. 55, no. 5, pp. 546-58.